Dissertation zur Erlangung des Doktorgrades
der Fakultät für Chemie und Pharmazie
der Ludwig-Maximilians-Universität München

Novel Dry Powder Inhalation System Based on Dispersion of Lyophilisates

Sarah Christina Claus
aus Groß-Gerau

2012

ERKLÄRUNG

Diese Dissertation wurde im Sinne von § 7 der Promotionsordnung vom 28. November 2011 von Herrn Prof. Dr. Wolfgang Frieß betreut.

EIDESSTATTLICHE VERSICHERUNG

Diese Dissertation wurde eigenständig und ohne unerlaubte Hilfe erarbeitet.

München, am 15.11.2012

Sarah Claus

Dissertation eingereicht am 15.11.2012

1. Gutachter: Prof. Dr. Wolfgang Frieß

2. Gutachter: Prof. Dr. Gerhard Winter

Mündliche Prüfung am 18.12.2012

ACKNOWLEDGMENTS

This thesis was prepared at the Department of Pharmacy, Pharmaceutical Technology and Biopharmaceutics at the Ludwig-Maximilians-University (LMU) in Munich in cooperation with the Respiratory Drug Delivery Unit of Boehringer Ingelheim Pharma GmbH & Co. KG (BI) in Ingelheim.

Foremost, I would like to express my gratitude to my supervisor, Prof. Dr. Wolfgang Frieß for the possibility to join his research group and particularly for his valuable scientific support and enthusiastic guidance over the last years. Furthermore, I am thankful for the great opportunities to present my work at numerous international conferences. I also very much appreciated his personal advice and the creation of a pleasant and creative working atmosphere in the group.

I also would like to thank the leader of the chair, Prof. Dr. Gerhard Winter, for creating excellent working conditions and for supporting numerous social activities. Thank you also very much for taking over the role of co-referee of this work.

Boehringer Ingelheim Pharma GmbH &Co. KG is gratefully acknowledged for scientific, experimental, and financial support. Special thanks go to Dr. Tilo Schönbrodt for the initiation of the project and for giving me the opportunity to conduct this study at the LMU in cooperation with BI. I would also like to thank him for his guidance and valuable scientific support during the first year. Special thanks also go to Dr. Claudius Weiler for taking over the supervision of this project at BI, for his enthusiastic guidance, and for all the scientific input. Many thanks are also expressed to Dr. Jörg Schiewe, Dr. Markus Wolkenhauer and Dr. Herbert Wachtel for their support and the interesting scientific discussions we had. I would also like to express special thanks to Marion Dörner, Ronald Frieß, Benjamin Welter, and Stefan Walter for their support with experiments in the lab, Holger Holakovsky and Gilbert Wuttke for the possibility to perform the high speed camera recordings, Dr. Herbert Wachtel and Andree Jung for the support to do the Aerosizer measurements, as well as Dr. Karl Wagner and Birgit Schwarz for the support with the compression analysis.

From the Department of Chemistry of the LMU I want to thank Christian Minke for his support with SEM analysis and Wolfgang Wünschheim for the access to the x-ray diffractometer.

I want to thank Prof. Dr. Franz Paintner, Prof. Dr. Stefan Zahler, Prof. Dr. Christian Wahl-Schott, and Prof. Dr. Ernst Wagner for kindly serving as a member for my examination board.

My thanks are also extended to the assisting students Florian Prändl, Elisabeth Berto, Felicitas Keller, Alexandra Pickel, Katharina Hümpfner and Annette Starke for the good job they did during their internships.

I want to thank all my PhD colleagues from the research groups of Prof. Frieß and Prof. Winter for their warm welcome, their contribution to the great working atmosphere, the inspiring scientific discussions, the nice coffee breaks and the various leisure-time activities. Particularly I want to mention Julia, Eva, Kerstin, Winnie, Tim, Philipp, Katja, and Lars. Thank you for your support, your friendship, and for the good time we spent together in- and outside the lab. I want to express special thanks to Julia for scientific input and all the valuable discussions about freeze-drying. Special thanks go also to my lab and office mates Eva, Kerstin, Imke, Katja and Miriam for the nice atmosphere and the great time we spent together.

I want to thank my parents Nannette and Günter, my “parents-in-law” Waltraud and Martin and my brother Nicolai with Katherine for their encouragement and great support in all the years.

Finally, I would like to thank Tobias for proofreading of this work, all his support and patience. Heartfelt thanks for your love.

For my parents
and Tobias

TABLE OF CONTENTS

Chapter 1

General Introduction and Objective of the Thesis

Abstract

In the last decades, dry powder inhalation has become a very attractive option for pulmonary drug delivery to treat lung diseases like cystic fibroses and lung infections. In contrast to the traditional pulmonary application of drugs for asthma and chronic obstructive pulmonary disease, these therapies require higher lung doses to be administered. The developments and improvements towards high dose powder pulmonary drug delivery are summarized and discussed in this chapter. These include the invention and improvement of novel inhaler devices as well as the further development of formulation principles and new powder engineering methods. The implementation of these strategies is subsequently described for some prototypes and formulations in research and development stage as well as for already marketed dry powder products. Finally, possible adverse effects which can occur after inhalation of high powder doses are shortly addressed.

1 GENERAL INTRODUCTION

1.1 WHY PULMONARY DRUG DELIVERY?

The main benefit of pulmonary drug administration is the delivery directly to the location of the disease while minimizing systemic exposure and toxicity [1]. Pulmonary delivery is characterized by rapid clinical response and allows to bypass therapeutic barriers such as poor gastrointestinal absorption and first-pass metabolism in the liver [2]. It can achieve a similar or superior therapeutic effect at a fraction of the systemic dose. For example, an oral dose of 2–4 mg salbutamol is therapeutically equivalent to 100–200 µg by inhalation [2]. This is particularly important when considering aminoglycoside antibiotics for the treatment of *Pseudomonas aeruginosa* infections of the lung. Only low sputum aminoglycoside concentrations are achieved by administration of relatively high intravenous doses which carry the potential for systemic toxicity whereas high sputum concentrations can be achieved by inhalation without the risk of systemic toxicity [3]. For the treatment of lung diseases like asthma and chronic obstructive pulmonary disease (COPD) inhaled medications have been available for many years. Devices and formulations were designed for the administration of relatively low doses ranging from 6 to 500 µg [4]. In recent years, the treatment of other diseases like cystic fibroses and lung infections, as well as systemic diseases by pulmonary administration, became more attractive. However, these therapies in general require higher doses to be effectively administered to the lung.

1.2 DEVICES FOR PULMONARY DRUG DELIVERY

Systems for pulmonary delivery include pressurized metered dose inhalers (pMDI), soft mist inhalers, nebulizer and dry powder inhalers (DPI). With respect to delivered dose, pMDIs and the Respimat® soft mist inhaler were designed for the delivery of highly potent drugs for the treatment of asthma and COPD but face several factors limiting high dose delivery. Due to a poor delivery efficiency (mean lung deposition of 12%), a small metering valve of 25-100 µl [5], and limited increase in concentration [6] only small delivered doses of less than a milligram per puff can be achieved with pMDIs [7]. The Respimat® soft mist inhaler improved delivery efficiency to about 40% but high dose delivery is still limited by a small metering chamber of only 15 µl [8]. Thus, pulmonary delivery of high drug doses has been realized by nebulization of liquid formulations. This way of administration has some drawbacks such as restricted portability of jet and ultrasonic nebulizers due to the required

power source as well as a noisy compressor for jet nebulizers. These drawbacks were improved for portable battery-powered vibrating mesh nebulizers. The administration is nevertheless time-consuming and regular cleaning and disinfection of the systems are required [9]. Particularly for cystic fibrosis (CF) patients, applying several aerosol therapies, the time burden is immense. It may take up to three hours per day for administration of drugs and then to clean and sanitize the aerosol equipment [7].

DPIs have the capacity to deliver higher payloads of drug to the lung. The first DPI (Aerohaler) was used in 1964 for the inhalation of 100,000 units of crystalline penicillin G sodium dust (approximately 60 mg) three times a day to treat patients with various infections of the respiratory tract [10]. In 1971 the Spinhaler® was developed [11] and approved for the delivery of 20 mg of the anti-asthmatic drug cromolyn sodium [12]. However, early DPI devices featured poor delivery efficiencies (only 4 to 17% lung delivery for cromolyn sodium) and the dosing performance depends on the patient's inspiratory flow rate [13, 14]. In order to be effectively delivered to the alveolar region, particles must have an aerodynamic size between 1 and 5 µm [2]. Particles in this size range are extremely adhesive and cohesive. To improve powder fluidization and aid in de-aggregation, the micronized drug is either formulated with controlled agglomeration (soft pellets) or, most often, blended with larger carrier particles [15] in a drug-carrier ratio of usually 1:67.5 [16, 17]. The high percentage of carrier particles and the poor delivery efficiency limit the maximum lung dose which can be delivered in one actuation to just a few milligrams [6]. For administration of an appropriate lung dose of the antiviral drug zanamivir, for example, the patient needs to inhale two blisters containing 5 mg zanamivir formulated with 20 mg lactose-monohydrate twice a day [18]. Additionally, the large variations in lung deposition which depend on the inspiratory flow rate restrict the standard blending technology to drugs with a relatively large therapeutic index [19]. To overcome these limitations, DPIs experienced continuous further development. A specific de-agglomeration zone was introduced for enhanced fine drug particle separation by turbulences and multi-dose DPIs were designed [4]. The Novolizer® and the AirMax™ device use tangential air flow which forms a cyclone in the device for optimized powder dispersion [20]. This approach improves lung delivery [21] but still shows variable performance at different flow rates [22, 23]. In contrast, drug delivery of the Taifun® device, which incorporates a vortex chamber, is relatively independent of the inhalation flow [24]. Constant drug deposition at different flow rates is also shown for the Turbospin® device where the inspiratory air is drawn through aerodynamically designed slits of the capsule chamber, putting it in a vortical motion. This causes shaking and twisting of the capsule for efficient

powder release [25, 26]. DPIs which include an active mechanism for powder dispersion are less dependent on the patient's inspiratory flow, which is particularly important when considering systemic drug delivery. The Exubera® and the Aspirair™ device are aimed for systemic delivery and use compressed air for powder aerosolization [27-29]. Nevertheless, all of the devices described above are designed for the delivery of small doses. DPI with drugs like anticholinergics, beta-2-agonists or glucocorticoids to treat asthma and COPD contain between 6 and 500 µg drug per dose [4]. An apomorphine hydrochloride formulation at 400 – 800 µg for the treatment of male erectile dysfunction was recently developed using the Aspirair™ device [29]. The Exubera® device was designed for the delivery of 1 or 3 mg of a dry powder insulin formulation to treat diabetes [27, 28].

In spite of still existing limitations for the delivery of larger doses, Crowther-Labiris et al. [3] delivered a lactose-blended micronized gentamicin dry powder formulation from the Clickhaler® device (nominal dose of 160 mg gentamicin) to ten chronically *Pseudomonas aeruginosa* infected patients, which had to take 32 inhalations to achieve a cumulative lung dose of 60 mg gentamicin. A new device, designed for the delivery of high powder doses, is the Twincer® for the application of antibiotics and sugar glass formulations containing, for example, therapeutic proteins. De Boer et al. [30] demonstrated that powder doses up to 25 mg of pure drug can effectively be de-agglomerated, which possibly could be further optimized to a dose of 50 mg. For 8 mg colistin sulfomethate, fine particle fractions between 40 and 60% were achieved, depending on the size of the classifier chamber. The Twincer® was designed as a low cost disposable inhaler, which makes it also interesting for medications that have to be given only once (e.g. vaccines) [30]. Another interesting novel dry powder inhaler for the delivery of high dose (25-250 mg) cohesive powders was described by Young et al. [31, 32]. The inhaler aerosolizes powder by using pressurized canisters filled with nitrogen gas at a pressure of 6-14 bar. An FPF between approximately 20 and 40% related to delivered dose could be achieved with a loading dose of 120 mg. A similar approach by using a standard propellant canister is described by Winkler et al. [33]. Up to 16 mg fine particle dose is reported in combination with that device. Recently the Novartis Podhaler® (T-326 Inhaler) was approved, which evolved from the Turbospin® device, to address the needs of high-payload delivery of engineered tobramycin particles of around 50 mg. Similar to the Turbospin® device, the vortical air flow causes the capsule to spin while powder is shaken out of two pierced holes and aerosolized [34]. *In vitro* particle deposition were found to be largely independent of the inhalation maneuver [35].

1.3 NEW POWDER FORMULATION METHODS

New powder formulation methods are equally important as sophisticated devices for an efficient delivery of high dose DPI products. Owing to their small size, micronsized particles are extremely adhesive and cohesive. To enhance powder flowability and dispersibility, the main formulation method is blending with large (30-90 μm) lactose carrier particles [17]. For these formulations two oppositional requirements must be fulfilled. On the one hand, adhesion between carrier and drug must be sufficient for the blend to be stable enough to allow handling like filling. On the other hand, it needs to be weak enough to enable the release of drug after inhalation when the carrier particles retain in the inhaler device or deposit in the oropharynx due to their large size. Drug detachment from the carrier during aerosolization is therefore crucial for efficient lung delivery [36]. To prevent incomplete de-agglomeration and improve lung delivery, different methods have been applied to weaken the drug adhesion including smoothing the carrier surface [37], reducing the particle size of the carrier [38], and using ternary mixtures with fines of e.g. lactose or hydrophobic components like magnesium stearate or amino acids [37, 39, 40]. Surface roughness of the carrier particles (in contrast to the surface roughness of small inhalable particles) may introduce asperities which could entrap drug particles and may resist its detachment from the carrier during inhalation [41, 42]. Two mechanisms by which fines improve de-aggregation are suggested because the aerosolization performance of the drug was shown to be both affected and unaffected by the blending order [43]. First, fines could prevent the drug particles from adhering to the strongest binding sites on the carrier [39] and, second, fine excipient and drug particles form agglomerates which are more easily dispersed and de-aggregated during aerosolization [44].

A second strategy to overcome uncontrolled agglomeration of micronsized particles is the controlled agglomeration into soft aggregates by spheronization. These soft pellets exhibit large particle sizes, which provide the required flow properties for accurate dosing and are hard enough to be handled and loaded into the inhaler but still easily break apart into primary particles during inhalation [45]. Nevertheless, the variability of dose emissions from such DPI systems has been found to be relatively high, with a total relative standard deviation of more than 15% of the average emitted dose [46]. Additionally, the formed soft aggregates can harden on the surface when exposed to moisture, which influences the dosing characteristics and the ability to disaggregate into primary particles at inhalation. Therefore, the inhaler (Turbohaler®) contains a desiccant, which is stored in the operating unit of the inhaler [45].

1.4 ENGINEERED PARTICLES

Drug delivery to the lung can also be improved by particle engineering, which aims at the production of drug particles of optimal size, morphology and structure [42]. At best, these engineered formulations can overcome the need of carrier blends to enhance powder flowability and thus reduce the need for large amounts of excipient in the formulation. Direct controlled crystallization, for example, enables the production of uniform crystal drug particles with better physical stability due to a lower amorphous content compared to micronized material [42]. Through the use of an antisolvent precipitation technique with growth-retarding stabilizers like hydroxypropylmethylcellulose, characteristic particle morphologies depending on crystalline polymorphs can be achieved [47]. Elongated particles show improved lung delivery because the aerodynamic diameter of a fiber is mainly determined by its width rather than by its length [48]. Ikegami et al. [49] performed solid-state transformation of a steroid from one polymorph to another and demonstrated an eightfold increase of the FPF for the needle-like particles of the β-form compared to the plate-like α-form. Nevertheless, particle size control remains a big challenge because most molecules tend to form relatively large crystals [42].

Several particle engineering technologies with the supercritical fluid carbon dioxide have been applied for pulmonary powder production. Particles form either as the result of rapid expansion of the supercritical fluid in which the components are dissolved or when the supercritical fluid acts as an antisolvent and causes precipitation from a solution [50]. It has been shown that powders produced by supercritical antisolvent precipitation typically exhibit a platelet particle morphology with lower bulk density and smaller cohesive-adhesive interactions compared to micronized powder, which enhances its dispersibility at low airflow rates [42]. Additionally, the controlled production of different polymorphic forms of high purity has been demonstrated [51]. The rapid expansion technique is only applicable if the compound has a significant solubility in the supercritical fluid and, if so, it is the technique of choice because of its simple, direct, solvent-free and continuous production of respiratory powder [42].

Spray drying is a well-established method in food and pharmaceutical industries with increasing popularity due to its applicability to formulate biopharmaceuticals [50, 52]. It is one of the most sophisticated drying techniques and offers many possibilities for modification and particle engineering. The product characteristics can be modified by process and formulation parameters like nozzle type and nozzle parameters, feed concentration and rate,

solvent, drying gas flow rate, temperature and humidity as well as excipients used [53, 54]. Spray drying is also applicable for many liquid systems like solutions, suspensions, as well as emulsions and it offers the possibility of mixing fluids immediately prior to or simultaneously with the atomization process [54]. Beside conventional spherical particles, spray drying permits also the controlled production of particles of different morphology. Corrugated particles can be attained, for example, by changing the spray drying process conditions [55-57], by employing polymeric excipients like dextran to increase the solution viscosity [58] or by adding low soluble components like leucine and trileucine [59-61]. These particles have a lower density and thus a larger geometrical size which improves powder dispersibility due to higher drag forces in the air stream. In addition, cohesive forces are reduced due to a smaller radius of curvature in the contact zone [58]. Spray drying has also been used in various methods for the preparation of porous particles. Vanbever et al. [62] prepared large porous particles by spray drying of a combination of water soluble (e.g. lactose) and water insoluble materials (e.g. dipalmitoylphosphatidylcholine) in an 87% ethanolic solution at a relatively low solid content (0.1% w/v). The particles had mean geometric diameters between 3 and 15 µm but very small densities (tap density of 0.04-0.06 g/cm^3), resulting in high emitted doses and respirable fractions. Another technique for the production of porous particles by spray drying is the PulmoSphere® technology [63]. PulmoSphere® particles are manufactured by an emulsion-based spray drying process. The drug is incorporated in an oil-in-water emulsion, which is composed of perfluorooctyl bromide and water and stabilized by the phospholipid distearoylphosphatidylcholine (DSPC), an endogenous pulmonary surfactant. During spray drying the drug diffuses to the center of the atomized droplet whereas the excipients form a shell at the surface. The volatile perflubron evaporates after further drying, leaving behind pores in the particle which form a sponge-like morphology. The particles have geometric sizes between 1 and 5 µm and are spherical in shape with a porous surface. This decreases the contact area between particles and leads to less particle agglomeration. Additionally, the accumulated DSPC at the surface lowers the surface energy, which further aids in decreasing interparticle cohesive forces. Consequently, PulmoSphere® particles have good flow and dispersing properties [63], allowing processing and aerosolization without the need to blend with carriers [64].

Spray freeze-drying is a related method and a useful process for drying thermosensitive molecules like proteins. An atomized liquid is frozen in liquid nitrogen and freeze-dried for the production of micronsized porous powder particles. Nevertheless, the atomization step and the extremely rapid freezing of droplets impose substantial stresses on proteins distinct

from those stresses created by conventional lyophilization [65]. Compared to spray drying the technique allows higher production yield and superior aerosol performance because of the particles' porosity. On the downside, the process is more complex, time-consuming, and cost intensive [66]. Additionally, the fast freezing of small droplets produce very fine microstructures after drying resulting in friable powders [65, 67].

Particles for sustained release can be formed from liquid dispersed systems via emulsion-based methods using biodegradable polymers like poly(lactide-co-glycolide) (PLGA) for microencapsulation of the drug. Traditionally, these methods have been applied for the preparation of injectables [42]. Numerous examples of sustained release microspheres for pulmonary delivery are published, which contain drugs like isoproterenol for sustained bronchodilation [68] or isoniazid/rifampicin for treatment of pulmonary tuberculosis [69]. Porous particles with increased delivery efficiency have also been prepared from liquid dispersed systems using PLGA. Applying this method, Edwards et al. [70] demonstrated improved bioavailability of large porous insulin particles which were about seven times bigger than small nonporous insulin particles. The positive effect was explained by two factors: first, the increased particle size results in decreased tendency to aggregate and therefore more efficient aerosolization; second, large particles may escape from phagocytosis by alveolar macrophages [70, 71]. However, it is important to note, that polylactide has been shown to cause adverse immunological responses, which result in a significant damage of the lung after 24 h [72].

Another particle engineering method for pulmonary drug delivery is a drug carrier technology developed by MannKind Biopharmaceuticals, which captures and stabilizes peptides or proteins in small precipitated particles. These light microspheres (Technospheres®) with a rough surface are formed by the pH-induced intermolecular self-assembly of 3,6-bis(N-fumaryl-N-(n-butyl)amino)-2,5-diketopiperazine. During the precipitation process, peptides and proteins which are present in the solution are microencapsulated. The precipitates are freeze-dried and become a light powder [73]. Efficacy, reliability and short-term tolerability of this drug delivery system has been demonstrated in clinical studies for parathyroid hormone [74] and insulin [75].

1.5 HIGH DOSE DPI FORMULATIONS ON THE MARKET AND IN RESEARCH AND DEVELOPMENT

As the first high dose antibiotic dry powder formulation (european medicines agency (EMA) approval in July 2011), tobramycin PulmoSphere® reached the market with the TOBI® Podhaler® (Novartis AG, Basel, Switzerland). The total amount of 112 mg of tobramycin formulation is administered by the inhalation of four capsules twice a day [76]. This portable passive delivery system demonstrates the same delivery efficiency as the jet nebulized 300 mg tobramycin solution for inhalation (TOBI® Pari-LC Plus), which is powered by an air compressor and requires an administration time of 15 to 20 min [77] as well as additional cleaning time. Fine particle dose (FPD) values of the market product are not published, however, an earlier study with 25 mg/capsule demonstrated a mean lung deposition of 34% [78].

In February 2012, the EMA approved Colobreath® (Forest Laboratories, Inc.). It is a dry powder formulation of colistimethate sodium administered using the Turbospin® DPI. One capsule contains 125 mg colistimethate to be inhaled twice a day [79]. The lung delivery efficiency is not published.

Several other high dose dry powder antibiotic formulations are in development. A ciprofloxacin PulmoSphere® formulation (Cipro Inhale) is currently in phase II clinical trial [80]. For a study in healthy volunteers, capsules were filled with 50 mg powder containing an active dose corresponding to 32.5 mg ciprofloxacin betain and was administered via the T-326 Nektar Inhaler (Podhaler®) [81]. The achieved FPD is not published.

Positive results were recently demonstrated in a phase I clinical study for AeroVanc® (Savara Inc.), a dry powder formulation of vancomycin. It is the first inhaled antibiotic being developed for the treatment of respiratory methicillin-resistant *Staphylococcus aureus* (MRSA) infection in patients with CF. The dose-escalating study included doses between 16 and 80 mg and examined the tolerability, safety, and pharmacokinetics of AeroVanc in non-MRSA infected CF patients in comparison to a 250 mg dose of vancomycin administered intravenously [82]. The lung delivery efficiency is not published, however, sputum concentrations of vancomycin known to effectively kill MRSA could be demonstrated [83].

Aquino et al. developed a dry powder formulation of gentamicin by particle engineering via spray drying. The formulation including 15% (w/w) leucine was spray dried from a water/co-

solvent system containing 30% (w/v) isopropyl alcohol and resulted in corrugated particles. A capsule charged with 120 mg powder introduced into the Turbospin® emitted almost the whole dose and achieved an in vitro FPD of 56 mg [59].

Not only antibiotics exist among high dosed dry powder formulations for inhalation. Mannitol (Aridol®, Pharmaxis Pharmaceuticals Limited), for example, is used in asthma diagnosis to identify persons with bronchial hyper-responsiveness [84]. For the bronchial provocation test patients are supposed to inhale the mannitol powder in increasing doses with the following protocol: 0 (empty capsule acting as a placebo), 5, 10, 20, 40, 80, 160, 160, and 160 mg mannitol whereby the 80-, and 160-mg doses are given in multiples of 40-mg capsules [85]. Another inhalative mannitol product is Bronchitol®, which was recently approved by the EMA for the treatment of CF patients aged 18 years and above for the improvement of lung function. A dose of 400 mg spray-dried mannitol is administered twice a day by inhalation of 10 capsules using the Cyclohaler®. The osmotic active mannitol helps in rehydration and clearance of the tenacious mucus [86, 87]. Achieved FPDs are not published.

Several other drugs for high dose pulmonary administration are considered in research. Among them are, for example, low molecular weight heparin [88], lung surfactant [89] and an NK1 receptor antagonist [90].

1.6 ADVERSE EFFECTS OF HIGH DOSED POWDER PULMONARY DELIVERY

The inhalation of large powder doses is regarded critical compared to nebulized liquids because of potential induction of bronchoconstriction in hyper-responsive lungs (e.g. asthma patients). Dry powder mannitol has been shown to present an osmotic challenge to hyper-responsive lungs at high dose and is therefore used for asthma diagnosis [84, 91]. Nevertheless, in non-asthmatic patients, large amounts of inhaled powder can also provoke upper-airway irritation, coughing, and bronchospasm which were reported as primary adverse events in various clinical studies. For Colobreath® these adverse effects normally diminish upon continued application or can be weakened by additional inhalation of β_2-agonists [79]. Mannitol for inhalation in CF patients provoked cough during the first treatment but was overall well tolerated [87]. The inhalation of tobramycin dry powder formulation most commonly caused cough, followed by lung disorders (generally reported as a pulmonary or CF exacerbation) and pharyngolaryngeal pain (sore throat) but were considered as not serious. Both phase III studies demonstrated that tobramycin inhalation powder was well tolerated in CF patients [92, 93]. Crowther-Labiris et al. [3] reported in a comparative study of dry

powder versus intravenous and nebulized gentamicin, that nebulization of gentamicin caused significantly more mouth and throat irritation, induced coughing, and an unpleasant taste compared to the dry powder inhalation.

1.7 CONCLUSION

The growing interest in the pulmonary administration of larger powder doses triggered both, the invention of novel inhaler devices with enhanced efficiency and the development of improved inhalation formulations. Another goal was to minimize variations in the aerosolization and delivery performance and to reduce the dependency on the patient's inspiratory flow. New sophisticated systems demonstrated their capability to deliver significantly increased lung doses compared to the simple early devices. Active as well as some passive devices achieved also inspiratory flow-independent delivery. In particular, particle engineering to improve powder properties play a significant role in leading dry powder formulations towards efficient delivery of large powder quantities. The engineered PulmoSphere® particles, for example, facilitated the development of the first marketed high dose antibiotic dry powder for pulmonary administration. Nevertheless, to achieve sufficiently high lung doses, every drug administration consists of multiple inhalations, which still leaves enough room for further improvement. The reported advances in particle engineering also opened the opportunity for the formulation and delivery of more complex and labile drugs like biopharmaceuticals.

2 OBJECTIVE OF THE THESIS

For pulmonary delivery of small molecules, as well as high-molecular-weight drugs like proteins and peptides, Yamashita et al. [94] developed a new dry powder inhalation system based on the dispersion of lyophilisates by impacting air. As the freeze-dried preparation is disintegrated into fine inhalable particles at the time of inhalation, the formulation is stored as a coherent bulk in a non-powdered form. This avoids formulation problems like poor flowability and re-dispersibility. The objective of the thesis was to evaluate the new concept of Yamashita et al. [94] and prove the possibility of creating individual inhalable particles from a coherent bulk via disintegration of lyophilisates by an air jet. It was aimed to assess possible methods for improvement of this technology as well as to explain underlying mechanisms. This includes first the development and evaluation of an output test system with reproducible and optimized performance as well as its characterization (Chapter 2). Second, in order to understand the aerosolization behavior, various placebo formulations were examined with respect to lyophilisate characteristics and particle size distributions (Chapter 3). In the following the suitability of this technology for the delivery of high powder doses was to be investigated. The main focus was thereby on the improvement of the formulation in order to achieve high fine particle doses (FPD - amount of drug that can be delivered to the side of action, the alveolar region of the lung). In a first approach ways and limitations to elevate the metered dose were studied (Chapter 4). For optimization of the FPD of a model drug which demonstrated poor delivery efficiency the addition of excipients was investigated (Chapter 5). To possibly increase the FPD of various freeze-dried substances, the impact of different lyophilisate morphologies on lyophilisate characteristics and their aerosolization performance was evaluated (Chapter 5 and Chapter 6). Furthermore, storage stability for three months at 25°C/60% RH and 40°C/75% RH was investigated for selected formulations (Chapter 5 and Chapter 7).

3 REFERENCES

[1] D.E. Geller, Aerosol Antibiotics in Cystic Fibrosis, Respir. Care., 54 (2009) 658-670.

[2] N.R. Labiris, M.B. Dolovich, Pulmonary drug delivery. Part I: Physiological factors affecting therapeutic effectiveness of aerosolized medications, Brit. J. Clin. Pharmaco., 56 (2003) 588-599.

[3] N. Crowther-Labiris, A. Holbrook, H. Chrystyn, S. MacLeod, M. Newhouse, Dry Powder versus Intravenous and Nebulized Gentamicin in Cystic Fibrosis and Bronchiectasis, Am. J. Respir. Crit. Care Med., 160 (1999) 1711-1716.

[4] I.J. Smith, M. Parry-Billings, The inhalers of the future? A review of dry powder devices on the market today, Pulm. Pharmacol. Ther., 16 (2003) 79-95.

[5] S.P. Newman, A Comparison of Lung Deposition Patterns Between Different Asthma Inhalers, J. Aerosol Med., 8 (1995) 21-27.

[6] J. Weers, A. Clark, P. Challoner, High dose inhaled powder delivery: challenges and techniques, in: R.N. Dalby, P.R. Byron, J. Peart, J.D. Suman, S.J. Farr (Eds.) Respiratory Drug Delivery IX, Davis Healthcare International Publishing (River Grove, IL, USA), Palm Desert, CA, USA, 2004, pp. 281-288.

[7] K.C. Kesser, D.E. Geller, New Aerosol Delivery Devices for Cystic Fibrosis, Respir. Care., 54 (2009) 754-768.

[8] S.P. Newman, K.P. Steed, S.J. Reader, G. Hooper, B. Zierenberg, Efficient delivery to the lungs of flunisolide aerosol from a new portable hand-held multidose nebulizer, J. Pharm. Sci., 85 (1996) 960-964.

[9] M.B. Dolovich, R. Dhand, Aerosol drug delivery: developments in device design and clinical use, The Lancet, 377 (2011) 1032-1045.

[10] K.M.R.P. Krasno L, Inhalation of penicillin dust, JAMA - J. Am. Med. Assoc., 138 (1948) 344-348.

[11] J.H. Bell, P.S. Hartley, J.S.G. Cox, Dry powder aerosols I: A new powder inhalation device, J. Pharm. Sci., 60 (1971) 1559-1564.

[12] M.M. Dykes, Evaluation of an antiasthmatic agent cromolyn sodium (aarane, intal), JAMA - J. Am. Med. Assoc., 227 (1974) 1061-1062.

[13] S.P. Newman, A. Hollingworth, A.R. Clark, Effect of different modes of inhalation on drug delivery from a dry powder inhaler, Int. J. Pharm., 102 (1994) 127-132.

[14] H. Steckel, B.W. Müller, In vitro evaluation of dry powder inhalers I: drug deposition of commonly used devices, Int. J. Pharm., 154 (1997) 19-29.

[15] M.J. Telko, A.J. Hickey, Dry Powder Inhaler Formulation, Respir. Care., 50 (2005) 1209-1227.

[16] F. Buttini, P. Colombo, A. Rossi, F. Sonvico, G. Colombo, Particles and powders: Tools of innovation for non-invasive drug administration, J. Control. Release, (2012) doi: 10.1016/j.jconrel.2012.1002.1028.

[17] M.P. Timsina, G.P. Martin, C. Marriott, D. Ganderton, M. Yianneskis, Drug delivery to the respiratory tract using dry powder inhalers, Int. J. Pharm., 101 (1994) 1-13.

[18] Fachinformation Relenza 5 mg/Dosis (German Summary of Product Characteristics), in, GlaxoSmithKline GmbH & Co. KG, München, Germany, 2011.

[19] J.G. Weers, T.E. Tarara, A.R. Clark, Design of fine particles for pulmonary drug delivery, Expert Opin. Drug Deliv., 4 (2007) 297-313.

[20] Y.-J. Son, J.T. McConville, Advancements in Dry Powder Delivery to the Lung, Drug Dev. Ind. Pharm., 34 (2008) 948-959.

[21] X.M. Zeng, S. Jones, D. O'Leary, M. Phelan, J. Colledge, Delivery of formoterol from a novel multi-dose inhaler AirmaxTM, Respir. Med., 96 (2002) 397-403.

[22] X.M. Zeng, D. O'Leary, M. Phelan, S. Jones, J. Colledge, Delivery of salbutamol and of budesonide from a novel multi-dose inhaler AirmaxTM, Respir. Med., 96 (2002) 404-411.

[23] S. Newman, G. Pitcairn, P. Hirst, R. Bacon, E. O'Keefe, M. Reiners, R. Hermann, Scintigraphic comparison of budesonide deposition from two dry powder inhalers, Eur. Resp. J., 16 (2000) 178-183.

[24] G.R. Pitcairn, T. Lankinen, O.-P. Seppälä, S.P. Newman, Pulmonary Drug Delivery from the Taifun Dry Powder Inhaler Is Relatively Independent of the Patient's Inspiratory Effort, J. Aerosol Med., 13 (2000) 97-104.

[25] PH&T web site: http://www.phtpharma.com/images/volantino-turbospin.pdf, in, (accessed July 5, 2012).

[26] L. Valentini, M. Maiorano, Inhalation device, in: United States Patent 4,069,819, Societa Farmaceutici S.p.A. (Milan, Italy), United States, 1978.

[27] S. White, D.B. Bennett, S. Cheu, P.W. Conley, D.B. Guzek, S. Gray, J. Howard, R. Malcolmson, J.M. Parker, P. Roberts, N. Sadrzadeh, J.D. Schumacher, S. Seshadri, G.W. Sluggett, C.L. Stevenson, N.J. Harper, EXUBERA®: Pharmaceutical Development of a Novel Product for Pulmonary Delivery of Insulin, Diabetes Technol. Ther., 7 (2005) 896-906.

[28] D.R. Owens, B. Zinman, G. Bolli, Alternative routes of insulin delivery, Diabetic Med., 20 (2003) 886-898.

[29] M. Tobyn, J.N. Staniforth, D. Morton, Q. Harmer, M.E. Newton, Active and intelligent inhaler device development, Int. J. Pharm., 277 (2004) 31-37.

[30] A.H. de Boer, P. Hagedoorn, E.M. Westerman, P.P.H. Le Brun, H.G.M. Heijerman, H.W. Frijlink, Design and in vitro performance testing of multiple air classifier technology in a new disposable inhaler concept (Twincer®) for high powder doses, Eur. J. Pharm. Sci., 28 (2006) 171-178.

[31] P.M. Young, J. Thompson, R. Price, D. Woodcock, K. Davies, The use of a novel handheld device to deliver high respirable fractions of high-dose dry powder active agents to the lung, J. Aerosol Med., 16 (2003) 192.

[32] P.M. Young, J. Thompson, D. Woodcock, M. Aydin, R. Price, The Development of a Novel High-Dose Pressurized Aerosol Dry-Powder Device (PADD) for the Delivery of Pumactant for Inhalation Therapy, J. Aerosol Med., 17 (2004) 123-128.

[33] R. Winkler, H. Wachtel, P. Langguth, Dose Range of a Propellant Driven High-Dose Dry Powder Inhaler, in: RDD Europe, Berlin, 2013, pp. 251-255.

[34] D.S. Maltz, S.J. Paboojian, Device Engineering Insights into TOBI Podhaler: A Development Case Study of High Efficient Powder Delivery to Cystic Fibrosis Patients, in: R.N. Dalby, P.R. Byron, J. Peart, J.D. Suman, P.M. Young (Eds.) Respiratory Drug Delivery Europe 2011, Davis Healthcare International Publishing (River Grove, IL, USA), Berlin, Germany, 2011, pp. 55-65.

[35] J. Weers, K. Ung, J. Le, N. Rao, B. Ament, G. Axford, D. Maltz, L. Chan, Dose Emission Characteristics of Placebo PulmoSphere((R)) Particles Are Unaffected by a Subject's Inhalation Maneuver, J. Aerosol. Med. Pulm. Drug Deliv., (2012).

[36] G. Pilcer, N. Wauthoz, K. Amighi, Lactose characteristics and the generation of the aerosol, Adv. Drug Delivery Rev., 64 (2012) 233-256.

[37] P.M. Young, D. Cocconi, P. Colombo, R. Bettini, R. Price, D.F. Steele, M.J. Tobyn, Characterization of a surface modified dry powder inhalation carrier prepared by “particle smoothing”, J. Pharm. Pharmacol., 54 (2002) 1339-1344.

[38] H. Steckel, B.W. Müller, In vitro evaluation of dry powder inhalers II: influence of carrier particle size and concentration on in vitro deposition, Int. J. Pharm., 154 (1997) 31-37.

[39] X.M. Zeng, G.P. Martin, S.-K. Tee, C. Marriott, The role of fine particle lactose on the dispersion and deaggregation of salbutamol sulphate in an air stream in vitro, Int. J. Pharm., 176 (1998) 99-110.

[40] J.N. Staniforth, Powder comprising anti-adherent materials for use in dry powder inhalers, in: United States patent 6475523, Vectura Limited, United States, 2002.

[41] M.-P. Flament, P. Leterme, A. Gayot, The influence of carrier roughness on adhesion, content uniformity and the in vitro deposition of terbutaline sulphate from dry powder inhalers, Int. J. Pharm., 275 (2004) 201-209.

[42] A. Chow, H. Tong, P. Chattopadhyay, B. Shekunov, Particle Engineering for Pulmonary Drug Delivery, Pharm. Res., 24 (2007) 411-437.

[43] M. Jones, R. Price, The Influence of Fine Excipient Particles on the Performance of Carrier-Based Dry Powder Inhalation Formulations, Pharm. Res., 23 (2006) 1665-1674.

[44] P. Lucas, K. Anderson, J.N. Staniforth, Protein Deposition from Dry Powder Inhalers: Fine Particle Multiplets as Performance Modifiers, Pharm. Res., 15 (1998) 562-569.

[45] K. Wetterlin, Turbuhaler: A New Powder Inhaler for Administration of Drugs to the Airways, Pharm. Res., 5 (1988) 506-508.

[46] G. Pilcer, K. Amighi, Formulation strategy and use of excipients in pulmonary drug delivery, Int. J. Pharm., 392 (2010) 1-19.

[47] N. Rasenack, H. Steckel, B.W. Müller, Micronization of anti-inflammatory drugs for pulmonary delivery by a controlled crystallization process, J. Pharm. Sci., 92 (2003) 35-44.

[48] H.-K. Chan, What is the role of particle morphology in pharmaceutical powder aerosols?, Expert Opin. Drug Deliv., 5 (2008) 909-914.

[49] K. Ikegami, Y. Kawashima, H. Takeuchi, H. Yamamoto, N. Isshiki, D.-i. Momose, K. Ouchi, Improved Inhalation Behavior of Steroid KSR-592 in Vitro with Jethaler® by Polymorphic Transformation to Needle-Like Crystals (β-Form), Pharm. Res., 19 (2002) 1439-1445.

[50] R.J. Malcolmson, J.K. Embleton, Dry powder formulations for pulmonary delivery, Pharm. Sci. Technol. Today, 1 (1998) 394-398.

[51] H.H.Y. Tong, B. Yu Shekunov, P. York, A.H.L. Chow, Characterization of Two Polymorphs of Salmeterol Xinafoate Crystallized From Supercritical Fluids, Pharm. Res., 18 (2001) 852-858.

[52] S. Schüle, W. Frieß, K. Bechtold-Peters, P. Garidel, Conformational analysis of protein secondary structure during spray-drying of antibody/mannitol formulations, Eur. J. Pharm. Biopharm., 65 (2007) 1-9.

[53] K. Cal, K. Sollohub, Spray drying technique. I: Hardware and process parameters, J. Pharm. Sci., 99 (2010) 575-586.

[54] R. Vehring, Pharmaceutical Particle Engineering via Spray Drying, Pharm. Res., 25 (2008) 999-1022.

[55] N.Y.K. Chew, H.-K. Chan, Use of Solid Corrugated Particles to Enhance Powder Aerosol Performance, Pharm. Res., 18 (2001) 1570-1577.

[56] N.Y.K. Chew, P. Tang, H.-K. Chan, J.A. Raper, How Much Particle Surface Corrugation Is Sufficient to Improve Aerosol Performance of Powders?, Pharm. Res., 22 (2005) 148-152.

[57] R. Fuhrherr, Spray-dried antibody powders for pulmonary application, PhD Thesis, in, Ludwig-Maximilians Universität München, Germany, 2005.

[58] C. Weiler, M. Egen, M. Trunk, P. Langguth, Force control and powder dispersibility of spray dried particles for inhalation, J. Pharm. Sci., 99 (2010) 303-316.

[59] R.P. Aquino, L. Prota, G. Auriemma, A. Santoro, T. Mencherini, G. Colombo, P. Russo, Dry powder inhalers of gentamicin and leucine: formulation parameters, aerosol performance and in vitro toxicity on CuFi1 cells, Int. J. Pharm., 426 (2012) 100-107.

[60] D. Lechuga-Ballesteros, C. Charan, C.L.M. Stults, C.L. Stevenson, D.P. Miller, R. Vehring, V. Tep, M.-C. Kuo, Trileucine improves aerosol performance and stability of spray-dried powders for inhalation, J. Pharm. Sci., 97 (2008) 287-302.

[61] K. Bechtold-Peters, W. Friess, S. Schuele, S. Bassarab, P. Garidel, T. Schultz-Fademrecht, Spray-dried amorphous powder with a low residual moisture and excellent

storage stability, in, Boehringer Ingelheim Pharma GmbH & Co. KG (Binger Strasse 173, 55216 Ingelheim, DE), 2008.

[62] R. Vanbever, J.D. Mintzes, J. Wang, J. Nice, D. Chen, R. Batycky, R. Langer, D.A. Edwards, Formulation and Physical Characterization of Large Porous Particles for Inhalation, Pharm. Res., 16 (1999) 1735-1742.

[63] D.E. Geller, J. Weers, S. Heuerding, Development of an Inhaled Dry-Powder Formulation of Tobramycin Using PulmoSphere™ Technology, J. Aerosol. Med. Pulm. Drug Deliv., 24 (2011) 175-182.

[64] J. Weers, Dispersible powders for inhalation applications, Innov. Pharm. Tech., 7 (2001) 111-116.

[65] H.R. Costantino, L. Firouzabadian, K. Hogeland, C. Wu, C. Beganski, K.G. Carrasquillo, M. Córdova, K. Griebenow, S.E. Zale, M.A. Tracy, Protein Spray-Freeze Drying. Effect of Atomization Conditions on Particle Size and Stability, Pharm. Res., 17 (2000) 1374-1382.

[66] Y.-F. Maa, P.-A. Nguyen, T. Sweeney, S.J. Shire, C.C. Hsu, Protein Inhalation Powders: Spray Drying vs Spray Freeze Drying, Pharm. Res., 16 (1999) 249-254.

[67] H.R. Costantino, L. Firouzabadian, C. Wu, K.G. Carrasquillo, K. Griebenow, S.E. Zale, M.A. Tracy, Protein spray freeze drying. 2. Effect of formulation variables on particle size and stability, J. Pharm. Sci., 91 (2002) 388-395.

[68] Y.-L. Lai, R.C. Mehta, A.A. Thacker, S.-D. Yoo, P.J. McNamara, P.P. DeLuca, Sustained Bronchodilation with Isoproterenol Poly(Glycolide-co-Lactide) Microspheres, Pharm. Res., 10 (1993) 119-125.

[69] R. Sharma, D. Saxena, A.K. Dwivedi, A. Misra, Inhalable Microparticles Containing Drug Combinations to Target Alveolar Macrophages for Treatment of Pulmonary Tuberculosis, Pharm. Res., 18 (2001) 1405-1410.

[70] D.A. Edwards, J. Hanes, G. Caponetti, J. Hrkach, A. Ben-Jebria, M.L. Eskew, J. Mintzes, D. Deaver, N. Lotan, R. Langer, Large Porous Particles for Pulmonary Drug Delivery, Science, 276 (1997) 1868-1872.

[71] D.A. Edwards, A. Ben-Jebria, R. Langer, Recent advances in pulmonary drug delivery using large, porous inhaled particles, Journal of Applied Physiology, 85 (1998) 379-385.

[72] D.J. Armstrong, P.N.C. Elliott, J.L. Ford, D. Gadsdon, G.P. McCarthy, C. Rostron, M.D. Worsley, Poly-(d,l-Lactic Acid) Microspheres Incorporating Histological Dyes for Intra-pulmonary Histopathological Investigations, J. Pharm. Pharmacol., 48 (1996) 258-262.

[73] A. Pfützner, T. Forst, Pulmonary insulin delivery by means of the Technosphere™ drug carrier mechanism, Expert Opin. Drug Deliv., 2 (2005) 1097-1106.

[74] A. Pfützner, F. Flacke, R. Pohl, D. Linkie, M. Engelbach, R. Woods, T. Forst, J. Beyer, S.S. Steiner, Technopshere/PTH(1-34) – a new approach for effective pulmonary delivery of parathyroid hormone(1-34). Horm. Metab. Res., 35 (2003) 319-323.

[75] A. Pfützner, A.E. Mann, S.S. Steiner, Technosphere/Insulin--a new approach for effective delivery of human insulin via the pulmonary route, Diabetes Technol Ther, 4 (2002) 589-594.

[76] Fachinformation TOBI Podhaler (German Summary of Product Characteristics), in, Novartis Pharma GmbH, Nürnberg, Germany, 2011.

[77] D.E. Geller, M.W. Konstan, J. Smith, S.B. Noonberg, C. Conrad, Novel tobramycin inhalation powder in cystic fibrosis subjects: Pharmacokinetics and safety, Pediatr. Pulm., 42 (2007) 307-313.

[78] M.T. Newhouse, P.H. Hirst, S.P. Duddu, Y.H. Walter, T.E. Tarara, A.R. Clark, J.G. Weers, Inhalation of a Dry Powder Tobramycin PulmoSphere Formulation in Healthy Volunteers, Chest, 124 (2003) 360-366.

[79] Colobreath product information, WC500123690, in, European medicines agency, 2012.

[80] Tief in den Lungen, in, Bayer research 21, Bayer AG, Leverkusen, Germany, 2011.

[81] H. Stass, S. Baumann-Noss, H. Delesen, J. Nagelschmitz, S. Willmann, A. Edginton, Ciprofloxacin PulmoSpere Inhalation Powder: a healthy volunteer study, in: American Thoracic Society International Conference, Toronto, Canada, 2008.

[82] Inhaled Vancomycin Tolerability, Safety and Pharmacokinetics (NCT01537666), in, ClinicalTrails.gov, (accessed June 20, 2012).

[83] Savara Pharmaceuticals, USA, news section of web site: http://www.savarapharma.com/news.html, in, (accessed June 20, 2012).

[84] S.D. Anderson, J. Brannan, J. Spring, N. Spalding, L.T. Rodwell, K. Cahn, I. Gonda, A. Walsh, A.R. Clark, A New Method For Bronchial-provocation Testing in Asthmatic Subjects Using a Dry Powder of Mannitol, Am. J. Respir. Crit. Care Med., 156 (1997) 758-765.

[85] Fachinformation Aridol Pulver zur Inhalation (German Summary of Product Characteristics), in, Pharmaxis Pharmaceuticals Limited, Burnham, United Kingdom, 2010.

[86] P. Jungmayr, Ergänzender Baustein zur Therapie der Mukoviszidose, Deutsche Apotheker Zeitung, 152 (2012) 38-40.

[87] A. Jaques, E. Daviskas, J.A. Turton, K. McKay, P. Cooper, R.G. Stirling, C.F. Robertson, P.T.P. Bye, P.N. LeSouëf, B. Shadbolt, S.D. Anderson, B. Charlton, Inhaled Mannitol Improves Lung Function in Cystic Fibrosis*, Chest, 133 (2008) 1388-1396.

[88] A. Rawat, Q.H. Majumder, F. Ahsan, Inhalable large porous microspheres of low molecular weight heparin: In vitro and in vivo evaluation, J. Control. Release, 128 (2008) 224-232.

[89] K.S. Babu, D.A. Woodcock, S.E. Smith, J.N. Staniforth, S.T. Holgate, J.H. Conway, Inhaled synthetic surfactant abolishes the early allergen-induced response in asthma, Eur. Resp. J., 21 (2003) 1046-1049.

[90] T. Nakate, H. Yoshida, A. Ohike, Y. Tokunaga, R. Ibuki, Y. Kawashima, Formulation development of inhalation powders for FK888 using the E-haler® to improve the inhalation performance at a high dose, and its absorption in healthy volunteers, Eur. J. Pharm. Biopharm., 59 (2005) 25-33.

[91] K. Holzer, S.D. Anderson, H.-K. Chan, J. Douglass, Mannitol as a Challenge Test to Identify Exercise-induced Bronchoconstriction in Elite Athletes, Am. J. Respir. Crit. Care Med., 167 (2003) 534-537.

[92] M.W. Konstan, D.E. Geller, P. Minić, F. Brockhaus, J. Zhang, G. Angyalosi, Tobramycin inhalation powder for P. aeruginosa infection in cystic fibrosis: The EVOLVE trial, Pediatr. Pulm., 46 (2011) 230-238.

[93] M.W. Konstan, P.A. Flume, M. Kappler, R. Chiron, M. Higgins, F. Brockhaus, J. Zhang, G. Angyalosi, E. He, D.E. Geller, Safety, efficacy and convenience of tobramycin inhalation powder in cystic fibrosis patients: The EAGER trial, J. Cyst. Fibros., 10 (2011) 54-61.

[94] C. Yamashita, A. Akagi, Y. Fukunaga, Dry powder inhalation system for transpulmonary administration, in: United States Patent 7735485 2010.

Chapter 2

The Test System

Abstract

Dry powder inhalers and dry powder formulations experience a growing interest and are the subject of continuous further development. The objective of this study was to evaluate the possible aerosolization of lyophilisates by an air impact. Therefore an output test system for disintegration of the lyophilisate and for delivery of the generated fine particles was developed. The output system uses compressed air at a preselectable pressure for reproducible generation of inhalable particles. The influence of several variable parameters on the fine particle output was investigated to decide for a standard setting for further development work. With respect to the compressed air, the final standard setting included a pressure of 3 bar and a volume for dispersion of 20 ml. Regarding the air inlet and outlet capillaries, the position was fixed at 5 mm below the stopper and the diameter to 0.75 mm. To possibly further improve the powder delivery, the influence of vial and stopper geometry of the implemented container housing the formulation and a modified mouthpiece with sheath air were investigated. In order to characterize and understand the disintegration and aerosolization process, the air flow through the test system was simulated and the lyophilisate dispersion was visualized by high speed camera recordings. Although the air flow impacted at about 90 m/s on the lyophilisate, the cake was not compressed but was lifted up and broken apart into fragments, which swirled around the endings of the capillaries. The aerosol finally had a velocity of 3 m/s when leaving the mouthpiece. The investigation of the influence of particle size on the output revealed an enhanced emission of larger particles due to larger target surfaces to the expelling air flow and less wall adhesion. However, also very fine particles (D (v, 0.5) of 3 µm) demonstrated a slightly increased emitted dose as a result of superior flight properties. Beside the successful dispersion of lyophilisates in the novel active test system, the possibility to disintegrate very soft lyophilisates was also demonstrated for the passive capsule based HandiHaler®. However, only small fine particle doses could be achieved.

1 INTRODUCTION

Inhalation therapy is the most common treatment for pulmonary diseases like asthma and chronic obstructive pulmonary disease (COPD). In the last decades, the evolution of dry powder inhalers (DPIs) experienced increasing attraction, which led to the development of several different devices and powder formulations. Islam and Gladki [1] divided the DPI devices available on the market into three generations of DPIs. The first generation DPIs are breath activated single unit dose devices like the Spinhaler®, for which the doses are factory metered into single capsules. Among the second generation DPIs, there are multi-dose reservoir inhalers and multiple unit dose inhalers, which are both breath activated devices as well. The Turbohaler®, for example, includes a powder reservoir and a disk with metering holes where the dose is metered right before inhalation [2]. The MAGhaler®, another multi-dose reservoir inhaler with a different metering system, is loaded with a ring-tablet from which small amounts are grated with a ceramic milling disk [3]. A multiple unit dose inhaler like the Diskus® contains a coiled blister strip with every blister containing one factory metered dose which is opened and inhaled [4]. The third generation DPIs are active devices like the Exubera® device, which uses patient-generated compressed air for powder aerosolization [5]. A new system, described by Yamashita et al. [6], consists of a freeze-dried preparation which is disintegrated into fine particles by impacting air at the time of inhalation. Therefore, it is a DPI system in which the formulation is stored in a non-powdered form. Formulation problems like inadequate flowability and redispersibility of powders are thereby avoided. The disintegration and delivery of the lyophilisate is achieved by an air jet, produced by contracting a bellows. Another interesting novel dry powder inhaler for the delivery of high dose (25-250 mg) cohesive powders was described by Young et al. (2003, 2004). The inhaler aerosolizes powder by using pressurized canisters filled with nitrogen gas at a pressure of 6-14 bar. The objective of this study was to prove the possibility of disintegrating lyophilisates by an air impact. For this purpose, an output test system with reproducible air jet generation was designed and evaluated with respect to the volume and pressure of the compressed air as well as position and diameter of in and outlet. Potential causes for reduced output of the test system like vial and stopper geometry as well as the mouthpiece were examined. To understand the aerosolization behavior of the system, high speed camera recordings were performed as well as a simulation of the air flow through the test system for a better understanding of the air flow upon impact on the cake. Furthermore, output characteristics were inspected separately from the disintegration process to understand how

different particle sizes generated from the lyophilisate can escape the container. Additionally, the possibility of disintegrating lyophilisates in the capsule-based passive HandiHaler® was investigated.

2 MATERIALS AND METHODS

2.1 MATERIALS

Excipients used were: L-isoleucine (Ile) (Fluka Chemie GmbH, Buchs, Switzerland), L-phenylalanine (Phe) (Merck KGaA, Darmstadt, Germany), L-valine (Val) (Fagron GmbH&Co KG, Barsbüttel, Germany), lactose-monohydrate (Lac) (Fagron GmbH&Co. KG, Barsbüttel, Germany), trehalose (Tre) (Hayashibara Co Ltd, Okayama, Japan); dye for quantification was rhodamine B (Sigma-Aldrich, Chemie GmbH, Steinheim, Germany); filters used in Andersen cascade impactor analysis were type A/E glass fiber filters 76 mm (Pall Corporation, Ann Arbor, MI, USA)

Lactose samples of different particle size were obtained from DFE pharma (Goch, Germany) in the following qualities: Lactohale® LH 100 (sieved), Lactohale® LH 200 (milled), Lactohale® LH 201 and Lactohale® LH 300.

2.2 DESIGN OF EXPERIMENTS (DOE)

A design of experiments was planned and evaluated with Modde 8 (Umetrics AB, Umeå, Sweden)

2.3 FORMULATION PREPARATION IN GLASS VIALS

0.5 ml solutions containing 4 mg/ml of the excipient and 0.2 mg/ml rhodamine B were filled into 2R glass vials (Fiolax® clear, Schott AG, Müllheim, Germany) and vials were equipped with rubber stoppers (C1503, Stelmi, Villepinte, France). Freeze-drying was carried out in a laboratory scale freeze-drier (Lyostar II, FTS Systems, Stone Ridge, NY, USA). The samples were frozen at -1°C/min to -45°C. Primary drying was performed at a shelf temperature of -20°C and a pressure of 34 mtorr for 14 h. In the secondary drying step shelf temperature was increased to 30°C and the pressure was decreased to 8 mtorr for 6 h.

For evaluation of serum stoppers (1104-PH 701/40/ow/wine-red, West Pharmaceutical Services, Eschweiler, Germany) as closure material, stoppers were exchanged after lyophilization in a glove box at approximately 10% relative humidity.

For evaluation of tubes, Rotilabo®-sample vials (Carl Roth GmbH & Co. KG, Karlsruhe, Germany) were cut to the same height as 2R vials. 0.5 ml solution containing 4 mg/ml trehalose and 0.2 mg/ml rhodamine B was filled into the tube and freeze-dried according to the above process. Afterwards, tubes were removed from the freeze-dryer to a glove box and sealed with 20 mm serum stoppers (1242 4110/40/grey West, Pharmaceutical Services, Eschweiler, Germany).

2.4 FORMULATION PREPARATION IN POLYETHYLENE CAPSULES

150 µl solution containing 4 mg/ml excipient and 0.2 mg/ml rhodamine B were filled into the base part of polyethylene capsules (size 3) arranged in a capsule tray of a handfill capsule machine (aponorm®, Wepa Apothekenbedarf GmbH & Co KG, Hillscheid, Germany). The tray was loaded onto a freeze-drier shelf and freeze-drying was carried out as described above. Afterwards, capsules were removed from the freeze-dryer to a glove box and closed with the corresponding top parts in the capsule machine. Until usage capsules were stored in a desiccator above silica orange gel.

2.5 ANDERSEN CASCADE IMPACTOR (ACI) ANALYSIS

The emitted dose (ED), delivered dose (DD), and fine particle fraction (FPF) of the formulations were evaluated using an Andersen cascade impactor (ACI) (8-Stage Non-Viable Sampler Series 20-800, Thermo Andersen, Smyrna, GA, USA). The ACI was operated at a flow rate of 39 l/min (corresponds to a pressure drop of 4 kPa with the HandiHaler®). The baffle plates were coated with a solution of 83% glycerin, 14% ethanol and 3% Brij 35. In 6.15 s a total air volume of 4 l passed through the impactor. During this time period, the aerosol was sprayed into the induction port. The total particle mass impacting below stage 1 equals to the FPF. By removing stages 2 to 7, the FPF is collected on the filter of the ACI. This configuration is called short stack ACI in this study. The amount of powder deposited on the filter was determined by washing with water and rhodamine B quantification at 554 nm in an Agilent 8453 UV-Vis spectrophotometer (Agilent Technologies, Santa Clara, CA, USA). Therefore the filter solution was ultra-centrifuged (Optima™ TLX Ultracentrifuge, Beckman Coulter, Brea, CA, USA) at 186000 g for 45 min before UV-Vis spectroscopic analysis. The

FPF (= fraction of particles in an inhalable size range with an aerodynamic diameter below 4.94 µm), the DD (dose that could be delivered to the ACI) and the ED (dose that was emitted off the vial) were calculated as percentage of the metered dose (nominal dose). The comparability of the FPF measured with the normal eight-stage ACI and the short stack version was tested with a flow rate of 39 l/min using the HandiHaler® in an unpublished study showing no significant difference of the measured FPF. Therefore the experiments of this study were performed with a flow rate of 39 l/min instead of the recommended 28.3 l/min of the pharmacopoeia. All ACI measurements were performed in triplicate.

2.6 SIMULATION OF THE AIR FLOW THROUGH THE DEVICE

Simulation of the air flow through the device and the vial was simulated by Ralf Kröger of Ansys Germany GmbH using Ansys Workbench 13. Employed subprograms were Designmodeller for modeling of the geometry of the test system, Workbench Meshing for superimposing the calculation network comprising 3.14 million polygonal cells, and Fluent 13 for executing the simulation at time intervals of $1 \cdot 10^{-6}$ s. Due to the high time resolution and the fine calculation network, the simulation was terminated after 17 ms in order to keep the effort manageable.

2.7 HIGH SPEED CAMERA RECORDINGS

The aerosolization behavior of the lyophilisates in the vial was recorded using a Fastcam 1024 PCI (Photron, San Diego, CA, USA) with a sample rate of 1000 fps.

2.8 PARTICLE SIZE DISTRIBUTION (PSD) ANALYSIS

The PSD of lactose powder was measured by laser diffractometry using a Helos Sympatec (Sympatec GmbH, Clausthal-Zellerfeld, Germany) equipped with a Rodos dry dispersion unit and a Vibri feeding. The powder was dispersed at a pressure of 3 bar and extracted by suction. The size distribution was calculated as volume distribution using the Fraunhofer theory. The aerosolized powder was collected in a beaker and measured similarly to the basic powder.

2.9 ED ANALYSIS OF LACTOSE POWDERS OF DIFFERENT PARTICLE SIZE

For analysis of the ED independent of the cake disintegration process, 24 mg of lactose powder (2.1) was weighed into a 2R vial and aerosolized using the test system at default

settings. The generated aerosol was extracted by suction. ED was quantified by weighing the vial before and after aerosolization and calculated as percentage of the MD.

2.10 MECHANICAL TESTING

The mechanical properties of the lyophilisates were investigated using a Texture Analyzer (TA.XT.plus, Stable micro Systems, Godalming, UK) equipped with a 5 kg load cell and a cylindrical stainless steel probe with a diameter of 5 mm at a test speed of 1 mm/s and a maximal immersion into the lyophilisate of 2 mm. The resulting immersion-force curve demonstrated steady fracture at a constant force visible as a horizontal plateau. For comparison of different formulations, the measured data points of the plateau were averaged. The obtained force value represents the force necessary to fracture the lyophilisate.

3 RESULTS AND DISCUSSION

3.1 CONSTRUCTION OF AN OUTPUT TEST SYSTEM

For disintegration of lyophilisates into fine particles suitable for inhalation and delivery of these fine particles, an output test system was developed (Figure 1). The system was designed on the basis of an active DPI described by Yamashita et al. [6], but with the focus on reproducibility. It consists of two capillaries pierced through the stopper of the vessel housing the lyophilisate. One capillary is the air inlet, the other capillary is the air outlet, which is connected to the mouthpiece. The test system uses compressed air for disintegration of the

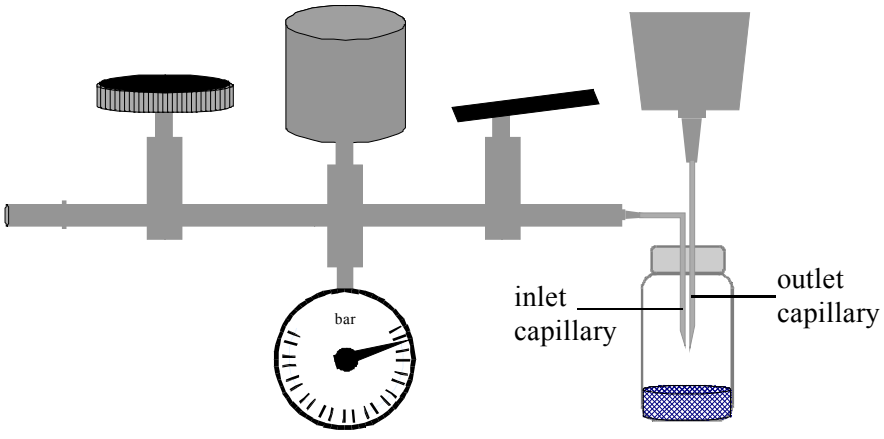

Figure 1: Schematic drawing of the output test system for disintegration of the lyophilisates.

lyophilisate into fine particles. For reproducible performance of the test system, the compressed air is stored in a pressure reservoir, holding a defined air volume at a preselectable pressure. Pressing a lever releases the compressed air through the inlet capillary. This pressure impulse starts dispersion and delivery of the powder. For comparison, the system of Yamashita et al. [6] has a similar configuration, but the air jet is generated manually by contraction of a 20 ml bellows.

The output test system has several variable parameters: the pressure and the volume of the compressed air reservoir, the diameter of the air inlet and air outlet capillary as well as their position. To identify the parameters influencing the FPF, DoE was used (see Table 1 for factors and corresponding settings). A fractional factorial resolution 4 screening design was performed which consisted of 19 runs, including 3 center points. The fine particle fraction was determined by short stack ACI analysis of isoleucine.

Table 1: The design of experiments factors and settings for evaluation of the variable parameter of the output test system.

Name	**Settings**
Pressure	1 to 3 bar
Reservoir volume	10 to 30 ml
Air inlet capillary diameter	0.25 to 0.75 mm
Air outlet capillary diameter	0.25 to 0.75 mm
Air inlet capillary position	0 to 10 mm below stopper
Air outlet capillary position	0 to 10 mm below stopper

The coefficient plot of the DoE (Figure 2) shows that only the pressure had a significant influence on the FPF and higher pressure led to larger FPF. On closer inspection, the air outlet capillary diameter (OCD) possibly had an effect on the fine particle fraction as well. A bigger air outlet capillary diameter led to slightly larger fine particle fractions, which might be due to a different flow behavior in container and outlet capillary resulting in a more effective destruction of the lyophilisate. A higher pressure is responsible for a larger total amount of air in the reservoir which could aid in the fine particle output. The total amount of air is the same for a pressure of 1 bar and an air volume of 30 ml or a pressure of 3 bar and an air volume of 10 ml. However, the FPF was substantially higher for a pressure of 3 bar in comparison to a pressure of 1 bar. For example, capillary diameters of 0.75 mm, a volume of 10 ml and a pressure of 3 bar achieved a FPF (related to MD) of 27%, whereas a volume of 30 ml and a pressure of 1 bar only attained a FPF of 18%. For capillary diameters of 0.25 mm this effect

was even higher. A volume of 10 ml and a pressure of 3 bar achieved a FPF of 19%, whereas a volume of 30 ml and a pressure of 1 bar only attained a FPF of 9%. Therefore, it was not the total amount of air which led to a larger FPF, but the high pressure. A higher pressure induced a stronger impaction on the lyophilisate which consequently disintegrated into finer particles. By taking this into account, the output test system was fixed to the following parameters: The pressure was set to 3 bar and the compressed air reservoir to a volume of 20 ml. For the air inlet and air outlet capillary a diameter of 0.75 mm was chosen. The position of the ending of the capillaries was fixed to 5 mm below the stopper of the vessel. All further experiments were carried out using this standard setting of the output test system. This should allow for reproducible results and substantial FPF.

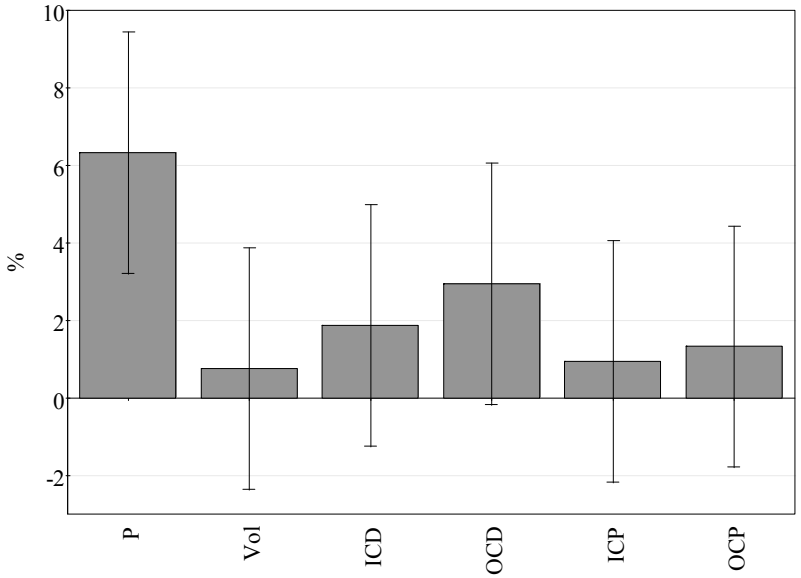

Figure 2: Scaled and centered coefficients for the fine particle fraction of the screening design DoE. The investigated factors were the compressed air pressure (P), reservoir volume (Vol), air inlet capillary diameter (ICD), air outlet capillary diameter (OCD), air inlet capillary position (ICP) and air outlet capillary position (OCP).

3.2 INFLUENCE OF VIAL AND STOPPER GEOMETRY ON FINE PARTICLE OUTPUT

When inspecting the vial after aerosolization, particles accumulated particularly in the cavity of the lyophilization stopper. In order to evaluate whether the geometry of the stopper hinders the particle output, lyo stoppers were replaced by flat serum stoppers after freeze-drying. No significant difference for ED, DD and FPF of trehalose lyophilisates in 2R vials equipped with the two different stoppers were detected (Figure 3a). Visual inspection of the vial after

aerosolization revealed a particle accumulation in the neck of the vial for samples with serum stopper. Thus the stopper replacement could not prevent particle accumulation at the top of the vial and therefore an increase in the ED was not possible.

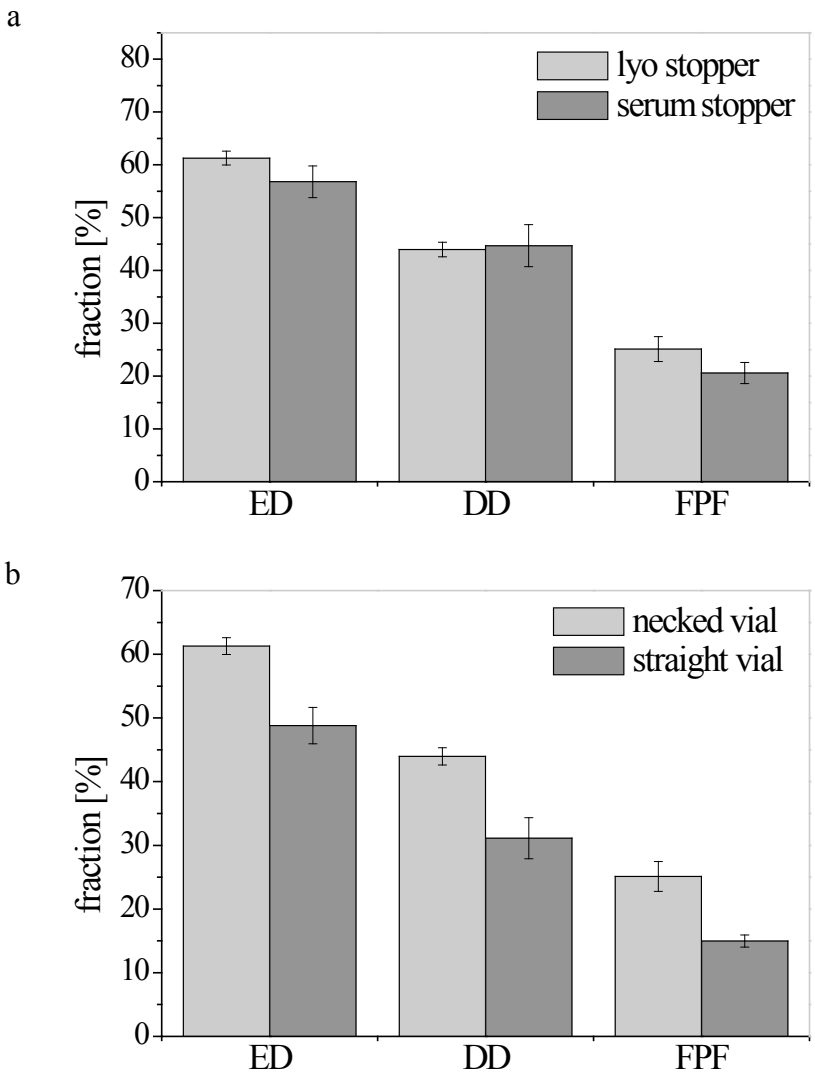

Figure 3: ED, DD and FPF of trehalose lyophilisates in a 2R vial equipped either with a lyophilization stopper or a serum stopper (a) or aerosolized from a necked 2R vial in comparison to a straight vial in the same dimensions (b).

To evaluate the influence of the vial neck on the ED, straight sample vials were compared to the normal 2R vials. The straight vials were sealed with 20 mm serum stoppers to eliminate any cavity where particles could accumulate. However, the straight vial geometry hindered the output from the vial as can be seen from Figure 3b. ED, DD, and FPF for trehalose lyophilisates decreased by about 10%. Possibly, the rounded neck edges of the vial benefit the output from the vial and the neck demonstrates a less negative effect compared to a straight geometry. The pass through of the air stream is generally enhanced with rounded edges,

whereas the sharp edges of the straight geometry could cause increased turbulences resulting in increased particle deposition. In conclusion, the 2R vial and lyo stopper geometry do not restrain fine particle output and can be used for all further studies.

3.3 INFLUENCE OF MOUTHPIECE WITH SHEATH AIR

After aerosolization a fine particle film covered the mouthpiece. The particles particularly deposited at the bottom of the mouthpiece due to a sudden expansion of the air flow leaving the narrow outlet capillary and entering the mouthpiece (Figure 4a). This sudden expansion to a larger diameter produces a zone of backflow with turbulences [7], resulting in a backward deposition at the bottom of the mouthpiece. In order to prevent this particle deposition and possibly enhance the FPF, a mouthpiece with sheath air was constructed. The sheath air is produced by suction through small holes positioned at the transition between outlet capillary and mouthpiece. It is supposed to focus the particle aerosol stream and guide it through the mouthpiece (Figure 4b). An adapter between the suction induction port (SIP) of the ACI and the mouthpiece assured for a tight connection. This enabled the vacuum pump simulating the inspiration to produce the sheath air inside the mouthpiece during the aerosolization process. The sheath air successfully reduced the deposition in the mouthpiece for phenylalanine and trehalose lyophilisates but increased the deposited fraction in the SIP as can be seen from Figure 5. All other fractions including the FPF remained the same. Visual inspection of the

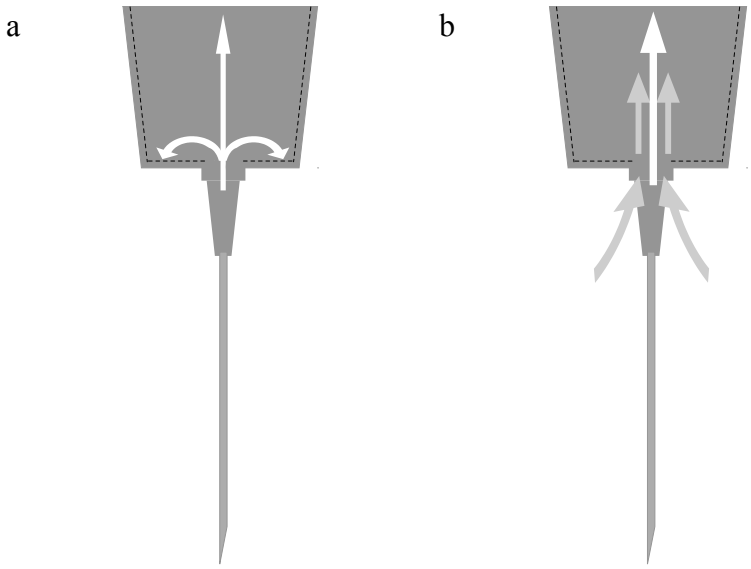

Figure 4: Schematic drawing of the aerosol behavior in the basic mouthpiece (a) and in the mouthpiece with sheath air (b).

SIP revealed a deposition of a particle film right at the beginning. Thus, the particle deposition which previously took place in the mouthpiece was only shifted to the beginning of the SIP when using the mouthpiece with sheath air. At this position, the same effect as reported for the mouthpiece without sheath air occurred. The air stream comprising the particle aerosol experienced a sudden expansion from the narrower sheath air to the broader diameter of the SIP, resulting in turbulences and consequently the deposition of finer particles. In summary, the improved mouthpiece with sheath air was not able to prevent the premature deposition of finer particles before entering the ACI. Therefore, the normal mouthpiece without sheath air will be used for all further experiments.

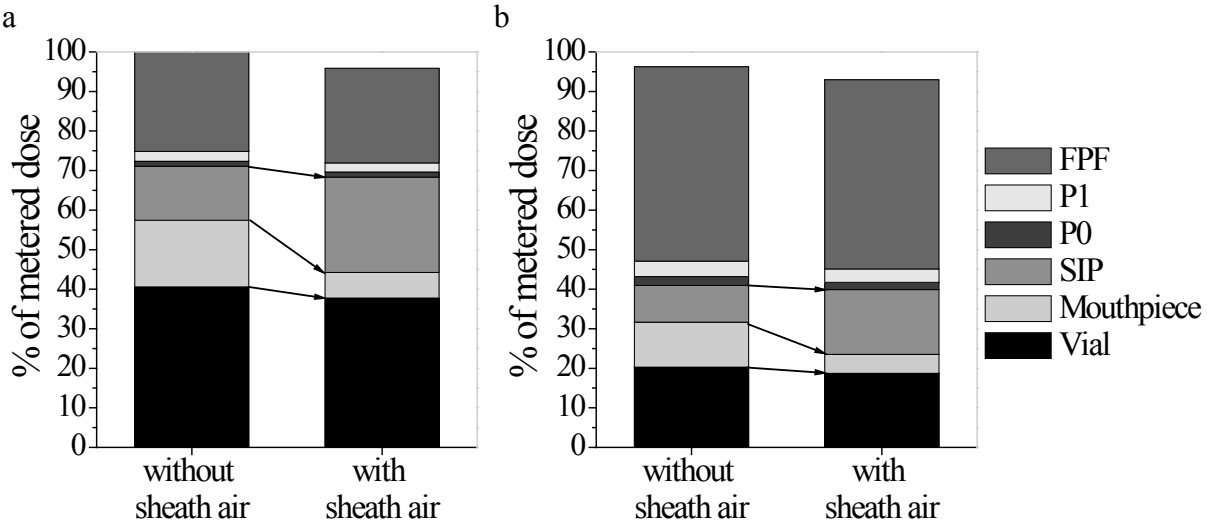

Figure 5: Material distribution after aerosolization of trehalose (a) or phenylalanine (b) lyophilisates using the basic mouthpiece or the one with sheath air.

3.4 SIMULATION OF THE AIR FLOW IN THE VIAL

To study the air flow through the device and the vial, a simulation was conducted. The geometry of the test system with the standard settings was modeled and a calculation network comprising 3.14 million polygonal cells was superimposed. The simulation was performed using very small time periods of $1 \cdot 10^{-6}$ s. For the first milliseconds the simulation revealed compressional waves which were reflected at edges and constrictions of the interior of the test system, resulting in pressure fluctuations until the inlet capillary was reached. The pressure fluctuations were eliminated in the narrow inlet capillary and therefore did not influence the air flow behavior in the vial. The pressure in the reservoir decreased from 3 bar overpressure to 2.8 bar within 17 ms, whereas the pressure in the vial increased to 0.7 bar (Figure 6).

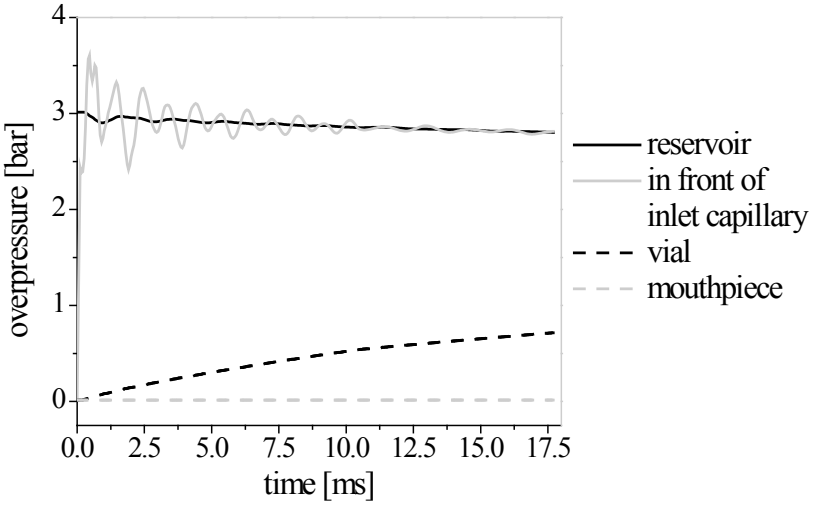

Figure 6: Simulated pressure variations of the air in the test system within 17 ms of actuation.

This huge pressure drop across the inlet capillary is a consequence of its small cross section and length. According to the equation of Hagen-Poiseuille when assuming laminar flow, the ratio of the length and the radius of the tube to the power of four determine the pressure drop across the tube. Hence, the radius of the tube plays a particularly important role: at a constant flow rate a reduction of the radius to the half, increases the pressure drop across the tube by 16-fold, which is an approximation because the equation of Hagen-Poiseuille is only valid for Newtonian and non-compressible fluids. Nevertheless, the DoE of the variable parameters of the test system revealed that the diameter of the capillaries, which were varied between 0.25 and 0.75 mm, did not significantly influence the FPF. On closer inspection, a capillary diameter of 0.75 mm achieved higher FPF than a capillary diameter of 0.25 mm, however the differences in FPF were considerably small compared to the pressure drop which should raise 81-fold. Comprising similar dimensions, the outlet capillary exhibited a comparable pressure drop, which caused the increasing pressure inside the vial. The pressure in the vial will rise until both capillaries demonstrate the same massflow. After 17 ms, the massflow into the vial was $1.1 \cdot 10^{-4}$ kg/s, whereas the massflow through the outlet capillary was only $4.0 \cdot 10^{-5}$ kg/s. Consequently, the vial still filled after 17 ms, which implies a still rising pressure in the vial.

The air flow achieved a velocity of approximately 350 m/s when leaving the inlet capillary and entering the vial during the first 2 ms (Figure 7). This air flow velocity was subsequently reduced to about 225 m/s after 17 ms. The velocity in the outlet capillary increased to 185 m/s within the 17 ms. The velocity of inlet and outlet flow will presumably average at 205 ms. Figure 8 shows the air movement inside the empty vial. The inlet air jet expands due to suction of surrounding air and finally impacts on the level of the cake surface at about 90 m/s.

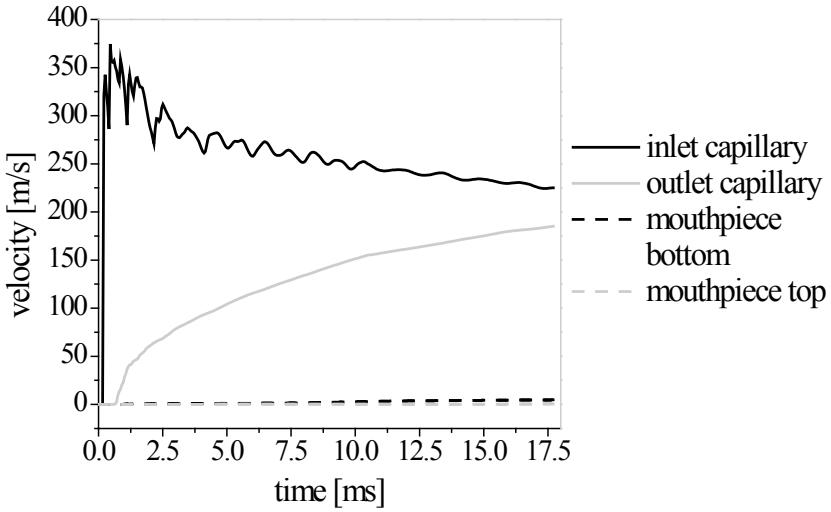

Figure 7: Simulated velocity variations of the air flow through the test system within 17 ms of actuation.

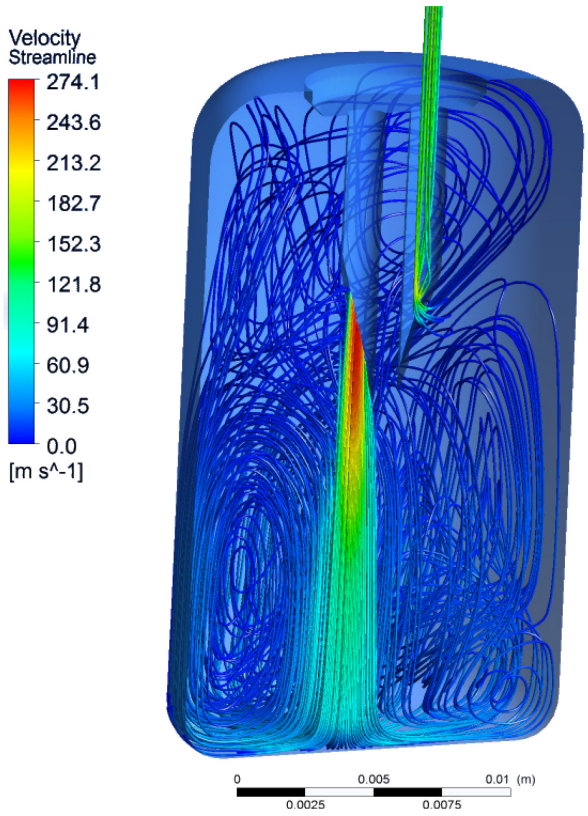

Figure 8: The pathlines of the air flow through the vial and its corresponding velocity at t=17 ms.

Turbulences of minor velocity occurred particularly at the bottom half of the vial, including some escapes to the top. At entering the outlet capillary, the air flow accelerated to 150 to 180 m/s. When considering aerosols, the velocity at which the aerosol leaves the device is of special interest because aerosol velocity influences lung deposition [8]. Inhalation devices

which emit aerosolized particles at a high velocity generally lead to a higher deposition in the oropharynx [9]. The air flow demonstrated a simulated velocity of 4.8 m/s at the bottom of the mouthpiece which was subsequently reduced to 0.7 m/s when leaving the mouthpiece. This velocity is comparable to the aerosol velocity of Respimat® Soft Mist™ Inhaler (0.8 m/s). The low velocity results in a higher lung and lower oropharyngeal deposition compared to pressurized metered dose inhalers (pMDI) [10] which have greater aerosol velocities (2 to 8 m/s) [11]. Nevertheless, the actual velocity of the powder aerosol needs to be tested (see 3.5).

3.5 THE AEROSOLIZATION BEHAVIOR OF THE LYOPHILISATE IN THE VIAL

In order to gain insights into the aerosolization behavior of the lyophilisate and understand the way of destruction and disintegration of the formulation by the air impact, the aerosolization of the lyophilisate was recorded with a high speed camera. As can be seen from Figure 9, the disintegration started on the left side of the vial, right below the air inlet capillary. The air impact on the lyophilisate caused an impact and eruption which disintegrated the lyophilisate into very small fragments. These fragments were lifted into the air and swirled around the endings of the capillaries. This swirling motion continued and after about 200 ms most of the fragments had left the vial. Thus, the lyophilisate was not compressed by the incoming airstream despite its high velocity of about 90 m/s, but broken apart and, with the reflection of the airstream in the bottom segment of the vial, the cake and cake fragments were lifted up in a circular and swirling fashion. The swirling particles were mainly focused on the upper half of the vial where air turbulences were less pronounced and at lower velocity compared to the bottom half (Figure 8). Whether this swirling motion induced further particle size reduction could not be clarified. The variable parameters tested with DoE (see 3.1) were also analyzed with the high speed camera in order to confirm and understand their influence. The position of the capillaries had no influence on the swirling behavior of the cake fragments: the center of the vortex was always located in the upper two thirds of the vial. Another parameter, the pressure for dispersion of the lyophilisates, had a significant effect on the size of the produced fragments. Reducing the pressure to 1 bar (Figure 9c), for example, led to apparently larger fragments as compared to the regular pressure of 3 bar (Figure 9a). Lyophilized cakes prepared of different excipients reacted differently to the air impact at the beginning of the aerosolization. For the valine lyophilisate, for example, shortly after the initial impact of the compressed air, the whole cake was lifted up and subsequently disintegrated into small fragments. For the phenylalanine lyophilisate, in contrast, the cake broke into large pieces

Figure 9: High speed recordings of the aerosolization behavior of lyophilized cakes prepared of different excipients like valine (a) and trehalose (b) as well as the disintegration of the valine lyophilisate using a reduced compressed air pressure of 1 bar (c).

which were then lifted up and disintegrated into smaller fragments. The lyophilisates produced of sugars such as lactose and trehalose mostly showed cracks on the surface which acted as predetermined breaking points, separating the cake into large pieces before further disintegration (Figure 9b). Apart from insights into the aerosolization process, high speed recordings also allowed to determine the aerosol velocity. Within a time period of 9 ms the aerosol covered a distance of 27 mm, resulting in an approximate velocity of 3 m/s at the end of the mouthpiece. This is comparable to pMDI, which have an aerosol velocity of 2.0-8.4 m/s [11]. The actual aerosol velocity was clearly greater compared to the simulated air flow velocity when leaving the mouthpiece (0.7 m/s). The particles might be accelerated to a high

velocity in the flow during the passage of the narrow outlet capillary, almost like darts in a blow-pipe and experience less deceleration compared to the air flow due to their mass inertia.

3.6 INFLUENCE OF THE PARTICLE SIZE ON THE OUTPUT

To investigate the influence of particle size on the ED, independent of the cake disintegration process, lactose powder (Lactohale®) of different particle sizes between 3 and 130 µm (D (v, 0.5)) were filled into vials (24 mg) and aerosolized using the output test system. The particle size distribution (PSD) of these powders was analyzed by laser diffractometry before and after aerosolization. Only the powder with the largest particle size (D (v, 0.5) of approx. 130 µm), showed a shift to smaller particle sizes after aerosolization (Table 2). Possibly the active aerosolization by compressed air caused a comminution of some accelerated larger particles like in a jet mill. A potential explanation could be also that very large particles were not able to pass the narrow capillary with a diameter of 0.75 mm and remained in the vial. The two coarse lactose qualities LH 200 and LH 201 experienced a reduced fraction of fines, possibly as a result of the fines remaining in the vial and mouthpiece because of adhesion to surfaces. Interparticulate interactions (cohesion and adhesion) are dominated by van der Waals forces for small particle (<<100 µm), whereas gravitational forces are expected to dominate for larger particles (>>100 µm) [12]. Adhesion to device surfaces is therefore reduced for larger particles which can influence the ED (see below). The fine lactose quality LH 300 demonstrated no difference of the PSD of the powder before and after aerosolization.

Table 2: PSD of the different sized lactose powders before and after aerosolization in the test system.

	D(v, 0.1) (µm)	D(v, 0.5) (µm)	D(v, 0.9) (µm)
LH 100, start	66.1	129.4	209.2
aerosolized	50.1	108.6	167.7
LH 200, start	8.8	73.8	143.4
aerosolized	10.2	69.9	139.0
LH 201, start	2.9	22.6	56.4
aerosolized	3.5	23.5	54.8
LH 300, start	0.7	2.5	6.3
aerosolized	0.7	2.6	6.4

Figure 10 shows a decrease in the ED for smaller particle sizes. The biggest particles with a median size of 129 µm demonstrated an ED of 31%, which decreased to 9% for particles with a median size of 23 µm. Fine particles having a median particle size of 3 µm exhibited an

increased ED of 18%. On the one hand, large particles should display a larger target surfaces to the discharging air flow compared to smaller particles. On the other hand, smaller particles demonstrate stronger adhesion to surfaces resulting in a greater loss of free particles in the aerosol and became apparent as particle films on the inner surfaces of the vial and the mouthpiece by visual inspection after aerosolization. This latter effect is stressed by the difference between ED and DD, which increased with decreasing particle size, indicating a greater particle loss by adhesion on the mouthpiece. It has been also considered that fine particles (D (v, 0.5) of 3 µm), exhibit superior flight properties partly compensating for the above described disadvantages. They can better follow changes of air flow direction, which is also used for particle size classification in cascade impactor analysis. An increased ED for lactose powders at increased particle size was already demonstrated by Bell et al. [13] for a capsule based DPI. The loss of powder from the capsule increased at increasing particle size between 4 and 100 µm but decreased again for powders of larger particle size until 400 µm due to intermittent blocking of the capsule holes. For the finer particles an extensive coating of the internal capsule walls was reported, leading to the conclusion that interparticulate and adhesive forces of finer particles hinder their discharge from the capsule. An increased emission of polyethylene glycol 8000 particles with increased particle size as a result of the diminished cohesive forces of the particles was also shown by French et al. [12].

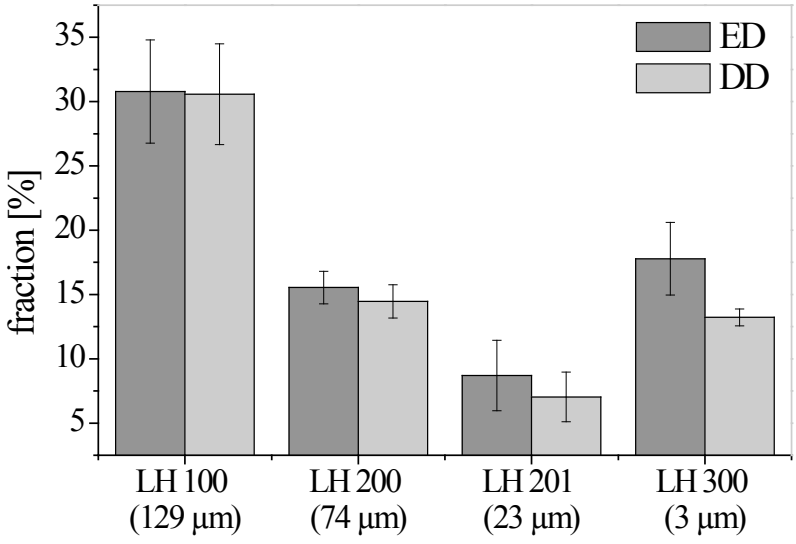

Figure 10: ED and DD of lactose powders aerosolized with the test system.

For the interpretation of this finding, one needs to consider that the delivery of particles to the alveolar region of the lung requires an aerodynamic size between 1 and 5 µm [14]. The aerodynamic diameter (d_A) is defined by the relationship

$$d_A \cong d_V \sqrt{\frac{\rho}{\chi \rho_0}} \quad (1)$$

and is dependent on the size (d_V), shape (χ) and mass density of the particle (ρ) for $\rho_0 = 1 g/cm^3$. It has been demonstrated that large porous particles display less cohesive and adhesive forces compared to small and nonporous particles and show more efficient delivery [15]. In order to take advantage of the improved emission, large porous particles with a small density could be beneficial.

3.7 EVALUATION OF LYOPHILISATE DISPERSION IN THE PASSIVE HANDIHALER®

Beside the advantage of inspiratory effort-independent delivery, active devices show some disadvantages such as the need for an energy source and the required coordination of activation and simultaneous inspiration by the patient. Alternatively, a high number of passive DPI devices are available on the market, which are easy to use and environmentally sustainable. In order to compare the described active system to a passive system, lyophilisate dispersion in a passive capsule-based device was studied. Excipient solutions of phenylalanine, valine and lactose in a concentration of 4 mg/ml were freeze-dried in polyethylene capsules for disintegration in the passive HandiHaler® and compared to lyophilisates in 2R vials aerosolized by the active test system. It is important to note that the base part of the capsule can only hold less than 200 µl for freeze-drying. Compared to a 2R vial, the metered dose is therefore limited. For aerosolization of a formulation in the HandiHaler®, a capsule is inserted into the device and pierced. The capsule vibrates in the capsule chamber as a result of the inspiratory flow. Particles which are arranged near one of the holes are sucked out of the capsule due to a flow dependent pressure difference (Venturi effect) and are subsequently carried along by the inspiratory air flow [16]. The lyophilisate needs to disintegrate into fine particles inside the capsule in order to pass through the small holes. This can either occur by agitation due to capsule vibration or by an air flow through the capsule. Figure 11 shows the high DD of around 80% for valine and lactose lyophilisates aerosolized by the passive HandiHaler® but only rather small FPF related to DD of 21.7% and 8.6%, respectively. For phenylalanine lyophilisates, in contrast, only a fraction of 10% left the capsule (data not shown). This demonstrates a successful disintegration of valine and lactose lyophilisates into particles which can leave the capsule. However, the disintegration was not very effective in producing fine particles with an aerodynamic diameter of less than 5 µm.

Phenylalanine lyophilisates, in contrast, were not adequately disintegrated into particles by the passive capsule-based device. Considering the FPD, the passive device demonstrated drastically reduced values in comparison to the active test system. The FPD of valine lyophilisates was reduced to about one tenth from 0.99 mg to 0.11 mg and for lactose lyophilisates from 0.42 mg to 0.04 mg. This was a result of a smaller metered dose in combination with a strongly decreased FPF.

In order to evaluate the mechanical stability of the lyophilisates inside the vials, texture analyses were performed. The cylindrical probe acts on the lyophilisate and the force needed for the immersion is recorded. The immersion-force curve of phenylalanine lyophilisates demonstrated a plateau indicating a force necessary to fracture the lyophilisate of about 0.014 N. Valine and lactose lyophilisates both exhibited softer cake structures with a force necessary to fracture the lyophilisate of less than 0.001 N, which was the lowest level of detection. Consequently, only very soft lyophilisates could be disintegrated in the passive HandiHaler®.

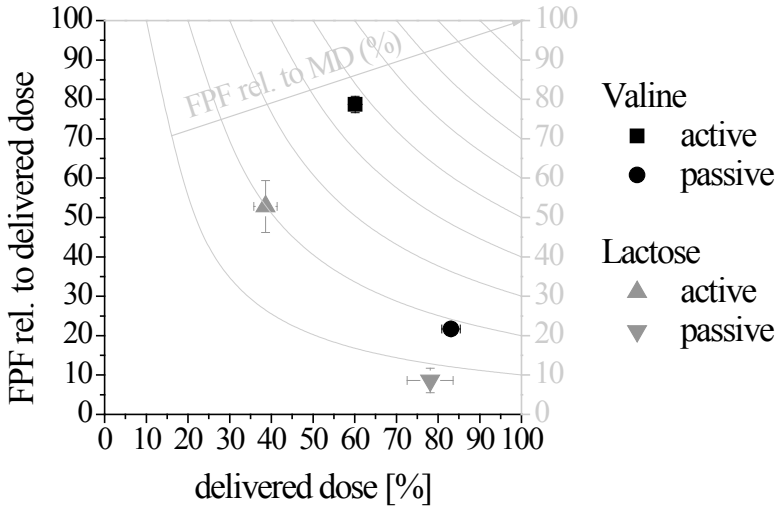

Figure 11: DD versus its related FPF as well as the FPF related to MD of valine and lactose lyophilisates aerosolized by the active test system in comparison to the passive HandiHaler®.

4 SUMMARY AND CONCLUSION

The output test system, which was designed with several variable parameters, enabled the disintegration of lyophilisates into fine particles in the vial and the delivery of these fine particles. With the exception of the factor pressure, the screening design DoE identified the

variable parameters of the output test system as not influencing FPF within the specified limits. For further experiments, the output test system was fixed to a standard parameter setting including a pressure of 3 bar, a compressed air reservoir of 20 ml, and a diameter of the air inlet and air outlet capillary of 0.75 mm. An observed particle accumulation in the cavity of the lyophilization stopper or neck of the 2R vial could neither be reduced via replacing the lyo stopper by a flat serum stopper nor by substituting the necked vial with a straight one. It was also not possible to increase the FPF by using a mouthpiece with sheath air. Although the deposition of fine particles in the mouthpiece was reduced, the same problem occurred at entering the SIP, resulting in deposition of finer particles due to turbulences of the expanding air stream. The test system was therefore by default used with a 2R vial equipped with lyophilization stoppers and with the basic mouthpiece.

A simulation of the air flow through the device demonstrated great pressure drops across the narrow inlet and outlet capillaries, resulting in a pressure increase inside the vial to 0.7 bar within the first 17 ms. At this time point, the pressure drop of the inlet capillary amounted to 2.1 bar. This can possibly explain the positive influence of a high compressed air pressure for a good disintegration and particle output. If considering a similar setting for a passive device, which was also described in the patent [6], such a high device resistance would not be acceptable. Taking only one capillary into account and assuming laminar flow (equation of Hagen-Poiseuille), an inspiration at 1.7 l/min over 2.3 min would be required to achieve the recommended pressure drop across the device of 4 kPa in combination with a suction volume of 4 l [17]. For a passive setup, the capillary must therefore have a much greater diameter and shorter length. The narrow capillaries contribute also to an acceleration of the air flow up to sonic velocity which was subsequently reduced at entering the vial. It finally impacted on the level of the cake surface at about 90 m/s. However, the cake was not compressed by the incoming air stream but was lifted up and broke apart into fragments, which swirled around the endings of the capillaries. Differences in the aerosolization behavior of different excipient formulations were identified. The produced particle aerosol had a velocity of 3 m/s at the exit of the mouthpiece, which is similar to pMDIs. Compared to capsule-based passive DPIs, the emission of larger particles is enhanced due to a larger cross-section and less wall adhesion. Only very fine particles (D (v, 0.5) of 3 µm) demonstrated a slightly increased ED as a result of superior flight properties.

The evaluation of the lyophilisate dispersion in the passive capsule based HandiHaler® demonstrated a possible disintegration for very soft lyophilisates like valine or lactose at a

concentration of 4 mg/ml. Nevertheless, the comminution process in the capsule was less effective compared to the air impact at high velocity of the active test system, resulting in a small FPF. In combination with the small metered dose, only small FPD were achieved.

5 REFERENCES

[1] N. Islam, E. Gladki, Dry powder inhalers (DPIs) - A review of device reliability and innovation, Int. J. Pharm., 360 (2008) 1-11.

[2] K. Wetterlin, Turbuhaler: A New Powder Inhaler for Administration of Drugs to the Airways, Pharm. Res., 5 (1988) 506-508.

[3] A.H. de Boer, D. Gjaltema, P. Hagedoorn, H.W. Frijlink, Comparative in vitro performance evaluation of the Novopulmon® 200 Novolizer® and Budesonid-ratiopharm® Jethaler: two novel budesonide dry powder inhalers, Pharmazie, 59 (2004) 692-699.

[4] I.J. Smith, M. Parry-Billings, The inhalers of the future? A review of dry powder devices on the market today, Pulm. Pharmacol. Ther., 16 (2003) 79-95.

[5] S. White, D.B. Bennett, S. Cheu, P.W. Conley, D.B. Guzek, S. Gray, J. Howard, R. Malcolmson, J.M. Parker, P. Roberts, N. Sadrzadeh, J.D. Schumacher, S. Seshadri, G.W. Sluggett, C.L. Stevenson, N.J. Harper, EXUBERA®: Pharmaceutical Development of a Novel Product for Pulmonary Delivery of Insulin, Diabetes Technol. Ther., 7 (2005) 896-906.

[6] C. Yamashita, A. Akagi, Y. Fukunaga, Dry powder inhalation system for transpulmonary administration, in: United States Patent 7735485 2010.

[7] G.H. Jirka, Einführung in die Hydromechanik, Universitätsverlag Karlsruhe, Karlsruhe, 2007

[8] D. Köhler, W. Fleischer, Theorie und Praxis der Inhalationstherapie, Arcis-Verlag, München, Germany, 2000.

[9] S.P. Newman, A Comparison of Lung Deposition Patterns Between Different Asthma Inhalers, J. Aerosol Med., 8 (1995) 21-27.

[10] S.P. Newman, K.P. Steed, S.J. Reader, G. Hooper, B. Zierenberg, Efficient delivery to the lungs of flunisolide aerosol from a new portable hand-held multidose nebulizer, J. Pharm. Sci., 85 (1996) 960-964.

[11] D. Hochrainer, H. Hölz, C. Kreher, L. Scaffidi, M. Spallek, H. Wachtel, Comparison of the Aerosol Velocity and Spray Duration of Respimat® Soft Mist™ Inhaler and Pressurized Metered Dose Inhalers, J. Aerosol Med., 18 (2005) 273-282.

[12] D.L. French, D.A. Edwards, R.W. Niven, The influence of formulation on emission, deaggregation and deposition of dry powders for inhalation, J. Aerosol Sci., 27 (1996) 769-783.

[13] J.H. Bell, P.S. Hartley, J.S.G. Cox, Dry powder aerosols I: A new powder inhalation device, J. Pharm. Sci., 60 (1971) 1559-1564.

[14] N.R. Labiris, M.B. Dolovich, Pulmonary drug delivery. Part I: Physiological factors affecting therapeutic effectiveness of aerosolized medications, Brit. J. Clin. Pharmaco., 56 (2003) 588-599.

[15] D.A. Edwards, A. Ben-Jebria, R. Langer, Recent advances in pulmonary drug delivery using large, porous inhaled particles, Journal of Applied Physiology, 85 (1998) 379-385.

[16] C. Weiler, Generierung leicht dispergierbarer Inhalationspulver mittels Sprühtrocknung, PhD Thesis, in, Johannes Gutenberg Universität Mainz, Germany, 2008.

[17] European Pharmacopoeia 7 Section 2.9.18 - Preparation for inhalation: aerodynamic assessment of fine particles, in, Council of Europe, Strasbourg, France, 2011.

Chapter 3

Evaluation of the Performance of the Test System

Abstract

During the last years, new technological ideas for dry powder inhalers were developed. A new concept is the creation of individual particles from a coherent bulk at the time of inhalation by disintegration of lyophilisates. The evaluation and characterization of the possible dispersion of lyophilisates by an air impact and the achievement of high fine particle fractions were the objectives of this study. In order to understand the aerosolization of lyophilisates, different formulations of amino acids and sugars were investigated. Besides the characterization of the different formulations by microscopy and x-ray diffractometry, the main focus was on the particle size distributions (PSD) of the dispersed particles. Thereby the geometric PSD was analyzed by laser diffraction, whereas the aerodynamic PSD was characterized by time of flight and Andersen cascade impactor analysis. The destruction of the porous structure of the lyophilisates resulted in large geometric particle sizes but aerodynamic particle sizes in the inhalable range with relatively large fine particle fractions (FPF) between 20 and 50% calculated as a percentage of the metered dose. Despite potential differences in freezing behavior and thus cake structure within lyophilization batches, reproducible fine particle fractions were attained. Overall, it could be concluded that the controlled disintegration of lyophilisates into inhalable particles by an air impact is possible and substantial FPF are achieved. Therefore, the method represents a promising new dry powder inhalation technology.

1 INTRODUCTION

Beside the local treatment of pulmonary diseases, a systemic delivery of therapeutic proteins by inhalation is of high commercial interest [1]. For their formulation, the proteins' limited physical and chemical stability pose additional challenges. Conventionally, the powders formulated for the use in dry powder inhalers (DPI) are produced by milling to micronize the drug or by spray drying [2, 3]. These powder production and formulation techniques have several disadvantages. Especially during milling the drug is exposed to high temperatures which can be a problem for thermolabile drugs. Micronization is also notorious for inducing electrostatic charges and generating amorphous domains on the particle surface [4]. Freeze-drying is a common method for stabilizing proteins and peptides. The result after a freeze-drying process is a cake in the size of the filling volume. For generation of an aerosol, the freeze-dried cake needs to be micronized for example by jet-milling to prepare fine particles. Additionally, spray drying or spray freeze drying are potential formulation methods to improve the stability and long term storage stability of these biological drugs. However, DPIs prepared by spray drying or freeze-drying-jet-milling method have been reported to cause partial deactivation of the peptides and proteins such as interferons [2].

A new DPI system initially introduced by Yamashita et al. [5], comprises a freeze-dried preparation which is aerosolized into inhalable particles by an air jet at the time of inhalation. The authors claim rather high fine particle fractions (FPF) of 10% or more, in some examples up to 81% related to delivered dose. Summarizing the advantages of this new system, it has a formulation process particularly suitable for thermolabile drugs like proteins and peptides and the manufacturing process is relatively simple, with extremely high accuracy at dose metering and high preparation yield as the formulation is metered as a liquid. On the other hand, the freeze-drying process could be a disadvantage concerning reproducibility and batch uniformity [6, 7]. Furthermore, freeze-drying is an energy intensive and time consuming manufacturing process [8].

The aim of this study was to verify the new concept of Yamashita et al. [5] of creating individual particles in an inhalable size range with high fine particle fraction from a coherent bulk by an air jet. To further understand the aerosolization behavior of the system, besides lyophilisate characteristics, the geometric and aerodynamic particle size distribution (PSD) of different placebo formulations were examined. In order to restrict influencing factors of the formulation, only placebo formulations containing a single excipient were used in this study.

2 MATERIALS AND METHODS

2.1 MATERIALS

Excipients used were: L-isoleucine (Ile) (Fluka Chemie GmbH, Buchs, Switzerland), L-phenylalanine (Phe) (Merck KGaA, Darmstadt, Germany), L-valine (Val) (Fagron GmbH&Co KG, Barsbüttel, Germany), lactose-monohydrate (Lac) (Fagron GmbH&Co. KG, Barsbüttel, Germany), D-mannitol (Man) (Riedel-de Haën, Seelze, Germany), trehalose (Tre) (Hayashibara Co Ltd, Okayama, Japan); dye for quantification was rhodamine B (Sigma-Aldrich, Chemie GmbH, Steinheim, Germany); filters used in Andersen cascade impactor analysis were type A/E glass fiber filters 76 mm (Pall Corporation, Ann Arbor, MI, USA)

2.2 FORMULATION PREPARATION

0.5 ml solutions containing 4 mg/ml of the excipient and 0.2 mg/ml rhodamine B were filled into 2R glass vials (Fiolax® clear, Schott AG, Müllheim, Germany) and vials were equipped with rubber stoppers (C1503, Stelmi, Villepinte, France). Freeze-drying was carried out in a laboratory scale freeze-drier (Lyostar II, FTS Systems, Stone Ridge, NY, USA). The samples were frozen at -1°C/min to -45°C. Primary drying was performed at a shelf temperature of -20°C and a pressure of 34 mtorr for 14 h. In the secondary drying step shelf temperature was increased to 30°C and the pressure was decreased to 8 mtorr for 6 h.

2.3 MICROSCOPY

The morphology of the lyo cakes was analyzed with a digital reflected light microscope (Keyence VHX-500F, Keyence Corporation, Osaka, Japan). The particle morphology of the dispersed particles was analyzed with a Jeol Scanning Electron Microscope (JSM-6500F, Jeol, Ebersberg, Germany). The samples were fixed with self-adhesive tape on aluminium stubs and were sputtered with carbon.

2.4 X-RAY DIFFRACTOMETRY (XRD)

The lyophilisates were investigated with a Seifert X-ray diffractometer XRD 3000 TT (Seifert, Ahrensburg, Germany). The samples were measured from 5 – 40° at a step rate of 2Θ=0.05° with 2 sec measuring time per step.

2.5 RESIDUAL MOISTURE CONTENT ANALYSIS

The residual moisture content of lyophilisates was determined by Karl-Fischer titration (Metrohm 756 KF Coulometer, Herisau, Switzerland) using Hydranal Coulomat AG (Riedel-de Haën, Seelze, Germany) as titration reagent. The lyophilisates were dissolved in 1.0 ml of anhydrous methanol (Hydranal-Methanol dry, Riedel-deHaën, Seelze, Germany), additionally dried with molecular sieve 3A (VWR International GmbH, Darmstadt, Germany), right in the production vials. As blanks, empty freeze-dried vials, similarly filled with 1.0 ml of dry methanol, were used. The injection volume was 500 µl each. The measurements were performed in triplicate.

2.6 DIFFERENTIAL SCANNING CALORIMETRY (DSC)

The DSC experiments were performed with 4 – 8 mg of freeze-dried sample sealed in aluminium pans (ME-26763) on a Mettler Toledo DSC821e (Mettler Toledo, Giessen, Germany). Phenylalanine samples were heated from 25°C to 295°C at 10°C/min.

2.7 PARTICLE SIZE DISTRIBUTION (PSD) ANALYSIS

2.7.1 Laser diffraction (LD) measurements

The geometric PSD was investigated with a Malvern Mastersizer X (Malvern Instruments Ltd, Worcestershire, England). A 300 mm lens with a measurement range of 0.5 to 600 µm was used. The size distribution was calculated using the Fraunhofer theory. The aerosol was sprayed into the laser beam using the output test system at a distance of approximately 5 cm and extracted by suction.

2.7.2 Time of flight (TOF) measurements

The aerodynamic PSD was determined with the API Aerosizer® LD (TSI Inc., Amherst, MA, USA) in combination with the Aero-Breather® for sample presentation. A 700 µm nozzle was used with a display range of 0.1 to 200 µm. The Aero-Breather® was operated at a breath rate of 39 l/min, a breath volume of 1 l with an acceleration of 19 l/s^2. For measurement, the aerosol was sprayed into the Aero-Breather® using the output test system.

2.7.3 Andersen cascade impactor (ACI) analysis

The aerodynamic PSD of the formulations was also evaluated using an Andersen cascade impactor (ACI) (8-Stage Non-Viable Sampler Series 20-800, Thermo Andersen, Smyrna, GA, USA). The ACI was operated at a flow rate of 39 l/min (corresponds to a pressure drop of 4 kPa with the HandiHaler®) with cut off diameters outlined in Table 1. The baffle plates were coated with a solution of 83% glycerin, 14% ethanol and 3% Brij 35. In 6.15 s a total air volume of 4 l passed through the impactor. During this time period, the aerosol was sprayed into the induction port. The amount of powder deposited on each stage of the impactor was determined by washing with water and rhodamine B quantification at 554 nm in an Agilent 8453 UV-Vis spectrophotometer (Agilent Technologies, Santa Clara, CA, USA). The FPF (= fraction of particles with an aerodynamic diameter below 4.94 µm) and the DD (dose that could be delivered to the ACI) were both calculated as percentage of the metered dose (nominal dose). A plot of the cumulative amount of powder deposited on each stage against the cut-off-diameter allowed calculation of the mass median aerodynamic diameter (MMAD) [9]. The total particle mass impacting below stage 1 equals to the FPF. By removing stages 2 to 7, the FPF is collected on the filter of the ACI. This configuration is called short stack ACI in this study. The filter solution was ultra centrifuged (Optima™ TLX Ultracentrifuge, Beckman Coulter, Brea, CA, USA) at 186000 g for 45 min before UV-Vis spectroscopic analysis. The comparability of the FPF measured with the normal eight-stage ACI and the short stack version was tested with a flow rate of 39 l/min using the HandiHaler® in an unpublished study showing no significant difference of the measured FPF.

All PSD measurements were performed in triplicate.

Table 1: Used cut off diameters for the ACI at flow rate of 39 l/min

Stage	Cut off diameter at 39 l/min
0	7.65
1	4.94
2	4.00
3	2.81
4	1.79
5	0.94
6	0.60
7	0.34

2.8 TAP DENSITY MEASUREMENT

The tap density measurements were performed using a 10 ml-graduated cylinder fixed in a jolting volumeter (STAV 2003, JEL Engelsmann AG, Ludwigshafen, Germany) and tapped 1250 times. Particles were generated by evacuation of the lyophilisate in the vial and stoppering of the vials (inside the freeze-dryer) at a pressure of <0.1 mtorr. Piercing a needle through the stopper of the vials caused quick ventilation and thereby destruction of the lyophilisate into small particles. The similarity of these particles and the particles generated by aerosolization with the output test system was verified by scanning electron microscopy (SEM). The measurements were performed in triplicate.

3 RESULTS AND DISCUSSION

3.1 PHYSICOCHEMICAL CHARACTERIZATION OF EXCIPIENT FORMULATIONS

In order to understand the impact of the lyophilisate characteristics on the aerosolization performance, the morphology of different placebo formulations was inspected with the reflected light microscope. The placebo formulations were single excipient formulations containing an amino acid (isoleucine, phenylalanine, valine) or a sugar (lactose, mannitol - knowing that mannitol is a sugar alcohol it is termed sugar in this study for the sake of simplicity - , trehalose) and were freeze-dried using a standard freeze-drying process with a cooling rate of -1°C/min. The lyophilisates had a porous comb like structure, with a skinny coating, covering the top of the cake. This is exemplarily shown for phenylalanine in Figure 1. An explanation for the feasible disintegration of the lyophilisate into inhalable particles is this highly porous structure with its filmy walls. The preparations have a very low mass density and feature big air filled cavities which enable easy penetration of the air into the whole cake and impact on the thin fragile wall structures.

Surface energy and adhesion/cohesion was considered less relevant for this system because the formulation is stored in a non-powdered form and the inhalable particles are generated at the time of inhalation.

For a better understanding of differences in the aerosolization behavior and fine particle output of different excipient formulations, the physical state of the formulations has to be

analyzed. The investigation of the lyophilisates by x-ray diffractometry demonstrated a crystalline structure for the isoleucine, valine and mannitol samples. The x-ray diffraction pattern of the freeze-dried mannitol sample showed the peak pattern of the δ-polymorph [10]. In contrast, the freeze-dried sugars lactose and trehalose were amorphous. For the freeze-dried phenylalanine sample the peaks reflected the monohydrate comparing the peak pattern with literature diffraction patterns [11]. The residual moisture analysis by Karl-Fischer titration indicated a content of phenylalanine monohydrate of approx. 50%. The existence of the hydrate could be confirmed by differential scanning calorimetry (DSC). Besides the melting endotherm of phenylalanine at 270°C, the DSC trace showed an endothermal event at 136°C, followed by an exothermal event at 146°C that was related to the crystallization of the anhydrous form of phenylalanine (data not shown). In a secondary reheating the thermal events at 136°C and 146°C did not occur. Phenylalanine exhibits pseudopolymorphism: it can exist as a monohydrate and in the anhydrous form. The transition point in water is at 37°C. The needle-shaped monohydrate is stable below, and the flake-shaped anhydrate above the transition point [11]. Thus it is not surprising that the phenylalanine solution crystallizes as the monohydrate during freeze-drying. Because the XRD pattern does not show any other peaks except those related to the monohydrate, and the moisture analysis indicated a phenylalanine monohydrate content of only 50%, the remaining 50% appeared to be present in the amorphous state.

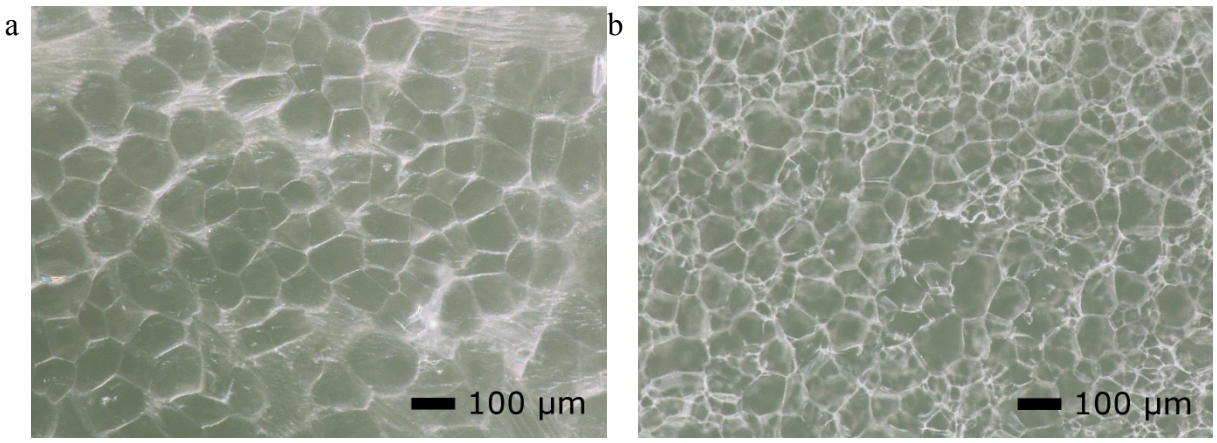

Figure 1: Morphology of the freeze-dried phenylalanine formulation: top of the cake (a) and bottom of the cake (b).

The different physical state of the formulations, being crystalline or amorphous, might have an effect on the stability and rigidity of the wall structures of the porous lyophilisates. This can furthermore influence the disintegration of the lyophilisates and the fine particle output which was analyzed in the following experiments. The physical state of the freeze-dried

excipients can also be important for stability issues. On the one hand, amorphous formulations are less stable against humidity as water has a plasticizing effect and amorphous regions can also change the physical state and crystallize during storage [12]. Considering incorporation of an active pharmaceutical ingredient, on the other hand, amorphous excipients might be favored e.g. for stabilizing proteins [13]. The following analysis of the PSD and the FPF of the different excipient formulations should give further information about the applicability of crystalline and amorphous formulations.

3.2 PSD OF DIFFERENT EXCIPIENT FORMULATIONS

The output test system was used to analyze the particle sizes which can be achieved by disintegration of the lyophilisates using the developed output system. In order to determine size and shape of the dispersed particles released from the output system, the particles were investigated with scanning electron microscopy (SEM). Specimens were prepared by collecting the aerosol leaving the output test system directly on a specimen stub. Particles observed were clearly separated from each other (Figure 2) having diameters between 5 µm and approximately 100 µm. Their shape appeared to reflect agglomerates of small fragments. During the disintegration process, the ordered pore structure of the lyophilisate was completely destroyed. Small fragments of the former pore walls formed these agglomerative particles, leading to a different morphology compared to the lyophilisates. The particles, however, still feature a highly porous structure and a low mass density.

Besides the agglomerative shape of all samples, particles of the various excipient formulations differed in shape. Phenylalanine particles had a netting structure formed by needles, whereas valine particles exhibited a platelet-like structure. A needle-shaped morphology has already been reported for phenylalanine monohydrate [11].

Using laser diffraction (LD) the geometric PSD was examined. The results of the PSD are outlined in Table 2. The distributions of the different excipient formulations were relatively broad. The particle sizes ranged from smaller than 1 µm to 100 µm and even larger as can be seen from Figure 3a. These particles are relatively large and rather unusual for pulmonary delivery. For non-spherical particles, such as plates and needles orientated randomly, the geometric volume diameter is typically overestimated because of the large projection diameter for these shapes [14]. This is certainly also the case for the non-spherical particles from this study. Furthermore, the PSD shown in Figure 3a is a volume distribution for which the calculation is based on the assumption that the particles measured are spherical. Nevertheless,

the microscopic pictures (Figure 2) of the dispersed particles confirmed that range of relatively large particles.

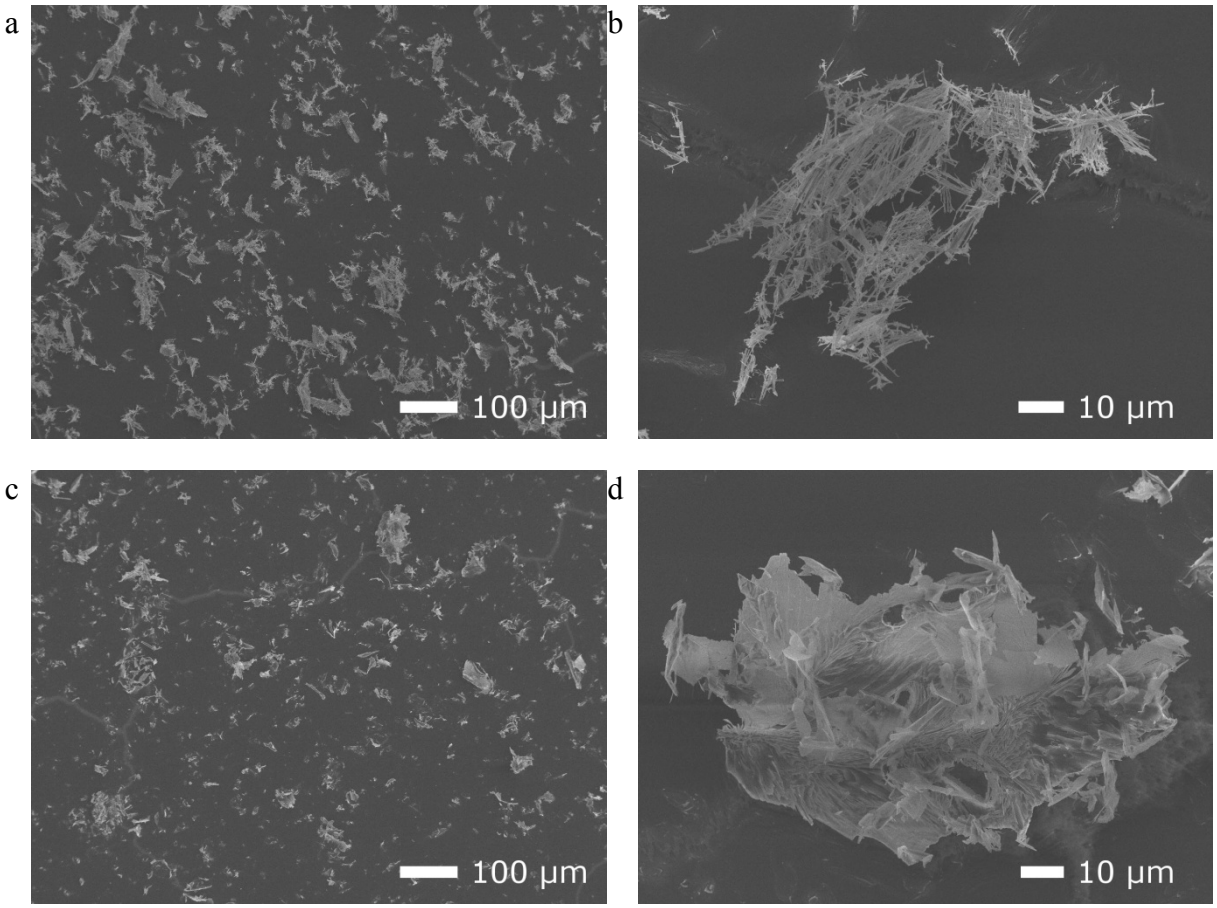

Figure 2: Scanning electron microscope pictures of dispersed particles of phenylalanine (a, c) and valine (b, d).

For evaluation of aerosols, the aerodynamic PSD is determining. Therefore the aerodynamic PSD was analyzed by time of flight (TOF) measurement with the Aerosizer®. The Aero-Breather®, which imitates the breath by moving a plunger, was used for sample presentation. The results of the PSD are outlined in Table 2 as well. The aerodynamic PSD was much narrower than the geometric PSD and shifted to smaller particle sizes (Figure 3b). It is also noticeable that the aerodynamic PSD of the amino acid formulations had a stronger relative variation compared to those of the geometric PSD. The FPF of the Aerosizer®, which corresponds to the analyzed amount of particles having an aerodynamic particle size <5 µm, differed between 51 and 100%. These results indicate the potential for very effective pulmonary delivery.

Table 2: The geometric and aerodynamic volume PSD (± S.D. n=3) of the different excipient formulations aerosolized with the standard output test system. The geometric PSD was measured by laser diffraction analysis, the aerodynamic PSD by time of flight analysis.

	D(v, 0.1) (µm)	D(v, 0.5) (µm)	D(v, 0.9) (µm)	≤ 5 µm (%)
Geometric PSD (by LD)				
Isoleucine	5.22 ± 0.11	20.49 ± 1.28	72.53 ± 8.15	10.06 ± 0.27
Phenylalanine	2.86 ± 0.13	15.81 ± 0.89	61.09 ± 5.61	20.57 ± 0.67
Valine	3.78 ± 0.28	14.44 ± 1.99	53.84 ± 8.91	16.35 ± 1.68
Lactose	3.23 ± 0.22	11.12 ± 0.64	41.16 ± 4.02	21.90 ± 0.76
Mannitol	3.10 ± 0.04	12.40 ± 0.42	57.51 ± 8.55	20.98 ± 0.23
Trehalose	3.04 ± 0.32	12.29 ± 1.43	61.68 ± 12.50	23.82 ± 2.85
	D(v, 0.1) (µm)	D(v, 0.5) (µm)	D(v, 0.9) (µm)	FPF rel. to DD (%)
Aerodynamic PSD (by TOF)				
Isoleucine	2.56 ± 0.07	3.64 ± 0.18	5.61 ± 0.68	83.64 ± 7.10
Phenylalanine	0.89 ± 0.03	1.58 ± 0.08	2.39 ± 0.19	99.92 ± 0.13
Valine	1.31 ± 0.05	2.73 ± 0.53	4.51 ± 0.22	96.96 ± 2.38
Lactose	20.8 ± 0.09	4.49 ± 0.05	7.82 ± 0.50	57.22 ± 0.67
Mannitol	2.09 ± 0.10	4.36 ± 0.27	7.49 ± 0.64	60.02 ± 4.20
Trehalose	2.40 ± 0.16	4.96 ± 0.37	7.63 ± 0.79	51.17 ± 6.60

Equation 1 is the simplified expression for Stokes aerodynamic diameter, widely used in aerosol literature:

$$d_A \cong d_V \sqrt{\frac{\rho}{\chi \rho_0}} \qquad (1)$$

Where d_A is the aerodynamic diameter, d_V is the volume-equivalent diameter, ρ_0 is the unit density of calibration spheres, ρ is the particle density and χ is the dynamic shape factor. A smaller aerodynamic particle size compared to the geometric particle size can thus be explained by a particle density smaller than 1 g/cm^3 or a large dynamic shape factor. Non-spherical particles have rather large shape factors. For a density of 1 g/cm^3, a sphere has a dynamic shape factor of 1, a fiber with a diameter of 3.56 µm and a length of 100 µm for example has a dynamic shape factor of 13.5 [15]. As the geometric and aerodynamic size of our dispersed particles differed to a great extent, the shape factor of our particles must be large and/or the particles must have a very low density. As the SEM pictures show, the particles consisted of fragments which are loosely agglomerated into particles, thus particle density should be very low. The tap density of the particles was measured as an estimate for

the particle density. For the valine particles e.g., a tap density of 0.009 g/cm^3 was measured. Using the obtained values for geometric and aerodynamic size (D(v,0.5)) as well as tap density in equation 1 renders a very small dynamic shape factor of 0.25. This indicates a high air resistance and deceleration resulting in good lung deposition. Vanbever et al [16] already reported on large porous particles for inhalation with tap densities between 0.04 and 0.6 g/cm^3.

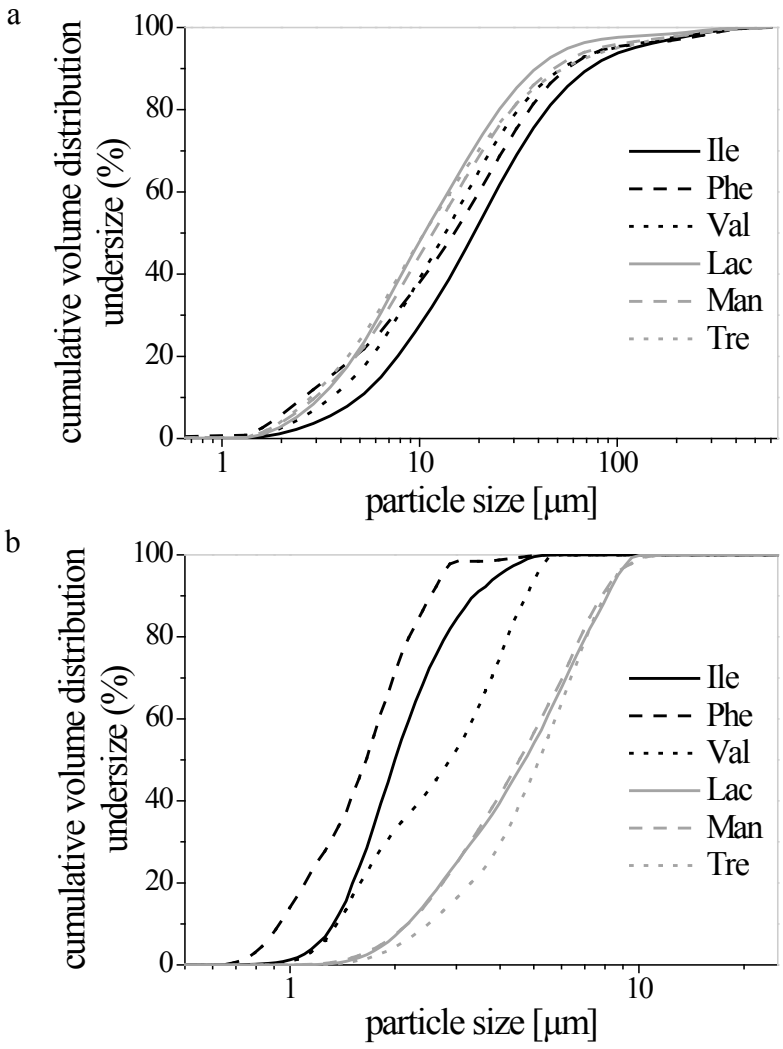

Figure 3: Cumulative geometric volume PSD of different excipient formulations investigated with LD (a) and TOF (b) measurements.

The aerodynamic PSD was also investigated using the ACI. Cascade impactor analysis is considered the most important and precise in vitro testing of aerosols. It is recommended by both the United States and the European pharmacopoeia. The detected FPF and DD of the different formulations are shown in Figure 4. Depending on the excipient, FPF between 20 and 50% calculated as a percentage of the metered dose (MD) could be determined. These

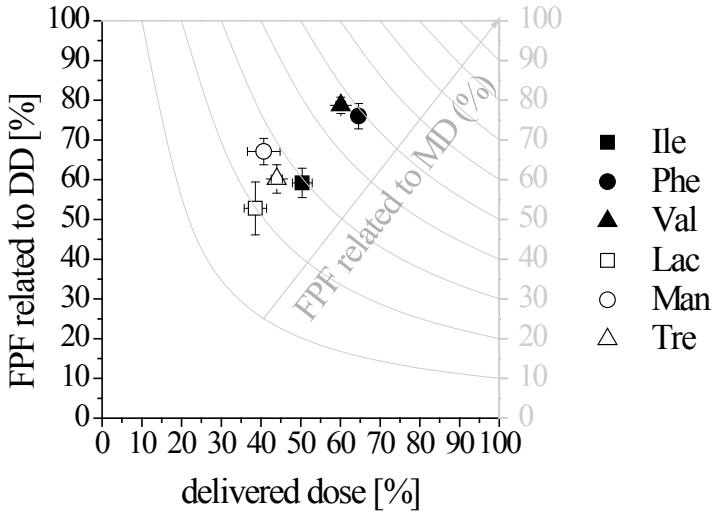

Figure 4: FPF related to DD as well as related to metered dose (MD) and DD of different excipient formulations investigated by short stack ACI analysis.

FPF are rather large compared to FPF of DPIs on the market which range from 9 to 36% [17, 18]. FPF related to DD ranged from 52 to 79%. These results are comparable to examples given by Yamashita et al. [19]. A novel DPI device described by Young et al. [20, 21], which also uses a pressurized gas (8 – 14 bar) for aerosolization of high powder loads of 120 mg, achieved lower mean FPF of 36% related to DD. The DD of the excipient formulations varied between 40 and 65%. Especially for the sugar formulation, this entails a major loss in the vessel and the mouthpiece (Figure 5). This has to be optimized in further studies. A MMAD of 3.2 µm was measured for the isoleucine and lactose formulation, and a MMAD of 3.1 µm for the mannitol formulation. These values are well below 5 µm, which is required for pulmonary delivery [22]. With a combination of SEM and ACI analysis it was possible to

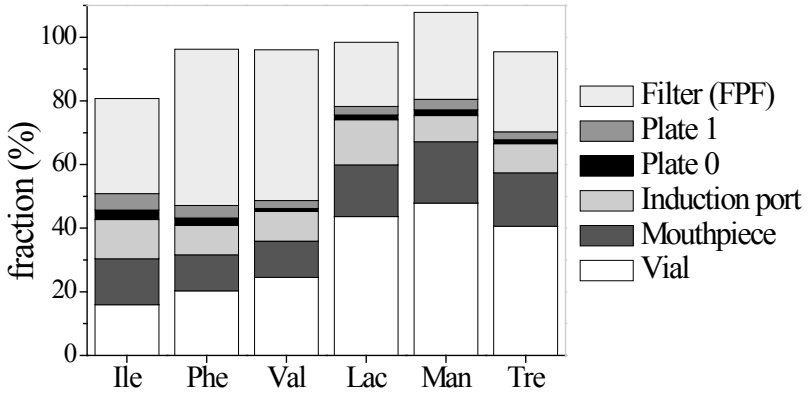

Figure 5: Fractions related to metered dose deposited on the different components of the short stack ACI.

measure the aerodynamic and geometric particle size of the same particle. Self-adhesive tapes for SEM were placed on each baffle plate of an eight stage ACI. Figure 6 shows the relation of the aerodynamic and the geometric size of dispersed isoleucine particles. It can be seen that large particles with mean diameters up to 100 µm are still in the respirable range with an aerodynamic size smaller than 5 µm. Therefore, the particle density must be very low.

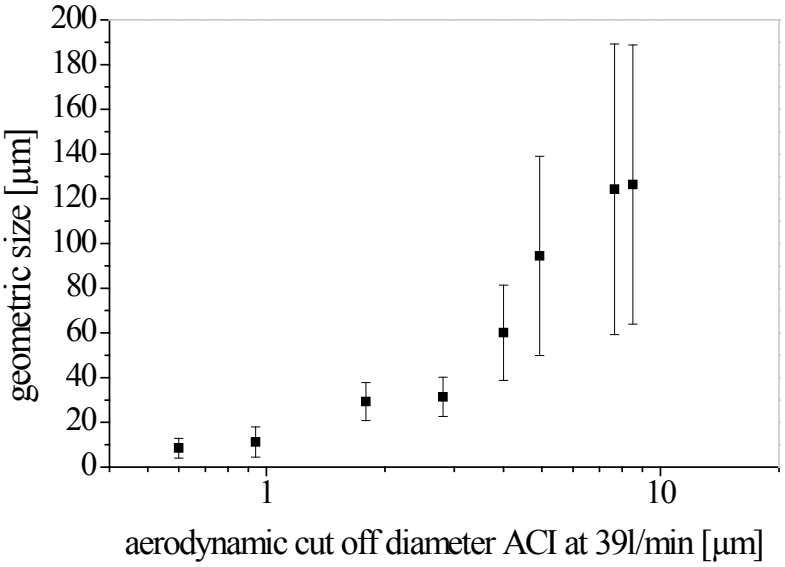

Figure 6: Relation between geometric and aerodynamic size of dispersed isoleucine particles analyzed with a combination of SEM and ACI.

By comparison of the two methods, TOF and ACI, it is noticeable that there is no significant difference in the FPF values for the sugar formulations. The FPF values of the amino acid formulations measured by TOF are overall greater compared to those measured by the ACI as can be seen from Figure 7. This poor agreement between TOF and ACI measured FPF was already reported by Vanbever et al. [16]. An explanation of this phenomenon may be found in the different analytical methods. The aerodynamic PSD measured by ACI is based on inertial impaction of the particles on coated plates comparable to the deposition mechanism in the upper human airways. Thereby bounce and blow-off at the stages and also wall or inter-stage losses may occur and bias the result [23]. Vanbever et al. [16], for example, assume that porous particles experience less lubrication-layer repulsion than small nonporous particles used for impactor calibration and are therefore overestimated. De Boer et al. [24] state in their critical evaluation of cascade impactor analysis that the aerodynamic diameter of irregular particles measured with an impactor is not necessarily the same as its equivalent diameter obtained from a sedimentation experiment, which yields the aerodynamic diameter by its definition. This is because there are different forces acting on a particle traveling between the

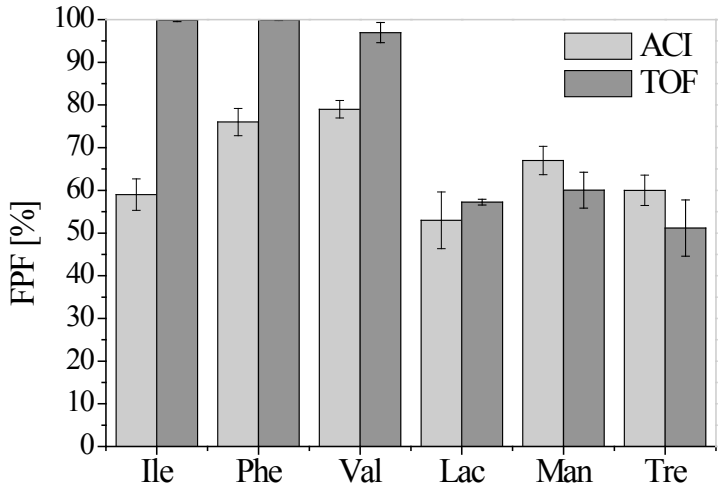

Figure 7: Comparison of the FPF of different excipient formulations measured by TOF and ACI analysis.

nozzle and the collection plate. The centrifugal force and the drag force are both not constant and additionally change their direction in contrast to the force of gravity. This results in a dynamic force system acting on the particle which reacts in a different way than during stationary settling. Irregular particles may start to rotate which affects in a different aerodynamic shape factor (χ) [24]. However, the magnitude of bias of the mentioned possible problems ought to be very small. Olsson et al. [25] i.e. reported total inter stage losses in an ACI of 1.6 – 3.5%. The Aerosizer®, in contrast, determines the aerodynamic particle size by measuring the time of particle flight. For transformation of the TOF data to an aerodynamic volume-weighted size distribution, the software uses the sample density and instrument calibration curves, assuming the particles to be spherical [26]. As the true particle density is not known, the material density was utilized for the TOF analysis in order to take differences between excipients into account. Furthermore, it has been reported that the Aerosizer® significantly undersizes non-spherical particles whereby the degree of size reduction is size-dependent. In the range between 7 and 19 µm, TOF results are 21 to 51% lower than the true aerodynamic diameter measured by sedimentation [27]. Potentially particle and material density were in better accordance for the sugar formulations as compared to the amino acid based formulations or the particles created from amino acid formulations are less spherical than the sugar based particles. Because the crystalline mannitol sample behaved similar to the other sugar formulations, which were amorphous, the physical state can not help explaining this phenomenon. Therefore most likely the differences could be explained by the unknown true density of the particles which is needed for the Aerosizer analysis. The Aerosizer® nevertheless can be used as a quick screening method for aerodynamic PSD.

As the freeze-drying process is known to have the problem of intra and inter-vial heterogeneity because of the stochastic nature of ice nucleation [6] as well as temperature gradients on the shelves and radiation from the wall [7], the reproducibility of the FPF is an important issue to analyze. Therefore all FPF analyses were performed in triplicate. The standard deviations of the FPF measured with the ACI and the Aerosizer® were both relatively small. For the FPF measured with the ACI and related to metered dose, the SD ranged from 1 to 4%. The SD of the FPF measured with the Aerosizer® ranged from 1 to 7% related to DD. Thus we can state that the FPF is robust against freeze-drying batch heterogeneity.

4 SUMMARY AND CONCLUSION

For dry powder formulations for inhalation it is of utmost importance that the particles generated can penetrate into the lung. Therefore the PSD produced by the novel inhalation system was analyzed by different methods considering geometric and aerodynamic PSD. The porous lyophilisates disintegrated into particles of large geometric size up to 100 µm and above. The aerodynamic size of these particles, however, was much smaller and a substantial fraction was in the respirable range of 1 – 5 µm due to low particle density. Overall, FPF of 20 – 50% calculated as a percentage of the metered dose could be determined by ACI measurements. Despite major losses in the vessel and the mouthpiece, these values were rather large compared to DPIs on the market. Fine Particle doses up to about 1 mg could be reached at relatively low DD of 40 – 65% which needs to be optimized in further studies. Differences in the aerosolization behavior of the different excipient formulations could be identified. Among the tested samples, the amino acid formulations of phenylalanine and valine performed best. The effect did not correlate with the physical state of being crystalline or amorphous and must therefore be caused by other material properties. Inhomogeneities in the structure of the lyophilisates were not identified to affect the reproducibility of the FPF of the different formulations. The standard deviations of the different samples measured in triplicate by ACI were relatively small between 1 and 4%. Therefore the aerosolization of the lyophilisates and its fine particle output was robust against freeze-drying batch heterogeneity in the investigated lab scale. Nevertheless, freeze-drying process parameters like freezing conditions can have an effect on the aerosolization of the lyophilisates and need to be analyzed in further studies. Overall, the disintegration and aerosolization of lyophilisates by an air impact is possible and a promising new concept for dry powder inhalation.

5 REFERENCES

[1] N.Y.K. Chew, H.-K. Chan, The Role of Particle Properties in Pharmaceutical Powder Inhalation Formulations, J. Aerosol Med., 15 (2002) 325-330.

[2] M.B. Chougule, B.K. Padhi, K.A. Jinturkar, A. Misra, Development of Dry Powder Inhalers, Recent. Pat. Drug Deliv. Formul., 1 (2007) 11-21.

[3] C. Parlati, P. Colombo, F. Buttini, P. Young, H. Adi, A. Ammit, D. Traini, Pulmonary Spray Dried Powders of Tobramycin Containing Sodium Stearate to Improve Aerosolization Efficiency, Pharm. Res., 26 (2009) 1084-1092.

[4] A. Chow, H. Tong, P. Chattopadhyay, B. Shekunov, Particle Engineering for Pulmonary Drug Delivery, Pharm. Res., 24 (2007) 411-437.

[5] C. Yamashita, A. Akagi, Y. Fukunaga, Dry powder inhalation system for transpulmonary administration, in: United States Patent 7735485 2010.

[6] J.A. Searles, J.F. Carpenter, T.W. Randolph, The ice nucleation temperature determines the primary drying rate of lyophilization for samples frozen on a temperature-controlled shelf, J. Pharm. Sci., 90 (2001) 860-871.

[7] A.A. Barresi, R. Pisano, V. Rasetto, D. Fissore, D.L. Marchisio, Model-Based Monitoring and Control of Industrial Freeze-Drying Processes: Effect of Batch Nonuniformity, Drying Technol., 28 (2010) 577-590.

[8] F. Franks, Freeze-drying of bioproducts: putting principles into practice, Eur. J. Pharm. Biopharm., 45 (1998) 221-229.

[9] European Pharmacopoeia 7 Section 2.9.18 - Preparation for inhalation: aerodynamic assessment of fine particles, in, Council of Europe, Strasbourg, France, 2011.

[10] A.I. Kim, M.J. Akers, S.L. Nail, The physical state of mannitol after freeze-drying: Effects of mannitol concentration, freezing rate, and a noncrystallizing cosolute, J. Pharm. Sci., 87 (1998) 931-935.

[11] R. Mohan, K.-K. Koo, C. Strege, A.S. Myerson, Effect of Additives on the Transformation Behavior of l-Phenylalanine in Aqueous Solution, Ind. Eng. Chem. Res., 40 (2001) 6111-6117.

[12] Y. Roos, M. Karel, Plasticizing Effect of Water on Thermal Behavior and Crystallization of Amorphous Food Models, J. Food Sci., 56 (1991) 38-43.

[13] K.-i. Izutsu, S. Kojima, Excipient crystallinity and its protein-structure-stabilizing effect during freeze-drying, J. Pharm. Pharmacol., 54 (2002) 1033-1039.

[14] B. Shekunov, P. Chattopadhyay, H. Tong, A. Chow, Particle Size Analysis in Pharmaceutics: Principles, Methods and Applications, Pharm. Res., 24 (2007) 203-227.

[15] K. Inthavong, J. Wen, Z. Tian, J. Tu, Numerical study of fibre deposition in a human nasal cavity, J. Aerosol Sci., 39 (2008) 253-265.

[16] R. Vanbever, J.D. Mintzes, J. Wang, J. Nice, D. Chen, R. Batycky, R. Langer, D.A. Edwards, Formulation and Physical Characterization of Large Porous Particles for Inhalation, Pharm. Res., 16 (1999) 1735-1742.

[17] B.J.B.J. O'Connor, The ideal inhaler: design and characteristics to improve outcomes, Respir. Med., 98 (2004) S10-S16.

[18] T.M. Crowder, J.A. Rosati, J.D. Schroeter, A.J. Hickey, T.B. Martonen, Fundamental Effects of Particle Morphology on Lung Delivery: Predictions of Stokes' Law and the Particular Relevance to Dry Powder Inhaler Formulation and Development, Pharm. Res., 19 (2002) 239-245.

[19] C. Yamashita, S. Ibaragi, Y. Fukunaga, A. Akagi, Dry powder inhalation system for transmulmonary administration, in: E.P. Office (Ed.), 2004.

[20] P.M. Young, J. Thompson, R. Price, D. Woodcock, K. Davies, The use of a novel handheld device to deliver high respirable fractions of high-dose dry powder active agents to the lung, J. Aerosol Med., 16 (2003) 192.

[21] P.M. Young, J. Thompson, D. Woodcock, M. Aydin, R. Price, The Development of a Novel High-Dose Pressurized Aerosol Dry-Powder Device (PADD) for the Delivery of Pumactant for Inhalation Therapy, J. Aerosol Med., 17 (2004) 123-128.

[22] S.P. Newman, S.W. Clarke, Therapeutic aerosols 1- physical and practical considerations, Thorax, 38 (1983) 881-886.

[23] J.P. Mitchell, M.W. Nagel, Cascade Impactors for the Size Characterization of Aerosols from Medical Inhalers: Their Uses and Limitations, J. Aerosol Med., 16 (2003) 341-377.

[24] A.H. de Boer, D. Gjaltema, P. Hagedoorn, H.W. Frijlink, Characterization of inhalation aerosols: a critical evaluation of cascade impactor analysis and laser diffraction technique, Int. J. Pharm., 249 (2002) 219-231.

[25] B. Olsson, L. Asking, M. Johansson, Choosing a cascade impactor, in: R.N. Dalby, P.R. Byron, S.J. Farr (Eds.) Respiratory Drug Delivery VI, Interpharm Press, Buffalo Grove, IL, 1998, pp. 133-138.

[26] J.P. Mitchell, M.W. Nagel, Time-of-Flight Aerodynamic Particle Sizer Analyzers: Their Use and Limitations for the Evaluation of Medical Aerosols, J. Aerosol Med., 12 (1999) 217-240.

[27] Y.S. Cheng, E.B. Barr, I.A. Marshall, J.P. Mitchell, Calibration and performance of an API Aerosizer, J. Aerosol Sci., 24 (1993) 501-514.

Chapter 4

Optimization of the FPD by Increase of the Solution Concentration and the Fill Volume

Abstract

There is a growing interest in the pulmonary administration of larger powder quantities, which would enable the treatment with high dosed drugs e.g. antibiotics. The aim of this study was to investigate the suitability of the lyophilisate based dry powder inhalation system for the delivery of high powder doses. This was to be achieved by elevation of the metered dose by varying the solution concentration and the fill volume of valine and cromolyn sodium lyophilisates. An increase in dose could be achieved by a controlled increase in the solution concentration at a low fill volume, whereas an increased fill volume as well as a substantially increased concentration resulted in a drastic decrease of the fine particle output. This latter negative impact was a consequence of impaired disintegration on the one hand due to increased cake hardness at elevated solution concentration. On the other hand, a higher fill volume resulted in reduced milling efficiency of softer cakes, whereas for harder cakes the product movement was reduced as less free space was available. The maximum fine particle dose (FPD) achieved was 1.2 mg for valine lyophilisates and 2.6 mg for cromolyn sodium lyophilisates. An increased pressure of the air used for dispersion resulted only in an increased emitted dose for the highest fill volume of 2 ml but did not further enhance the FPD of cromolyn sodium lyophilisates in 2R vials. However, utilization of a larger container in combination with an adapted amount of compressed air rendered a FPD of 3.7 mg cromolyn sodium in a single shot and is considered as a promising approach to deliver high drug doses to the lung.

1 INTRODUCTION

Currently marketed dry powder inhalers (DPI) mostly contain relatively low doses of drugs like anticholinergics, beta-2-agonists or glucocorticoids, ranging from 6 to 500 µg [1]. However, in the case of less potent drugs DPIs with e.g. 20 mg cromolyn sodium [2], 28 mg tobramycin [3] or 40 mg mannitol for asthma diagnosis [4] are used and there is a growing interest in the pulmonary administration of higher doses [5]. Some traditional dry powder formulations consist of micronized drug blended with larger lactose carrier particles to enhance flow and re-dispersibility [6]. The high percentage of carrier to drug particle ratios of typically 67.5:1 (w/w) [7] and the moderate lung delivery efficiencies limit the maximally delivered lung dose with these mixtures to just a few milligrams per inhalation [8]. This was for example illustrated for gentamicin in a study, where 32 inhalations were necessary for the delivery of a therapeutic dose because of only 1.9 mg fine particle dose (FPD) per inhalation [9]. To overcome the poor delivery efficiency of DPIs, de Boer et al. [5] developed the DPI Twincer® which was designed for effective de-agglomeration of high powder doses up to 25 mg of pure drug. Young et al. [10] introduced an active device utilizing pressurized gas for aerosolization and delivery 20-250 mg of highly cohesive pumactant powder and in vitro studies showed fine particle fractions (FPF) of >30% (~30 mg FPD) when loaded doses of 120 mg were delivered using 8–14 bar aerosolization pressures. A new dry powder inhalation system based on dispersion of lyophilisates which was initially introduced by Yamashita et al. [11] and developed further within this thesis (see Chapter 2 for details) also comprises an active test system utilizing compressed air for aerosolization and delivery of fine particles. The aim of this study was to investigate the suitability of this technology for the delivery of high powder doses. Possible approaches to increase the FPD of such a lyophilisate based DPI system were the elevation of the metered dose (MD) by varying the solution concentration and the fill volume of valine and cromolyn sodium lyophilisates. In a second attempt the influence of increased pressure of the compressed air used for dispersion was tested to further increase the FPD. Additionally, a bigger container holding the freeze-dried formulation was evaluated. Finally, the FPD achieved for the model drug cromolyn sodium were compared to commercial products.

2 MATERIALS AND METHODS

2.1 MATERIALS

L-valine and cromolyn sodium were purchased from Fagron GmbH&Co KG (Barsbüttel, Germany). Solutions were prepared with highly purified water (Purelab Plus, Elga LabWater, Celle, Germany). The commercial product Lomudal® cromolyn sodium Inhalatiepoeder 20 mg (Lot No. 0060K, Sanofi-Aventis Netherlands B.V., Gouda) was used for comparison.

2.2 FORMULATION PREPARATION

0.5 to 2 ml aqueous solutions of 6 – 36 mg/ml valine or 12 – 28 mg/ml cromolyn sodium were filled into 2R glass vials (Fiolax® clear, Schott AG, Müllheim, Germany) equipped with rubber stoppers (1079-PH 701/40/ow/wine-red, West Pharmaceutical Services, Eschweiler, Germany). Freeze-drying was carried out in a laboratory scale freeze-drier (Lyostar II, FTS Systems, Stone Ridge, NY, USA). The samples were frozen at -1°C/min to -45°C for 2 h including two 30 min holding steps at +5°C and -5°C for temperature equilibration across the high fill depth. Primary drying was performed at a shelf temperature of -15°C (shelfs were ramped at +0.2°C/min) and a pressure of 100 mtorr for 30 h. For secondary drying the shelf temperature was increased to +30°C at a ramp rate of +0.1°C/min for 10 h. Additionally, 0.5 to 3 ml aqueous solutions of 12 mg/ml cromolyn sodium were filled into 6R glass vials (Fiolax® clear, Schott AG, Müllheim, Germany) equipped with rubber stoppers (1319 PH 4023/50, gray, 20 mm, West Pharmaceutical Services, Eschweiler, Germany) and freeze-dried as mentioned above.

2.3 FPF ANALYSIS

The formulations were aerosolized using a custom design inhaler (see chapter 2 for details) with the standard setting of 20 ml compressed air at a pressure of 3 bar, 0.75 mm of inlet and outlet capillary diameter and a capillary position of 5 mm below the stopper for 0.5 to 1.5 ml lyophilisates or right below the stopper for 2 ml lyophilisates. The FPF was measured using a short stack version of the Andersen Cascade Impactor (8-Stage Non-Viable Sampler Series 20-800, Thermo Andersen, Smyrna, GA, USA) at a flow rate of 39 l/min (corresponds to a pressure drop of 4 kPa with the HandiHaler®). Baffle plates were coated with a solution of 83% glycerin (AppliChem GmbH, Darmstadt, Germany), 14% ethanol (central supply LMU, Munich, Germany) and 3% Brij 35 (Serva Electrophoresis GmbH, Heidelberg, Germany).

Filters used were type A/E glass fiber filters 76 mm (Pall Corporation, Ann Arbor, MI, USA). By removing stages 2 to 7, the whole FPF (particle fraction <4.94 µm) is collected on the filter directly below stage 1 and can easily be quantified by weighing the filter before and after powder deposition. The resulting amount of powder is the FPD. The emitted dose (ED) was measured by weighing the vial before and after aerosolization and calculated as the percentage of the MD. The FPF was calculated either as the percentage of the MD or of the ED. The measurements were performed in triplicate.

2.4 MECHANICAL TESTING

The mechanical properties of the lyophilisates were investigated using a Texture Analyzer (TA.XT.plus, Stable micro Systems, Godalming, UK) equipped with a 5 kg load cell and a cylindrical stainless steel probe with a diameter of 5 mm at a test speed of 1 mm/s and a maximal immersion into the lyophilisate of 2 mm for 0.5 ml fill volume or 5 mm for 1-2 ml fill volume. The resulting immersion-force curve demonstrated steady fracture at a constant force visible as a horizontal plateau. For comparison of different formulations, the measured data points of the plateau were averaged. The obtained force value represents the force necessary to fracture the lyophilisate. At the end of the immersion, the probe touches the bottom of the vial which results in a steep increase of the immersion force curve and can therefore be disregarded.

2.5 HIGH SPEED CAMERA RECORDING

The aerosolization behavior of the lyophilisates in the vial was recorded using a Fastcam 1024 PCI (Photron, San Diego, CA, USA) with a sample rate of 1000 fps.

3 RESULTS AND DISCUSSION

3.1 OPTIMIZATION OF THE FPD OF VALINE LYOPHILISATES

In order to enhance the FPD of the inhalation systems based on dispersion of lyophilisates, the MD was elevated. Therefore, lyophilisates with increasing solution concentrations from 6 mg/ml to 36 mg/ml valine and increasing fill volume from 0.5 ml to 2 ml were prepared and the aerosolization performance was tested. Figure 1a shows the FPF related to MD of the different formulations. The FPF decreased drastically with increasing solution concentration

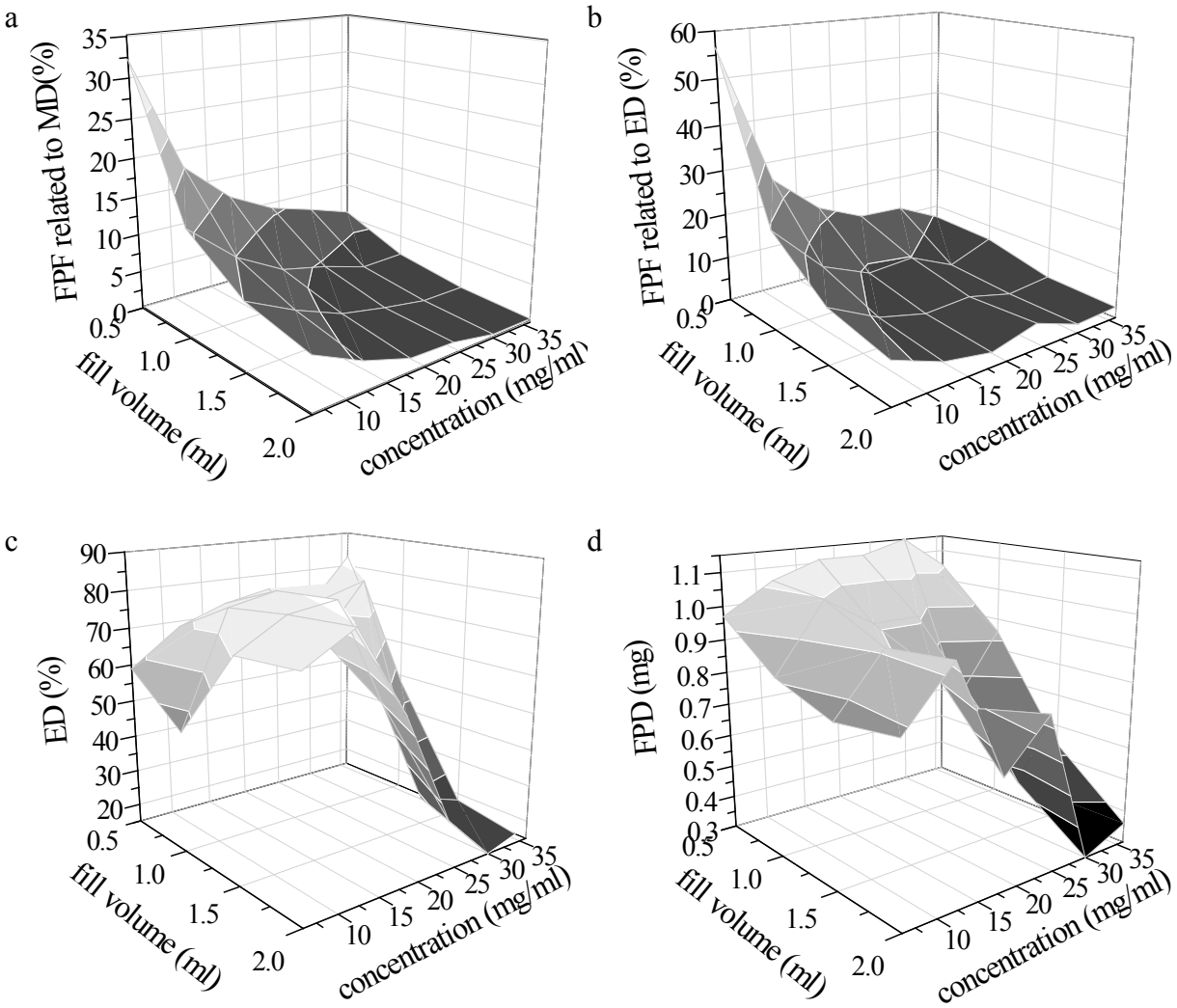

Figure 1: Effect of elevated MD by increased fill volume and concentration on the FPF related to MD (a), on FPF related to ED (b) as well as on ED (c) and the consequently resulting FPD (d) for valine lyophilisates.

as well as with increasing fill volume. Similar to an increased drug concentration for metered dose inhalers reported in [8], the increased loading resulted in a significantly decreased delivery efficiency. This led to the question whether the decrease in FPF is a result of a less effective disintegration into larger particles or a decreased output from the vial. In Figure 1b the FPF related to ED of the different formulations is plotted against the fill volume and the concentration. The graph similarly demonstrates a dramatic decrease of the FPF at increasing solution concentration and at increasing fill volume. The ED, as can be seen from Figure 1c, markedly decreased only for combinations of fill volume and concentration, starting at 18 mg/ml, 24 mg/ml and 36 mg/ml for fill volumes of 2, 1.5 and 1 ml, respectively. For these samples, a residual piece of cake was observed in the vial after the active disintegration process. The decrease in FPF could therefore be mainly referred to an impaired disintegration.

With respect to FPD, the increased initial loading at higher concentration or fill volume partially compensated for the reduced FPF as can be seen from Figure 1d. The maximum FPD of 1.2 mg was obtained at 30 mg/ml/0.5 ml. Thus, a dose increase could be achieved by increasing the solution concentration at a low fill volume. However, due to the rather low FPF of 7.7%, the loss in dose is substantial and, particularly when considering expensive drugs, possibly not economical.

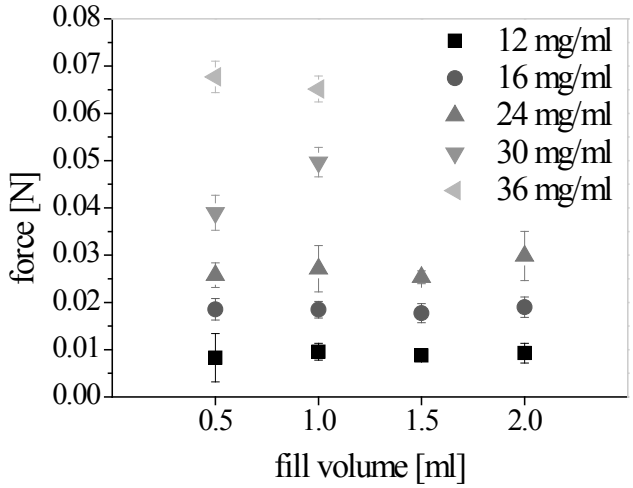

Figure 2: Mechanical testing of valine lyophilisates at varying concentration and fill volume. The shown force is the average value of the immersion-force-curve plateau and represents the force necessary to fracture the lyophilisate.

Obviously, the impact of the compressed air was not able to adequately break up lyophilisates of elevated fill volume and concentration. In order to gain insights into the mechanical properties of the different formulations, texture analyzer measurements were performed. The mechanical testing revealed that a higher force was necessary for fracturing the lyophilisates with increasing concentration as can be seen from Figure 2. As a consequence, the impact force of the compressed air on the lyophilisate becomes insufficient for adequate comminution of the harder cakes into fine particles at higher initial solution concentration. In contrast, the force necessary for fracturing the lyophilisate was independent of the fill volume and the cake hardness can therefore not explain the disintegration problems for lyophilisates of higher fill volume. To further elucidate the disintegration and aerosolization behavior of the lyophilisates at the lower concentration of 8 mg/ml, high speed camera recordings were performed. For the lowest fill volume of 0.5 ml (Figure 3a), the cake was lifted up in a rotational movement and was subsequently disintegrated in the impacting air stream. The fragments swirled in the upper part of the vial around the endings of the capillaries until they

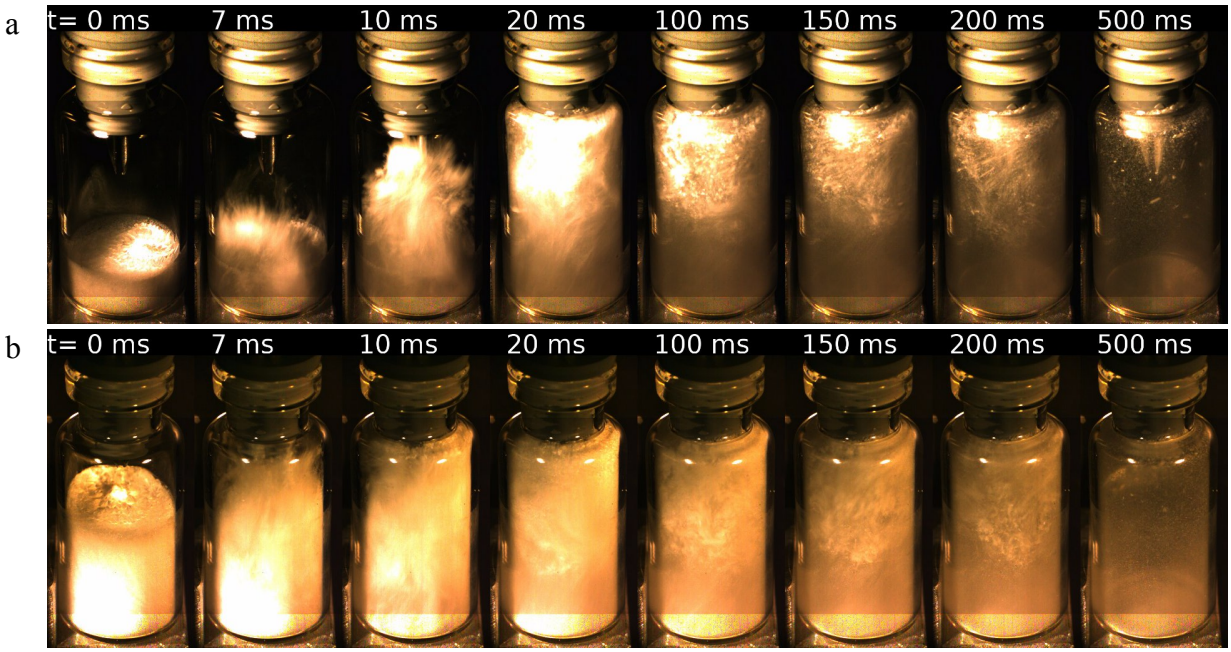

Figure 3: Aerosolization behavior of 8 mg/ml valine lyophilisates at 0.5 ml (a) and 2 ml (b) fill volume visualized with high speed camera recordings at 1000 fps.

left the vial through the outlet capillary. Lyophilisates at higher fill volume were also lifted up and disintegrated into particulate fragments. Because of an instantaneous and complete disintegration of the lyophilisates, larger lyophilisates result in a higher number of free swirling particles inside the vial. For a fill volume of 2 ml, a part of these particles initially accumulated right below the stopper in a waiting position as can be seen from Figure 3b (20 ms). Later, after enough particles had left the vial, these accumulated particles re-entered the swirling air flow. Probably, the amount of particles in the swirling air flow also affects the comminution into fine inhalable particles. The disintegration process of the lyophilisate by the swirling air flow is comparable to the jet-milling process. The particles to be pulverized are accelerated by pressurized gas whereby the grinding effect is produced either by interparticle collision or by impact against solid surfaces [12]. Thereby an important variable is the amount of particles inside the mill chamber because the frequency and intensity of collisions determines the grinding efficiency [13]. An increase of the feed rate and therefore an increased particle amount leads to a coarser product [14]. Not every particle in the mill will break upon colliding with another particle or with the wall, the kinetic energy of the collision has to be taken into account [13]. A high number of particles cause more frequent collision whereupon the kinetic energy of these particles is reduced resulting in less impact velocity at following collisions. This probably can explain the less effective size reduction of the fragmented lyophilisate to inhalable fine particles at higher fill volume.

3.2 OPTIMIZATION OF THE FPD OF CROMOLYN SODIUM LYOPHILISATES AND COMPARISON TO A HIGH DOSE MARKET PRODUCT

Options for enhancing the FPD of the lyophilisate based DPI system were also evaluated for the model drug cromolyn sodium. The MD was raised by increasing the initial solution concentrations from 12 to 28 mg/ml cromolyn sodium, and the fill volume from 0.5 to 2 ml.

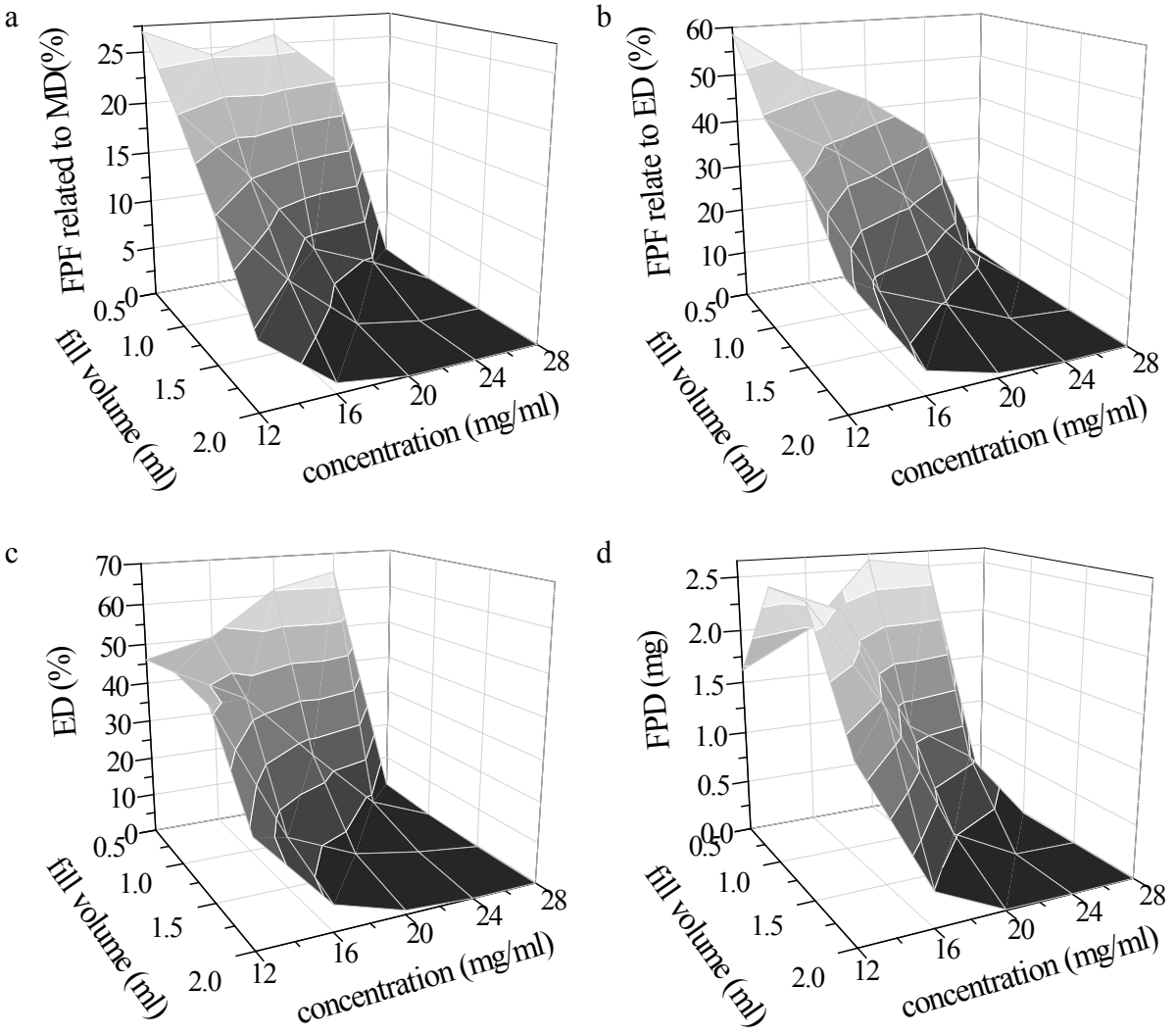

Figure 4: Effect of elevated MD by increased fill volume and concentration on the FPF related to MD (a), on FPF related to ED (b) as well as on ED (c) and the consequently resulting FPD (d) for cromolyn sodium lyophilisates.

Similar to valine lyophilisates, the FPF related to MD (Figure 4a) dropped with increasing fill volume and in particular with increasing solution concentration from 24 mg/ml on. The decrease in FPF must be also a result of a hindered cake disintegration because FPF related to ED (Figure 4b) demonstrated similar to valine lyophilisates a strong decrease with increasing concentration as well as with increasing fill volume. The ED in contrast increased with

increasing concentration at a fill volume of 0.5 ml until a concentration of 24 mg/ml but strongly decreased at elevated fill volume as can be seen from Figure 4c. Probably a higher loading dose is necessary to compensate for the loss due to particle accumulation at the top of the vial and in the cavity of the lyophilization stopper. The maximum FPD of approx. 2.6 mg was obtained with a concentration of 20 mg/ml and a fill volume of 0.5 ml. As already observed for valine, a dose increase could be best achieved by increasing the solution concentration at a low fill volume (Figure 4d). There appears to be a critical limit of dispersibility between 24 and 28 mg/ml of cromolyn sodium because 28 mg/ml showed a drastic decrease of ED and FPF already for the 0.5 ml lyophilisate.

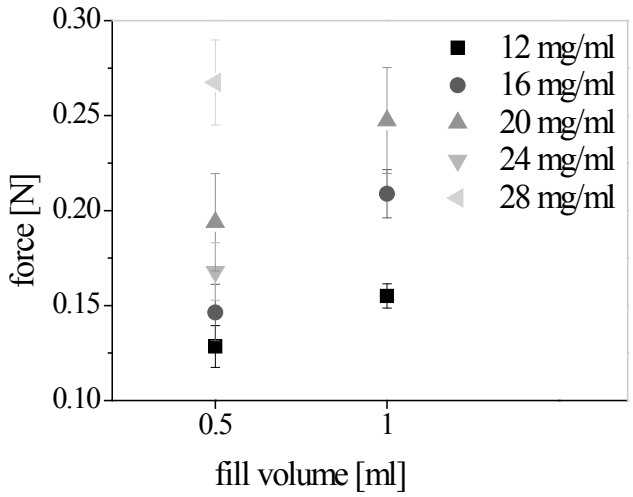

Figure 5: Mechanical testing of cromolyn sodium lyophilisates at varying concentration and fill volume. The shown force is the average value of the immersion-force-curve plateau and represents the force necessary to fracture the lyophilisate.

Mechanical testing revealed that higher forces are necessary for fracturing the lyophilisate of elevated concentration and fill volume as can be seen from Figure 5. It is noticeable, that the plateau indicating the force necessary for fracturing was attained later during the immersion process for lyophilisates of 1 ml fill volume compared to 0.5 ml. For fill volumes of 1.5 and 2 ml, the plateau was not reached within the tested 5 mm of immersion, but the immersion-force-curve steadily raised (Figure 6). The steady slope of the curve indicates a more elastic behavior of the lyophilisates at elevated fill volume where initially mainly compression takes place instead of steady fracture. This less brittle behavior of lyophilisates at elevated fill volume and their harder structure can possibly explain the inferior disintegration into fine particles. Approximately at 0.27 N, a critical hardness limit was reached for which disintegration by the impacting air stream was not possible anymore. Comparing the hardness

of valine and cromolyn sodium lyophilisates, it is important to note that valine lyophilisates were more than ten times softer and exhibited a less elastic lyophilisate structure. This could be the reason for a mostly complete disintegration of valine lyophilisates in contrast to only partly disintegration of cromolyn sodium lyophilisates until a critical hardness limit for disintegration. Beside already identified differences in the aerosolization behavior and fine particle output of different excipient formulations (see chapter 2 and 3 for details), the hardness of a lyophilisate is also dependent on the freeze-dried material properties which again affects the dispersibility.

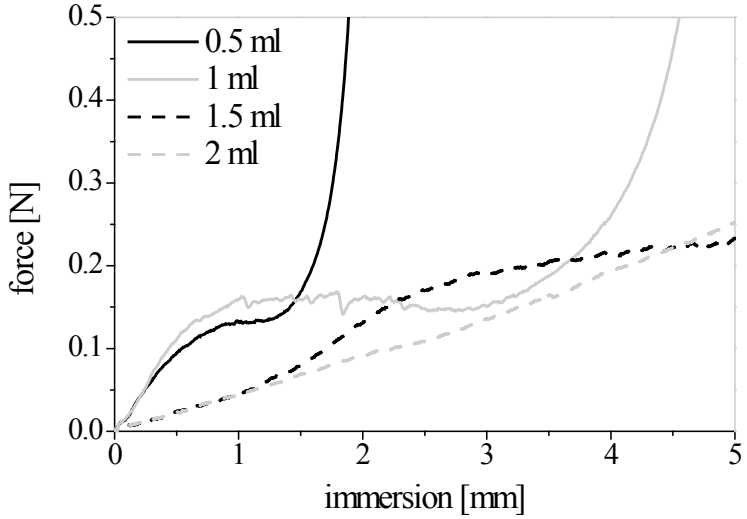

Figure 6: Immersion-force-curves of 12 mg/ml cromolyn sodium lyophilisates at varying fill volume.

Visualization of the disintegration process for 12 mg/ml cromolyn sodium lyophilisates by high speed camera recording revealed that it is of utmost importance that the lyophilisate can rotate in the vial for a good disintegration or that it is at least fractured into smaller pieces which can rotate in the vial. Large lyophilisates of 2 ml (Figure 7b) for example were not able to perform rotational movements and were not fractured into smaller pieces. In contrast, the whole cake was lifted up remaining more or less stationary at the top of the vial for a few milliseconds. At the end of the disintegration process, a substantial piece of the cake remained in the vial resulting in a low ED. In contrast, valine lyophilisates at low and high fill volume were also lifted up but subsequently disintegrated into fragments even if no rotational movement was possible. Furthermore, the complete disintegration process occurred within the first milliseconds whereas the cromolyn sodium lyophilisates were fractured into pieces rotating at the bottom of the vial while fine particles were scaled off (Figure 7a). Therefore, a possibly hindered comminution process due to a high number of fragments in the swirling air

flow was probably less important for cromolyn sodium lyophilisates. Nevertheless, the hindered disintegration indicated by the decrease in FPF related to ED was most likely attributed to the increased hardness.

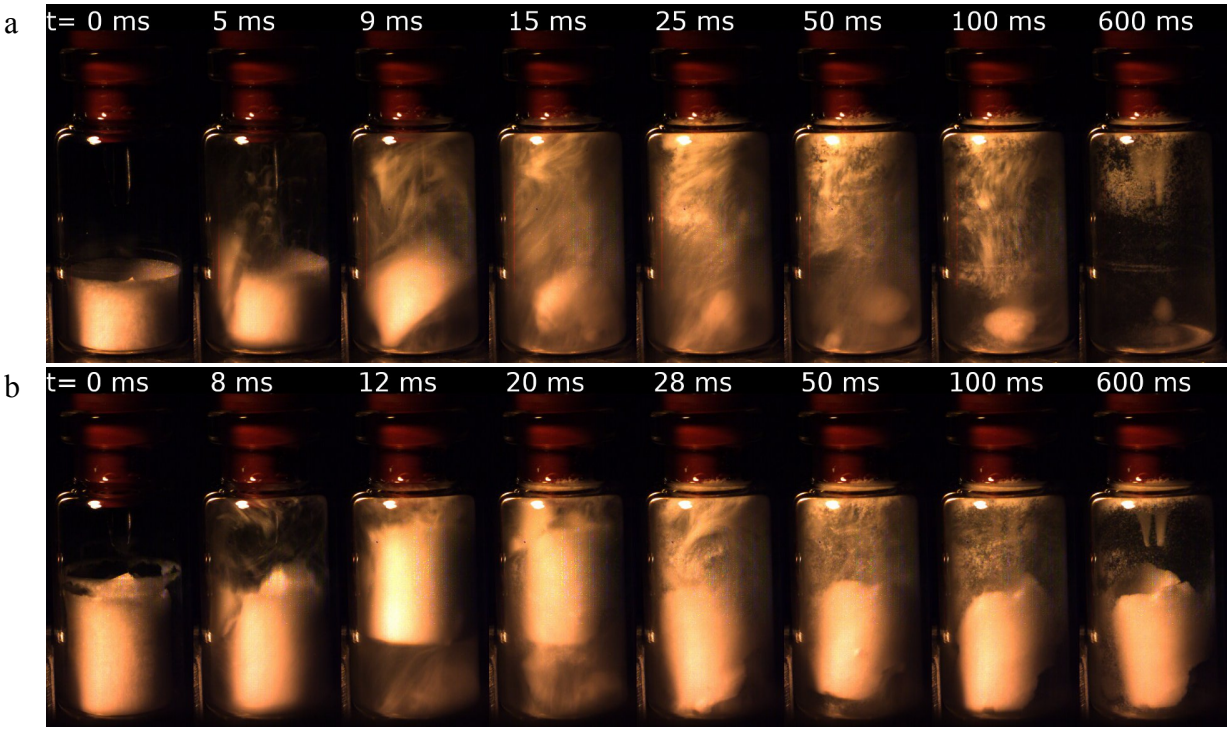

Figure 7: Aerosolization behavior of 12 mg/ml cromolyn sodium lyophilisates at 1 ml (a) and 2 ml (b) fill volume visualized with high speed camera recordings at 1000 fps.

This led to the question whether an increased pressure of 4 bar for dispersion compared to standard 3 bar can result in improved disintegration and elevated ED and FPF. Figure 8 shows the FPF related to MD of 12 mg/ml lyophilisates. A significant difference was only detectable for a fill volume of 2 ml where the FPF related to MD doubled from 6.2% to 12.4% for 3 and 4 bar pressure. The plot also clearly demonstrates that the FPF related to ED remained the same for all fill volumes. The increased FPF related to MD of the 2 ml-formulation was therefore only due to the enormous increase of the ED from 24.8% to 54.0%. An increased pressure for dispersion consequently resulted in an elevated output from the vial but not in an enhanced comminution process into finer particles. Therefore, an increased pressure for dispersion showed no benefit. Since the poorer disintegration of formulations with a high fill volume appeared to be the consequence of insufficient vial volume, freeze-dried formulations of various fill volumes were prepared in 6R vials, thus doubling the container volume, in order to further enhance the FPD. A fill volume of 2 ml in a 6R vial has about the same fill depth than a fill volume of 1 ml in a 2R vial. As can be seen from Figure 9, small fill volumes demonstrated less fine particle output compared to the normal 2R vials when disintegrated at

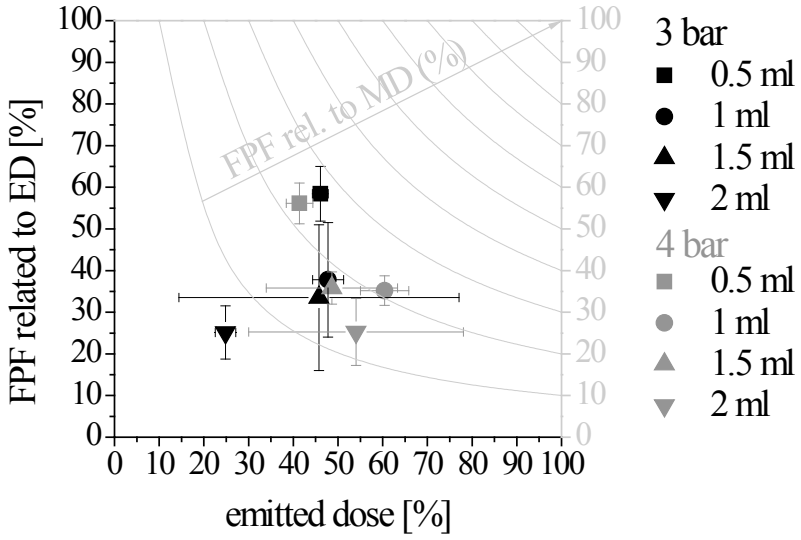

Figure 8: ED and FPF related to ED as well as FPF related to MD of 12 mg/ml cromolyn sodium lyophilisates aerosolized using 3 and 4 bar compressed air pressure for dispersion.

the standard test system settings. An elevated FPD compared to the same fill volume in a 2R vial was only achieved for the highest fill volume of 2 ml. This increase was a result of an improved comminution into fine particles because the FPF related to ED increased from 25% to 35% whereas the ED remained about the same. Figure 10a demonstrates the disintegration process in the larger 6R vial. The cake was lifted up and broke apart during a first rotation. The resulting pieces rotated at the bottom of the vial while particles were scaled off. This confirms the above statement that enough space for rotational movements of the cake is

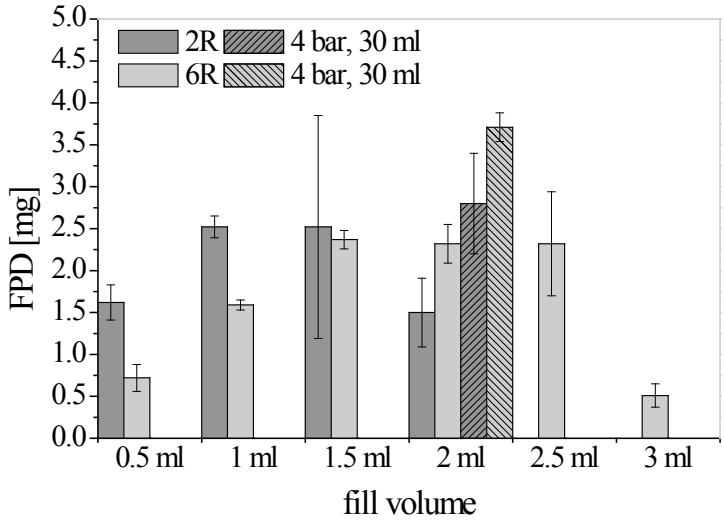

Figure 9: FPD of 12 mg/ml cromolyn sodium lyophilisates aerosolized from 2R or 6R vials applying the standard setting of 20 ml compressed air at 3 bar or an increased amount of compressed air with 30 ml at 4 bar.

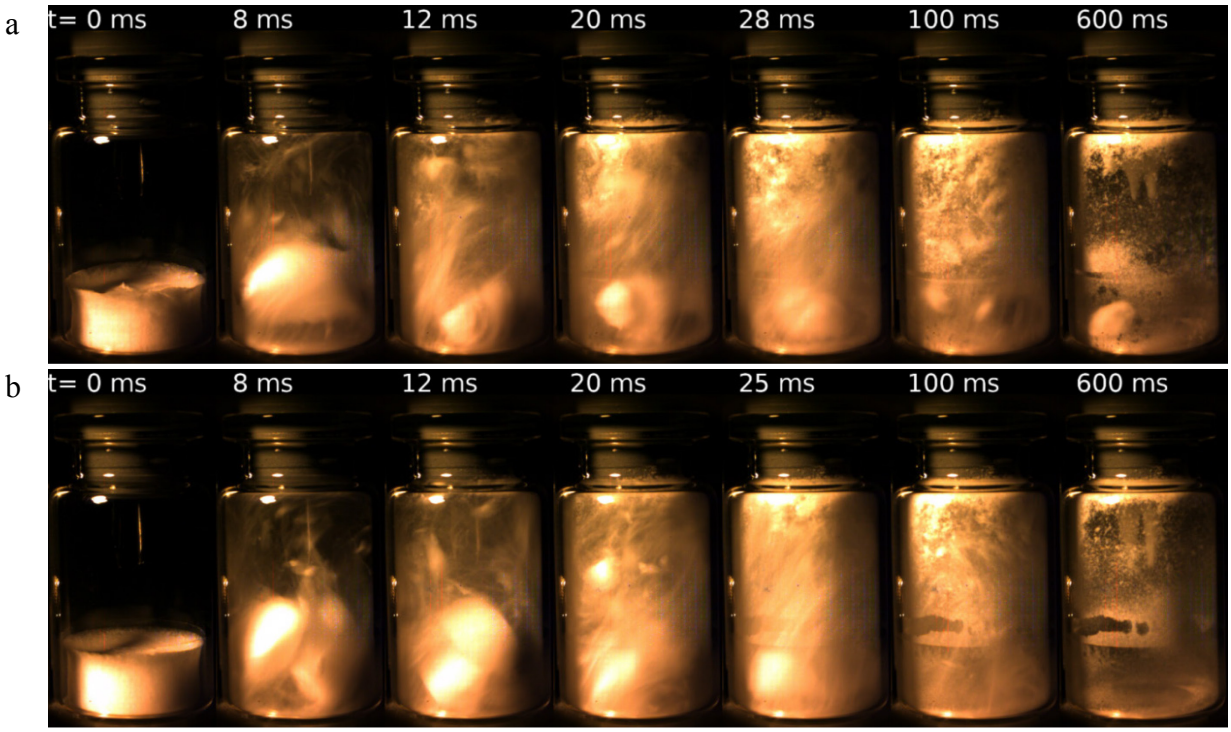

Figure 10: Aerosolization behavior of 12 mg/ml cromolyn sodium lyophilisates at 2 ml dispersed with 20 ml compressed air at 3bar (a) or with 30 ml at 4bar (b).

important for a good disintegration process. Nevertheless, the achieved FPD was not higher than the FPD of the 1 ml and 1.5 ml formulations in a 2R vial. The impact velocity/force of the incoming air stream must be about the same for both the 2R and 6R vial. The vial height differs only by 5 mm and the position of the capillaries of the test system was previously identified as not influencing the FPF (see chapter 2 for details). However, the same amount of air passed through the small 2R vial as well as the bigger 6R vial possibly resulting in a change in air flow behavior. Consequently a test was performed with a doubled volume of compressed air to 120 ml (30 ml at 4 bar) compared to the standard 60 ml (20 ml at 3 bar). Applying these adapted disintegration conditions, the FPD of the 2 ml formulation in 6R vials could be elevated to 3.7 mg. This increase was a result of an elevated ED from 28% to 48% whereas the FPF related to ED remained about the same similarly to the previous reported pressure increase for the 2R vials. The reference aerosolization of the 2R vial formulation at 4 bar and 30 ml revealed also an enhanced FPD as a result of the previously reported increased ED for a pressure of 4 bar but lacked the improved comminution due to the small vial volume. This showed that employing a bigger 6R vial with an adapted amount of compressed air could be used to further enhance the FPD of this lyophilisate based DPI system. Furthermore this clearly demonstrated that the disintegration of harder lyophilisates

like of cromolyn sodium required a certain amount of space which enables rotational movements for an effective comminution into fine particles.

For comparison, the micronized cromolyn sodium from one capsule of the commercial product Lomudal® (~26 mg) was filled into a 2R vial and aerosolized using the same conditions. The micronized drug achieved a FPD of 2.1 mg which corresponds to a FPF of 7.8%. The lyophilisate in 2R vial with the best performance (20 mg/ml and 0.5 ml) achieved a higher FPD of 2.6 mg in combination with a substantially lower metered dose of only 10 mg because of a markedly higher FPF of 26%. However, the FPF of Lomudal® could be higher when aerosolized using the original Eclipse® inhaler. For another commercial cromolyn sodium product formulated without excipient (Intal®), Steckel et al. [2] obtained a FPF of 14.1% and a FPD of 3.5 mg aerosolized using the intended inhalation device (Spinhaler®) and a Multistage Liquid Impinger (MLI) at a flow rate of 100 l/min. In a former study Steckel et al. [15] demonstrated a lower FPF for Intal® Spinhaler® of only 10% when measuring with the Twin Stage Impinger or 4% FPF using the MLI both operated at a flow rate of 60 l/min. Employing a 6R vial with an adapted amount of compressed air, a similar FPD of 3.7 mg was achieved while the FPF was again slightly higher at 15.5%. In both comparator products the FPF was significantly lower, and therefore a substantially higher MD was needed compared to the lyophilisate to deliver an appropriate FPD. A particularly high FPD is achieved with the PulmoSphere™ tobramycin dry powder formulation. In a study in healthy volunteers using gamma scintigraphy a mean FPF of 34% which corresponds to a FPD of 4.6 mg tobramycin following inhalation of a single capsule containing 25 mg of radiolabeled PulmoSphere™ tobramycin formulation was determined [16]. The marketed product TOBI® Podhaler® with an MD of 112 mg tobramycin (4 capsules) shows systemic tobramycin exposure comparable to a 300 mg nebulized tobramycin solution (TOBI® PARI-LC® Plus) [3] the latter resulting in 5% or 9% total lung deposition [16, 17]. Thus, the FPD of the TOBI® Podhaler® formulation must be around 3.75-6.75 mg per capsule.

With the novel dry powder inhalation system a FPD comparable to high dose market products could be achieved. Considering valine lyophilisates, the maximum FPD of 1.2 mg was significantly lower compared to cromolyn sodium. It is therefore dependent on the material properties whether the novel DPI system is suitable for the delivery of higher doses. It is also important to note that the novel DPI system is an active device which requires compressed air in contrast to the mentioned passive DPIs.

4 SUMMARY AND CONCLUSION

The aim of this study was to investigate the suitability of the lyophilisate based inhalation system for the delivery of high powder doses. The idea was to enhance the FPD of the system by elevation of the MD. Therefore, valine and cromolyn sodium lyophilisates at increasing solution concentration and at increasing fill volume were evaluated with respect to their aerosolization behavior and mechanical properties. An increase in dose could only be achieved by increasing the solution concentration at a low fill volume. However, the increase of the solution concentration was also limited. Although valine lyophilisates were ten times softer, the mechanical testing revealed for both substances an increasing hardness at increasing solution concentration ultimately responsible for an inferior disintegration and decrease in FPF. At a solution concentration of 28 mg/ml, cromolyn sodium lyophilisates reached a critical hardness limit for which disintegration was not possible anymore. The decrease in FPF at higher fill volume was also caused by an impaired disintegration of the lyophilisate. This was primarily a result of a reduced milling efficiency in the case of softer lyophilisates (e.g. valine lyophilisates) which were instantaneously and completely disintegrated into particles by the air impact. For harder lyophilisates (e.g. cromolyn sodium lyophilisates), the hindered disintegration was attributed to the increased hardness which prevented an immediate and complete fragmentation into particles. These harder lyophilisates required enough space to perform rotational movements in order to fracture in smaller pieces for a following scaling off of particles. With respect to FPD, the higher initial MD due to higher solution concentration partially compensated for the decrease in FPF so that a maximum FPD of 1.2 mg was achieved for valine and 2.6 mg for cromolyn sodium lyophilisates. Nevertheless, due to the small FPF, the loss in dose was immense. An increased pressure for dispersion of 4 bar resulted only in an increased ED for the highest fill volume of 2 ml and was not able to further enhance the FPD in the standard 2R vial for cromolyn sodium. Taking the required space for rotational movements into account, employing bigger 6R vials enabled improved cake disintegration. By applying an adapted amount of compressed air to the doubled vial volume (30 ml at 4 bar), the increased pressure for dispersion enhanced the ED and therefore the FPD to 3.7 mg. Overall, the novel DPI system based on dispersion of lyophilisates can keep up with marketed DPI products of higher metered dose.

5 REFERENCES

[1] I.J. Smith, M. Parry-Billings, The inhalers of the future? A review of dry powder devices on the market today, Pulm. Pharmacol. Ther., 16 (2003) 79-95.

[2] H. Steckel, N. Rasenack, B.W. Müller, In-situ-micronization of disodium cromoglycate for pulmonary delivery, Eur. J. Pharm. Biopharm., 55 (2003) 173-180.

[3] D.E. Geller, J. Weers, S. Heuerding, Development of an Inhaled Dry-Powder Formulation of Tobramycin Using PulmoSphere™ Technology, J. Aerosol. Med. Pulm. Drug Deliv., 24 (2011) 175-182.

[4] S.D. Anderson, J. Brannan, J. Spring, N. Spalding, L.T. Rodwell, K. Cahn, I. Gonda, A. Walsh, A.R. Clark, A New Method For Bronchial-provocation Testing in Asthmatic Subjects Using a Dry Powder of Mannitol, Am. J. Respir. Crit. Care Med., 156 (1997) 758-765.

[5] A.H. de Boer, P. Hagedoorn, E.M. Westerman, P.P.H. Le Brun, H.G.M. Heijerman, H.W. Frijlink, Design and in vitro performance testing of multiple air classifier technology in a new disposable inhaler concept (Twincer®) for high powder doses, Eur. J. Pharm. Sci., 28 (2006) 171-178.

[6] M.J. Telko, A.J. Hickey, Dry Powder Inhaler Formulation, Respir. Care., 50 (2005) 1209-1227.

[7] F. Buttini, P. Colombo, A. Rossi, F. Sonvico, G. Colombo, Particles and powders: Tools of innovation for non-invasive drug administration, J. Control. Release, (2012) doi: 10.1016/j.jconrel.2012.1002.1028.

[8] J. Weers, A. Clark, P. Challoner, High dose inhaled powder delivery: challenges and techniques, in: R.N. Dalby, P.R. Byron, J. Peart, J.D. Suman, S.J. Farr (Eds.) Respiratory Drug Delivery IX, Davis Healthcare International Publishing (River Grove, IL, USA), Palm Desert, CA, USA, 2004, pp. 281-288.

[9] N. Crowther-Labiris, A. Holbrook, H. Chrystyn, S. MacLeod, M. Newhouse, Dry Powder versus Intravenous and Nebulized Gentamicin in Cystic Fibrosis and Bronchiectasis, Am. J. Respir. Crit. Care Med., 160 (1999) 1711-1716.

[10] P.M. Young, J. Thompson, D. Woodcock, M. Aydin, R. Price, The Development of a Novel High-Dose Pressurized Aerosol Dry-Powder Device (PADD) for the Delivery of Pumactant for Inhalation Therapy, J. Aerosol Med., 17 (2004) 123-128.

[11] C. Yamashita, A. Akagi, Y. Fukunaga, Dry powder inhalation system for transpulmonary administration, in: United States Patent 7735485 2010.

[12] R. Tuunila, L. Nyström, Effects of grinding parameters on product fineness in jet mill grinding, Miner. Eng., 11 (1998) 1089-1094.

[13] H.J.C. Gommeren, D.A. Heitzmann, J.A.C. Moolenaar, B. Scarlett, Modelling and control of a jet mill plant, Powder Technol., 108 (2000) 147-154.

[14] N. Midoux, P. Hošek, L. Pailleres, J.R. Authelin, Micronization of pharmaceutical substances in a spiral jet mill, Powder Technol., 104 (1999) 113-120.

[15] H. Steckel, B.W. Müller, In vitro evaluation of dry powder inhalers I: drug deposition of commonly used devices, Int. J. Pharm., 154 (1997) 19-29.

[16] M.T. Newhouse, P.H. Hirst, S.P. Duddu, Y.H. Walter, T.E. Tarara, A.R. Clark, J.G. Weers, Inhalation of a Dry Powder Tobramycin PulmoSphere Formulation in Healthy Volunteers, Chest, 124 (2003) 360-366.

[17] P. Challoner, M. Flora, P. Hirst, M. Klimowicz, S. Newman, B. Schaeffler, R. Speirs, S. Wallis, Gamma scintigraphy lung deposition comparison of TOBI in the Pari LC Plus nebulizer and the Aerodose inhaler, Am. J. Respir. Crit. Care Med., 163 (2001) 83.

Chapter 5

Optimization of the FPF of a Lyophilized Lysozyme Formulation for Dry Powder Inhalation

Abstract

Purpose: A new dry powder inhalation technology creates inhalable particles from a coherent lyophilized bulk at the time of inhalation. The aim of this study was to evaluate several approaches to improve the fine particle output and to understand underlying aerolization mechanisms.

Methods: Lysozyme was chosen as model drug. Phenylalanine and valine were added, and the freezing process employed in lyophilization was varied (shelf ramped, with annealing, on precooled shelf, in liquid nitrogen, and vacuum induced). For characterization of the lyophilisates, x-ray diffractometry, residual moisture analysis, mechanical testing, and microscopy was performed. The fine particle fraction (FPF) was measured and the aerosolization behavior was recorded with a high speed camera. Furthermore, the particles were investigated by scanning electron microscopy.

Results: The addition of 14 to 40% of the crystalline amino acids phenylalanine and valine to the lysozyme solution prior to freeze-drying rendered a dose independent increase of the FPF from 5% to 17% and 14%, respectively. This is possibly due to enhanced fracture properties of the lyophilisates upon impact of the air stream as well as reduced particle agglomeration and cohesion caused by a rougher surface. This positive effect on aerosolization performance was well preserved over three months of storage at 40°C/75% RH. The structure of the freeze-dried product was influenced by the freezing process which in turn affected the aerosolization behavior. Freezing by immersion in liquid nitrogen and vacuum-induced freezing performed best, doubling the FPF. Despite poor fracture properties, the special cake morphology with elongated channels enabled easy disintegration. The resulting large particles comprise a very low density and a high porosity, which are advantageous for a high emitted dose and FPF.

Conclusion: The variation of the lyophilization process and formulation utilizing excipients enabled an optimization of the FPF of the novel lyophilisate based DPI system.

1 INTRODUCTION

Since first marketed in 1970, dry powder inhalers (DPIs) have been subject to continuous improvement. Device technology developed continuously to overcome the relatively low efficiency in fine particle fraction (FPF) and inconsistencies in the emitted dose (ED) of the first generation DPIs [1]. Most DPIs are breath-activated passive systems where powder aerosolization is achieved by the patient's own inspiration. These devices mostly have the disadvantage of inspiratory flow-dependent de-agglomeration of the powder [2]. Some newer devices like the Clickhaler® and the Taifun® show an in vivo deposition which is relatively independent from the inspiratory effort [3, 4]. Furthermore, active devices were developed which enable respiratory force independent dosing precision and reproducible aerosolization [5]. These devices are primarily designed for systemic pulmonary delivery and for conditions where the inspiratory power of the patient cannot be relied upon [6]. Examples for active devices are the Nektar Pulmonary Inhaler for Exubera® or the Aspirair™ device, which both use compressed air for the powder de-agglomeration and aerosolization process [6, 7].

New powder formulation methods are equally important to sophisticated devices. The two main formulation methods to enhance powder flowability and dispersibility are carrier systems mainly utilizing lactose and controlled agglomeration of pure drug particles, called pelletization [8]. The growing interest in pulmonary delivery of therapeutic proteins, nucleic acid nanocarriers, and vaccines as dry powder aerosols demands for alternative formulation methods to replace the commonly used but problematic micronization of the active pharmaceutical ingredient (API). Micronization may generate local hot spots in the processed materials and reduces their stability which is particularly a problem for thermolabile biopharmaceuticals [9]. A variety of new methods like controlled crystallization, supercritical fluid precipitation, spray drying, and spray freeze-drying were recently summarized by Chow et al. [9] with regards to the production of more uniform particles in terms of morphological state (e.g. crystallinity), particle size distribution, and shape. All these particle engineering methods directly produce a powder, which can reduce some challenges of micron-sized powder particles such as poor flow behavior and a high tendency to aggregate, but handling and precise metering remain difficult.

Freeze-drying is a common method for the stabilization of labile bioproducts. The lyophilized products are porous cakes in the dimensions of the former fill volume. For the production of inhalable particles the lyophilisate can be milled, which adds another manufacturing step and additional stress for the API. Alternatively, impacting air can be used for the disintegration of a freeze-dried preparation into inhalable particles [10]. Thus, DPI formulation is stored in a non-powdered form and the formation of fine particles occurs at the time of inhalation, thereby avoiding formulation problems like inadequate flowability and dispersibility of the powder. In addition, the manufacturing process is suitable for chemical entities as well as labile biopharmaceuticals. Because the formulation is metered as a liquid, extremely high accuracy at dose metering and a high preparation yield are further advantages of this technology. Nevertheless, freeze-drying is a time consuming and energy intensive manufacturing process [11]. A previous study revealed that placebo lyophilisates, disintegrated by compressed air in a custom designed test device, show material dependent differences in the fine particle output (Chapter 3). This led to the question whether the FPF of lyophilisates which exhibit poor dispersing behavior can be enhanced by the addition of excipients which demonstrate good aerosolization performance. The freeze-drying process or, more specifically, the freezing step is considered as another possible approach to increase fine particle output. The freezing process is a key step in lyophilization because it determines the ice crystal structure (shape and dimensions) and therefore governs the resulting lyophilisate morphology [12, 13]. The morphology of the lyophilisate should impact the dispersibility and aerosolization of the freeze-dried cake. Overall, the ice nucleation temperature, the freezing rate, as well as the freezing mechanism influence the ice crystal formation [14]. Shelf-ramped freezing renders a low ice nucleation temperature and fast ice crystal growth, resulting in a high number of small ice crystals. The addition of an annealing step enables a rearrangement and secondary ice crystal growth [15]. Freezing on a precooled shelf causes higher nucleation temperatures and slower freezing rates from vial bottom to top compared to shelf-ramped freezing and leads to a large heterogeneity between vials [16]. Vacuum-induced freezing allows controlled ice nucleation at a defined temperature. The ice nucleation starts at the top surface, followed by a top-down freezing which results in vertical ice crystals [17]. A very fast cooling method is immersion in liquid nitrogen, where freezing occurs by directional solidification resulting in small lamellar-oriented pores [18].

The aim of this study was to optimize the fine particle output of the model API lysozyme which demonstrated a poor emitted dose and fine particle fraction when lyophilized solitarily. High molecular weight species such as proteins form soft and elastic sponges after freeze-

drying, which is utilized, for example, in flexible gelatin-containing wound dresses [19]. For the disintegration into small particles by an air impact, these properties could be impedimental. Lysozyme was used as a model substance and the intention was to develop a pulmonary delivery system for lyophilisted formulations in general. Therefore protein stability and activity was not tested specifically. Instead, in a first approach, it was intended to achieve an optimized FPF by the addition of excipients. The two amino acids phenylalanine and valine performed best as single excipient lyophilisates in a previous study, showing FPF related to metered dose (MD) of nearly 50% (Chapter 3). They were therefore chosen as potential excipients to enhance the fine particle output of lysozyme. To gain a better understanding of the underlying mechanisms of the improvement, lyophilisate characteristics as well as aerosolization properties were investigated in addition to fine particle measurements. Furthermore, storage stability for three months at 25°C/60% RH and 40°C/75% RH was evaluated for a selected formulation. In a second approach to increase the fine particle output, various freezing methods as part of the lyophilization process of two selected formulations were applied. The obtained lyophilisates were investigated with respect to their morphology, mechanical properties, and aerosolization performance.

2 MATERIALS AND METHODS

2.1 MATERIALS

The model protein lysozyme from chicken egg white (Lys) was purchased from Serva Electrophoresis GmbH (Heidelberg, Germany) as a crystalline powder in hydrochloride form. Excipients used were L-phenylalanine (Phe) (Merck KGaA, Darmstadt, Germany) and L-valine (Val) (Fagron GmbH&Co KG, Barsbüttel, Germany). Solutions were made with highly purified water (Purelab Plus, Elga LabWater, Celle, Germany).

2.2 FORMULATION PREPARATION

0.5 ml aqueous solutions of 12 mg/ml lysozyme with 2 to 8 mg/ml phenylalanine or valine were filled into 2R glass vials (Fiolax® clear, Schott AG, Müllheim, Germany) and vials were equipped with rubber stoppers (1079-PH 701/40/ow/wine-red, West Pharmaceutical Services, Eschweiler, Germany). Freeze-drying was carried out in a laboratory scale freeze-drier (Lyostar II, FTS Systems, Stone Ridge, NY, USA). The samples were frozen at -1°C/min to

-45°C for 1 h. Primary drying was performed at a shelf temperature of -15°C (shelfs were ramped at +0.2°C/min) and a pressure of 100 mtorr for 20 h. For secondary drying the shelf temperature was increased to +30°C at a ramp rate of +0.1°C/min for 6 h. For comparison purposes also 4 mg/ml phenylalanine and 12 mg/ml valine solutions were freeze-dried similarly.

Additional four different freezing methods were tested besides the normal shelf ramped freezing at -1°C/min:

- Annealing at -10°C for 10 h: The samples were frozen at -1°C/min to -45°C with a hold at -45°C for 1 h, followed by a shelf temperature increase to -10°C at +1°C/min and annealing for 10 h at -10°C before the samples were frozen again at -1°C/min to -45°C with another hold at -45°C for 1 h.
- Precooled shelf at -70°C: The samples were placed on a precooled shelf at -70°C for 1.5 h.
- In liquid nitrogen: Samples were immersed in liquid nitrogen for 1 min and were subsequently placed on a precooled shelf.
- Vacuum-induced at -3°C: The samples were equilibrated on the shelfs at -3°C for 1 h. According to [17] the chamber was evacuated as fast as possible to 600 mtorr to induce freezing. Afterwards the shelf temperature was quickly decreased to -45°C for 1 h.

2.3 X-RAY DIFFRACTOMETRY (XRD)

The content of three vials was pooled for investigation with a Seifert X-ray diffractometer XRD 3000 TT (Seifert, Ahrensburg, Germany) equipped with a copper anode (40 kV, 30 mA, wavelength 154.17 pm). The samples were measured from 5 – 40° 2-Θ at a step rate of 0.05° 2-Θ with 2 s measuring time per step.

2.4 DEVICE

The lyophilized formulations were dispersed into aerosols using a custom-designed device (Chapter 2). Briefly, it consists of two capillaries with a diameter of 0.75 mm pierced through the stopper of the vial housing the lyophilisate. One capillary is the air inlet, the other capillary the air outlet, which is connected to the mouthpiece. Compressed air is stored in a

20 ml pressure reservoir at a pressure of 3 bar. Pressing a lever releases the compressed air through the inlet capillary, thereby starting dispersion of the powder.

2.5 FINE PARTICLE FRACTION (FPF) ANALYSIS

The FPF was measured using a short stack version of the Andersen cascade impactor (ACI) (8-Stage Non-Viable Sampler Series 20-800, Thermo Andersen, Smyrna, GA, USA) at a flow rate of 39 l/min (corresponds to a pressure drop of 4 kPa with the HandiHaler®, which is recommended by USP <601> [20]). Baffle plates were coated with a solution of 83% glycerin (AppliChem GmbH, Darmstadt, Germany), 14% ethanol (central supply LMU, Munich, Germany) and 3% Brij 35 (Serva Electrophoresis GmbH, Heidelberg, Germany). Filters used were type A/E glass fiber filters 76 mm (Pall Corporation, Ann Arbor, MI, USA). By removing stages 2 to 7, the whole FPF (particle fraction <4.94 µm) is collected on the filter directly below stage 1 and can easily be quantified by weighing the filter before and after powder deposition. The herein contained total lysozyme content was calculated by taking the varying amount of excipients into account. The FPF was calculated as the percentage of the total lysozyme content in the vial. The emitted dose (ED) was measured by weighing the vial before and after aerosolization and also calculated as the percentage of the total lysozyme content in the vial. The FPF analyses were performed in triplicate and the mean value including the standard deviation is presented in the figures.

2.6 MECHANICAL TESTING

The mechanical properties of the lyophilisates were investigated using a Texture Analyzer (TA.XT.plus, Stable micro Systems, Godalming, United Kingdom) equipped with a 5 kg load cell and a cylindrical stainless steel probe with a diameter of 5 mm at a test speed of 1 mm/s and a maximal immersion into the lyophilisate of 2 mm. The cylindrical probe acts on the lyophilisate by proceeding at constant speed and the force needed for the immersion is recorded. The resulting force represents the force necessary for breakage of the lyophilisate. At the end of the immersion, the probe touches the bottom of the vial which results in a steep increase of the immersion force curve and can therefore be disregarded. Measurements were performed in triplicate and averaged.

2.7 HIGH SPEED CAMERA RECORDING

The aerosolization behavior of the lyophilisates in the vial was recorded using a Fastcam 1024 PCI (Photron, San Diego, CA, USA) with a sample rate of 1000 fps. Dispersion of the lyophilisates was performed using the device (2.4) at standard settings (20 ml compressed air at 3 bar).

2.8 MICROSCOPY AND SCANNING ELECTRON MICROSCOPY (SEM)

The morphology of the lyophilisates was analyzed by digital light microscopy (VHX-500F, Keyence Corporation, Osaka, Japan) equipped with a VH-Z20R objective with variable lighting.

The particle morphology of the dispersed fine particles was analyzed with a Jeol Scanning Electron Microscope (JSM-6500F, Jeol, Ebersberg, Germany) at 5 kV. Sample preparation was performed using a second short stack version of the ACI where stages 3 to 7 have been removed. Conductive self-adhesive tape (Ø 12 mm Leit-Tabs, Plano GmbH, Wetzlar, Germany) was placed on the coated baffle plate after stage 2. The particles collected on the tape therefore have an aerodynamic cut off diameter between 4-4.94 µm at a flow rate of 39 l/min (Chapter 3). The samples were sputtered with carbon under vacuum.

2.9 STABILITY TESTING

For stability testing the sealed lyophilized samples were stored at 25°C and 60% relative humidity (RH) above a saturated ammonium nitrate (VWR International, Leuven, Belgium) solution or at 40°C and 75% RH above a saturated sodium chloride (Merck KGaA, Darmstadt, Germany) solution for three months. Stoppers used were dried before lyophilization at 105°C for 4 h.

The lyophilisates were analyzed for morphological state (2.3), moisture content (2.10), mechanical properties (2.6), microscopic morphology (2.8), as well as ED and FPF (2.5).

2.10 RESIDUAL MOISTURE CONTENT ANALYSIS

The residual moisture content of lyophilisates was determined by Karl-Fischer titration (Metrohm 756 KF Coulometer, Herisau, Switzerland) using Hydranal Coulomat AG (Riedel-deHaën, Seelze, Germany) as titration reagent. The lyophilisates were dissolved in the vials in

1.0 ml of anhydrous methanol (Hydranal-Methanol dry, Riedel-deHaën, Seelze, Germany), additionally dried with molecular sieve 3A (VWR International GmbH, Darmstadt, Germany). As blanks, empty freeze-dried vials, treated similarly, were used. The injection volume was 500 µl each. The measurements were performed in triplicate in order to calculate mean values.

3 RESULTS

3.1 OPTIMIZATION OF THE FPF BY ADDITION OF EXCIPIENTS

A custom-designed test device was used for disintegration of the lyophilisates and delivery of the fine powder. The resulting FPF of the lysozyme formulations were measured with a short-stack version of the ACI. Lyophilized lysozyme from 12 mg/ml lysozyme solution showed an ED of 37.4% and a small FPF of only 4.8% related to the MD of 6 mg. In order to improve the FPF, 2 to 8 mg/ml phenylalanine and valine, which demonstrated good performance in a previous study (Chapter 3), were added.

XRD demonstrated that freeze-dried lysozyme without excipients was completely amorphous. Mixtures with the amino acids demonstrated an increase in crystallinity of the formulations for concentrations > 4 mg/ml of phenylalanine or > 2 mg/ml of valine (Figure 1). The XRD patterns of these lyophilisates showed crystalline reflections of phenylalanine-monohydrate and valine, respectively.

The different lysozyme formulations demonstrate that the addition of phenylalanine or valine resulted in a dose-independent increase of the FPF of lysozyme. The ED is plotted against the FPF related to ED (left y-axis) in Figure 2. From the contour lines and the right y-axis, it is also possible to determine the FPF related to MD from the same plot. The ED was almost doubled to around 70% by addition of the excipients. The FPF related to MD was increased up to 17.0% by adding 4 mg/ml phenylalanine or elevated up to 14.1% by adding 6 mg/ml valine, mainly a consequence of the doubled ED.

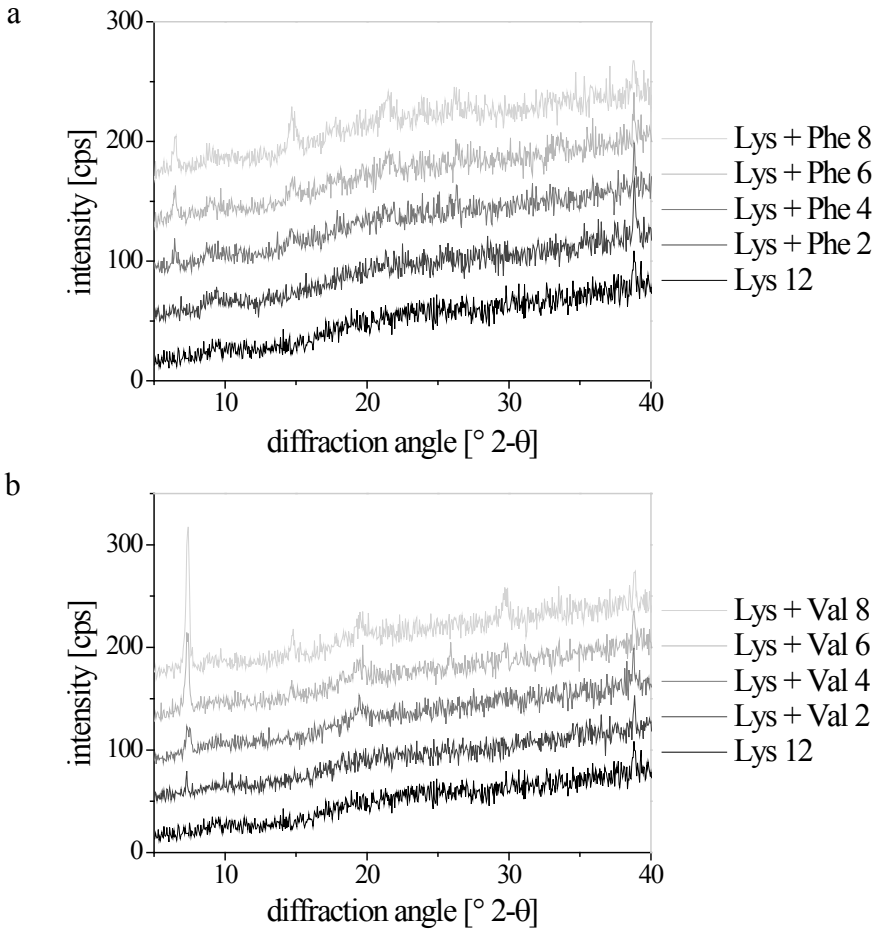

Figure 1: XRD patterns of 12 mg/ml lysozyme lyophilisates and the mixtures with phenylalanine (a) or valine (b) in the concentration of 2 to 8 mg/ml.

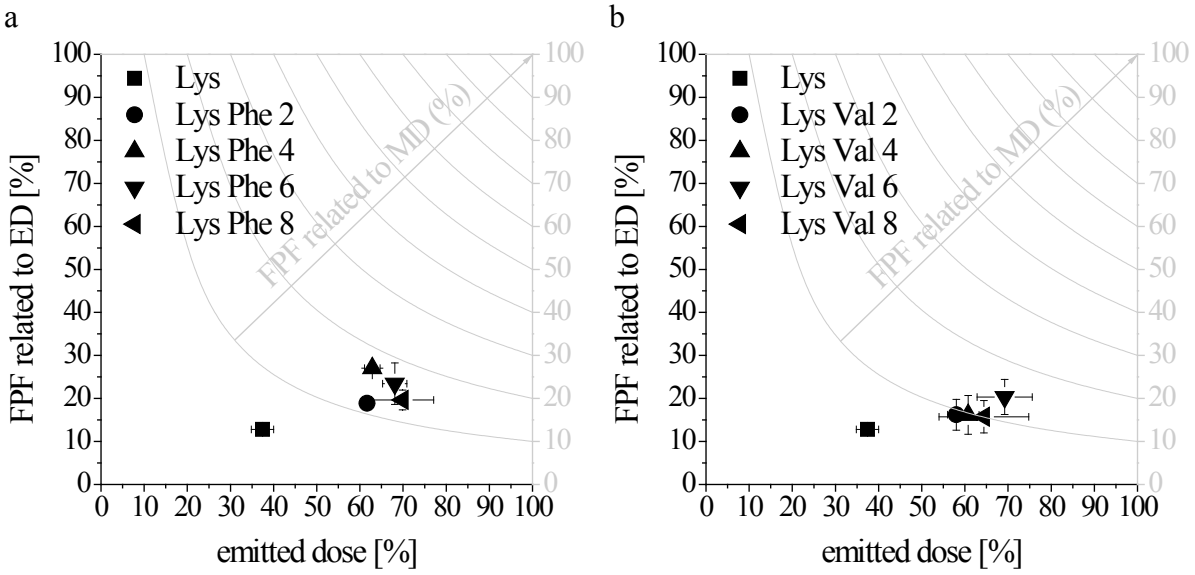

Figure 2: ED versus its related FPF as well as the FPF related to metered dose of lyophilisates of pure lysozyme and lysozyme formulated with 2-8 mg/ml phenylalanine (a) or valine (b).

To understand underlying mechanisms for the successful FPF optimization, the lyophilisate characteristics as well as the aerosolization properties were further investigated. The force necessary for breakage of the lyophilisate was tested by immersion of a cylindrical probe. Steady fracture at a constant force, resulting in a plateau, was found for pure phenylalanine and valine lyophilisates in the concentration of 4 mg/ml and 12 mg/ml (Figure 3) with force values of 0.014 N and 0.006 N, respectively. For lysozyme, a continuous increase of the immersion-force-curve at a slope of 0.07 N/mm was observed which represents a more elastic structure where mainly compression takes place. The immersion-force-curves of the mixtures, in contrast, revealed a plateau, indicating steady fracture at 0.08 N in the case of the phenylalanine mixture or 0.09 N for the valine mixture, exemplarily shown for the two formulations with the best performance.

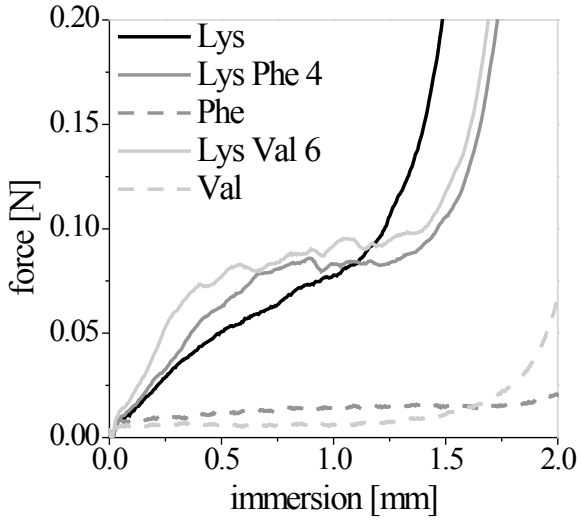

Figure 3: The texture characterization of lysozyme 12 mg/ml lyophilisates in comparison to lysozyme 12 mg/ml + phenylalanine 4 mg/ml, lysozyme 12 mg/ml + valine 6 mg/ml, phenylalanine 4 mg/ml and valine 12 mg/ml.

High speed camera recordings were performed in order to gain insights into the aerosolization behavior of the different lyophilisates. For all formulations the disintegration of the lyophilisate started by fragmentation into larger subunits (Figure 4). These pieces disintegrated further into fine particles which swirled around the endings of the capillaries until they left the vial. After aerosolization of pure lysozyme, a substantial amount of particles adhered to the capillaries (Figure 4a). If lysozyme was formulated with one of the crystalline amino acids, in contrast, adhesion of the dispersed particles to the capillaries and other surfaces in the vial was lower, as can be seen from Figure 4b/c. For the lysozyme lyophilisate almost all particles, which did not stick to the surfaces, left the vial after about 100 ms. Fine

particles of those formulations that included an amino acid in contrast swirled in the vial for a longer period of time until about 500 ms. This could be a result of the larger total content in the vial.

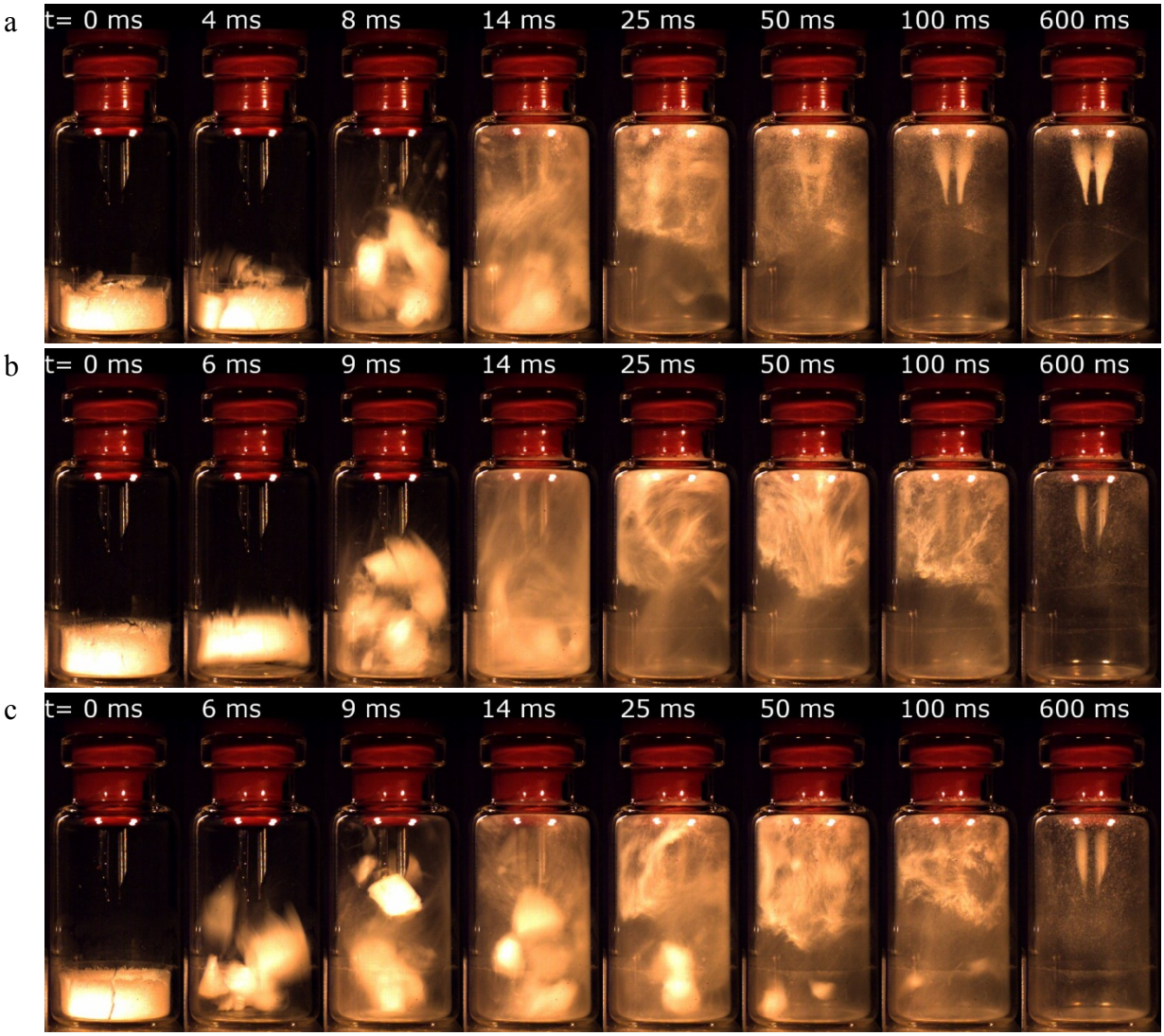

Figure 4: High speed camera recordings of lysozyme lyophilisate (a), lysozyme in the combination with 4 mg/ml phenylalanine (b) or with 6 mg/ml valine (c).

The microscopic morphology of the different freeze-dried formulations was inspected with the reflected light microscope. The lyophilisates of both pure lysozyme and the mixtures showed a porous comb-like structure. Figure 5 demonstrates the pore size for the upper surface of the lyophilisates of around 100 µm for pure freeze-dried lysozyme and slightly bigger pores of around 150 µm for the formulation with phenylalanine. The pore walls of pure lyophilized lysozyme were very thin and translucent. Whereas the pore walls of the mixtures appeared whitish and clearly visible. This is exemplarily shown for the phenylalanine mixture in Figure 5b.

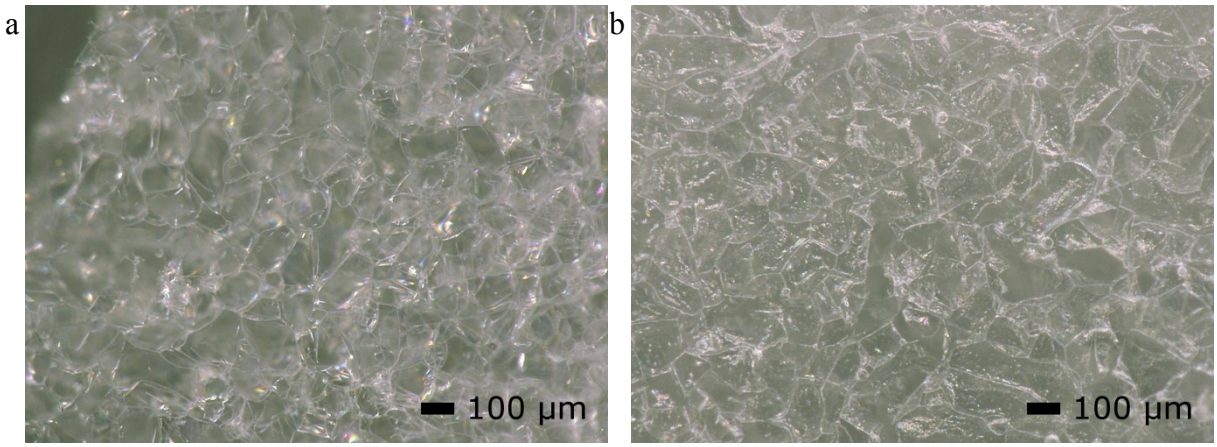

Figure 5: Microscopic morphology of lysozyme lyophilisates: upper surface of pure lysozyme (a) in comparison to lysozyme with 4 mg/ml phenylalanine (b).

In order to determine the geometric size and shape of the dispersed particles released from the test device, the particles were investigated with SEM. For comparison of particles with identical aerodynamic size, the specimens were collected on the baffle plate after stage 2 of the ACI, having an aerodynamic cut off diameter of 4-4.94 µm. At the border of the impacted particle spots (Figure 6a/c/e), it was possible to observe particles which were clearly separated from each other. These geometric particle sizes of approximately 10-30 µm were comparable for the different lysozyme formulations. The fragments of the pure lysozyme lyophilisates showed a very smooth surface (Figure 6b), whereas the fragments of the lysozyme phenylalanine formulation revealed a rough surface with needle-shaped crystal structures embedded (Figure 6d). The fragments of the lysozyme valine formulation demonstrated also a rougher surface (Figure 6f).

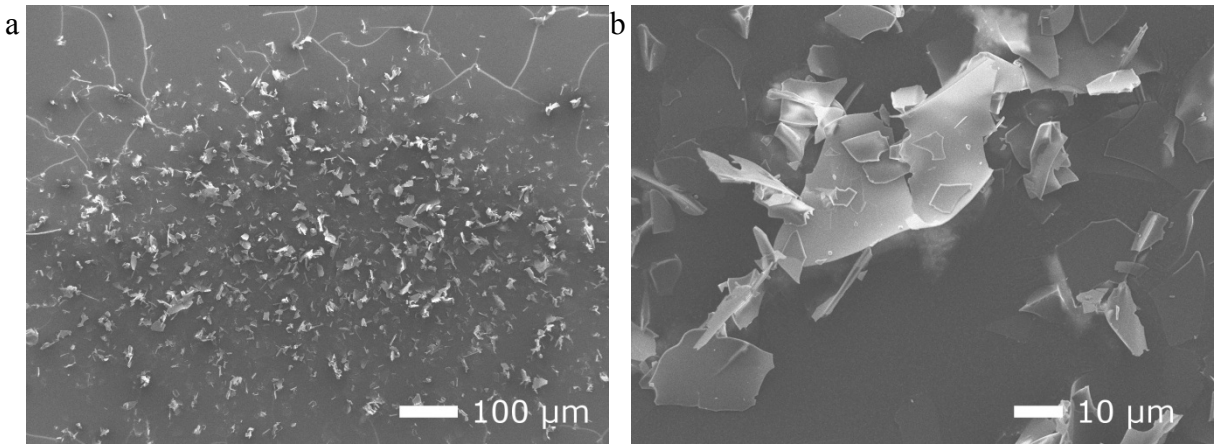

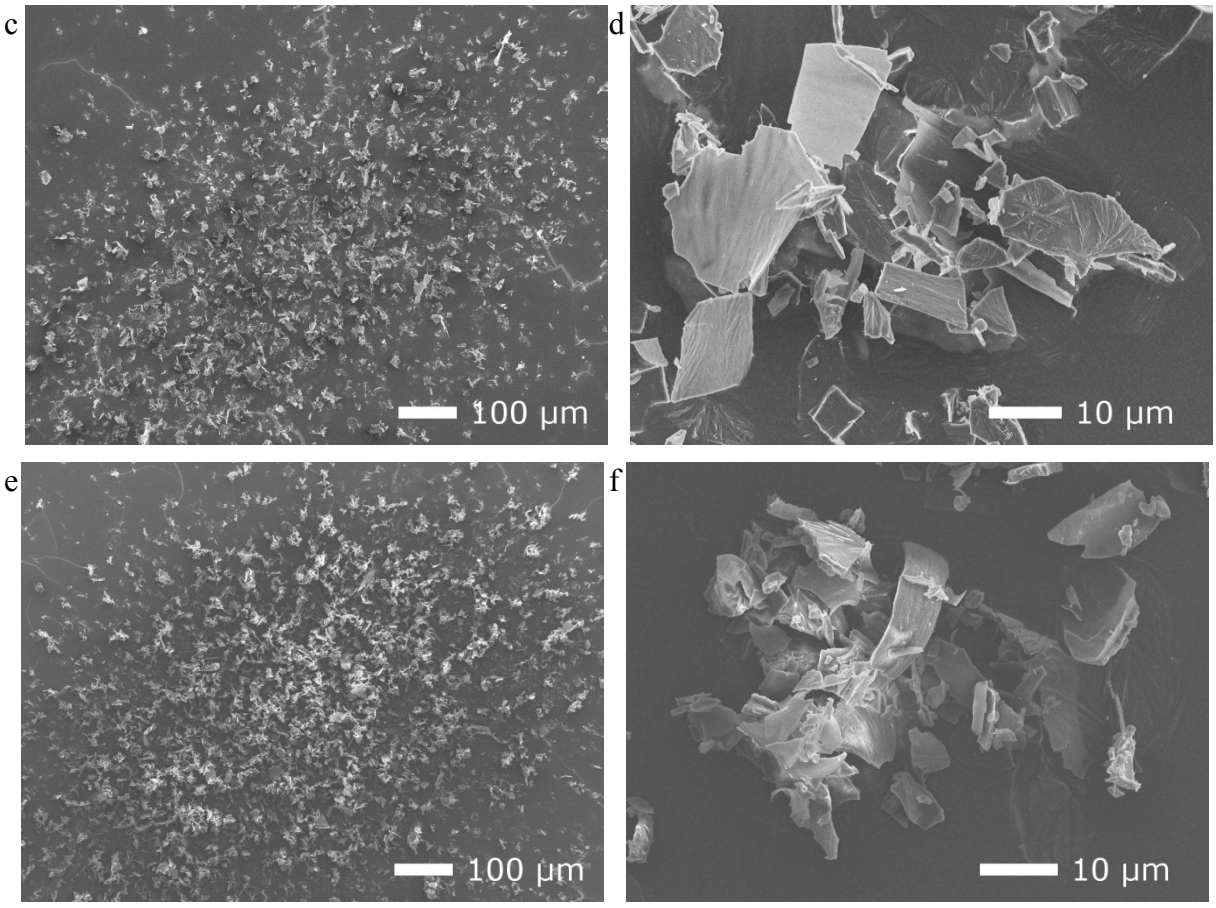

Figure 6: SEM of the particles with an aerodynamic cut off diameter between 4 and 4.94 µm of lysozyme 12 mg/ml (a, b) and lysozyme 12 mg/ml + phenylalanine 4 mg/ml (c, d) as well as lysozyme 12 mg/ml + valine 6 mg/ml (e, f).

3.2 STORAGE STABILITY OF 12 MG/ML LYSOZYME-4 MG/ML PHENYLALANINE-FORMULATION

Freeze-drying is known to improve the stability of labile drugs [21]. If a freeze-dried formulation contains amorphous or partially crystalline modifications which are thermodynamically unstable, one always has to consider the possibility of recrystallization during storage [13]. Furthermore, the moisture content of a freeze-dried formulation during storage may increase due to moisture coming from the vial stopper [22] or insufficient integrity of the container adversely influencing physicochemical stability and aerosol performance [9]. Consequently, freeze-dried 12 mg/ml lysozyme with 4 mg/ml phenylalanine formulation was stored at 25°C/60% RH and 40°C/75% RH up to three months.

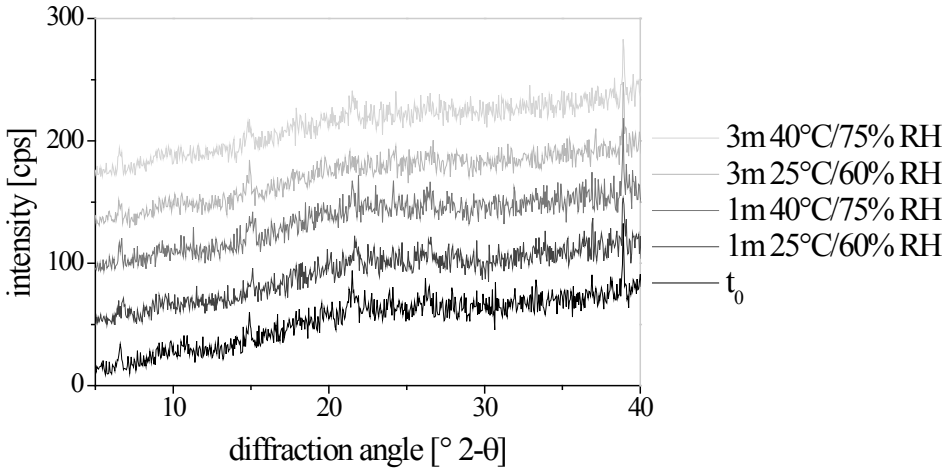

Figure 7: XRD pattern of 12 mg/ml lysozyme/4 mg/ml phenylalanine lyophilisates before and after one and three months of storage.

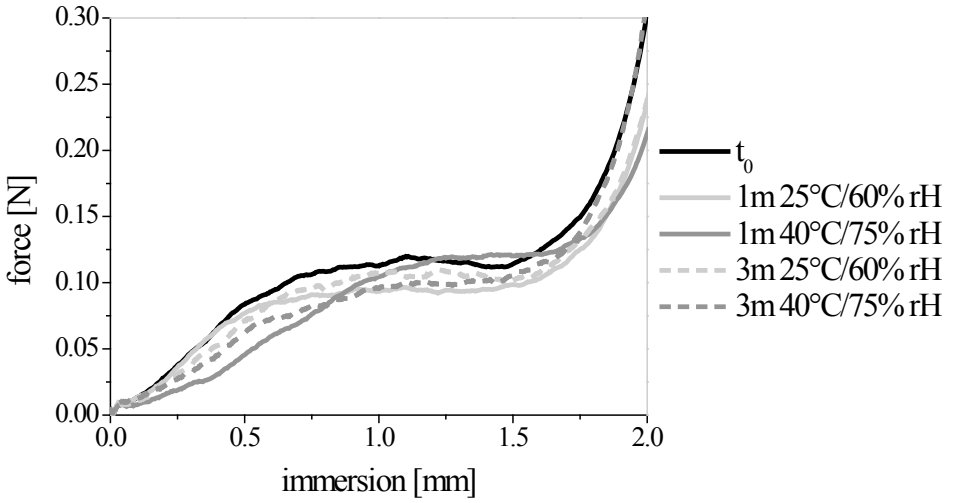

Figure 8: Mechanical testing of 12 mg/ml lysozyme/4 mg/ml phenylalanine lyophilisates before and after one and three month of storage.

The XRD pattern of the lyophilized lysozyme phenylalanine formulation showed no difference between freshly freeze-dried or stored lyophilisates (Figure 7). The crystalline reflections of phenylalanine-monohydrate remained at the same peak position and height. During storage the moisture increased from 0.3% to 0.8% and 1.9% after one month and to 1.5% and 2.7% after three month at 25°C/60% RH and 40°C/75% RH, respectively. Samples stored at the higher temperature and relative humidity absorbed significantly larger amounts of water. The mechanical behavior of the lyophilisates remained stable during storage. The position and shape of the immersion-force-curve of the mechanical testing did not change (Figure 8). Furthermore, no change in the microscopic morphology was detectable. ACI measurements revealed slight but not significant differences in ED as well as FPF of the lyophilisates. At t_0 samples demonstrated an ED of 57% which slightly increased to 64%

during storage. The FPF related to ED amounted to 34% at t_0 and varied between 30% and 34% after one and three months of storage. Thus, stability of the formulation with respect to physicochemical properties and aerosol performance over three months at 40°C/75% RH could be demonstrated.

3.3 VARIATION OF THE FPF BY VARIATION OF THE FREEZING METHOD

The morphology of the solid matrix of a lyophilisate is determined by the freezing process, comprising ice nucleation and ice crystal growth [17]. Different freezing methods were applied to alter the lyophilisate properties in order to improve ED and FPF. 12 mg/ml lysozyme solutions containing 4 mg/ml phenylalanine or 6 mg/ml valine were freeze-dried. Besides the normal shelf-ramped freezing at -1°C/min, an additional annealing step at -10°C for 10 h, freezing on a precooled shelf at -70°C, freezing by immersion into liquid nitrogen and vacuum-induced freezing at -3°C were performed. The crystallinity of the lyophilisates was analyzed by XRD. Lysozyme was always present in the amorphous state. All lyophilisates in the combination lysozyme and valine showed the characteristic peak pattern of crystalline valine with the main peaks at 7.4° and 19.5° 2θ (Figure 9a). Phenylalanine exhibited very small peaks, indicating a partial crystallinity in the form of the monohydrate for all different frozen lyophilisates (Figure 9b). The partial crystallinity of phenylalanine was analyzed in Chapter 3.

Mechanical testing revealed marked differences of the mechanical properties of lyophilisates prepared with different freezing processes, as can be seen in Figure 10. For samples frozen in liquid nitrogen, a constant positive slope of the immersion-force-curve was observed. Vacuum-induced freezing resulted in a force peak with a maximum at 0.09 N at the beginning of the immersion for the lysozyme/phenylalanine lyophilisates, whereas the lysozyme/valine lyophilisates required a higher overall force of 0.16 N for fracture. The lysozyme/valine lyophilisates frozen on a precooled shelf required also a higher force for breakage of 0.11 N compared to the lyophilisates frozen in the conventional shelf-ramped process or additionally with annealing, which both demonstrated a force of 0.09 N for breakage. Lysozyme/phenylalanine lyophilisates frozen on a precooled shelf as well showed a plateau of constant fracture at 0.09 N which was higher than the lyophilisate frozen by shelf-ramping (0.08 N) or including annealing (0.07 N).

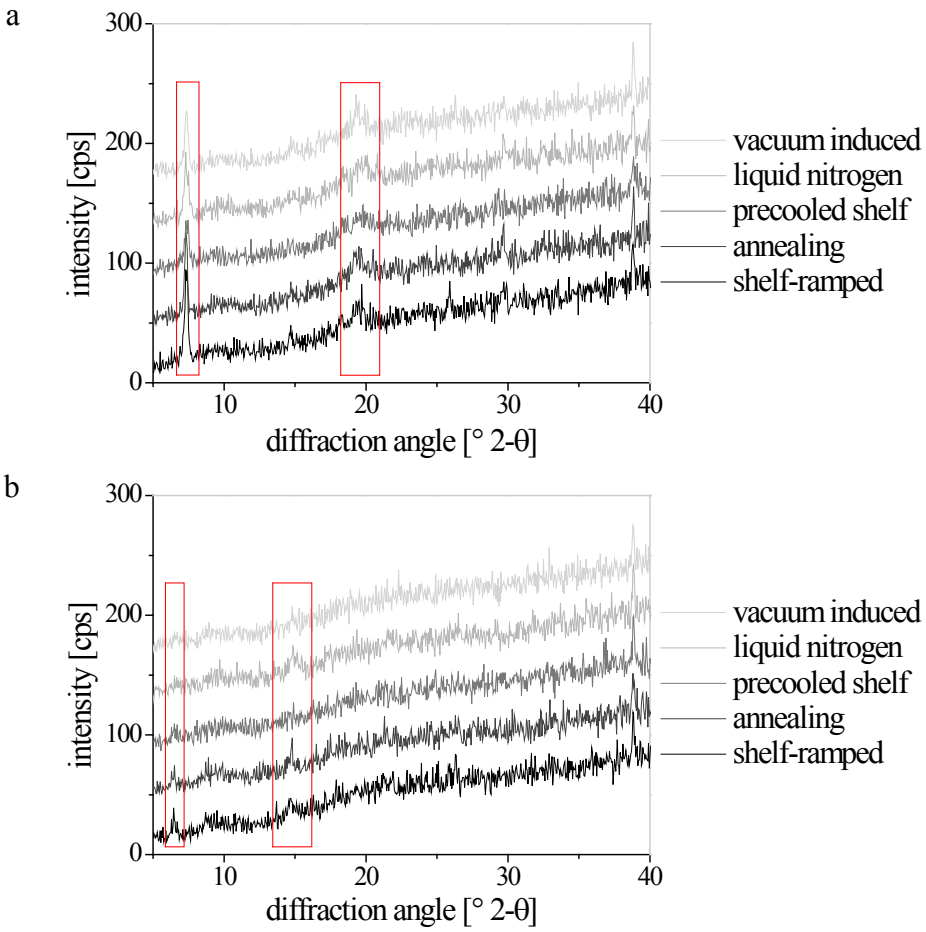

Figure 9: XRD pattern of 12 mg/ml lysozyme/6 mg/ml valine (a) and 12 mg/ml lysozyme/4 mg/ml phenylalanine (b) lyophilisates prepared with different freezing procedures.

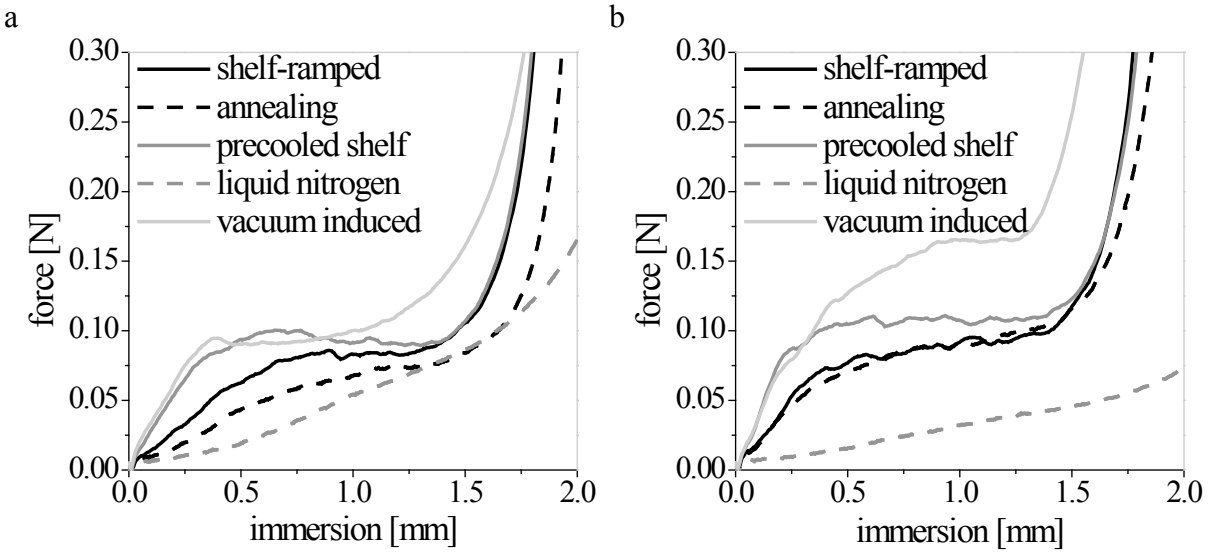

Figure 10: The mechanical testing of 12 mg/ml lysozyme/4 mg/ml phenylalanine (a) or 12 mg/ml lysozyme/6 mg/ml valine (b) prepared with different freezing procedures.

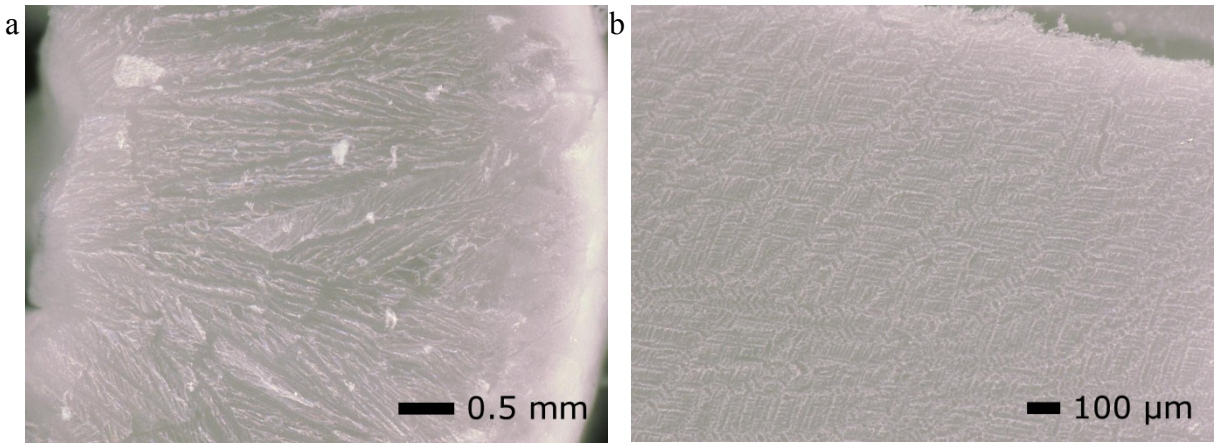

Figure 11: The bottom surface morphology of lyophilisates frozen in liquid nitrogen (a) and the upper surface morphology of the vacuum induced frozen lyophilisates (b) of 12 mg/ml lysozyme/4 mg/ml phenylalanine.

Microscopy of lyophilisates frozen via shelf-ramping, with an annealing step, or on a precooled shelf showed a similar pore structure. Differences in the pore sizes, particularly at the bottom side, were apparent. For the lysozyme/phenylalanine lyophilisates, for example, the pore size at the bottom was around 100 µm for samples frozen via shelf-ramping. Annealing caused an increase to about 160 µm, whereas precooled shelf freezing resulted in smaller pores of approximately 30 µm. Both samples frozen in liquid nitrogen demonstrated a special morphology with lamellar pores oriented in the direction from outside to the center, which was clearly visible for the inner and bottom structure of the lyophilisate (Figure 11a). The samples obtained by vacuum-induced freezing had a very dense upper surface structure with tiny little pores of approximately 30 µm for the formulation with phenylalanine (Figure 11b) and 20 µm for the formulation with valine. The bottom of these lyophilisates showed small pores of 50-60 µm as well.

Analysis of the dispersed particles by SEM demonstrated that the fragments of the conventionally frozen (at -1°C/min) lysozyme/phenylalanine lyophilisates had a platelet-like structure, whereas the samples frozen in liquid nitrogen or by vacuum-induced freezing were fluffy and porous. The fine particles with an aerodynamic size between 4 and 4.94 µm consisted of agglomerates of smaller fragments and demonstrated different geometric sizes, depending on the freezing process: particles from normal freezing were 10-30 µm, the particles from vacuum-induced freezing of approx. 80 µm, and the ones frozen in liquid nitrogen of approx. 110 µm in size (Figure 12). The aerodynamic diameter (d_A) is defined by the relationship

$$d_A \cong d_V \sqrt{\frac{\rho}{\chi \rho_0}} \quad (1)$$

and is dependent on the size (d_V), shape (χ) and mass density of the particle (ρ) for $\rho_0 = 1 g/cm^3$. By disregarding the shape assuming round particles, a particle density can be estimated based on the aerodynamic and geometric size. The particle density decreased from around 0.05 g/cm^3 for the small particles generated from lyophilisates prepared by normal freezing to a density of around 0.002 g/cm^3 for the large particles generated from lyophilisates prepared by liquid nitrogen freezing.

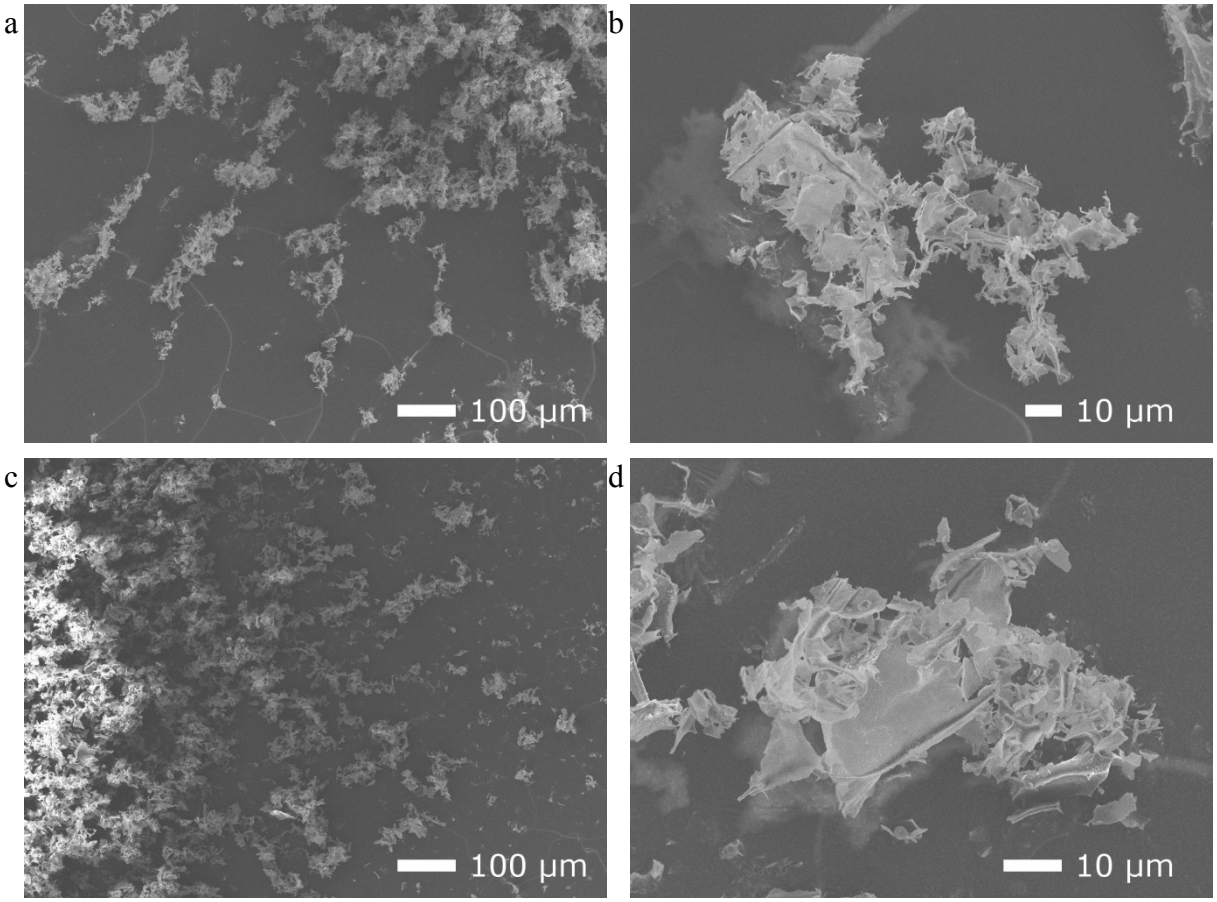

Figure 12: SEM of the particles with an aerodynamic cut off diameter between 4 and 4.94 µm. Aerosolized 12 mg/ml lysozyme/4 mg/ml phenylalanine lyophilisates frozen in liquid nitrogen (a, b) and frozen vacuum induced (c, d).

Additional high speed camera recordings revealed a different behavior of the various frozen lyophilisates during the disintegration process in the vial. For the lysozyme/phenylalanine formulation, for example, the disintegration into particles of the lyophilisates frozen at -1°C/min (Figure 4b) and with the annealing step (Figure 13a) was already finished after about 25 ms. The disintegration into small particles of samples prepared by precooled shelf

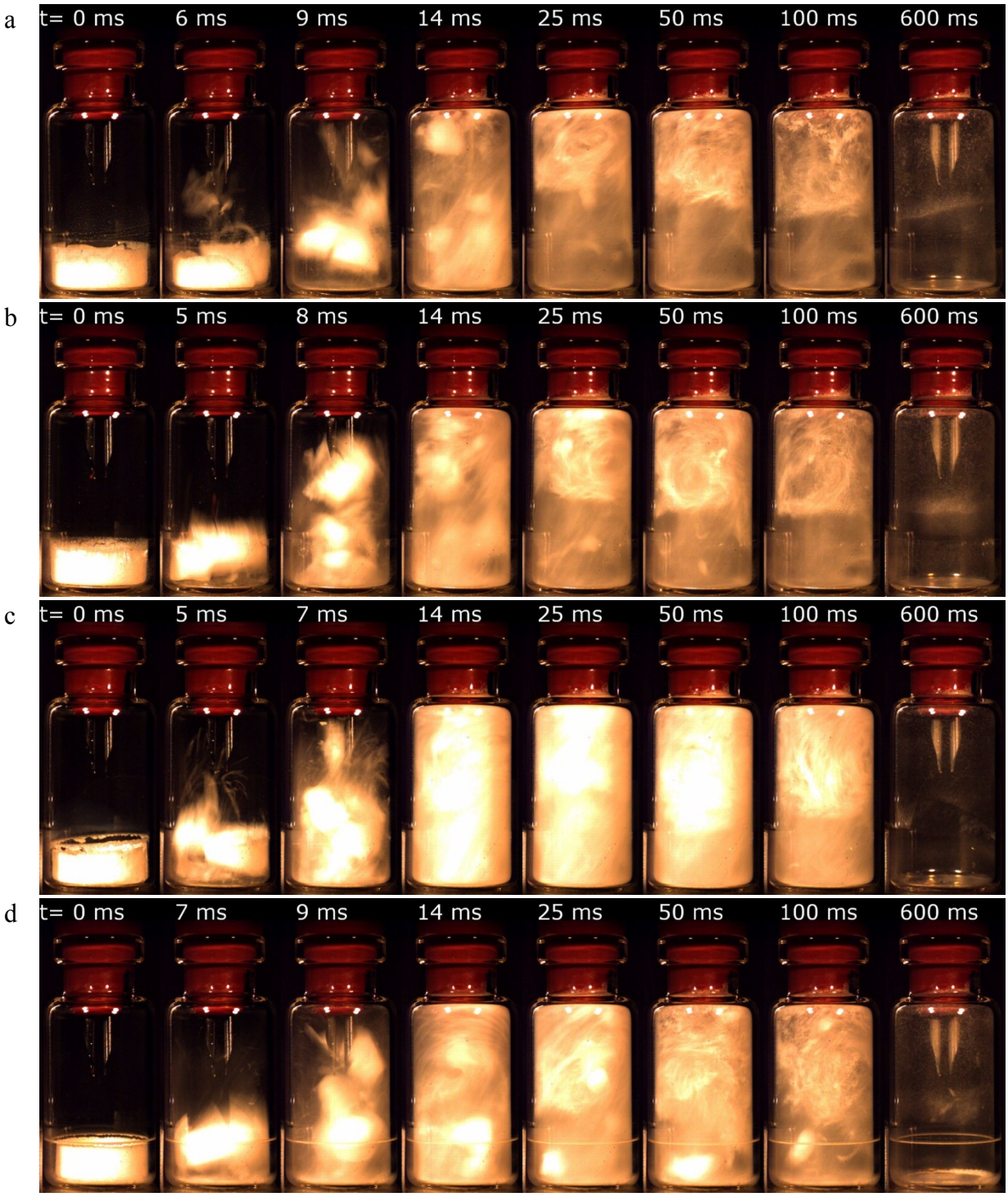

Figure 13: High speed camera recordings of 12 mg/ml lysozyme/4 mg/ml phenylalanine lyophilisates frozen with annealing (a), on precooled shelf (b), in liquid nitrogen (c) and vacuum induced (d).

freezing lasted about 50 ms (Figure 13b). Lyophilisates from vacuum-induced freezing (Figure 13d), in contrast, disintegrated into smaller subunits from which particles were scaled off over a longer period of time (more than 100 ms). The lyophilisates frozen in liquid

nitrogen disintegrated quickly into voluminous particles, resulting in a complete fill of the vial (Figure 13c). The valine formulations showed similar aerosolization behavior.

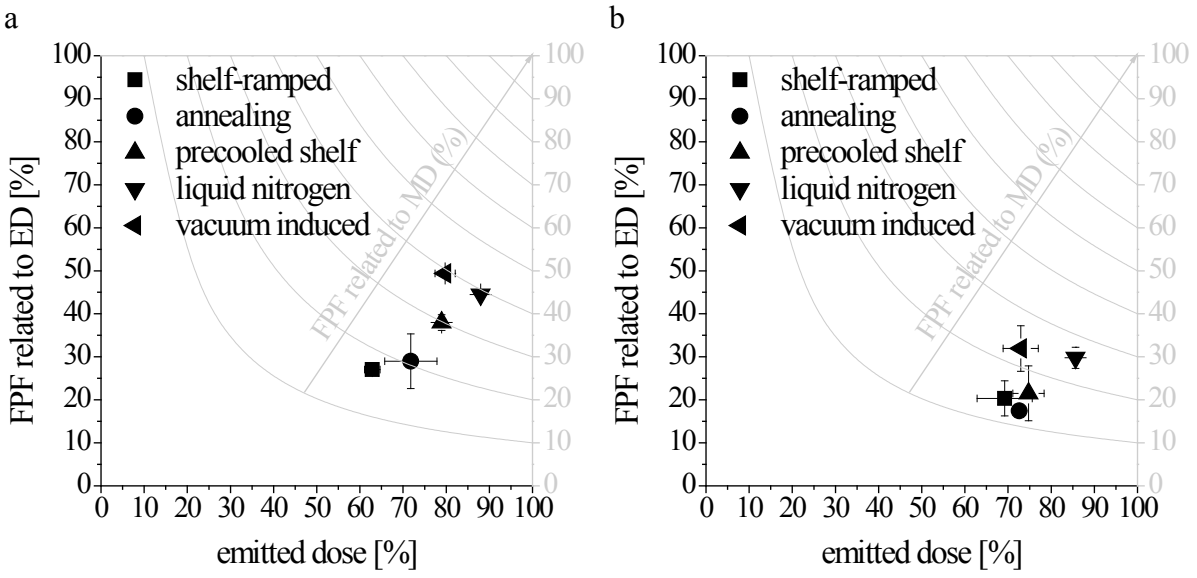

Figure 14: The impact of the different freezing processes of lyophilized 12 mg/ml lysozyme/4 mg/ml phenylalanine (a) or 12 mg/ml lysozyme/6 mg/ml valine (b) on the ED and the FPF related to ED as well as the FPF related to metered dose.

The described variations of lyophilisate morphology and properties partly resulted in differences in the fine particle output, as can be seen from Figure 14. For both, lysozyme/phenylalanine and lysozyme/valine formulations annealing did not result in a significant difference in ED and FPF compared to regular shelf freezing. The precooled shelf method in comparison to shelf-ramped freezing led to a significant increase of the ED from 63% to 79% and therefore also to an increase of the FPF related to MD from 17% to 30% for the phenylalanine formulation. The valine formulation, in contrast, showed no significant differences. By freezing in liquid nitrogen, it was possible to significantly enhance the ED and the FPF for both formulations. The ED increased to 88% in the case of the phenylalanine formulation with an increase in the FPF related to ED from 27% to 44% while the valine formulation showed an enhanced ED from 69% to 86% and FPF related to ED from 20% to 30%. The samples from vacuum-induced freezing also exhibited a significant escalation of the FPF for both formulations to 49% and 32% as well as a significant increase of the ED to 80% for the phenylalanine formulation. Freezing in liquid nitrogen and vacuum-induced freezing resulted for the phenylalanine formulation in a more than twofold elevation of the FPF related to MD from 17% to 39%.

4 DISCUSSION

4.1 OPTIMIZATION OF THE FPF BY ADDITION OF EXCIPIENTS

It was possible to significantly increase the FPF of the lyophilized model API lysozyme by addition of the amino acids phenylalanine or valine. These two excipients are not commonly used in freeze-drying or dry powder formulation for inhalation but were chosen because of their good performance in a previous study exhibiting high FPF related to MD of nearly 50% (Chapter 3). In principle, most amino acids crystallize during freeze-drying and are therefore suitable as bulking agents [23]. Glycine, for example, is a commonly used bulking agent in freeze-dried formulations [24]. Valine crystallizes as well during freeze-drying whereas phenylalanine forms a monohydrate and is only present in a partially crystalline state (Chapter 3).

The magnitude of the FPF elevation of 12 mg/ml lyophilized lysozyme was independent of the amount of excipient added. A small amount of 2 mg/ml phenylalanine or valine was sufficient to double the FPF related to MD from 4.8% to 11.7% and 9.4%, respectively. Consequently, the amino acids had a great effect on the lyophilisate properties and aerosolization behavior of freeze-dried lysozyme. These lyophilisate properties and characteristics are discussed in the following to understand underlying mechanisms.

As expected, lysozyme was present in the amorphous state in all formulations. Proteins, in general, do not crystallize during freezing but form an amorphous solid at the glass transition temperature of the freeze concentrate (Tg') [13]. This purely amorphous glass appeared translucent in light microscopy, resulting in a glassy sheen on the lyophilisate surface [25], whereas the pore walls appeared whitish in the formulations with an amino acid. As intended, valine crystallized during freeze-drying. In contrast, phenylalanine was partly present in the amorphous state. Because crystallization is dependent on the presence of other solutes [26], the amorphous protein prevented phenylalanine from crystallization at the highest protein to amino acid ratio of 6:1. At higher phenylalanine concentrations, the amino acid was only partially crystalline as indicated by small crystalline reflections appearing in combination with an amorphous halo. This was not only caused by the presence of the amorphous protein since pure freeze-dried phenylalanine also exists in a partly amorphous state (Chapter 3). During freeze-drying phenylalanine crystallizes in the form of the needle-shaped monohydrate which is the stable pseudo-polymorph when crystallization occurs at

temperatures below 37°C [27]. The crystalline nature of formulations containing an amino acid corresponded to a rough surface of the pore wall fragments in SEM. The distinct striped appearance of the needle-shaped phenylalanine-monohydrate crystals coated with a thin layer of amorphous material was also reported previously [28]. This surface roughness could explain the lower adhesiveness of the particles to the capillaries and the vial surface, as well as to each other, because of a smaller effective contact area compared to the planar surface of lyophilized lysozyme fragments. The enhanced dispersibility of particles with irregular surfaces was also observed for spray-dried particles [8, 29, 30]. Less adhesion to the capillaries and vial surface enhanced the ED and consequently the FPF related to MD. A longer time period during which particles swirled in the vial until their escape through the outlet capillary was noticeable, which could be an effect of a larger total content in the vial or of less adhesion resulting in a larger amount of free swirling particles in the vial.

The rough surface is not the only parameter responsible for the successful increase of the FPF by addition of phenylalanine or valine. Mechanical properties of the lyophilisates can be examined by texture analysis. The cylindrical probe acts on the lyophilisate by proceeding at a constant speed. The resulting force needed for the immersion is constantly measured and represents the force necessary for breakage of the lyophilisate. The texture analysis revealed that lyophilisates containing phenylalanine or valine, which show steady fracture at a constant force, have good aerosolization properties with a high ED and FPF. It is important to note, that the force necessary to fracture the lyophilisate was much higher in the lysozyme/amino acid combinations (0.08-0.09 N) compared to the pure amino acid (0.006-0.014 N) but did not hinder the disintegration of the lyophilisates. Lysozyme, on the other hand, showed a continuous positive slope of the immersion-force curve, which points to an elastic structure for which mainly compression takes place instead of breakage. Since the lyophilisate needs to fracture into fine particles during the dispersion process, one can easily conclude that brittleness and fragility of lyophilisates shown by a plateau in the immersion-force curve of the mechanical testing and therefore steady fracture at a constant force are beneficial for a good dispersibility and a high fine particle output. By the addition of crystalline excipients it was possible to improve the fracture properties of lyophilized lysozyme and consequently the FPF.

4.2 STORAGE STABILITY OF 12 MG/ML LYSOZYME-4 MG/ML PHENYLALANINE-FORMULATION

During storage the aerosolization performance of the lyophilisates may become reduced and amorphous material may recrystallize due to moisture uptake. The formulation was stored at 25°C and 60% RH or 40°C and 75% RH, as recommended by the International Conference on Harmonization [31]. The morphological state of the lyophilisate did not change during storage of 3 months. Even during storage at 40°C, which is above the transition point of phenylalanine in water where the anhydrous form is more stable [27], phenylalanine remained a monohydrate. Furthermore, the partly amorphous phenylalanine state was preserved over the storage period. The residual moisture of lyophilisates immediately after freeze-drying was less than 1%, which is considered optimal for storage stability [21]. The moisture content of the freeze-dried formulation increased during storage. The higher the storage temperature, the greater was the increase in moisture content, which agrees with other storage stability studies [23, 32]. Residual moisture in the stopper is often responsible for the moisture uptake of the formulation up to an equilibrium value which is characteristic for the product, amount of product, and stopper treatment method, whereby the time to the equilibrium is dependent on the temperature [22]. Lyophilisates stored at 25°C did not reach the equilibrium of greater or equal to 2.7% within three months. Since water has a plasticizing effect on amorphous materials [33], variations in the mechanical characteristics were expected. Nevertheless, the mechanical property of the formulation did not change for all storage conditions and time periods. Potentially the crystalline component had a stabilizing effect on the mechanical behavior of the lyophilisate. The cascade impactor measurements demonstrated that an increased moisture content was not detrimental for the aerosolization performance of the formulation.

4.3 VARIATION OF THE FPF BY VARIATION OF THE FREEZING METHOD

As the manner of ice crystal formation and growth during the freezing process fixes the texture and porosity of the final dried product, the degree of supercooling, the freezing rate, and the time required for complete solidification directly impact ice crystal morphology [14]. In general, freezing methods for which supercooling exceeds 5°C result in a freezing of samples by global supercooling, which causes a spherulitic morphology. This was the case for lyophilisates prepared with standard shelf-ramped freezing, annealing, and precooled shelf freezing. Directional solidification, in contrast, is often seen at very high cooling rates, or

when ice nucleation is induced close to the equilibrium freezing point [14]. Lyophilisates frozen by directional solidification show lamellar plate morphology [34], which was in this study only observed for freezing by immersion in liquid nitrogen. It causes extreme temperature gradients along the vial bottom and sides, resulting in directional solidification from those surfaces inward [16]. The microscopic morphology of both liquid nitrogen frozen formulations showed the characteristic thin pores of lamellar-orientation in the direction from outside toward the middle. A supercooling of less than 5°C occurred also for the controlled nucleation at -3°C by vacuum-induced freezing. Nevertheless, these formulations were frozen by global supercooling, which resulted in spherulitic pore morphology visible on the bottom of the lyophilisates (Figure 9a). In addition, observation of the formulations during the freezing process showed a sudden change in the appearance of the vial content from a clear liquid to an opaque/translucent slush, which is indicative of global supercooling [35].

As Table 1 summarizes, the different freezing processes applied resulted not only in a varied morphology but also in a variation of cake characteristics and aerosolization performance. For both lysozyme formulations (with 4 mg/ml phenylalanine or 6 mg/ml valine), freezing in liquid nitrogen and vacuum induced freezing demonstrated the best results for ED and FPF by about doubling again the FPF related to metered dose. In the following, differences and commonalities of the samples prepared by the different freezing procedures are discussed in order to understand underlying mechanisms of the aerosolization performance improvement.

The physical state of the compounds in a lyophilisate can be influenced by the freezing procedure. In addition to enabling rearrangement and growth of ice crystals, annealing or thermal treatment of frozen systems is a process which facilitates crystallization of a bulking agent such as glycine or mannitol [13]. On the other hand, fast freezing, for example by immersion into liquid nitrogen, can prevent solutes from crystallizing. XRD, however, showed no differences in the peak height of the different frozen lyophilisates. Thus, no further crystallization of phenylalanine occurred during annealing and fast freezing by immersion into liquid nitrogen did not prevent valine or phenylalanine from crystallization.

For the differently frozen lyophilisates, texture analysis revealed a different mechanical behavior. Because the physical state remained the same, the differences must be a result of the structural properties. Conventional shelf-ramped freezing and annealing resulted, for all samples, in an immersion-force curve with a plateau that indicates brittle cake fracture. Both samples prepared by precooled shelf freezing demonstrated a steeper slope of the immersion-

Table 1: Results overview of the cake characteristics and aerosolization performance of lysozyme/phenylalanine or lysozyme/valine lyophilisates prepared with different freezing procedures.

Lyozyme 12 mg/ml + phenylalanine 4 mg/ml	**standard shelf-ramped**	**annealing**	**precooled shelf**	**liquid nitrogen**	**vacuum induced**
pore structure	spherulitic	spherulitic	spherulitic	lamellar	spherulitic
mechanical testing	force plateau at 0.08 N	force plateau at 0.07 N	force plateau at 0.09 N	constant slope of 0.06 N/mm	force peak max at 0.09 N
disintegration characteristics	fast, within 25 ms	fast, within 25 ms	within 50 ms	fast into voluminous particles	into subunits and scaling off
ED	63%	72%	79%	88%	80%
FPF (ED)	27%	29%	38%	44%	49%
FPF (MD)	17%	21%	30%	39%	39%
particle morphology	platelet-like	-	-	fluffy, porous	fluffy, porous
particle size	10-30 µm	-	-	80 µm	110 µm

Lysozyme 12 mg/ml + valine 6 mg/ml	**standard shelf-ramped**	**annealing**	**precooled shelf**	**liquid nitrogen**	**vacuum induced**
pore structure	spherulitic	spherulitic	spherulitic	lamellar	spherulitic
mechanical testing	force plateau at 0.09 N	force plateau at 0.09 N	force plateau at 0.11 N	constant slope of 0.03 N/mm	force plateau at 0.16 N
ED	69%	73%	75%	86%	73%
FPF (ED)	20%	17%	22%	30%	32%
FPF (MD)	14%	13%	16%	25%	23%

force-curve until the plateau was reached, suggesting that a higher force was needed to break at least the upper half of the cake. Freezing on a precooled shelf can cause an enormous temperature gradient throughout the fill volume, which leads to smaller pores at the bottom and large pores near the top [14] as observed in this study. Phenylalanine samples from vacuum-induced freezing demonstrated a peak at the beginning of the immersion-force-curve, indicating that a higher force was needed to break the top part. Compared to the other freezing methods, the microscopic picture revealed a very dense upper surface of this sample, which therefore can explain the harder and more destruction resistant structure. The reduction of the pressure to 600 mtorr for vacuum-induced freezing results in an evaporation of water, which lowers the temperature on the surface of the solution and induces ice nucleation [17]. During this vaporization process, the solutes concentrate at the surface [12] and thus form a dense upper surface layer. Both formulations frozen in liquid nitrogen showed a constant slope of the immersion-force-curve without a plateau and thus demonstrated an elastic behavior. These

sample characteristics conflict with the above conclusion that brittleness of the lyophilisate instead of an elastic behavior is beneficial for a good disintegration and a high fine particle output. This demonstrates, however, that there must be several factors influencing the aerosolization behavior which more or less can compensate for other characteristics. While a brittle structure can improve the disintegration behavior for lyophilisates with a spherulitic morphology, it is not essential for good disintegration of samples with a special morphology such as the narrow lamellar oriented pores resulting from directional solidification. Possibly, the narrow pore structure does not fracture in the same way as the spherulitic pores but particles form due to separation and rupture of the lamellae.

High speed camera recordings demonstrated quick and complete disintegration of lyophilisates frozen in liquid nitrogen into voluminous particles. Consequently, the directional lamellar pore structure of the cake can easily disaggregate into particles without the need of superfine breakup. SEM showed highly porous particle agglomerates with a huge geometric size of about 110 µm but an aerodynamic size in the respirable size range. Therefore, these porous particles must have a very small density. The harder samples of vacuum-induced or precooled shelf freezing disintegrated first into smaller pieces, from which fine particles were scaled off continuously. SEM revealed that cakes from vacuum-induced freezing disintegrated also into porous particles which had a bigger geometric size of about 80 µm compared to the conventionally frozen samples with a geometric particle size of approx. 20 µm. Porous particles with a big geometric size and a low density are therefore advantageous for a high ED and FPF, which can be most effectively achieved by freezing by immersion in liquid nitrogen prior to lyophilization. It has been already demonstrated in literature that porous particles can be efficiently aerosolized from standard DPIs, exhibiting elevated respirable fractions. These porous particles were produced by spray drying [36].

Despite good performance of the sample frozen in liquid nitrogen, one should consider that freezing sensitive proteins by immersing the vial in liquid nitrogen can result in increased protein aggregation or decreased enzyme activity compared to a slow cooling rate [37]. The reason for this is the formation of higher surface areas by quench freezing [35], resulting in increased surface denaturation at the ice-water interface. A protection can be achieved by the addition of surfactants as cryoprotectants [37]. Furthermore, freezing in liquid nitrogen is not appropriate for full-scale GMP production of sterile pharmaceuticals [34]. Vacuum-induced freezing, in contrast, can be considered more suitable for production scale.

5 SUMMARY AND CONCLUSION

This study demonstrates two methods for a successful improvement of the FPF of a lyophilization-based novel formulation for inhalation. This includes the addition of excipients, as well as the variation of the lyophilisate structure by varying the freezing method. It was also possible to demonstrate some underlying mechanisms responsible for the improved disintegration and aerosolization behavior of the lyophilized formulations. Furthermore, storage stability and unchanged aerosolization property of a selected formulation was demonstrated.

In summary, the FPF of lyophilized lysozyme formulations could be enhanced by addition of the crystalline excipients phenylalanine or valine. The amount of excipient added was less important. The crystalline excipients improved the fracture properties of the lyophilisate and enhanced its dispersibility and fine particle output. Additionally, crystals possibly coated with a thin layer of amorphous material resulted in a rough surface of the fragments which reduced particle aggregation and adhesion to vial and capillary surfaces and therefore enhanced the ED.

Storage at 25°C/60% RH and 40°C/75% RH for three months demonstrated physical stability and unchanged aerosolization performance, despite a slight increase in the moisture content. Possibly, the crystalline excipients served as mechanical stabilizers.

Different freezing methods resulted not only in different pore structures of the lyophilisates but also in a variation of the mechanical properties as well as in the aerosolization behavior. A further improvement of the FPF of lyophilized lysozyme formulated with phenylalanine or valine could be achieved by freezing in liquid nitrogen or by vacuum-induced freezing at -3°C. Considering the mechanical behavior of these different frozen lyophilisates, it was obvious that not only improved fracture properties of the lyophilisates can have an enhancing effect on the fine particle output. In addition, a special structure, such as the fine directional lamellar pore structure resulting from freezing in liquid nitrogen, could positively affect the ED and FPF. This special structure disaggregated quickly and completely into particles having good aerodynamic properties without the need of superfine breakup. The resulting fine particles had a geometric size of about 110 µm but an aerodynamic size in the respirable size range because of a low density and high porosity.

In conclusion, the novel formulation for inhalation based on dispersion of lyophilisates enabled an improvement of the FPF by different strategies. This included the utilization of excipients showing good disintegration properties as well as the variation of the lyophilization process. The freezing method, in particular, resulted in a variation of the lyophilisate structure and thereby affected its aerosolization properties.

6 REFERENCES

[1] S.P. Newman, W.W. Busse, Evolution of dry powder inhaler design, formulation, and performance, Respir. Med., 96 (2002) 293-304.

[2] H.W. Frijlink, A.H. De Boer, Dry powder inhalers for pulmonary drug delivery, Expert Opin. Drug Deliv., 1 (2004) 67-86.

[3] M.T. Newhouse, N.P. Nantel, C.B. Chambers, B. Pratt, M. Parry-Billings, Clickhaler (a Novel Dry Powder Inhaler) Provides Similar Bronchodilation to Pressurized Metered-Dose Inhaler, Even at Low Flow Rates, Chest, 115 (1999) 952-956.

[4] G.R. Pitcairn, T. Lankinen, O.-P. Seppälä, S.P. Newman, Pulmonary Drug Delivery from the Taifun Dry Powder Inhaler Is Relatively Independent of the Patient's Inspiratory Effort, J. Aerosol Med., 13 (2000) 97-104.

[5] N. Islam, E. Gladki, Dry powder inhalers (DPIs) - A review of device reliability and innovation, Int. J. Pharm., 360 (2008) 1-11.

[6] M. Tobyn, J.N. Staniforth, D. Morton, Q. Harmer, M.E. Newton, Active and intelligent inhaler device development, Int. J. Pharm., 277 (2004) 31-37.

[7] D.R. Owens, B. Zinman, G. Bolli, Alternative routes of insulin delivery, Diabetic Med., 20 (2003) 886-898.

[8] N.Y.K. Chew, H.-K. Chan, The Role of Particle Properties in Pharmaceutical Powder Inhalation Formulations, J. Aerosol Med., 15 (2002) 325-330.

[9] A. Chow, H. Tong, P. Chattopadhyay, B. Shekunov, Particle Engineering for Pulmonary Drug Delivery, Pharm. Res., 24 (2007) 411-437.

[10] C. Yamashita, A. Akagi, Y. Fukunaga, Dry powder inhalation system for transpulmonary administration, in: United States Patent 7735485 2010.

[11] F. Franks, Freeze-drying of bioproducts: putting principles into practice, Eur. J. Pharm. Biopharm., 45 (1998) 221-229.

[12] A. Hottot, S. Vessot, J. Andrieu, Freeze drying of pharmaceuticals in vials: Influence of freezing protocol and sample configuration on ice morphology and freeze-dried cake texture, Chem. Eng. Process., 46 (2007) 666-674.

[13] J. Liu, Physical Characterization of Pharmaceutical Formulations in Frozen and Freeze-Dried Solid States: Techniques and Applications in Freeze-Drying Development, Pharm. Dev. Technol., 11 (2006) 3-28.

[14] J.C. Kasper, W. Friess, The freezing step in lyophilization: Physico-chemical fundamentals, freezing methods and consequences on process performance and quality attributes of biopharmaceuticals, Eur. J. Pharm. Biopharm., 78 (2011) 248-263.

[15] T.W. Patapoff, D.E. Overcashier, The Importance of Freezing on Lyophilization Cycle Development, BioPharm Int., March 2002 (2002) 16–21, 72.

[16] J.A. Searles, J.F. Carpenter, T.W. Randolph, The ice nucleation temperature determines the primary drying rate of lyophilization for samples frozen on a temperature-controlled shelf, J. Pharm. Sci., 90 (2001) 860-871.

[17] J. Liu, T. Viverette, M. Virgin, M. Anderson, P. Dalal, A Study of the Impact of Freezing on the Lyophilization of a Concentrated Formulation with a High Fill Depth, Pharm. Dev. Technol., 10 (2005) 261-272.

[18] S.D. Webb, J.L. Cleland, J.F. Carpenter, T.W. Randolph, Effects of annealing lyophilized and spray-lyophilized formulations of recombinant human interferon-γ, J. Pharm. Sci., 92 (2003) 715-729.

[19] K. Ulubayram, I. Eroglu, N. Hasirci, Gelatin Microspheres and Sponges for Delivery of Macromolecules, J. Biomater. Appl., 16 (2002) 227-241.

[20] United States Pharmacopeia 36 Chapter 601 - Physical tests and determinations: Aerosols, Nasal Sprays, Metered-Dose Inhalers, and Dry Powder Inhalers, in, United States Pharmacopoial Convention Inc., 2012.

[21] X. Tang, M. Pikal, Design of Freeze-Drying Processes for Pharmaceuticals: Practical Advice, Pharm. Res., 21 (2004) 191-200.

[22] M.J. Pikal, S. Shah, Moisture transfer from stopper to product and resulting stability implications, Dev. Biol. Stand., 74 (1992) 165-177; discussion 177-169.

[23] M. Mattern, G. Winter, U. Kohnert, G. Lee, Formulation of Proteins in Vacuum-Dried Glasses. II. Process and Storage Stability in Sugar-Free Amino Acid Systems, Pharm. Dev. Technol., 4 (1999) 199-208.

[24] M.J. Akers, N. Milton, S.R. Byrn, S.L. Nail, Glycine Crystallization During Freezing: The Effects of Salt Form, pH, and Ionic Strength, Pharm. Res., 12 (1995) 1457-1461.

[25] F. Franks, T. Auffret, Freeze-Drying of Pharmaceuticals and Biopharmaceuticals, RSC Publishing, Cambridge, UK, 2007.

[26] K. Chatterjee, E.Y. Shalaev, R. Suryanarayanan, Partially crystalline systems in lyophilization: I. Use of ternary state diagrams to determine extent of crystallization of bulking agent, J. Pharm. Sci., 94 (2005) 798-808.

[27] R. Mohan, K.-K. Koo, C. Strege, A.S. Myerson, Effect of Additives on the Transformation Behavior of l-Phenylalanine in Aqueous Solution, Ind. Eng. Chem. Res., 40 (2001) 6111-6117.

[28] C. Roth, G. Winter, G. Lee, Continuous measurement of drying rate of crystalline and amorphous systems during freeze-drying using an in situ microbalance technique, J. Pharm. Sci., 90 (2001) 1345-1355.

[29] D.L. French, D.A. Edwards, R.W. Niven, The influence of formulation on emission, deaggregation and deposition of dry powders for inhalation, J. Aerosol Sci., 27 (1996) 769-783.

[30] C. Weiler, M. Egen, M. Trunk, P. Langguth, Force control and powder dispersibility of spray dried particles for inhalation, J. Pharm. Sci., 99 (2010) 303-316.

[31] Stability Testing of New Drug Substances and Products Q1A(R2), in, International Confernece on Harmonisation of technical requirements for registration of pharmaceuticals for human use 2003.

[32] J.C. Kasper, D. Schaffert, M. Ogris, E. Wagner, W. Friess, Development of a lyophilized plasmid/LPEI polyplex formulation with long-term stability—A step closer from promising technology to application, J. Control. Release, 151 (2011) 246-255.

[33] Y. Roos, M. Karel, Plasticizing Effect of Water on Thermal Behavior and Crystallization of Amorphous Food Models, J. Food Sci., 56 (1991) 38-43.

[34] J.A. Searles, Freezing and Annealing Phenomena in Lyophilization, in: L. Rey, J.C. May (Eds.) Freeze-Drying/Lyophilization of Pharmaceutical and Biological Products, Marcel Dekker, Inc., New York - Basel, 2004.

[35] C.C. Hsu, H.M. Nguyen, D.A. Yeung, D.A. Brooks, G.S. Koe, T.A. Bewley, R. Pearlman, Surface Denaturation at Solid-Void Interface—A Possible Pathway by Which Opalescent Participates Form During the Storage of Lyophilized Tissue-Type Plasminogen Activator at High Temperatures, Pharm. Res., 12 (1995) 69-77.

[36] R. Vanbever, J.D. Mintzes, J. Wang, J. Nice, D. Chen, R. Batycky, R. Langer, D.A. Edwards, Formulation and Physical Characterization of Large Porous Particles for Inhalation, Pharm. Res., 16 (1999) 1735-1742.

[37] B.S. Chang, B.S. Kendrick, J.F. Carpenter, Surface-induced denaturation of proteins during freezing and its inhibition by surfactants, J. Pharm. Sci., 85 (1996) 1325-1330.

Chapter 6

Effect of Variation of the Lyophilisate Morphology on the Fine Particle Fraction

Abstract

New inhaler devices as well as innovative dry powder formulations are important areas of research in advanced pulmonary drug delivery. A novel dry powder inhalation system based on dispersion of lyophilisates is an interesting technology which was proposed recently. Produced via freeze-drying, the system offers the possibility to adapt the inhaled powder quality by varying the characteristics of the coherent bulk from which the aerosol is produced. Lyophilisates of several model compounds including phenylalanine, valine, lactose, trehalose, and cromolyn sodium were investigated. Variations of the solid matrix structure of the lyophilisate were achieved by changing the freezing procedure as part of the lyophilization process and by addition of tertiary butyl alcohol as co-solvent. The applied freezing methods enabled to generate different pore structures of the lyophilisates, which again allowed variation of the mechanical properties of the lyophilisates. Only strong changes in the solid matrix characteristics, such as a lamellar-oriented morphology or a loss of the ordered structure by consolidation compared to the conventional spherulitic morphology, caused significant changes in the aerosolization performance. Samples comprising a fine lamellar pore morphology (by freezing in liquid nitrogen) were beneficial with respect to emitted dose (ED) and predominantly also with respect to fine particle fraction. The ED of liquid nitrogen frozen valine cakes, for example, increased to 85% and the FPF doubled. Lactose, trehalose, and phenylalanine cakes rendered also an increased ED to 78%, 56%, and 72%, respectively. This special structure disaggregated quickly and completely into large, highly porous particles with good aerodynamic properties, despite of an elastic behavior of the lyophilisate. The addition of tertiary butyl alcohol in the range of 5% to 20% as a co-solvent led to large needle-shaped ice crystals resulting in an elastic, lamellar structure and in most cases also increased ED of larger particles. Cromolyn sodium samples prepared from 5% to 20% TBA

solutions exhibited an increased ED of approx. 70% compared to 48% for the water based lyophilisate. Overall, this study also revealed a great influence of the material property, when comparing the different compounds tested, on the lyophilisate characteristics and the aerosolization performance.

1 INTRODUCTION

For the successful development of dry powder inhalation products (DPIs), the focus has to be on both the inhaler device and on the powder formulation [1, 2]. With regard to novel, improved powder formulations, a variety of new particle engineering methods emerged such as direct controlled crystallization, spray drying and spray freeze-drying, particle formation from liquid dispersed systems as well as supercritical fluid technologies [1]. For DPIs, the disadvantage of inspiratory flow-dependent de-agglomeration of the powder [3] of the mainly breath-activated passive devices was compensated by the introduction of active inhaler devices. These devices use, for example, compressed air (Nektar Pulmonary Inhaler [4] or Aspirair [5]), a pressurized gas (Pressurized Aerosol Dry-Powder Device [6]), or a high frequency piezoelectric vibrator (MicroDose DPI [7]) for powder deagglomeration and aerosolization. The combination of an active device with appropriate formulation technologies offers a promising approach to minimize patient to patient variation and improve efficacy across the full range of patient groups [5]. Yamashita et al. [8] introduced a new active system for disintegration of a freeze-dried product into inhalable particles by impacting air at the time of inhalation. The formulation is thereby stored as a coherent bulk, avoiding formulation problems like poor flowability and redispersibility of powders. Freeze-drying as a manufacturing process entails on the one hand accurate dose metering, high preparation yield, and suitability for thermolabile (bio)pharmaceuticals but on the other hand it is energy intensive and time consuming [9]. Additionally, it could possess the disadvantage of batch nonuniformity according to the stochastic nature of ice crystallization [10]. Freezing fixes the ice crystal structure and determines cake appearance by the retention of the solid matrix. Therefore, freezing is a very critical step in the freeze-drying process [11]. During the disintegration process, the lyophilisate structure is completely destroyed and fragments of the former pore walls form agglomerative particles with a new morphology (Chapter 3). If changes in the matrix morphology affect the aerosolization process, this characteristic could potentially be used for an intentional variation and possibly for an optimization of the fine particle output. The impact of several freezing process variations on the matrix morphology is

already described in the literature and in Chapter 5. The most prevalent freezing method used in the pharmaceutical industry is shelf-ramped freezing [12]. It shows a low ice nucleation temperature and fast ice crystal growth resulting in a high number of small spherulitic ice crystals. Equilibration of the vials at a lowered shelf temperature or two-step freezing with a "supercooling" holding is a modification of the shelf-ramped freezing process to obtain a more homogeneous temperature distribution across the total fill volume and thus freezing [11, 13]. Annealing is a secondary holding step after an initial freezing at a temperature above the final freezing temperature and is generally performed to allow for complete crystallization of crystalline components [13]. The annealing step enables also a rearrangement and further ice crystal growth [14]. For freezing on a precooled shelf, higher nucleation temperatures as well as slower freezing rates from vial bottom to top compared to shelf-ramped freezing are observed and result in a large heterogeneity between vials [10]. The temperature gradient inside the sample leads to smaller pores at the bottom and larger pores near the top [15]. Immersion of vials in liquid nitrogen is a very fast cooling method where freezing occurs by directional solidification, resulting in small lamellar-oriented pores [16]. Vacuum-induced freezing allows controlled ice nucleation at a defined temperature. The ice nucleation starts at the top surface, followed by a top-down freezing resulting in vertical ice crystals [11]. Besides different freezing processes, the presence of high melting point solvents such as tertiary butyl alcohol (TBA) results in solvent crystallization between the ice matrix altering the crystal habit of the formed ice [17]. Depending on the TBA concentration, the freezing of the co-solvent system results in crystals of different size and shape [18]. The aim of this study was to evaluate the impact of different lyophilisate morphologies on their aerosolization performance and applicability for dry powder inhalation. Therefore, six different freezing methods as part of the lyophilization process were applied using solutions of several model substances (valine, phenylalanine, lactose, trehalose and cromolyn sodium). The morphology and the mechanical properties of the lyophilisates were analyzed. The aerosolization performance was assessed by the use of high speed camera recordings, emitted dose (ED), and fine particle fraction (FPF) analysis as well as investigation of particle morphology. In a second approach, several TBA/water co-solvent systems were evaluated according to their ability to change lyophilisate properties and aerosolization performance. In order to possibly explain material related differences in lyophilisate characteristics and aerosolization performance of different substances, mechanical properties of the pulverized freeze-dried substances were additionally evaluated by compaction analysis.

2 MATERIALS AND METHODS

2.1 MATERIALS

Substances used in this study were L-valine (Val), lactose-monohydrate (Lac), cromolyn sodium (CS) (all Fagron GmbH&Co. KG, Barsbüttel, Germany), L-phenylalanine (Phe) (Merck KGaA, Darmstadt, Germany) and trehalose (Tre) (Hayashibara Co Ltd, Okayama, Japan). Solutions were prepared with highly purified water (Purelab Plus, Elga LabWater, Celle, Germany).

2.2 FORMULATION PREPARATION (AQUEOUS SOLUTIONS)

1 ml aqueous solutions of 12 mg/ml of valine, lactose, trehalose and cromolyn sodium or 8 mg/ml of phenylalanine was filled into 2R glass vials (Fiolax® clear, Schott AG, Müllheim, Germany) and vials were equipped with rubber stoppers (1079-PH 701/40/ow/wine-red, West Pharmaceutical Services, Eschweiler, Germany). Freeze-drying was carried out in a laboratory scale freeze-drier (Lyostar II, FTS Systems, Stone Ridge, NY, USA). The samples were frozen at -1°C/min to -45°C for 1 h. Primary drying was performed at a shelf temperature of -15°C (shelfs were ramped at +0.2°C/min) and a pressure of 100 mtorr for 30 h. For secondary drying the shelf temperature was increased to +30°C at a ramp rate of +0.1°C/min for 10 h. Five additional freezing methods were tested and compared to the standard procedure:

- Shelf-ramped freezing including two holding steps: The samples were frozen at -1°C/min to -45°C including 30 min holding steps at 5°C and -5°C.
- Annealing at -10°C for 10 h: The samples were frozen at -1°C/min to -45°C with a hold at -45°C for 1 h, followed by a shelf temperature increase to -10°C at +1°C/min and annealing for 10 h at -10°C before the samples were frozen again at -1°C/min to -45°C with another hold at -45°C for 1 h.
- Precooled shelf at -70°C: The samples were placed on a precooled shelf at -70°C for 1.5 h.
- Freezing in liquid nitrogen: Samples were immersed in liquid nitrogen for 1 min and were subsequently placed on a precooled shelf at -45°C.
- Vacuum-induced freezing at -3°C: The samples were equilibrated on the shelfs at -3°C for 1 h. According to [11] the chamber was evacuated as fast as possible to 600 mtorr

to induce freezing. Subsequently, the shelf temperature was decreased to -45°C for 1 h at -3.5°C/min.

2.3 FORMULATION PREPARATION (TBA/WATER CO-SOLVENT SYSTEMS)

Four different TBA/water co-solvent systems were produced by mixing TBA (Sigma-Aldrich Chemie GmbH, Steinheim, Germany) with highly purified water at 5%, 10%, 20% or 70% w/w TBA. Formulations were prepared by solving cromolyn sodium or valine at 12 mg/ml or 8 mg/ml trehalose in the different co-solvent systems. In each case 1 ml of the formulation was filled into 2R glass vials, equipped with rubber stoppers and freeze-dried using shelf-ramped freezing including two holding steps as described above.

2.4 X-RAY DIFFRACTOMETRY (XRD)

The lyophilisates were investigated with a Seifert X-ray diffractometer XRD 3000 TT (Seifert, Ahrensburg, Germany) equipped with a copper anode (40 kV, 30 mA, wavelength 154.17 pm). The samples were measured from 5 – 40° 2-Θ at a step rate of 0.05° 2-Θ with 2 s measuring time per step.

2.5 MECHANICAL TESTING OF LYOPHILISATES

The mechanical properties of the lyophilisates were investigated using a Texture Analyzer (TA.XT.plus, Stable micro Systems, Godalming, United Kingdom) equipped with a 5 kg load cell and a cylindrical stainless steel probe with a diameter of 5 mm at a test speed of 1 mm/s and a maximal immersion into the lyophilisate of 5 mm.

2.6 DEVICE

The lyophilized formulations were dispersed into aerosols using a custom-designed inhaler (Chapter 2). Briefly, it consists of two capillaries with a diameter of 0.75 mm pierced through the stopper of the vial housing the lyophilisate. One capillary is the air inlet, the other capillary the air outlet, which is connected to the mouthpiece. Compressed air is stored in a 20 ml pressure reservoir at a pressure of 3 bar. Pressing a lever releases the compressed air through the inlet capillary, thereby starting dispersion of the powder.

2.7 FINE PARTICLE FRACTION (FPF) ANALYSIS

The FPF was measured using a short stack version of the Andersen cascade impactor (ACI) (8-Stage Non-Viable Sampler Series 20-800, Thermo Andersen, Smyrna, GA, USA) at a flow rate of 39 l/min (corresponds to a pressure drop of 4 kPa with the HandiHaler®). Baffle plates were coated with a solution of 83% glycerin (AppliChem GmbH, Darmstadt, Germany), 14% ethanol (central supply LMU, Munich, Germany) and 3% Brij 35 (Serva Electrophoresis GmbH, Heidelberg, Germany). Filters used were type A/E glass fiber filters 76 mm (Pall Corporation, Ann Arbor, MI, USA). By removing stages 2 to 7, the whole FPF (particle fraction <4.94 µm) is collected on the filter directly below stage 1 and can easily be quantified by weighing the filter before and after powder deposition. The emitted dose (ED) was measured by weighing the vial before and after aerosolization and calculated as the percentage of the metered dose (MD). The FPF was calculated as the percentage of the ED and of the MD. The measurements were performed in triplicate.

2.8 MICROSCOPY

The morphology of the lyophilisates was analyzed by digital light microscopy (VHX-500F, Keyence Corporation, Osaka, Japan) equipped with a VH-Z20R objective with variable lighting.

The particle morphology of the dispersed fine particles was analyzed with a Jeol Scanning Electron Microscope (JSM-6500F, Jeol, Ebersberg, Germany) at 5 kV. Sample preparation was performed using a second short stack version of the ACI where stages 3 to 7 have been removed. Conductive self-adhesive tape (Ø 12 mm Leit-Tabs, Plano GmbH, Wetzlar, Germany) was placed on the coated baffle plate after stage 2. The particles collected on the tape therefore have an aerodynamic cut off diameter between 4-4.94 µm at a flow rate of 39 l/min (Chapter 3). The samples were sputtered with carbon under vacuum.

2.9 HIGH SPEED CAMERA RECORDING

The aerosolization behavior of the lyophilisates in the vial was recorded using a Fastcam 1024 PCI (Photron, San Diego, CA, USA) with a sample rate of 1000 fps.

2.10 MECHANICAL PROPERTY TESTING OF FREEZE-DRIED SUBSTANCES VIA COMPACTION

5 ml of higher concentrated aqueous solutions of valine (50 mg/ml), phenylalanine (20 mg/ml), lactose (100 mg/ml), trehalose (100 mg/ml), and cromolyn sodium (100 mg/ml) were filled into 10R glass vials (Fiolax® clear, Schott AG, Müllheim, Germany) equipped with rubber stoppers (1319 PH 4023/50, gray, 20 mm, West Pharmaceutical Services, Eschweiler, Germany) and freeze-dried. The samples were frozen at -1°C/min to -45°C for 2.5 h. Primary drying was performed at a shelf temperature of -18°C (shelfs were ramped at +0.1°C/min) and a pressure of 100 mtorr for 50 h. For secondary drying the shelf temperature was increased to +30°C at a ramp rate of +0.1°C/min for 10 h.

The mechanical properties of the freeze-dried solid substances were analyzed with a compaction simulator (Flexitab®, Röltgen GmbH & Co. KG, Solingen, Germany) at a compression pressure of approx. 18 kN. The lyophilisates were scraped out of the vials and 150-300 mg powder was filled into a 10 mm cylindrical biplane die while the lower indenter was positioned at -8.5 mm. To facilitate compaction of freeze-dried lactose and trehalose, the die was lubricated with oleic acid. During compression, compact heights and compression loads were measured. These recorded data of the compaction process and the measured true density (see below) were used to generate an "in die" Heckel plot for which the relative porosity (D_{rel}) was plotted against the applied pressure (P). The Heckel parameters were determined by regression analysis of the terminal linear part of the compression phase of the Heckel plot. The slope of the linear regression is the Heckel constant (k) and A the intercept according to:

$$\ln\left(\frac{1}{1-D_{rel}}\right) = k * P + A$$

The mean yield pressure is inversely proportional to the slope and renders the material's resistance to deformation. The elastic recovery is calculated as the compact height during decompression related to the minimum compact height in percent. Relaxation is the increase of compact height in percent after the maximum pressure was reached. Six compaction analyses were performed for each substance.

The true density of the powder was assumed to be equal to the density after compaction at approx. 50 kN, calculation using the dimensions at maximum pressure and the weight of the compact. Measurements were performed in triplicate.

3 RESULTS

3.1 VARIATION OF THE FREEZING PROCESS

The freezing step is a key element in lyophilization [19] because the cake structure is controlled by the retention of the solid matrix structure formed by freezing [11]. A variation of the freezing process and thereby a variation of the ice crystal shape and dimensions determines size and morphology of the resulting pores. In this study different freezing methods were applied to solutions of the amino acids phenylalanine and valine, the sugars lactose and trehalose, as well as the model drug cromolyn sodium to evaluate influences of the freezing process on characteristics and ultimately the aerosolization behavior of these lyophilisates. Besides the conventional shelf-ramped freezing at -1°C/min, the following five additional freezing methods were selected: The addition of two holding steps at 5°C and -5°C (to ensure a better equilibration of the solution temperature), the addition of an annealing step at -10°C for 10 h, freezing on a precooled shelf at -70°C, freezing by immersion into liquid nitrogen, and vacuum-induced freezing at -3°C. An overview of the results is provided in Table 1.

At first, the physical state of the lyophilisates was characterized by XRD. Independent of the freezing process, the amino acid lyophilisates showed the crystalline peak pattern of valine and phenylalanine monohydrate, respectively. Valine demonstrated the characteristic main peaks at 7.45°, 14.75°, 22.2°, and 29.7° 2θ. The characteristic peaks of phenylalanine-monohydrate were located at 6.55, 14.85, 21.5, and 26.35° 2-θ. Freeze-dried lactose, trehalose, and cromolyn sodium were in all cases present in the amorphous state.

3.1.1 Microscopic appearance

For the normal shelf-ramped freezing at -1°C/min, microscopy revealed a sponge-like matrix with spherulitic pores at the top of the cake and the pore size between 70 and 170 µm depending on the substance. Valine and cromolyn sodium exhibited the smallest and phenylalanine the biggest pore diameters. The valine lyophilisate demonstrated a whitish crystalline skin on the top where crystals were partly arranged in rosettes. In comparison to the top, pores at the bottom of the cake were smaller with pore diameters of 30 to 40 µm except for the phenylalanine lyophilisate, which demonstrated both small pores and areas with pores of approximately 90 µm. Freezing with annealing caused a complete loss of the ordered spherulitic pore structure for lactose (Figure 1a) and trehalose lyophilisates with a translucent

Table 1: Tabular overview of the freezing process variation results

	-1°C/min	**-1°C/min with hold**	**annealing**	**precooled shelf**	**liquid nitrogen**	**vacuum induced**
Valine						
Physical state	crystalline	crystalline	crystalline	crystalline	crystalline	crystalline
Lyophilisate morphology	spherulitic	spherulitic	-	spherulitic	lamellar	spherulitic
Pore size [µm]	top: 65 bottom: 40	-	-	top: 70 bottom: 55	-	bottom: 60
Particle morphology	porous agglomerates	-	porous agglomerates	-	porous agglomerates	-
Particle size	61 µm	-	42 µm	-	80 µm	-
Mechanical testing	plateau at 0.004 N	plateau at 0.003 N	-	plateau at 0.003 N	slope of 0.001 N/mm	plateau at 0.006 N
Disintegration characteristics	fast and complete	fast and complete	-	fast and complete	fast and complete	fast and complete
ED	73%	77%	50%	71%	85%	67%
FPF (ED)	8%	9%	9%	9%	19%	10%
FPF (MD)	6%	7%	5%	6%	16%	7%
Lactose						
Physical state	amorphous	amorphous	amorphous	amorphous	amorphous	amorphous
Lyophilisate morphology	spherulitic	spherulitic	consolidated	spherulitic	lamellar	spherulitic
Pore size [µm]	top: 80 bottom: 40	-	top: 100	top: 104 bottom: 35	-	-
Particle morphology	porous agglomerates	-	Different shaped fragments	-	porous agglomerates	-
Particle size	35 µm	-	8 µm	-	82 µm	-
Mechanical testing	peak of max. 0.089 N	peak of max. 0.088 N	plateau at 0.006 N	peak of max. 0.105 N	slope of 0.035 N/mm	plateau at 0.025 N
Disintegration characteristics	separation into subunits and scaling off[l]	separation into subunits and scaling off[l]	fast and complete (finished after 100 ms)	separation into subunits and scaling off	fast and complete	fast and complete
ED	46%	46%	18%	40%	78%	46%
FPF (ED)	32%	34%	14%	31%	34%	26%
FPF (MD)	15%	16%	2%	12%	27%	12%
Trehalose						
Physical state	amorphous	amorphous	amorphous	amorphous	amorphous	amorphous
Lyophilisate morphology	spherulitic	spherulitic	consolidated	spherulitic	lamellar	spherulitic
Pore size [µm]	top: 110 bottom: 30	-	top: 140	top: 90 bottom: 25	-	-
Particle morphology	-	-	-	-	-	-
Particle size	-	-	-	-	-	-
Mechanical testing	peak of max. 0.113 N	peak of max. 0.088 N	plateau at 0.006 N	peak of max. 0.118 N	slope of 0.041 N/mm	plateau at 0.025 N
Disintegration characteristics	separation into subunits and scaling off[l]	separation into subunits and scaling off[l]	fast and complete (finished after 100 ms)	separation into subunits and scaling off	fast and complete	fast and complete
ED	41%	44%	13%	26%	56%	44%
FPF (ED)	38%	33%	19%	44%	41%	34%
FPF (MD)	16%	14%	2%	10%	23%	15%

	-1°C/min	-1°C/min with hold	annealing	precooled shelf	liquid nitrogen	vacuum induced
Phenylalanine						
Physical state	crystalline	crystalline	crystalline	crystalline	crystalline	crystalline
Lyophilisate morphology	spherulitic	spherulitic	spherulitic	spherulitic	lamellar	spherulitic
Pore size [µm]	top: 170 bottom: 30-40 / 90	-	top: 170 bottom: 110	top: 130 bottom: 35	-	top: 4 bottom: 100
Particle morphology	porous agglomerates	-	porous agglomerates	porous agglomerates	porous agglomerates	porous agglomerates
Particle size	70 µm	-	74 µm	68 µm	109 µm	91 µm
Mechanical testing	plateau at 0.067 N	plateau at 0.060 N	plateau at 0.079 N	plateau at 0.062 N	slope of 0.005 N/mm	peak of max. 0.108 N
Disintegration characteristics	separation into subunits and scaling off[1]	separation into subunits and scaling off[1]	separation into subunits and scaling off[1]	separation into subunits and scaling off	fast and complete	separation into subunits and scaling off[1]
ED	49%	43%	38%	63%	72%	68%
FPF (ED)	57%	59%	61%	45%	42%	55%
FPF (MD)	27%	25%	23%	29%	30%	36%
Cromolyn sodium						
Physical state	amorphous	amorphous	amorphous	amorphous	amorphous	amorphous
Lyophilisate morphology	spherulitic	spherulitic	spherulitic	lamellar (bottom to top)	lamellar (outside to middle)	spherulitic
Pore size [µm]	top: 80 bottom: 30	-	top: 50 bottom: 30	top: lamellar bottom: 14	-	top: 15 bottom: 90
Particle morphology	porous agglomerates	-	porous agglomerates	porous agglomerates	porous agglomerates	porous agglomerates
Particle size	44 µm	-	40 µm	75 µm	123 µm	58 µm
Mechanical testing	plateau at 0.135 N	plateau at 0.153 N	plateau at 0.121 N	slope of 0.062 N and 0.017 N	slope of 0.070 N	peak of max. 0.124 N
Disintegration characteristics	separation into subunits and scaling off[1]	separation into subunits and scaling off[1]	separation into subunits and scaling off[1]	fast and complete	fast and complete	separation into subunits and scaling off[1]
ED	67%	48%	37%	64%	68%	50%
FPF (ED)	28%	44%	45%	38%	18%	42%
FPF (MD)	19%	21%	16%	24%	12%	21%

[1]incomplete disintegration

skin on top of the cake. The structure of the valine lyophilisates could not be evaluated due to destruction during the ventilation process in the freeze-drier. For phenylalanine lyophilisates, the annealing process had no effect on the morphology except that the upper surface skin appeared thicker. Cromolyn sodium lyophilisates revealed a more homogenous pore size distribution after the annealing step (Figure 1b), with a mean pore diameter of 30 µm. After freezing on a -70°C precooled shelf most lyophilisates showed small spherulitic pores of 25-35 µm at the bottom and bigger pores of 73-100 µm near the top of the cake. The top layer of valine lyophilisates was again composed of crystal rosettes, whereas phenylalanine lyophilisates showed needle shaped furrows and the sugars lactose and trehalose showed

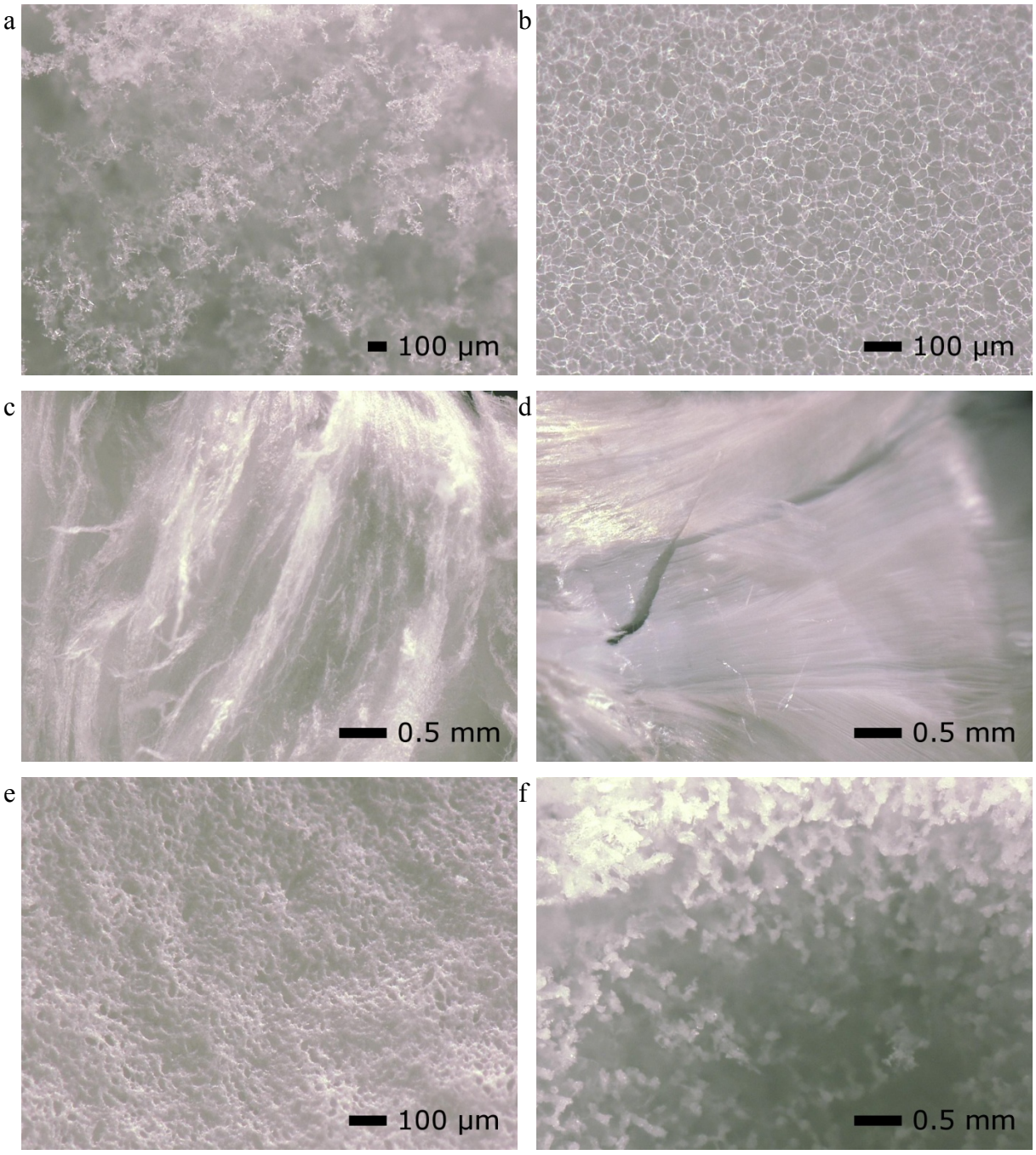

Figure 1: Microscopic appearance of lyophilisates: bottom of 12 mg/ml lactose frozen with annealing (a), bottom of 12 mg/ml cromolyn sodium frozen with annealing (b), cross section of 12 mg/ml cromolyn sodium frozen on a precooled shelf (c), cross section of 8 mg/ml phenylalanine frozen in liquid nitrogen (d), cromolyn sodium 12 mg/ml frozen vacuum induced (e) and lactose 12 mg/ml frozen vacuum induced (f).

rectangular pores on top of the cake. A cross sectional cut of cromolyn sodium lyophilisates demonstrated lamellar pores in the direction from bottom to top (Figure 1c) and also the upper surface showed a lamellar pore morphology, whereas the bottom of the cakes exhibited very small pores of around 14 µm. For all samples freezing by immersion into liquid nitrogen

resulted in a fine lamellar morphology in the direction from outside to inside. The cross sectional cut (exemplarily shown for phenylalanine in Figure 1d) showed directed narrow pores reaching from the walls of the vials towards the middle and finally upwards. Besides fine disruptions in lactose and trehalose lyophilisates, liquid nitrogen frozen cromolyn sodium cakes exhibited distinctive cracks directing from outside to the middle. Vacuum-induced freezing at -3°C resulted in a dense upper layer with small pores for cromolyn sodium (15 µm), phenylalanine (4 µm), and valine lyophilisates (not distinguishable). Lactose and trehalose lyophilisates demonstrated upward pointing villi on top of the cake and irregularly shaped oblong pores at the bottom. The inner pore structure of all lyophilisates is composed of spherulitic pores.

3.1.2 Mechanical characterization of the lyophilisates by indentation

In order to characterize the mechanical properties of the lyophilisates, texture analyzer measurements were performed. The cylindrical probe acts on the lyophilisate by proceeding at a constant speed. The resulting force needed for the immersion into the cake and therefore the force necessary for its breakage is recorded. For the normal shelf-ramped freezing process (Figure 2a), steady fracture of the lyophilisate at a constant force resulting in a plateau was found for valine, phenylalanine, and cromolyn sodium lyophilisates at 0.004 N, 0.067 N, and 0.135 N, respectively. For lactose and trehalose cakes, the immersion-force-curve rose until 1.7 mm immersion to 0.09 N and 0.11 N, followed by a decreasing force for the next 1 mm of immersion, thus demonstrating nonuniform fracture properties. Shelf-ramped freezing with two holding steps did not change the mechanical properties of all lyophilisates compared to the common shelf-ramped process apart from slightly different force values (Figure 2b). The annealing step (Figure 2c) caused a dramatic decrease of the force necessary to fracture lactose and trehalose cakes and a modification to steady fracture at 0.006 N. Valine lyophilisates were not measurable because of the destruction of the cake mentioned above. The mechanical properties of phenylalanine and cromolyn sodium lyophilisates were not substantially changed compared to the conventional shelf-ramped freezing. Precooled shelf freezing (Figure 2d) resulted in a variation of the mechanical properties only for cromolyn sodium lyophilisates. Instead of a plateau the force required for immersion into the lyophilisate showed a continuous incline, indicating an elastic behavior where mainly compression takes place. Similarly, all liquid nitrogen frozen lyophilisates (Figure 2e) demonstrated an immersion-force-curve with an almost constant increase as a result of an elastic structure. Thereby, the slope of the curve differed for different freeze-dried substances

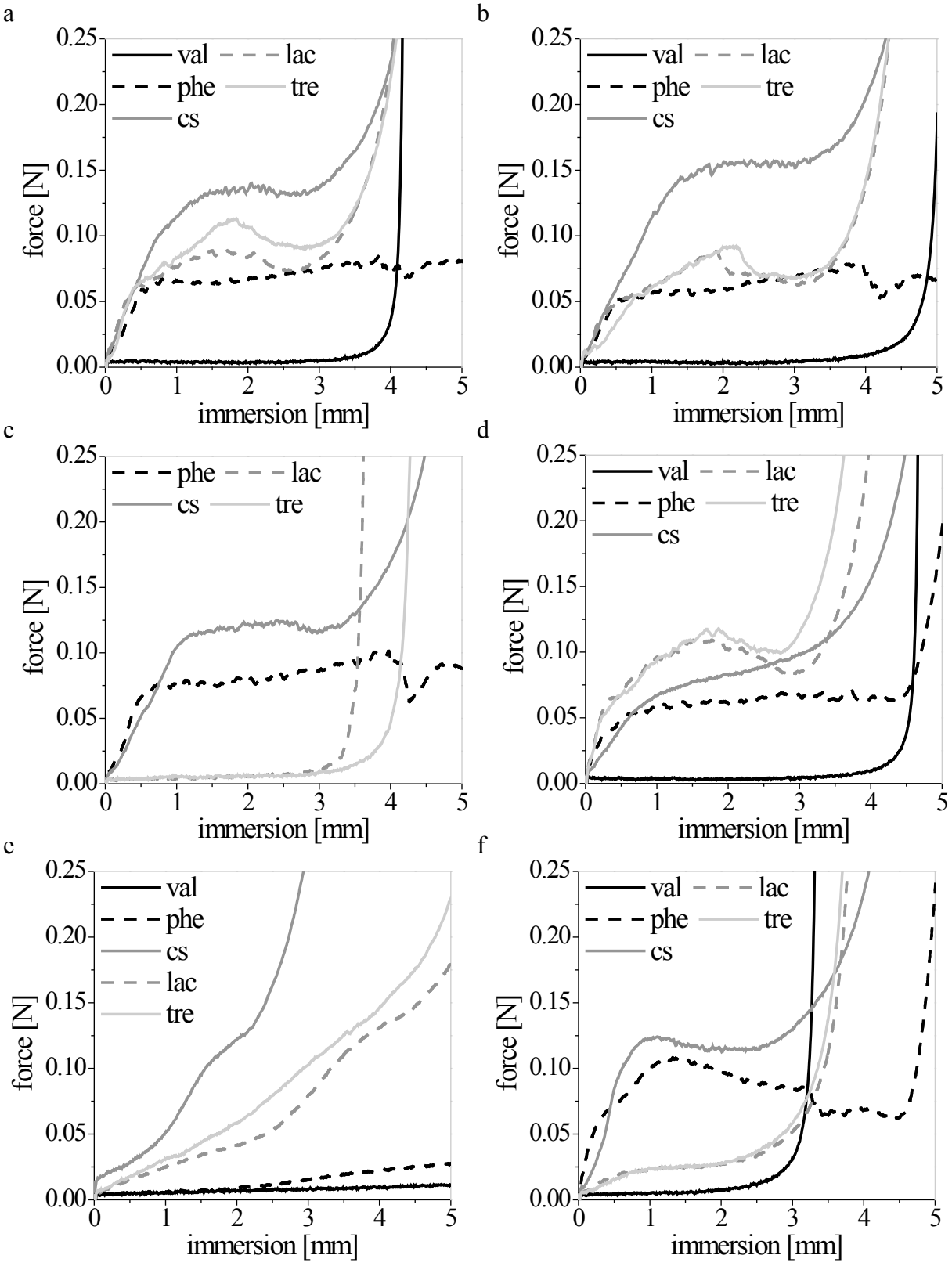

Figure 2: Mechanical testing of lyophilisates prepared with different freezing methods: shelf-ramped freezing (a), shelf-ramped freezing including two holding steps (b), shelf-ramped freezing including an annealing step (c), freezing on a precooled shelf (d), freezing in liquid nitrogen (e) and vacuum induced freezing (f).

as follows: 12 mg/ml valine lyophilisates 0.001 N/mm, 8 mg/ml phenylalanine lyophilisates 0.005 N/mm, 12 mg/ml lactose lyophilisates 0.035 N/mm, 12 mg/ml trehalose lyophilisates 0.041 N/mm, and 12 mg/ml cromolyn sodium lyophilisates 0.070 N/mm. After immersion of the probe an elastic relaxation of the compressed cakes occurred, which confirmed the elastic behavior. Vacuum-induced freezing showed again steady fracture at a constant force at 0.025 N, 0.025 N, and 0.006 N for lactose, trehalose and valine lyophilisates, respectively. For phenylalanine and cromolyn sodium lyophilisates, the required force for fracture increased at the beginning to 0.108 N and 0.124 N, followed by a decreasing force, demonstrating a harder top layer of the lyophilisate.

3.1.3 Aerosolization characteristics

The aerosolization of the lyophilisates into inhalable particles was achieved by a custom designed inhaler which uses compressed air for dispersion (see Chapter 2 for details). To analyze the impact of the freezing process on the aerosolization properties several characterization methods were applied. For visualization of the disintegration behavior of the lyophilisate in the vial, high speed camera recordings were performed. Figure 3 exemplarily shows the impact of the freezing process on the disintegration behavior of 12 mg/ml lactose lyophilisates. The cakes prepared by conventional shelf-ramped freezing were separated by the impacting and swirling air jet into two to three subunits, followed by a scaling off of fine particles (Figure 3a). This was the case for all lyophilisates prepared by conventional shelf-ramped freezing except for valine cakes, which showed fast and complete disintegration. After disintegration, particles swirled in the vial until their escape through the outlet capillary. At the end, a larger lyophilisate piece was not disintegrated completely and remained in the vial, except for valine cakes. The disintegration process for lyophilisates frozen via shelf-ramping including holding steps were comparable to the normal shelf ramped freezing for all substances (Figure 3b). Annealing revealed a disintegration behavior similar to normal freezing for phenylalanine and cromolyn sodium. Lactose and trehalose experienced a very fast and complete disintegration whereby almost all particles had left the vial already after 100 ms (Figure 3c). Valine lyophilisates were not taken into account due to the fact that the cake was already fragmented after the ventilation process in the freeze-drier. Precooled shelf freezing caused a fast and complete disintegration for cromolyn sodium lyophilisates. For all other substances the disintegration behavior was similar to the normal shelf-ramped freezing but with an always complete disintegration (Figure 3d). For all substances freezing in liquid nitrogen delivered cakes which showed very fast and complete disintegration into fibrous and

voluminous particles (Figure 3e). These particles partly collected in the top region of the vial before reentering the swirling air stream and finally escaping through the outlet capillary. Vacuum-induced freezing resulted in a fast and complete disintegration for valine, lactose, and trehalose lyophilisates (Figure 3f). A disintegration behavior similar to the conventional freezing process was demonstrated for phenylalanine and cromolyn sodium lyophilisates, whereby the cromolyn sodium lyophilisate disintegrated into more voluminous particles compared to cakes which had been conventionally frozen.

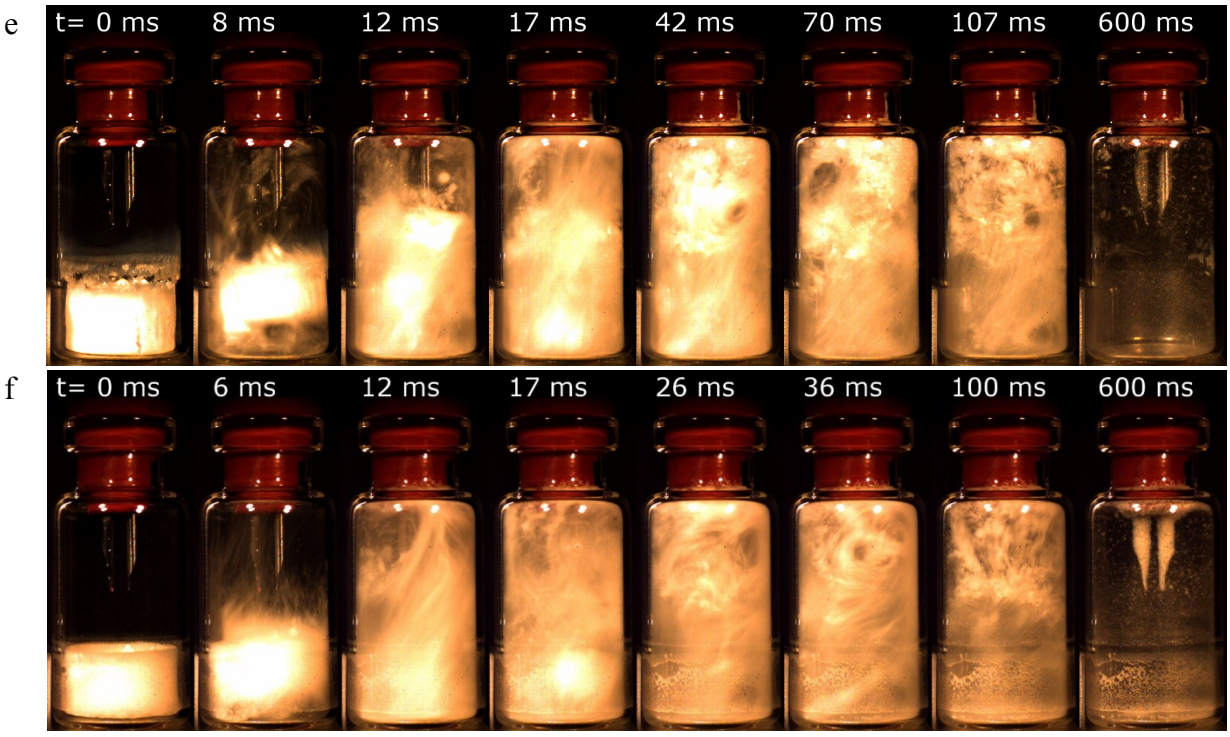

Figure 3: High speed camera recordings of lactose lyophilisates prepared with shelf-ramped freezing (a), shelf-ramped freezing including two holding steps (b), shelf-ramped freezing including an annealing step (c), freezing on a precooled shelf (d), freezing in liquid nitrogen (e) and vacuum induced freezing (f).

3.1.4 Aerosolization performance

Short stack ACI measurements were performed to evaluate the differently frozen lyophilisates with respect to ED and FPF. Figure 4 shows the ED-FPF-plots of the five substances prepared with different freezing processes. The ED is thereby plotted against the FPF related to ED (right y-axis). From the contour lines and the left y-axis, it is also possible to determine the FPF related to MD from the same plot. For valine, lactose, and trehalose lyophilisates freezing with holding steps, precooled shelf freezing, and vacuum-induced freezing had no significant influence on ED and FPF when compared to the conventional shelf-ramped freezing. The annealing step caused a reduction of the ED from 73% to 50% for valine lyophilisates and a decreased ED and FPF for lactose and trehalose cakes, resulting in a reduction of the FPF related to MD from about 15% to only 2%. Freezing in liquid nitrogen resulted in an increased ED for valine, lactose, and trehalose lyophilisates to 85%, 78%, and 56%, respectively. Additionally, the valine cakes exhibited a twofold elevation of the FPF related to ED. With respect to FPF related to ED, the various phenylalanine and cromolyn sodium lyophilisates showed a different outcome than valine, lactose, and trehalose

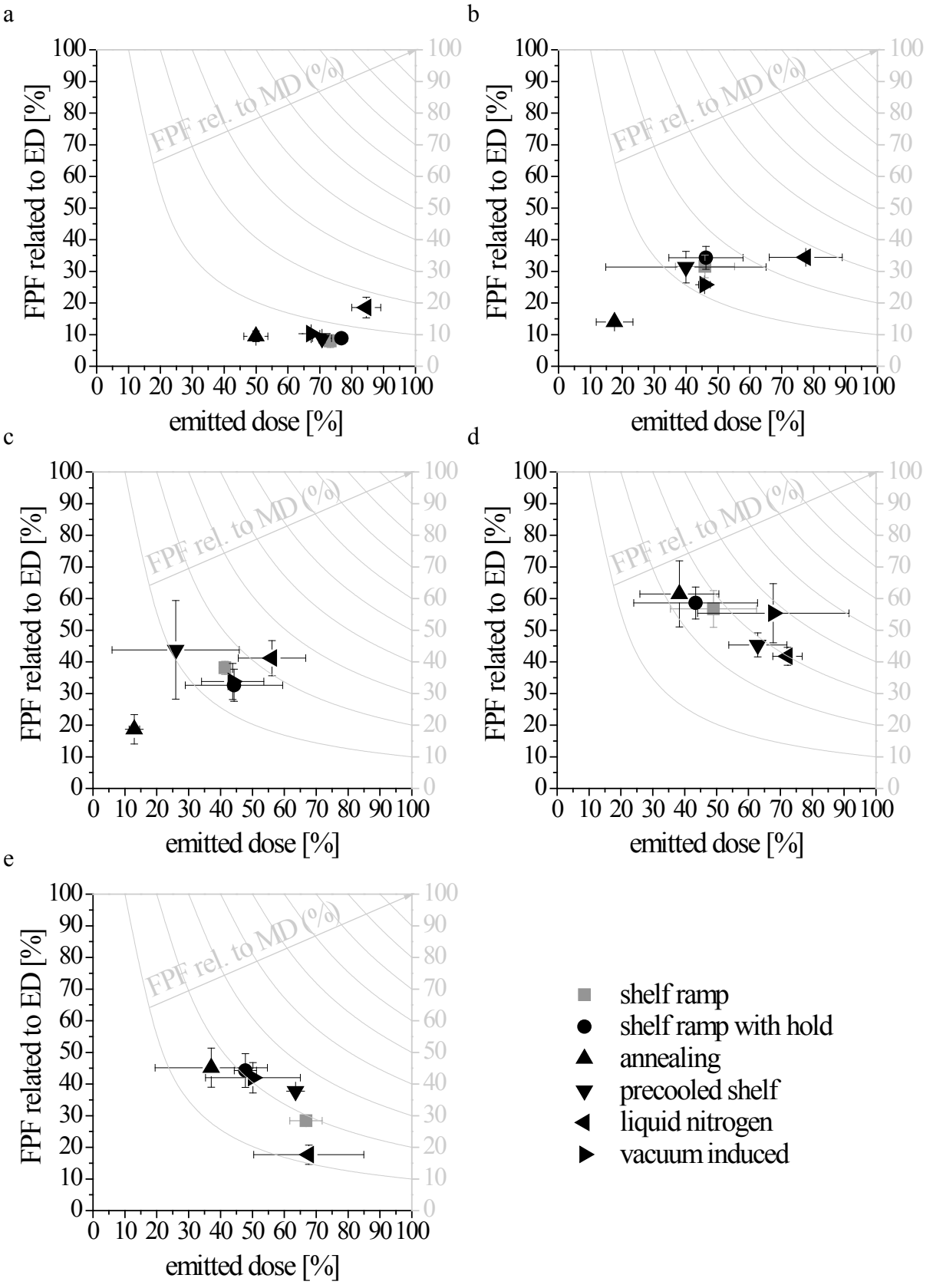

Figure 4: ED versus its related FPF as well as the FPF related to MD of 12 mg/ml valine (a), 12 mg/ml lactose (b), 12 mg/ml trehalose (c), 8 mg/ml phenylalanine (d) and 12 mg/ml cromolyn sodium lyophilisates (e) prepared with different freezing procedures.

lyophilisates. Phenylalanine lyophilisates showed a significant increase in the ED for the liquid nitrogen frozen lyophilisates from 49% to 72% but a decrease in FPF related to ED from 57% to 42%. Compared to the conventional shelf-ramped freezing method all other freezing processes had no significant influence on the ED. However, freezing with an annealing step rendered a change towards a smaller ED (38%). The cromolyn sodium lyophilisate frozen via shelf-ramping revealed a relatively high ED of 67% which could not be increased by changing the freezing process. Nevertheless, freezing in liquid nitrogen and precooled shelf freezing resulted in about the same ED but showed a reduction in FPF related to ED from 28% to 18% for liquid nitrogen freezing, whereas precooled shelf freezing exhibited a higher FPF related to ED of 38%. The cakes prepared with an annealing step demonstrated again a significant decrease in the ED to 37% but an increased FPF related to ED of 45%.

3.1.5 Particle characteristics

In order to analyze and compare the geometric particle sizes as well as the structural properties of the aerosolized particles they were investigated with SEM. For comparison of particles with identical aerodynamic size, the specimens were collected on the baffle plate after stage 2 of the ACI, which has an aerodynamic cut off diameter of 4 to 4.94 µm at a flow rate of 39 l/min. At the border of the impacted particle spots it was possible to observe particles which were clearly separated from each other. These isolated particles were used for comparison of geometric particle sizes and morphological properties. The particles were composed of agglomerates of smaller fragments. Particles generated from valine, lactose, and trehalose lyophilisates showed altered particle morphologies for those samples that demonstrated a different ED in comparison to shelf-ramped freezing. Exemplarily for lactose samples, Figure 5 shows an increasing geometric particle size with increasing ED in the following order: lyophilisates frozen with annealing (8 µm), frozen via shelf-ramping (35 µm), and frozen in liquid nitrogen (82 µm). Of particular note is thereby an increasing porosity combined with decreasing wall thickness of the fragments. The annealing step caused a wall thickness of approximately 1 µm, whereas freezing at -1°C/min resulted in approximately 0.6 µm and was again reduced to approx. 0.4 µm for freezing in liquid nitrogen. Variations in the particle morphologies were less pronounced for phenylalanine and cromolyn sodium lyophilisates. For phenylalanine lyophilisates, freezing in liquid nitrogen caused particle agglomerates of bigger geometric size and of higher porosity with more filigree structures, whereas the annealing step had no influence on the particle morphology.

For cromolyn sodium samples, precooled shelf freezing resulted in bigger geometric particle sizes compared to normal shelf-ramped freezing but similar structural properties, whereas freezing in liquid nitrogen led to even bigger particle sizes with a more porous particle morphology.

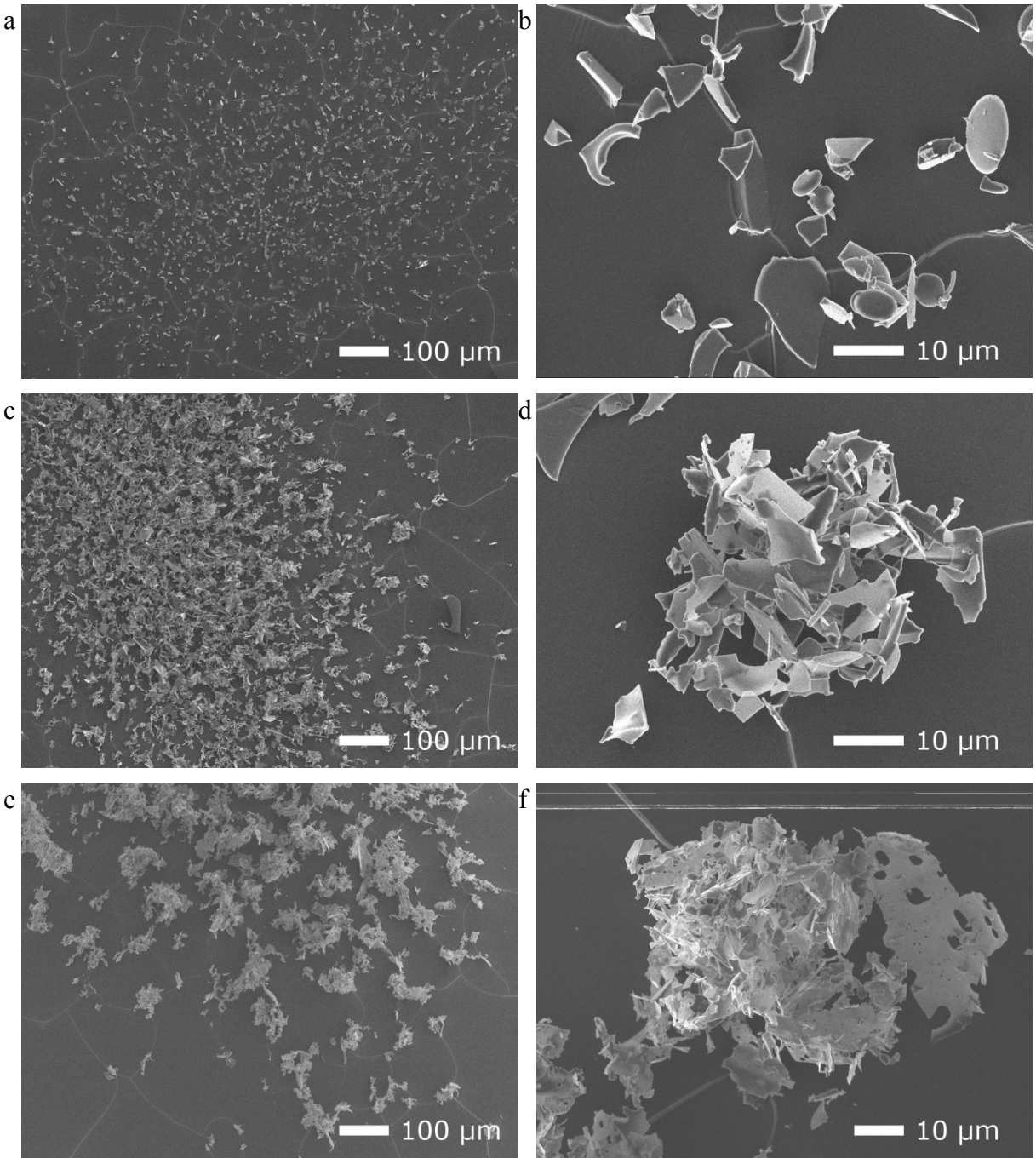

Figure 5: SEM structure of particles with an aerodynamic cut off diameter between 4 and 4.94 µm. Aerosolized 12 mg/ml lactose lyophilisates frozen with annealing (a/b), via shelf-ramping (c/d) or in liquid nitrogen (e/f).

3.2 CHANGING THE ICE CRYSTAL HABITUS USING TBA AS CO-SOLVENT

The great majority of lyophilized products are freeze-dried from aqueous solutions. The presence of an organic co-solvent has been shown to affect the freezing characteristics of the solution and to subsequently influence the drying rate and physical appearance of the freeze-dried product [20]. For the purpose of freeze-drying, the most favored co-solvent is TBA because it possesses miscibility with water, a high vapor pressure, freezes completely in most commercial freeze-dryers, can increase sublimation rates, and has low toxicity [17]. The size and shape of the ice crystals has been found to vary dependent on the concentration of the co-solvent [18]. In order to alter the lyophilisate morphology and evaluate the effect on characteristics and aerosolization behavior, 12 mg/ml solutions of cromolyn sodium and valine as well as 8 mg/ml solutions of trehalose with 5%, 10%, 20%, and 70% (w/w) TBA as co-solvent were prepared and freeze-dried. None of the substances was soluble in the 70% TBA/water co-solvent system, only cromolyn sodium formed a milky crystal suspension after ultrasonic treatment and was freeze-dried.

The morphology of the freeze-dried products was microscopically examined and is exemplarily presented for cromolyn sodium samples in Figure 6. In contrast to the aqueous lyophilisate with its spherulitic pore morphology (Figure 6a), the sample with 5% TBA showed large dendritic pore structures (Figure 6b). Samples with 10% and 20% TBA revealed long needle-shaped pores arranged in parallel, as can be seen from Figure 6c/d. A totally different appearance was found for the freeze-dried 70% TBA cromolyn sodium crystal suspension (Figure 6e/f). The top of the cake showed a coralline morphology composed of small spherulitic pores of approximately 25 µm in diameter which homogeneously distributed over the whole cake.

The mechanical properties of the lyophilisates obtained from TBA mixtures were characterized using the force necessary for a probe to penetrate into the cake. As already reported above, the aqueous cromolyn sodium, valine, and trehalose lyophilisates demonstrated steady fracture at a constant force resulting in a plateau at 0.153 N, 0.003 N, and 0.013 N, respectively. Samples obtained from 5%, 10%, or 20% TBA containing solutions, in contrast, showed an immersion-force-curve with a constant gradient, indicating an elastic structure as can be seen for cromolyn sodium lyophilisates in Figure 7. The slope of the curves increased with increasing TBA content from 0.020 to 0.071 N/mm. The 70% TBA sample in turn exhibited again steady fracture at a smaller force of 0.005 N. The 12 mg/ml valine and 8 mg/ml trehalose lyophilisates freeze-dried from a TBA/water co-solvent system

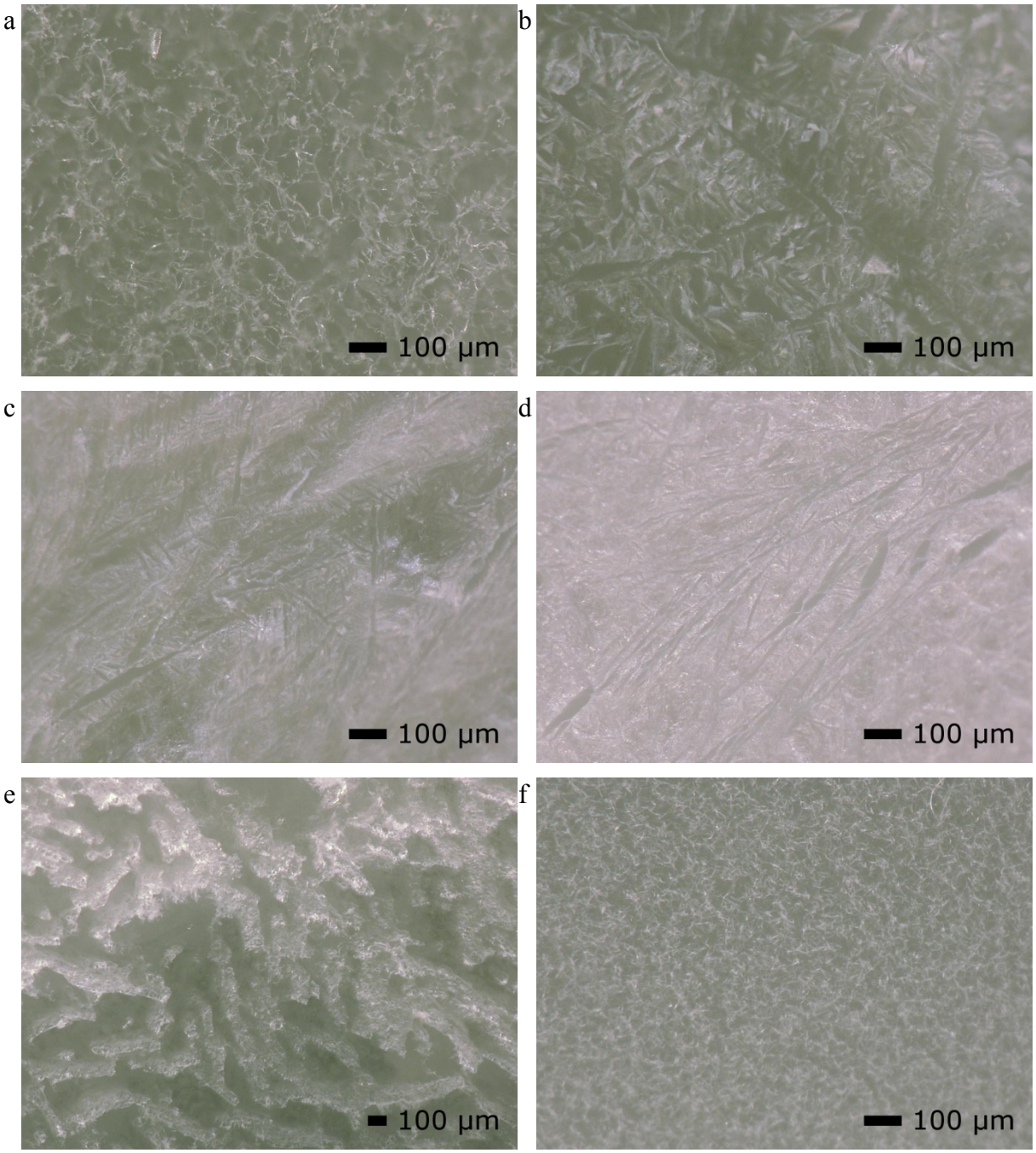

Figure 6: Microscopic appearance of freeze-dried TBA/water co-solvent systems. 12 mg/ml cromolyn sodium lyophilisates freeze-dried from aqueous solution (a), from the co-solvent system containing 5% TBA (b), 10% TBA (c), 20% (d) TBA or 70% TBA: top of the cake (e) and bottom of the cake (f).

demonstrated very soft properties which were below the texture analyzer's detection limit of 0.001 N. When doubling the solution concentration of valine to 24 mg/ml, the lyophilisates of the TBA/water co-solvent systems demonstrated also an immersion-force-curve with a constant gradient between 0.005 and 0.008 N/mm.

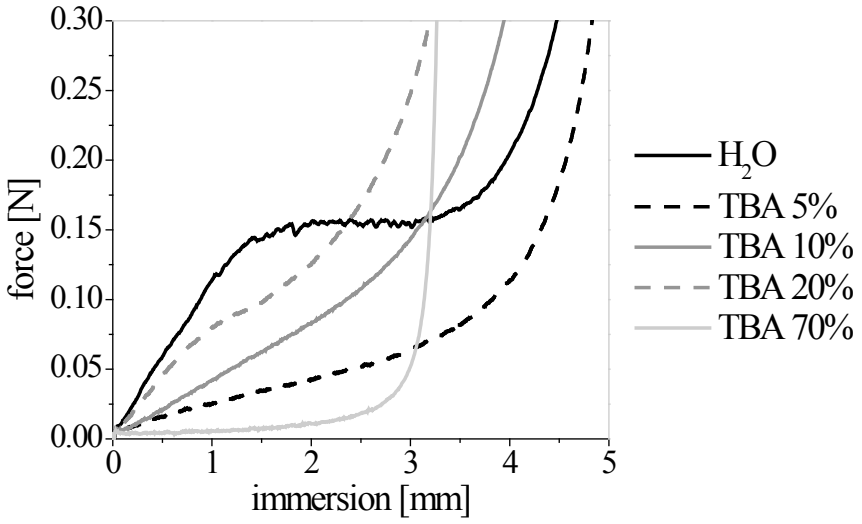

Figure 7: Mechanical testing of the different TBA/water co-solvent systems of 12 mg/ml cromolyn sodium lyophilisates

The effect of the varied lyophilisate morphology on the aerosolization behavior was evaluated based on changes in the ED and FPF of these samples. As can be seen from Figure 8a, cromolyn sodium samples prepared with 5%, 10%, and 20% TBA resulted in an increase of the ED from 48% to approximately 70% but simultaneously in a strong decrease of the FPF related to ED from 44% to approximately 15%. The 70% TBA sample, in contrast, showed a decreased ED of 28% and a similar FPF related to ED compared to the aqueous sample. Overall, the resulting FPF related to MD of only 10% was the same for all cromolyn sodium TBA samples. For valine freeze-dried from different TBA/water co-solvent systems, Figure 8b demonstrates a slight increase in ED from 76% to nearly 90%, whereas the FPF related to ED remains consistent between 8% and 13%. In contrast, trehalose lyophilisates from 5%, 10% and 20% TBA/water systems on the one hand showed a decreased ED from 49% to 37%, 32%, and 15%, respectively. On the other hand the FPF related to ED increased from 25% to around 36% (Figure 8c).

Aerosolized particles with an aerodynamic cut off diameter between 4 and 4.94 µm were investigated with SEM to analyze and compare the geometric particle size and structural properties. Cromolyn sodium lyophilisates from the 20% TBA/water co-solvent system (Figure 9c) demonstrated a bigger geometric particle size of approximately 100 µm compared to the aqueous lyophilisates (52 µm) (Figure 9a). The morphology changed from a smooth platelet like structure (Figure 9b) to a wrinkled structure (Figure 9d). For valine lyophilisates the particle size of the 20% TBA sample compared to the aqueous sample remained about the same of around 94 µm while the particle morphology changed from a very filigree structure

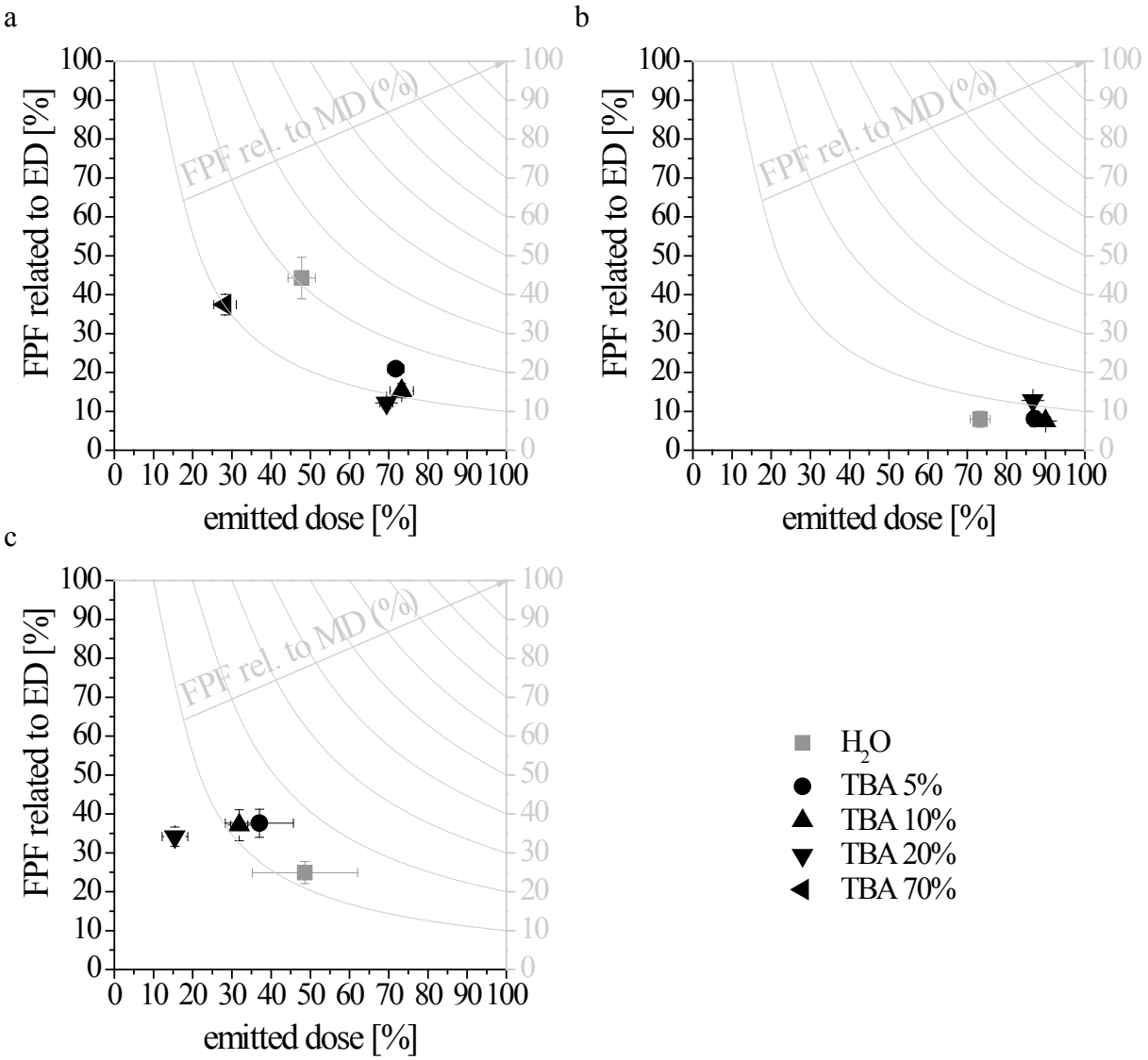

Figure 8: ED versus its related FPF as well as the FPF related to MD of 12 mg/ml cromolyn sodium lyophilisates (a), 12 mg/ml valine lyophilisates (b) and 8 mg/ml trehalose (c) lyophilisates freeze-dried from different TBA/water co-solvent systems.

into a more leafy structure. The particle morphology of trehalose samples could not be evaluated since the particles smoothened and coalesced upon contact with environmental humidity.

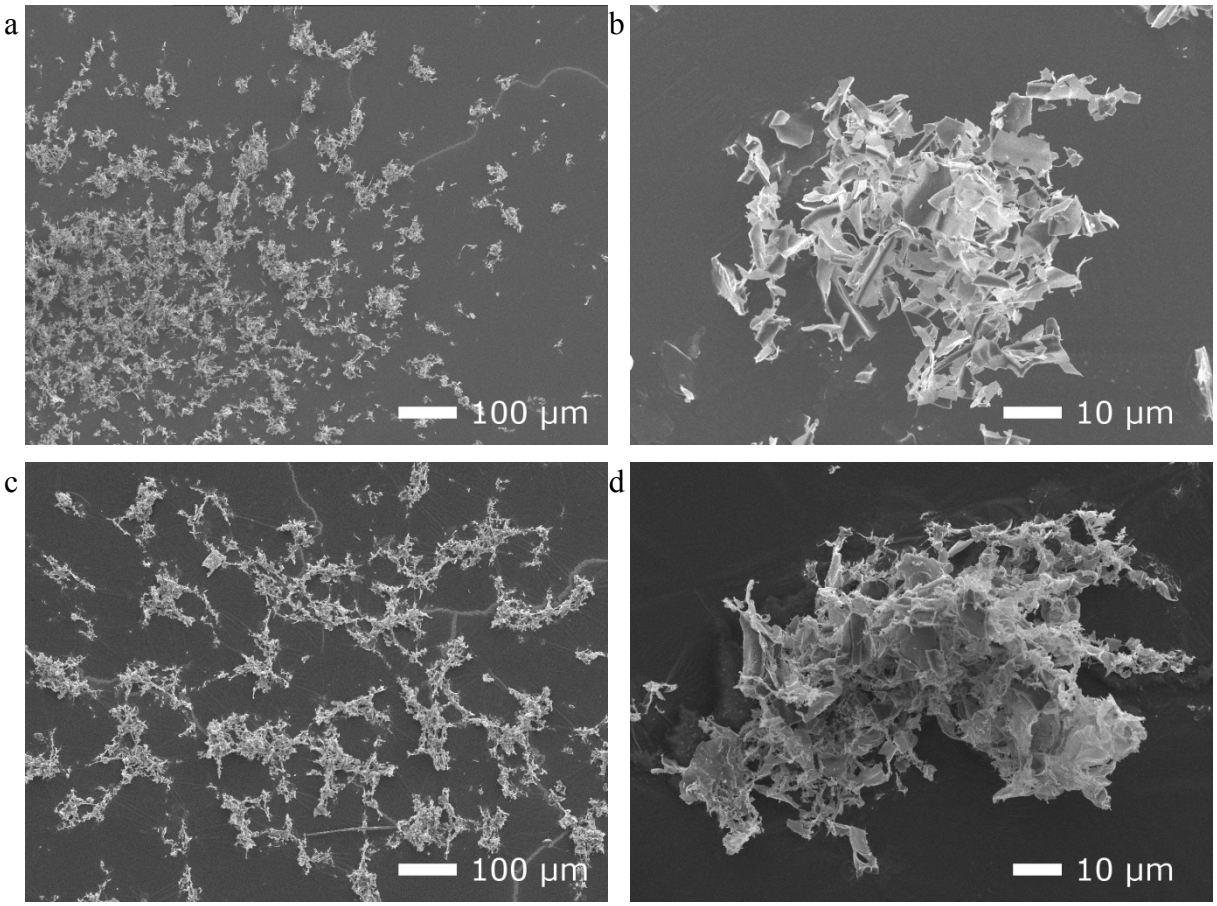

Figure 9: SEM structure of particles with an aerodynamic cut off diameter between 4 and 4.94 µm. Aerosolized 12 mg/ml cromolyn sodium lyophilisates frozen from an aqueous solution (a/b) and from a 20% TBA/water co-solvent system (c/d).

3.3 ANALYSIS OF THE MATERIAL PROPERTIES BY COMPRESSION STUDIES

Compaction of substances with an instrumented press gives the opportunity to analyze material properties like the degree of elastic recovery and relaxation of the compact. This should allow to draw conclusions whether a substance behaves more elastic, plastic, or brittle. All substances used in this study were conventionally freeze-dried at higher solution concentrations (lactose, trehalose, and cromolyn sodium at 100 mg/ml; valine at 50 mg/ml, and phenylalanine at 20 mg/ml due to their limited solubility in water) for analysis by instrumented compaction. From the recorded data, the porosity-pressure function according to Heckel [21] was calculated for both the compression and decompression phases (Figure 10). The obtained Heckel and compression parameters are outlined in Table 2. For all parameters, valine showed markedly different values in comparison to all other substances. The Heckel plot of valine powder rendered the smallest slope of $4.7*10^{-3}$ and the largest intercept of 1.75. The valine compact experienced the smallest relaxation of 0.16% during compression and the

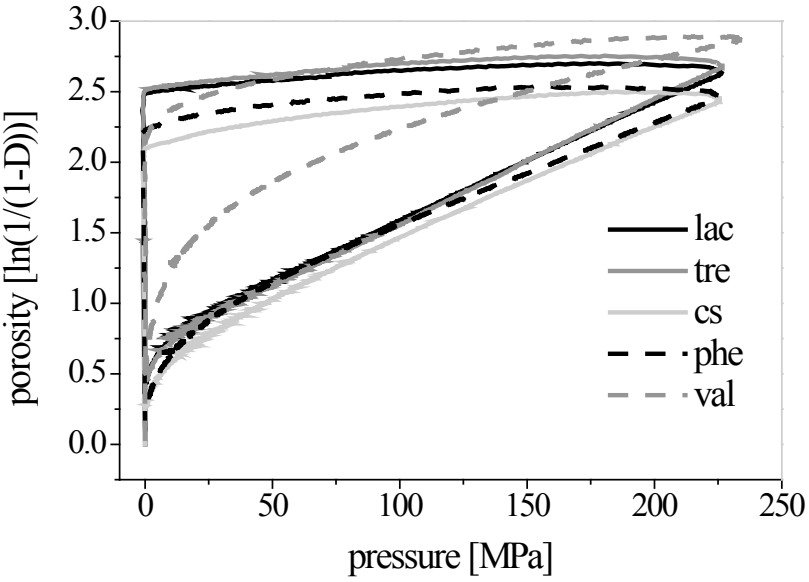

Figure 10: Heckel plot of freeze-dried lactose, trehalose, cromolyn sodium, phenylalanine and valine powder (one analysis curve shown exemplarily for each substance).

highest elastic recovery of 8% after load removal. Lactose, trehalose, and cromolyn sodium demonstrated rather similar values with respect to the compaction behavior. The compacts showed a relaxation between 0.52% and 0.56% and the Heckel plots revealed high slopes of around $9*10^{-3}$ and small intercepts of around 0.7. The Heckel parameters obtained for phenylalanine arranged between the ones from valine and the other three substances with a slop of $6.5*10^{-3}$ and an intercept of 0.87. The phenylalanine compact, in contrast, experienced the highest relaxation of 0.69%.

Table 2: Characteristic Heckel and compression parameters obtained by compression analysis of valine, phenylalanine, trehalose, cromolyn sodium and lactose (± S.D. n=6).

	val	**phe**	**tre**	**cs**	**lac**
heckel-slope $*10^{-3}$	4.7 ± 1.2	6.5 ± 0.5	8.5 ± 0.1	8.9 ± 1.1	8.9 ± 0.4
heckel-intercept	1.75 ± 0.05	0.87 ± 0.04	0.72 ± 0.05	0.71 ± 0.08	0.73 ± 0.01
residual	$4.80*10^{-6}$	$2.33*10^{-6}$	$2.67*10^{-6}$	$3.33*10^{-6}$	$1.67*10^{-6}$
max. pressure [MPa]	231 ± 3	227 ± 2	230 ± 2	229 ± 3	227 ± 2
elastic recovery [%]	8.4 ± 1.7	2.7 ± 1.0	1.9 ± 0.1	4.3 ± 0.6	1.6 ± 0.1
relaxation [%]	0.16 ± 0.03	0.69 ± 0.04	0.56 ± 0.05	0.54 ± 0.08	0.52 ± 0.3
yield pressure [MPa]	224 ± 53	154 ± 11	118 ± 2	114 ± 15	112 ± 5

4 DISCUSSION

4.1 VARIATION OF THE FREEZING PROCESS

The size and shape of ice crystals formed during freezing essentially determines the morphology of the resulting pores and thereby controls the solid matrix structure [22]. The effect of ice formation is thereby strongly dependent on the degree of supercooling and the freezing rate [23]. A high degree of supercooling creates a homogeneous, sponge-like structure whereas the cake texture changes to an oriented lamellar structure for samples with a low degree of supercooling [15]. A lamellar structure was found in this study for all samples frozen in liquid nitrogen and also for cromolyn sodium lyophilisates frozen on a precooled shelf. Large thermal gradients promote directional solidification, resulting in a directional lamellar morphology with connected pores [12] because secondary nucleation will only comprise those areas of the liquid volume with sufficient supercooling [10]. Freezing on the -70°C precooled shelf caused a large thermal gradient across the fill height, which was particularly pronounced for the cromolyn sodium solution. The freezing of this solution occurred with a very low supercooling of 1°C whereas, for example, the precooled frozen valine solution exhibited a supercooling of approximately 6°C, showing the normal sponge-like matrix structure after drying. This agrees with the finding that if supercooling exceeds 5°C, the solution in general freezes by global supercooling, resulting in a dispersed spherulitic morphology [15]. However, vacuum-induced freezing led to a normal sponge-like matrix for all substances despite the controlled nucleation at -3°C and therefore little supercooling. Liquid nitrogen freezing causes extreme temperature gradients along the vial bottom and sides, resulting in directional solidification from those surfaces inward as already reported [10, 24]. By studying a model food system, Quast and Karel [25] detected that samples frozen in liquid nitrogen cracked intensively during drying, which was also noticed for some lyophilisates evaluated in the current study. Among those, cromolyn sodium lyophilisates exhibited particularly distinctive cracks. These cracks enhance the water vapor flow during drying [25] but also allow to start the disintegration process in the vial with a cake that is almost separated into several subunits. For all substances the lamellar cake morphology caused an elastic structure, which is indicated by the constant gradient of the immersion-force-curve lacking a horizontal plateau. Instead of fracture mainly compression of the sample takes place, which was also confirmed by the observed elastic relaxation of the compressed cake after the immersion of the texture analyzer probe. Nevertheless, considering the aerosolization process, an elastic structure as a result of lamellar morphology did not hinder a

good disintegration. All samples with a lamellar morphology showed a fast and complete disintegration in the high speed camera recordings. This special matrix structure fragments into aerosol particles without the need for brittleness. In high speed camera recordings, the disintegrated particles appeared more voluminous than particles generated by disintegration of a sponge-like cake matrix. SEM confirmed a bigger geometric particle size for the same aerodynamic size in the case of particles produced from cakes with lamellar morphology. This is possible if the particles exhibit a decreased density, which was demonstrated by the more filigree and more porous appearance of these particles in SEM. All freeze-dried substances featuring a lamellar matrix showed an increased ED or at least a similar value (in the case of an already high ED of samples frozen via shelf-ramping). The increased output from the vial can be explained by the enlarged particle size because large particles offer greater contact surface to the discharging air flow and show reduced adhesion to surfaces. They demonstrate in general increased emission (Chapter 2). For a successful delivery of large particles to the lung, these particles need to possess a low density in order to meet the required aerodynamic size of less than 5 µm. The group of Edwards and Langer [26, 27] already successfully demonstrated the enhanced aerosolization efficiency of large porous particles for inhalation.

Annealing on the one hand is a process to facilitate crystallization of a bulking agent and on the other hand allows the unfrozen water to diffuse through the frozen matrix. This leads to ice crystal growth due to a ripening effect which may also create channels as a result of ice crystal interconnections [22]. After freezing and complete solidification, the frozen formulation is treated at a higher temperature between the glass transition temperature of the maximally freeze concentrated solution (Tg') and the ice melting point for a certain period of time before refreezing below Tg' [22]. All samples demonstrated similar XRD patterns compared to the conventionally frozen references. Therefore, no further crystallization or recrystallization occurred. The annealing temperature at -10°C is clearly above the Tg' of lactose and trehalose (-28°C and -29°C) [28]. This caused a local collapse phenomenon with consolidation of fine amorphous structures, which is similarly reported by Searles et al. [29] and by Webb et al. [16] for sucrose and hydroxyethyl starch formulations. This can be explained by the fact that the initial morphology has an extremely high surface-to-volume ratio, and super-Tg' annealing allows the system to relax to a morphology with a lower interfacial area [29]. The consolidation of the fine structures caused a complete loss of the ordered spherulitic morphology, resulting in a disordered network comprising large void volume. Solely the translucent skin on top of the cake still showed the spherulitic morphology. This loss of the ordered structure was mirrored in the changed outcome of the

mechanical testing. Compared to conventionally frozen samples, the annealed lyophilisates demonstrated steady fracture at a substantially smaller force because an ordered spherulitic structure increases resistance against the pressure of the probe, a principle which is for example utilized in lightweight construction [30]. The aerosolization behavior in the vial visualized by the high speed camera recordings showed also distinctive changes. These are possibly a consequence of the consolidation which results in thicker wall and network structures forming less porous particles. Visualizing these particles with SEM, a wall thickness of approximately 1 µm compared to 0.6 µm for the conventionally frozen lactose sample was observed. It was also noticeable that the particles did not demonstrate the same agglomerative highly porous structure as all other lactose samples and therefore exhibited a significantly smaller geometric size of 8 µm (Figure 5). As a consequence of these characteristics, the ED as well as the FPF decreased. A similar effect was also observed for the annealed valine sample despite its crystalline nature. Although the evaluation of the lyophilisate structure was not possible, the matrix must be very soft in order to fracture during the ventilation process in the freeze-dryer. The aerosolized particles generated from cakes which were prepared with an annealing step exhibited a smaller geometric size of 41 µm compared to approximately 90 µm of the conventionally frozen lyophilisate, which can be an explanation for the reduced ED. Annealing of phenylalanine and cromolyn sodium samples, in contrast, showed no significant effects. Microscopy revealed no changes in the lyophilisate morphology except of a change to more homogeneous pore size distribution. Mechanical testing revealed similar results as for the conventional shelf-ramped freezing. Particle morphology and size was neither influenced by the annealing step. This resulted altogether in comparable aerosolization behavior and only small variations in ED or FPF.

Further freezing methods resulting in spherulitic pore morphology are conventional shelf-ramped freezing, shelf-ramped freezing with holding steps, mostly precooled shelf freezing, and vacuum-induced freezing. These solutions froze by global supercooling. Hereby the entire liquid volume achieves a similar level of supercooling, and the secondary nucleation zone comprises the entire liquid volume [10]. As aforementioned, vacuum-induced freezing demonstrated freezing by global supercooling despite of the controlled nucleation at -3°C. When nucleation was induced by reduced pressure, the solution in the vial changed suddenly from a clear liquid into an opaque/translucent slush, which is indicative of global supercooling [12]. The mechanical testing of lyophilisates with a spherulitic matrix mostly showed steady fracture at a constant force, which is characteristic of a brittle structure. Only small variations were observed such as an increased force needed for fracturing the dense

upper layer of phenylalanine and cromolyn sodium samples from vacuum-induced freezing. A slightly reduced brittleness of lactose and trehalose samples frozen via shelf-ramping was indicated by the observed peak, instead of a horizontal plateau, in the immersion-force-curve. For disintegration of a spherulitic matrix, the cake is typically first separated into smaller subunits by the impacting air, followed by scaling off of fine particles. Some samples showed again small variations. Valine frozen via shelf-ramping, for example, disintegrated fast and completely as a result of its very soft structure. Lactose, trehalose, and valine prepared with vacuum-induced freezing showed also a fast and complete disintegration process and demonstrated a soft matrix structure as well. SEM of the aerosolized particles always showed agglomerates composed of smaller fragments, giving the particle a highly porous structure. The exact appearance varied among the different substances from more smooth and platelet like structures to wrinkled or filigree structures. The fragments of phenylalanine, for example, showed always the distinctive netting structure of phenylalanine-monohydrate crystals which develop when phenylalanine is freeze-dried (Chapter 3, Chapter 5). For lactose, trehalose and valine samples, ACI measurements demonstrated about the same FPF and ED values for all lyophilisates with a spherulitic matrix, whereas a changed matrix morphology exhibited a significantly different aerosolization performance. Phenylalanine and cromolyn sodium lyophilisates did not demonstrate such clear differences for the aerosolization performance of various matrix structures. Lyophilisates with a spherulitic matrix showed about the same ED and FPF as lyophilisates with a lamellar morphology.

4.2 CHANGING THE ICE CRYSTAL HABITUS USING TBA AS CO-SOLVENT

As mentioned before and reported by Kasraian and DeLuca [18], TBA alters the ice crystal habitus dependent on the amount of co-solvent added. A concentration of at least 3% TBA changes the ice structure to large dendritic ice crystals. The addition of 10% TBA results in even finer needle-shaped ice crystals whereas at the eutectic at 20% TBA, the frozen solution is composed of small eutectic crystals. The 70% TBA solution corresponds to the melting of pure TBA-hydrate and results in the formation of very large hydrate crystals [18]. The lyophilisate morphologies of the TBA/water co-solvent systems in the concentration of 5% and 10% were in accordance with the appearance reported by Kasraian and DeLuca [18], showing large-needle shaped pore structures. Liu et al. [11] reported also the formation of needle-like ice crystals for a formulation containing 5% TBA. The 20% TBA system, in contrast, did not demonstrate the mentioned small eutectic crystals but also needle-shaped structures for all lyophilisates. This can be a consequence of solutes influencing crystal

formation. Similarly, the 70% TBA/cromolyn sodium system did not show large pore formation due to very large TBA-hydrate crystals but a network of small spherulitic pores. Possibly the suspended cromolyn sodium crystals prevented the formation of large TBA-hydrate crystals. The samples with 5%, 10%, and 20% TBA demonstrated large needle-shaped aligned pores after freeze-drying. The mechanical testing revealed an elastic structure which was comparable to the liquid nitrogen frozen samples mentioned above. The spherulitic matrix of the 70% TBA/cromolyn sodium sample, in contrast, exhibited steady fracture at a constant force comparable to other samples with a sponge-like matrix described above. The aerosolization performance demonstrated a decrease in the ED for the 70% TBA sample compared to the aqueous sample for cromolyn sodium despite of the similar spherulitic matrix. The lamellar samples with 5%, 10%, and 20% TBA showed an increased ED compared to the spherulitic aqueous sample for cromolyn sodium and valine lyophilisates. An increase in the ED for samples with a lamellar morphology compared to those with a spherulitic matrix structure was also described above for various frozen lyophilisates of different substances. Trehalose samples, in contrast, demonstrated a decreased ED despite similar cake morphology. The samples showed a very soft cake structure, incomplete disintegration is therefore unlikely to occur. Visual inspection of the vial after disintegration revealed complete cake disintegration but a large particle fraction was collected at the top of the vial. Either the expelling air stream was not able to adequately catch the particles and export them out of the vial or most of the particles had a geometric size which was too large to escape through the outlet capillary (0.75 mm in diameter). Morphological aspects of the particles formed could not be evaluated due to destruction upon contact with environmental humidity. Most lyophilisates freeze-dried from a TBA/water co-solvent system demonstrated a softer structure in the texture analysis compared to the lyophilisates freeze-dried from aqueous solutions and the cake decomposed easily when extracted from the protective vial. In the literature, lyophilisates produced from TBA/water co-solvent systems were already described as readily breaking apart [31]. Possibly residual solvent levels of TBA act as a plasticizer and cause the softening of the lyophilisate structure. Wittaya-Areekul et al. [31] demonstrated increased residual TBA levels for higher initial TBA concentrations. The soft structure of the 70% TBA cromolyn sodium sample could therefore be a result of high residual TBA levels. Wittaya-Areekul and Nail [32] showed in another study that residual TBA levels were smaller for the crystallizing excipient glycine in contrast to higher levels for the amorphous excipient sucrose. Flink and Karel [33] postulated that residual solvents are entrapped within microregions of the freeze-dried solids of carbohydrates rather than being

adsorbed to the surface and thus are hard to remove. However, crystalline valine and amorphous trehalose exhibited both a softening of the structure for the TBA/water co-solvent systems. Possibly, the special lyophilisate structure contributed also to the mechanical properties of the cake. Considering intravial homogeneity, Liu et al. [11] obtained the best results by implementing two-step freezing or by adding TBA to a concentrated formulation with high fill depth. In this study, the TBA samples and the aqueous reference were frozen via a two-step freezing, including two holding steps at 5°C and -5°C. The very small standard deviations (Figure 8) indicate a good vial to vial homogeneity within the batch.

4.3 ANALYSIS OF THE MATERIAL PROPERTIES BY COMPRESSION STUDIES

In order to possibly explain material-dependent differences in lyophilisate characteristics and aerosolization performance, the material properties of the different substances were analyzed under compression. Under an applied load, materials can undergo brittle fracture or elastic or plastic deformation. Compaction profiles were recorded and several parameters like elastic recovery, relaxation, Heckel-slope, yield pressure, and Heckel-intercept were calculated to evaluate differences in plastic deformation or brittle fracture of the substances used. In order to compare compacted samples of different height, the tablet porosity was plotted against the pressure to obtain a Heckel plot. The Heckel-intercept is a measure for the degree of densification by fragmentation and particle reorganization until plastic deformation begins. Lactose, trehalose, and cromolyn sodium showed a similarly small value for the intercept of about 0.7 compared to the significantly higher values for phenylalanine and valine. Therefore, plastic deformation starts earlier for lactose, trehalose, and cromolyn sodium. Another indicator for plastic deformation is a high slope of the linear regression of the Heckel plot or a small yield pressure, which is inversely related to the slope and the minimum pressure required to cause deformation of the material [34]. Additionally, plastic deformation causes a high stress relaxation of the compact because of plastic flow [35]. Lactose, trehalose, and cromolyn sodium showed similarly high values for the Heckel-slope of around 0.009 and for the relaxation of around 0.5%, demonstrating good plastic deformation. The Heckel plot of valine, in contrast, showed the largest intercept of 1.75 and a small slope of 0.0047, indicating a high degree of fragmentation during compaction [36]. This was additionally confirmed by a small relaxation of 0.16%, which points to a brittle material with a low degree of plastic flow. Less consolidation of the powder during compaction results in more elastic recovery [34], which is the case for valine demonstrating the highest elastic recovery of 8.4%. This exceptionally high elastic recovery could also be a result of entrapped air, which is

compressed during compaction and will expand again after load removal [37]. The freeze-dried valine powder had a very low bulk density despite precompaction and therefore included large void volume, which potentially could not escape during the compaction process. A high degree of elastic deformation during compaction and entrapped air results in weaker tablet strength, leading to higher capping tendencies of the compacts [37]. For valine compacts a strong capping was noticed. Phenylalanine compacts showed on the one hand the highest relaxation of 0.69%, which points to plastic deformation. On the other hand, phenylalanine demonstrated a Heckel-slope of 0.0065 which was significantly smaller than the slope of lactose, trehalose, and cromolyn sodium and significantly larger than the slope of valine. The elastic recovery of 2.7% is considered small in comparison to all other substances, which indicates plastic deformation. In summary, phenylalanine demonstrated a more plastic deformation than brittle fracture.

By comparison of the material properties from compaction studies with the mechanical properties of the lyophilisates, the brittle behavior of valine is consistent with the very good fracture properties of the lyophilisate from texture analysis. This is indicated by the horizontal plateau over the complete way of immersion at small force values (Figure 2a). Phenylalanine lyophilisates demonstrated good fracture properties as well because of a relatively leveled plateau of the immersion-force-curve over a long way of immersion but at higher force values. Trehalose and lactose, in contrast, demonstrated plastic deformation during compaction and nonuniform fracture properties at texture analysis because of a force peak during immersion instead of a horizontal plateau. Cromolyn sodium, in turn, showed also good plastic deformation during compaction but a plateau in texture analysis. However, the plateau was first reached after 1.25 mm of immersion and extended only over an immersion of 1.5 mm. This demonstrates poorer fracture properties compared to valine or phenylalanine. In conclusion, the mechanical properties of the freeze-dried substances estimated by compaction roughly agree with the mechanical properties of the lyophilisates measured by texture analysis. For the characterization of lyophilisate properties texture analysis is therefore considered as a useful and easy to perform analysis. Both methods, however, were not able to explain commonalities and differences of the aerosolization performance of different substances. The sugars and valine demonstrated a similar correlation between the freezing process and the aerosolization performance but markedly different material properties. The sugars and cromolyn sodium, in contrast, exhibited similar material properties but different effects of varied freezing procedures on the aerosolization performance. This demonstrates that parameters affecting the aerosolization performance are way too complex for prediction.

The aerosolization performance and its possible variation need therefore to be assessed for every new substance.

5 SUMMARY AND CONCLUSION

This study evaluates several methods for altering the lyophilisate morphology to influence the aerosolization performance of the freeze-dried product. Variations of the solid matrix structure of a lyophilisate were achieved by changing the freezing process resulting in a different shape and size of ice crystals. Furthermore, the addition of TBA as co-solvent changed the ice crystal habitus and therefore also the matrix morphology. Significant changes in the aerosolization performance were mostly caused only by a strong variation of the solid matrix structure for example by a lamellar-oriented morphology or a loss of the ordered structure by consolidation. This shows in turn, that small changes in lyophilisate morphology which arise as vial to vial inhomogeneities and batch to batch variations according to stochastic ice nucleation [10] or differences in drying kinetics due to radiation phenomena, shelf fluid temperature gradients and vapor fluid dynamics in the freeze-drying chamber [38] will not dramatically impact the aerosolization outcome.

In conclusion samples with a lamellar morphology showed good results for the ED and dependent on the freeze-dried substance also for the FPF. Analyzed mechanical properties of the substances could not explain differences in FPF despite similar cake morphology. A lamellar matrix structure was achievable by freezing in liquid nitrogen or for a single case in this study by freezing on a precooled shelf. In literature directional solidification was also realized by immersion of the vial into dry ice/isopropanol [39] or dry ice/ethanol [14] and for samples containing *Pseudomonas syringae* as nucleating agent [10]. Although all quench freezing methods of immersing vials into an extremely cold liquid demonstrate a lamellar morphology which showed good aerosolization results, they are not applicable in large scale-manufacturing [40]. Similarly the addition of *P. syringae* as ice nucleating agent is also not of practical use for FDA-regulated and approved pharmaceuticals products [15]. A TBA/water co-solvent system in a TBA range of 5% to 20% demonstrated large needle-shaped ice crystals resulting in kind of a lamellar morphology with the characteristic elastic structure and mostly high ED. For pharmaceutical product manufacturing, the use of such an organic co-solvent must be properly estimated taking the following issues into account: proper safe handling of the flammable solvent, determination and control of residual solvent levels,

qualification of an appropriate GMP purity and the toxicity of the remaining solvent [17]. The residual solvent in the final product for TBA is influenced by the initial TBA concentration, the freezing rate, and the physical state of the solutes [31]. The fact, that the marketed pharmaceutical product Caverject® uses an organic co-solvent system for freeze-drying (20% v/v TBA/water system) [17] shows that safety, toxicity and regulatory issues are manageable.

An important aspect of this study is also the great influence of the material property. The diverse substances formed different solid matrix structures varying in pore shape and size distribution, wall appearance as well as in the mechanical behavior for the same freezing process. The variation of the freezing process again had a variable effect on the lyophilisate morphology and mechanical property depending on the selected substance. Altogether this can result in a different aerosolization behavior demonstrating a different fine particle output. Detected variations were thereby independent of morphological aspects like a crystalline or amorphous nature. Similar substances like the two amorphous sugars lactose and trehalose showed for all freezing variations the same behavior. The crystalline amino acid valine revealed similar results. The crystalline amino acid phenylalanine and the amorphous cromolyn sodium in contrast demonstrated different outcomes for the same variations in the freezing process compared to lactose, trehalose and valine. Mechanical properties of the freeze-dried substance analyzed by compression revealed a decrease of brittle fracture and an increase of plastic deformation for the substances in the following order: valine, phenylalanine, lactose/trehalose/cromolyn sodium. The different mechanical behavior of valine compared to the sugars but a similar aerosolization performance of the various frozen samples as well as the similar mechanical behavior of the sugars and cromolyn sodium but a different outcome for the aerosolization performance demonstrate, that the evaluation of these characteristics are not enough to explain substance related variation. Therefore not only the formation of a different crystal structure with different properties or distinct mechanical properties are responsible for a variation in lyophilisate characteristics but also other material properties of the freeze-dried substance.

6 REFERENCES

[1] A. Chow, H. Tong, P. Chattopadhyay, B. Shekunov, Particle Engineering for Pulmonary Drug Delivery, Pharm. Res., 24 (2007) 411-437.

[2] H.-K. Chan, P.M. Young, D. Traini, M. Coates, Dry powder inhalers: challenges and goals for next generation therapies, Pharmaceutical Technology Europe, (2007).

[3] H.W. Frijlink, A.H. De Boer, Dry powder inhalers for pulmonary drug delivery, Expert Opin. Drug Deliv., 1 (2004) 67-86.

[4] D.R. Owens, B. Zinman, G. Bolli, Alternative routes of insulin delivery, Diabetic Med., 20 (2003) 886-898.

[5] M. Tobyn, J.N. Staniforth, D. Morton, Q. Harmer, M.E. Newton, Active and intelligent inhaler device development, Int. J. Pharm., 277 (2004) 31-37.

[6] P.M. Young, J. Thompson, D. Woodcock, M. Aydin, R. Price, The Development of a Novel High-Dose Pressurized Aerosol Dry-Powder Device (PADD) for the Delivery of Pumactant for Inhalation Therapy, J. Aerosol Med., 17 (2004) 123-128.

[7] J. Whelan, Electronic DPI for insulin, Drug Discov. Today, 7 (2002) 213-214.

[8] C. Yamashita, A. Akagi, Y. Fukunaga, Dry powder inhalation system for transpulmonary administration, in: United States Patent 7735485 2010.

[9] F. Franks, Freeze-drying of bioproducts: putting principles into practice, Eur. J. Pharm. Biopharm., 45 (1998) 221-229.

[10] J.A. Searles, J.F. Carpenter, T.W. Randolph, The ice nucleation temperature determines the primary drying rate of lyophilization for samples frozen on a temperature-controlled shelf, J. Pharm. Sci., 90 (2001) 860-871.

[11] J. Liu, T. Viverette, M. Virgin, M. Anderson, P. Dalal, A Study of the Impact of Freezing on the Lyophilization of a Concentrated Formulation with a High Fill Depth, Pharm. Dev. Technol., 10 (2005) 261-272.

[12] J.A. Searles, Freezing and Annealing Phenomena in Lyophilization, in: L. Rey, J.C. May (Eds.) Freeze-Drying/Lyophilization of Pharmaceutical and Biological Products, Marcel Dekker, Inc., New York - Basel, 2004.

[13] X. Tang, M. Pikal, Design of Freeze-Drying Processes for Pharmaceuticals: Practical Advice, Pharm. Res., 21 (2004) 191-200.

[14] T.W. Patapoff, D.E. Overcashier, The Importance of Freezing on Lyophilization Cycle Development, BioPharm Int., March 2002 (2002) 16–21, 72.

[15] J.C. Kasper, W. Friess, The freezing step in lyophilization: Physico-chemical fundamentals, freezing methods and consequences on process performance and quality attributes of biopharmaceuticals, Eur. J. Pharm. Biopharm., 78 (2011) 248-263.

[16] S.D. Webb, J.L. Cleland, J.F. Carpenter, T.W. Randolph, Effects of annealing lyophilized and spray-lyophilized formulations of recombinant human interferon-γ, J. Pharm. Sci., 92 (2003) 715-729.

[17] D.L. Teagarden, D.S. Baker, Practical aspects of lyophilization using non-aqueous co-solvent systems, Eur. J. Pharm. Sci., 15 (2002) 115-133.

[18] K. Kasraian, P.P. DeLuca, Thermal Analysis of the Tertiary Butyl Alcohol-Water System and Its Implications on Freeze-Drying, Pharm. Res., 12 (1995) 484-490.

[19] A. Hottot, S. Vessot, J. Andrieu, Freeze drying of pharmaceuticals in vials: Influence of freezing protocol and sample configuration on ice morphology and freeze-dried cake texture, Chem. Eng. Process., 46 (2007) 666-674.

[20] H. Seager, C.B. Taskis, M. Syrop, T.J. Lee, Structure of products prepared by freeze-drying od solutions containing organic solvents, in: Symposium on Lyophilization presented at the Annual Meeting of the Academy of Pharmaceutical Sciences, San Diego, California, 1982.

[21] R.W. Heckel, Density pressure relationship in powder compaction, Trans. Metall. Soc. AIME, 221 (1961) 671-675.

[22] J. Liu, Physical Characterization of Pharmaceutical Formulations in Frozen and Freeze-Dried Solid States: Techniques and Applications in Freeze-Drying Development, Pharm. Dev. Technol., 11 (2006) 3-28.

[23] B.S. Bhatnagar, R.H. Bogner, M.J. Pikal, Protein Stability During Freezing: Separation of Stresses and Mechanisms of Protein Stabilization, Pharm. Dev. Technol., 12 (2007) 505-523.

[24] P.J. Dawson, D.J. Hockley, Scanning electron microscopy of freeze-dried preparations: relationship of morphology to freeze-drying parameters, Dev. Biol. Stand., 75 (1992) 185-192.

[25] D.G. Quast, M. Karel, Dry Layer Permeability and Freeze-Drying Rates in Concentrated Fluid Systems, J. Food Sci., 33 (1968) 170-175.

[26] D.A. Edwards, J. Hanes, G. Caponetti, J. Hrkach, A. Ben-Jebria, M.L. Eskew, J. Mintzes, D. Deaver, N. Lotan, R. Langer, Large Porous Particles for Pulmonary Drug Delivery, Science, 276 (1997) 1868-1872.

[27] R. Vanbever, J.D. Mintzes, J. Wang, J. Nice, D. Chen, R. Batycky, R. Langer, D.A. Edwards, Formulation and Physical Characterization of Large Porous Particles for Inhalation, Pharm. Res., 16 (1999) 1735-1742.

[28] L.-M. Her, S.L. Nail, Measurement of Glass Transition Temperatures of Freeze-Concentrated Solutes by Differential Scanning Calorimetry, Pharm. Res., 11 (1994) 54-59.

[29] J.A. Searles, J.F. Carpenter, T.W. Randolph, Annealing to optimize the primary drying rate, reduce freezing-induced drying rate heterogeneity, and determine Tg′ in pharmaceutical lyophilization, J. Pharm. Sci., 90 (2001) 872-887.

[30] B. Klein, Leichtbau-Konstruktion: Berechnungsgrundlagen Und Gestaltung, Vieweg+Teubner Verlag, Springer Fachmedien Wiesbaden GmbH, 2011.

[31] S. Wittaya-Areekul, G.F. Needham, N. Milton, M.L. Roy, S.L. Nail, Freeze-drying of tert-butanol/water cosolvent systems: A case report on formation of a friable freeze-dried powder of tobramycin sulfate, J. Pharm. Sci., 91 (2002) 1147-1155.

[32] S. Wittaya-Areekul, S.L. Nail, Freeze-drying of tert-butyl alcohol/water cosolvent systems: Effects of formulation and process variables on residual solvents, J. Pharm. Sci., 87 (1998) 491-495.

[33] J. Flink, M. Karel, Effects of process variables on retention of volatiles in freeze-drying, J. Food Sci., 35 (1970) 444-447.

[34] N.O. Iloañusi, J.B. Schwartz, The Effect of Wax on Compaction of Microcrystalline Cellulose Beads Made by Extrusion and Spheronization, Drug Dev. Ind. Pharm., 24 (1998) 37-44.

[35] J.A. Dressler, Vergleichende Untersuchungen pharmazeutischer Hilfsstoffe unter Einsatz eines inkrementalen Weggebers zur präzisen Wegmessung an einer Exzenter-Tablettenpresse, PhD Thesis, in, Eberhard-Karls-Universität Tübingen, Germany, 2002.

[36] M. Duberg, C. Nyström, Studies on direct compression of tablets VI. Evaluation of methods for the estimation of particle fragmentation during compaction., Acta Pharm. Suec., 19 (1982) 421-436.

[37] P. Lennartz, Untersuchungen zu speziellen Eigenschaften und zur inneren Struktur von Minitabletten aus Paracetamol und sprühgetrockneter Laktose, PhD Thesis, in, Universität Hamburg, Germany, 1998.

[38] A.A. Barresi, R. Pisano, V. Rasetto, D. Fissore, D.L. Marchisio, Model-Based Monitoring and Control of Industrial Freeze-Drying Processes: Effect of Batch Nonuniformity, Drying Technol., 28 (2010) 577-590.

[39] C.C. Hsu, H.M. Nguyen, D.A. Yeung, D.A. Brooks, G.S. Koe, T.A. Bewley, R. Pearlman, Surface Denaturation at Solid-Void Interface—A Possible Pathway by Which Opalescent Participates Form During the Storage of Lyophilized Tissue-Type Plasminogen Activator at High Temperatures, Pharm. Res., 12 (1995) 69-77.

[40] P. Cameron, Good Pharmaceutical Freeze-Drying Practice, Interpharm Press Inc., Buffalo Grove, USA, 1997.

Chapter 7

Storage Stability of Lyophilized Formulations for Dry Powder Inhalation

Abstract

Stability is an essential requirement for a drug product. The novel dry powder inhalation system comprises a freeze-dried formulation which is disintegrated into inhalable particles at the time of inhalation. In this case, the physic-chemical stability of the lyophilisate has to be in the focus and the stable disintegration and lung delivery of these products after storage need to be verified and was the subject of this study. Sealed lyophilisates of three different model substances (phenylalanine, lactose, and cromolyn sodium) were stored for a three month period at 25°C/60% RH and 40°C/75% RH, respectively and changes in lyophilisate characteristics as well as aerosolization performance were evaluated. A slight moisture absorption up to a maximum of 3% due to residual moisture in the stopper could be observed for all substances. This resulted in a softening of the lactose lyophilisate structure. Aerosolization performance for all samples, however, was not affected. A marginal but not relevant increase of the fine particle fraction or the emitted dose after three months storage was observed. In a second part of the study, the effect of higher moisture adsorption during unintended open storage at higher humidity was tested. For this purpose, lyophilisates were stored at 30% RH and 50% RH at RT for three days without stoppers. Despite substantial moisture uptake of the amorphous products, which was reflected in a reduction of the force necessary to break the cake structures of most samples, hardly any effect on the aerosolization performance was detectable.

1 INTRODUCTION

Dry powder formulations for pulmonary drug delivery, in general, comprise the active pharmaceutical ingredient in a size between 1 and 5 µm. These small drug particles have poor flow properties and are difficult to disperse due to their highly cohesive nature. To improve flow, reduce aggregation and aid in dispersion, the micronized drug particles are typically blended with larger carrier particles or are loosely agglomerated [1]. During inhalation, the drug particles need to disperse for penetration into the lung. The adhesive (drug-carrier interaction) and cohesive (drug-drug interaction) forces should therefore be adjusted to a level which not only provides a stable formulation but also allows for easy separation during inhalation [2]. It is important to note that the dispersibility of a powder formulation is affected by storage relative humidity (RH) whereby, in general, storage at high RH adversely affects dispersibility [3]. The mechanisms behind this effect are increased capillary forces, solid bridging [4] and increased interactions of nearby particles, which are caused by higher polar surface energy due to adsorbed moisture [3]. Since deposition characteristics of dry powder formulations are sensitive to moisture, the demonstration of stability in long-term storage is required [5]. The International Conference on Harmonization provides guidelines for stability testing of new drug substances or drug products which recommend the following storage conditions: a long-term storage (minimum 12 months) should be performed at either 25°C/60% RH or 30°C/65% RH and complemented with an accelerated study (minimum 6 months) under more extreme conditions of 40°C/75% RH [6]. The novel dry powder inhalation system is based on dispersion of lyophilisates. In this system the formulation is stored as a coherent bulk and disintegrated into fine particles at the time of inhalation. Problems like poor flowability and re-dispersibility are thereby avoided. Freeze-drying is widely used to improve long-term storage stability of labile drugs, especially biopharmaceuticals [7]. Nevertheless, instabilities during storage can occur which in parts are a consequence of moisture uptake. In amorphous products water can act as a plasticizer, which reduces the glass transition temperature and could induce recrystallization [8]. These changes can affect the mechanical properties of the lyophilisates. To be inhalable, the stable disintegration and lung delivery of the lyophilized products need to be verified. The aim of this study hence was to evaluate phenylalanine, lactose, and cromolyn sodium lyophilisates for inhalation with regard to storage stability of the aerosolization performance, in particular, over three month at 25°C/60% RH and 40°C/75% RH. In a second part of the study, a moisture stress test comprising an un-stoppered storage at 30% RH and 50% RH of several

freeze-dried substances for three days was performed to simulate an unintentional open storage at high humidity or an alternative moisture-permeable container. Before and after storage, lyophilisates were characterized with respect to morphological state by x-ray powder diffraction, moisture content, mechanical behavior of the cake up on penetration of a probe, as well as aerosolization performance.

2 MATERIALS AND METHODS

2.1 MATERIALS

Aqueous solutions were prepared of L-phenylalanine (Phe) (Merck KGaA, Darmstadt, Germany), lactose-monohydrate (Lac) (Fagron GmbH&Co. KG, Barsbüttel, Germany), cromolyn sodium (CS) (Fagron GmbH&Co. KG, Barsbüttel, Germany), L-isoleucine (Ile) (Fluka Chemie GmbH, Buchs, Switzerland), L-valine (Val) (Fagron GmbH&Co KG, Barsbüttel, Germany), D-mannitol (Man) (Riedel-de Haën, Seelze, Germany), trehalose (Tre) (Hayashibara Co Ltd, Okayama, Japan) lysozyme (Lys) from chicken egg white (Serva Electrophoresis GmbH, Heidelberg, Germany). Dye for quantification was rhodamine B (Sigma-Aldrich, Chemie GmbH, Steinheim, Germany).

2.2 FORMULATION PREPARATION

For the three-month stability 0.5 ml aqueous solutions of lactose or cromolyn sodium at 12 mg/ml or phenylalanine at 8 mg/ml were filled into 2R glass vials (Fiolax® clear, Schott AG, Müllheim, Germany) and vials were equipped with rubber stoppers (1079-PH 701/40/ow/wine-red, West Pharmaceutical Services, Eschweiler, Germany). Stoppers used were dried before lyophilization at 105°C for 4 h. Freeze-drying was carried out in a laboratory scale freeze-drier (Lyostar II, FTS Systems, Stone Ridge, NY, USA). The samples were frozen at -1°C/min to -45°C for 1 h. Primary drying was performed at a shelf temperature of -15°C (shelfs were ramped at +0.2°C/min) and a pressure of 100 mtorr for 20 h. For secondary drying the shelf temperature was increased to +30°C at a ramp rate of +0.1°C/min for 6 h. All samples were crimped with aluminium caps.

For the stress test 0.5 ml aqueous solutions of 12 mg/ml excipient (isoleucine, valine, lactose or trehalose) or model drug (cromolyn sodium or lysozyme) were filled into 2R glass vials and vials were equipped with rubber stoppers (C1503, Stelmi, Villepinte, France). Freeze-

drying was carried out in the laboratory scale freeze-drier. The samples were frozen at -1°C/min to -45°C for 1 h. Primary drying was performed at a shelf temperature of -20°C (shelfs were ramped at +0.2°C/min) and a pressure of 34 mtorr for 20 h. For secondary drying the shelf temperature was increased to +30°C at a ramp rate of +0.5°C/min for 10 h at a decreased pressure of 8 mtorr.

2.3 STORAGE

For three-month stability testing the sealed lyophilized samples were stored at 25°C and 60% relative humidity (RH) or at 40°C and 75% RH. The desired humidity was achieved by storage in a humidor containing saturated ammonium nitrate (VWR International, Leuven, Belgium) solution for 60% RH or a saturated sodium chloride (Merck KGaA, Darmstadt, Germany) solution for 75% RH in each case monitored by a hygrometer.

For the stress test, un-stoppered lyophilisates were stored at 30% RH or 50% RH at room temperature (RT) for 3 days. The desired humidity was achieved by storage in a humidor containing a saturated calcium chloride (Merck KGaA, Darmstadt, Germany) solution for 30% RH or a saturated calcium nitrate (central supply LMU, Munich, Germany) solution for 52% RH in each case monitored by a hygrometer. Regarding the saturated solution for control of RH see [9] for more details.

2.4 MOISTURE CONTENT ANALYSIS

The moisture content of lyophilisates was determined by Karl-Fischer titration (Metrohm 756 KF Coulometer, Herisau, Switzerland) using Hydranal Coulomat AG (Riedel-deHaën, Seelze, Germany) as titration reagent. The lyophilisates were dissolved in 1.0 ml of anhydrous methanol (Hydranal-Methanol dry, Riedel-deHaën, Seelze, Germany), additionally dried with molecular sieve 3A (VWR International GmbH, Darmstadt, Germany). The dissolution took place right in the production vials after injection of methanol through the stopper of the vial using a 1 ml-Hamilton syringe. As blanks, empty freeze-dried vials were treated the same way. The injection volume was 500 µl each. The measurements were performed in triplicate.

2.5 MOISTURE SORPTION ANALYSIS

The moisture sorption behavior of the freeze dried samples was measured using an IGASorp moisture sorption analyser (Hiden Isochema, Warrington, United Kingdom). Isothermes were

recorded at 25°C with RH from 5% up to 90% in steps of 10%. The samples were previously dried for at least 2 h in a dry nitrogen flow at 250 ml/min. During measurement the humidity-controlled flow had a rate of 200 ml/min. The sample mass was about 6 to 8 mg.

2.6 MECHANICAL TESTING

The mechanical properties of the lyophilisates were investigated using a Texture Analyzer (TA.XT.plus, Stable micro Systems, Godalming, United Kingdom) equipped with a 5 kg load cell and a cylindrical stainless steel probe with a diameter of 5 mm at a test speed of 1 mm/s and a maximal immersion into the lyophilisate of 2 mm. The resulting immersion-force curve approached steady fracture at a constant force reflected in a horizontal plateau. For comparison of the formulations before and after storage, the data points of the plateau were averaged and the obtained value represents the force necessary to fracture the lyophilisate.

2.7 X-RAY DIFFRACTOMETRY (XRD)

The lyophilisates were investigated with a Seifert X-ray diffractometer XRD 3000 TT (Seifert, Ahrensburg, Germany) equipped with a copper anode (40 kV, 30 mA, wavelength 154.17 pm). The samples were measured from 5 – 40° 2-Θ at a step rate of 0.05° 2-Θ with 2 s measuring time per step.

2.8 FINE PARTICLE FRACTION (FPF) ANALYSIS

For aerosolization of the lyophilisates, a custom-designed test system (Chapet 2) was used. The FPF was measured using a short stack version of the Andersen Cascade Impactor (8-Stage Non-Viable Sampler Series 20-800, Thermo Andersen, Smyrna, GA, USA) at a flow rate of 39 l/min (corresponds to a pressure drop of 4 kPa with the HandiHaler®). Baffle plates were coated with a solution of 83% glycerin (AppliChem GmbH, Darmstadt, Germany), 14% ethanol (central supply LMU, Munich, Germany) and 3% Brij 35 (Serva Electrophoresis GmbH, Heidelberg, Germany). Filters used were type A/E glass fiber filters 76 mm (Pall Corporation, Ann Arbor, MI, USA). By removing stages 2 to 7, the whole FPF (particle fraction <4.94 µm) is collected on the filter directly below stage 1.

For three-month stability testing the FPF was quantified by weighing the filter before and after powder deposition and was either calculated as the percentage of the metered dose (MD)

or the emitted dose (ED). ED was measured by weighing the vial before and after aerosolization and calculated as the percentage of MD.

For stress test FPF was determined by washing the filter with water and rhodamine B quantification at 554 nm in an Agilent 8453 UV-Vis spectrophotometer (Agilent Technologies, Santa Clara, CA, USA). Therefore the filter solution was ultra-centrifuged (Optima^{TM} TLX Ultracentrifuge, Beckman Coulter, Brea, CA, USA) at 186000 g for 45 min before UV-Vis spectroscopic analysis. FPF was again calculated as either the percentage of MD or ED. ED was measured by washing the vial with water and quantification by UV-Vis spectroscopy; it was calculated as the percentage of MD.

3 RESULTS AND DISCUSSION

3.1 THREE-MONTH STABILITY AT 25°C/60% RH AND 40°C/75% RH

To assess storage stability of freeze-dried formulations for inhalation, lyophilisates were stored in the sealed vials at 25°C/60% RH and at 40°C/75% RH for three months. Immediately after freeze-drying as well as after one and three months of storage, the formulations were characterized. Since the physicochemical stability of a freeze-dried product is often sensitive to the level of moisture, residual moisture needs to be reduced during the secondary drying process and subsequently controlled during storage [10]. Immediately after freeze-drying, all lyophilisates exhibited residual moisture of less than 1%, which is considered optimal for storage [7]. A critical aspect for the storage of freeze-dried formulations is the slightly rising moisture content caused by residual moisture in the stopper [10] and permeation of water through the stopper [11]. Non-dried stoppers can be considered as a water reserve, dried stoppers play the role of a buffer limiting the rate of water transfer to the product [11]. Stoppers used in this study were therefore dried at 105°C for 4 h prior to freeze-drying. Nevertheless, the moisture content of the lyophilisates increased during storage for all formulations up to 3%, as can be seen from Figure 1. A higher storage temperature caused a faster increase in moisture. This can be explained by the fact that water transfer out of the stopper to the lyophilisate is more pronounced at elevated temperature [12]. Pikal and Shah [10] demonstrated that the product moisture content increases over time until an equilibrium value is reached, which is characteristic for the product, amount of product, and stopper treatment method. The time period to reach this equilibrium is thus only dependent on

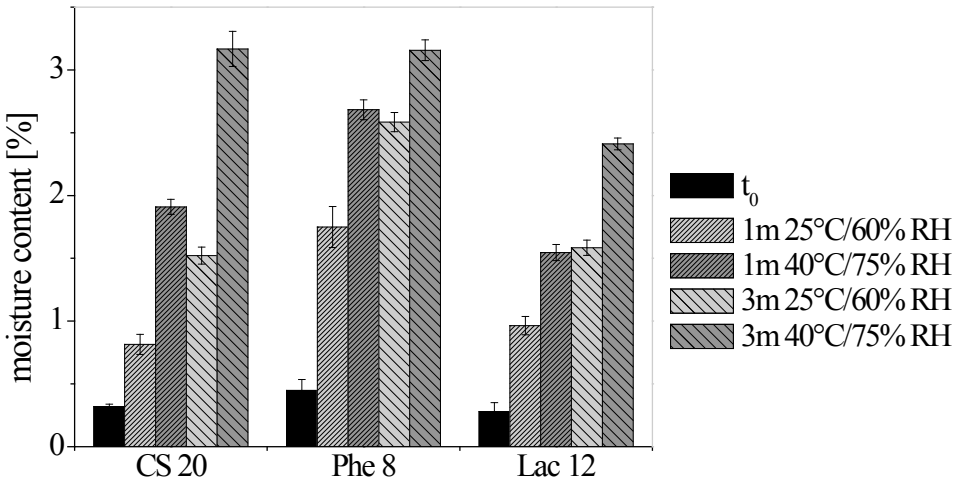

Figure 1: The moisture content of lyophilisates immediately after freeze-drying compared to samples after 1 and 3 month of storage at 25°C/60%RH and 40°C/75% RH.

temperature, whereas the equilibrium water content is temperature independent. Whether the equilibrium moisture content was already reached for the tested formulations within three months of storage at 40°C cannot be stated.

Since water has a plasticizing effect on amorphous materials [13], the increased moisture content of the freeze-dried product could affect its mechanical characteristics. Mechanical testing of the different formulations before and after storage revealed no significant changes for cromolyn sodium and phenylalanine lyophilisates. The immersion-force-curves of lactose lyophilisates, in contrast, demonstrated a shift to smaller forces after storage, as can be seen from Figure 2. Immediately after freeze-drying, the plateau force necessary to fracture the

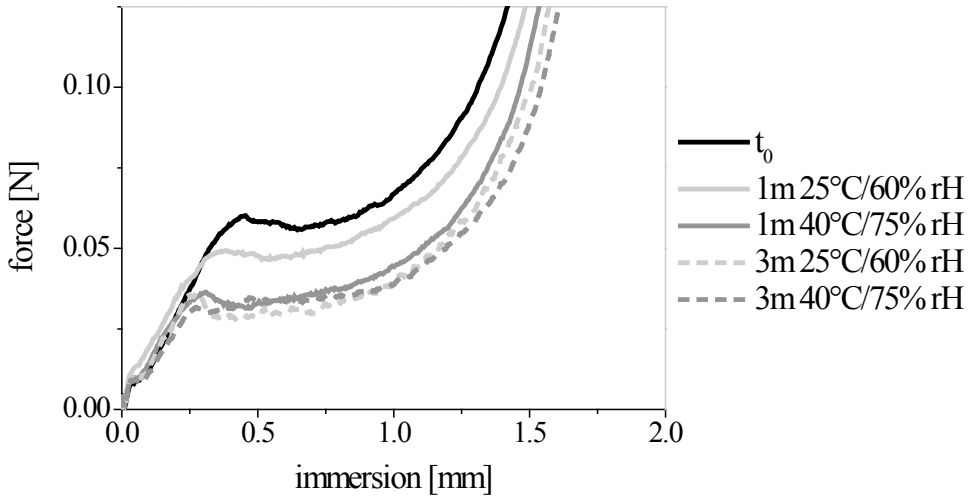

Figure 2: Immersion-force-curves for lactose lyophilisates immediately after freeze-drying and after storage.

lyophilisate amounted to 0.057 N. During storage, this force leveled at about 0.03 N for sample exhibiting a residual moisture content of 1.5% and did not drop further for samples with higher moisture levels up to 3%.

X-ray powder diffractometry (XRD) is perhaps the gold standard to characterize the physical state of freeze-dried solids. For freeze-dried formulations containing amorphous or partially crystalline modifications which are thermodynamically unstable, the possibility of recrystallization during storage needs to be considered [14]. For phenylalanine XRD demonstrated small crystalline reflections at 6.5, 14.85, 21.55 and 33.1° 2-θ, which are characteristic for phenylalanine-monohydrate [15]. Peak intensity and location did not change during storage. The residual water content immediately after freeze-drying and later during storage is remarkably low. Theoretically, the water content of pure phenylalanine-monohydrate is 9.8%. Therefore, phenylalanine must have been present in a partially crystalline state, including a large amorphous fraction. Lactose and cromolyn sodium, in contrast, showed a completely amorphous nature, which did not change during storage.

As mentioned before, the disintegration and deposition performance of traditional dry powder formulations are especially sensitive towards moisture exposure during storage. In order to identify potential effects of storage on the dispersibility and deposition of lyophilisates for inhalation, ED and FPF of the different samples was measured immediately after freeze-drying and compared to values after one and three months of storage (Figure 3). No significant decrease in aerosolization performance could be detected for all three formulations. On the contrary, a slightly increased FPF was determined for phenylalanine and lactose lyophilisates stored three months and a slightly increased ED was detectable for cromolyn sodium lyophilisates stored three months at 40°C. On the one hand, the higher FPF of lactose lyophilisates could be a result of a softer cake structure. If less force is needed for the fracturing of the cake, potentially the disintegration into inhalable particles becomes easier. On the other hand, the mechanical behavior remained stable for lyophilisates containing 1.5% moisture or more. This specific moisture content was already reached after one month of storage at 40°C/75% RH and those samples did not show significant changes in FPF. Furthermore, phenylalanine and cromolyn sodium revealed slightly increased FPF or ED for samples stored three months, but otherwise did not demonstrate any changes in the mechanical behavior or in the physical state. The slightly higher values after three months of storage are considered as not relevant in the context of the small number of samples and the

normal variations in the analytics. On this basis, the tested lyophilisates for inhalation were considered stable during three months of storage at 25°C/60% RH and 40°C/75% RH.

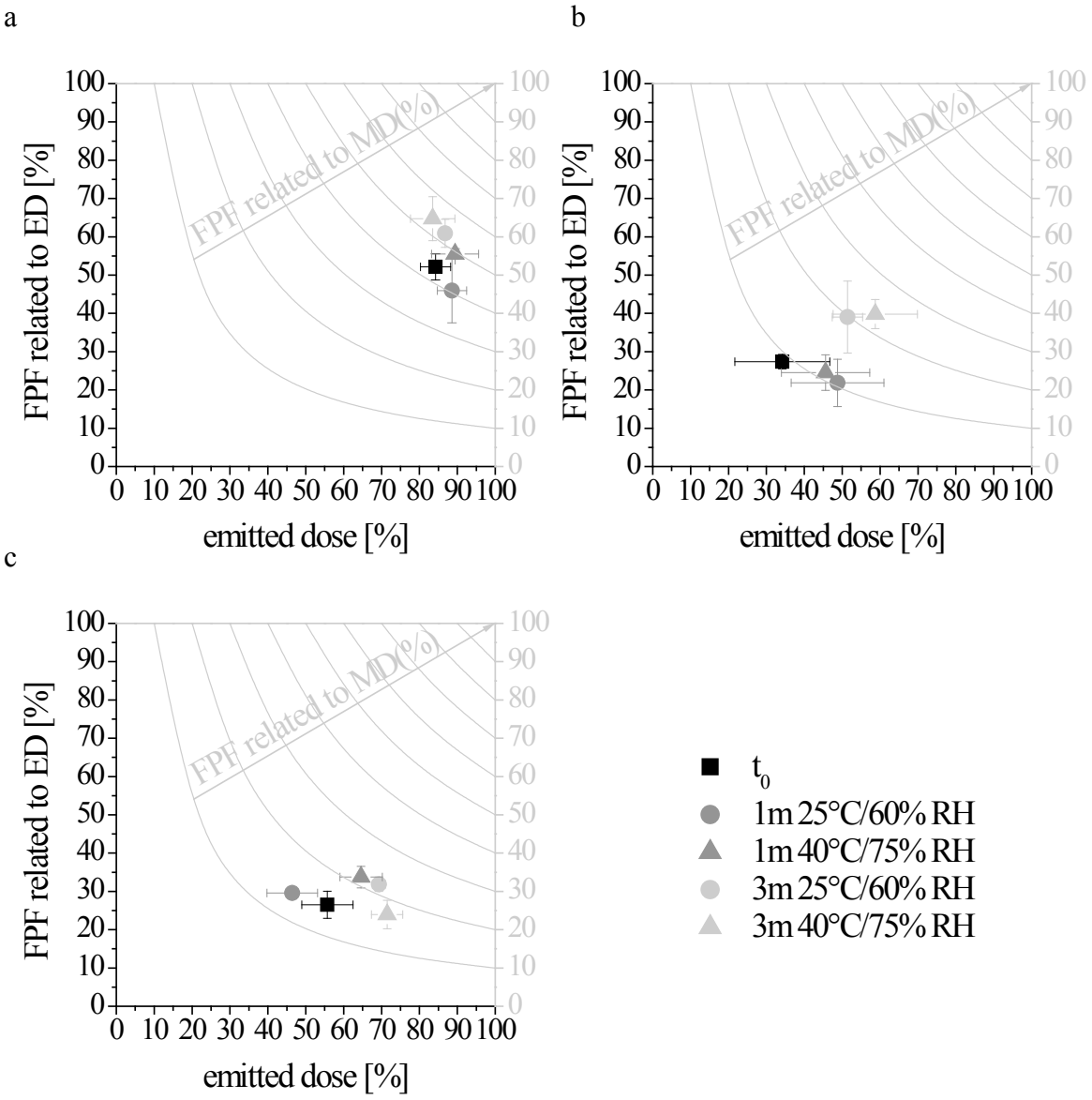

Figure 3: ED versus its related FPF as well as the FPF related to MD of the different lyophilisates before and after storage: phenylalanine (a), lactose (b) and cromolyn sodium (c).

3.2 STRESS TEST: OPEN STORAGE AT RT/30% RH AND RT/50% RH

In order to simulate potential higher moisture sorption due to an unintended open storage at high humidity or an alternative moisture-permeable container and to evaluate potential effects on the aerosolization performance, lyophilisates of various substances were equilibrated un-stoppered at 30% RH and 50% RH for three days. Substances included in this study were

amino acids (isoleucine and valine), sugars (lactose and trehalose), as well as the model API cromolyn sodium and the model protein lysozyme, each at 12 mg/ml. The lyophilisates of the two sugars did not survive the moisture stress at 50% RH but collapsed completely rendering aerosolization impossible.

XRD revealed a completely amorphous state for freeze-dried lactose, trehalose, cromolyn sodium, and lysozyme before and after moisture stress. Except for lactose and trehalose, which collapsed at 50% RH, the moisture stress did not cause crystallization. The amino acids demonstrated the characteristic peak pattern of crystalline isoleucine and valine, respectively. It has been demonstrated previously that most amino acids crystallize during freeze-drying and are therefore suitable as bulking agents [16]. For freeze-drying of protein formulations, it is known that proteins and sugars, in general, do not crystallize during freezing, but are transformed into an amorphous solid at the glass transition temperature of the maximally freeze concentrated solution (Tg') [14, 17].

Figure 4 shows the moisture content of the unstressed and stressed samples. The moisture content of the crystalline amino acids did not change after equilibration at 30% or 50% RH. The amorphous lyophilisates, in contrast, absorbed a substantial amount of water vapor. For cromolyn sodium, in particular, the moisture content increased to about 10 and 16 wt. % at 30% and 50% RH, respectively. Crystalline materials typically adsorb vapors only in small quantities at their surfaces or take up larger stoichiometric quantities to form solvates. Amorphous materials, in contrast, absorb water vapor in relatively large amounts [18].

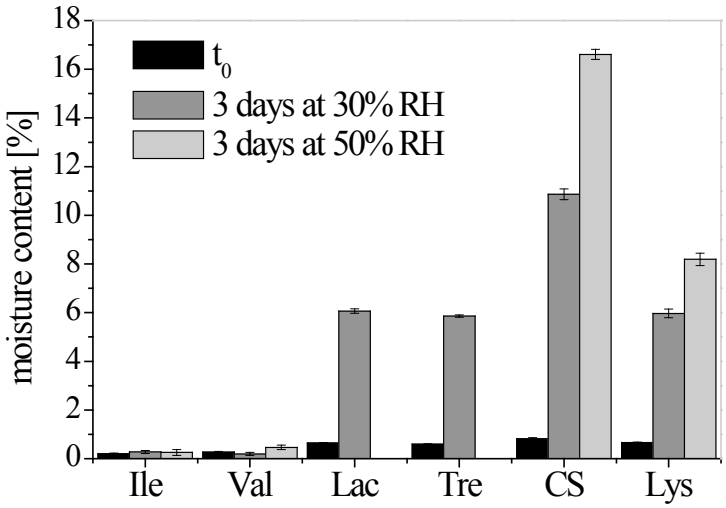

Figure 4: The moisture content of different lyophilisates stressed at 30% RH and 50% RH in open vials.

Consequently, the moisture sorption isotherm analysis of isoleucine demonstrated significant vapor sorption only at more than 80% RH, with a maximum adsorption at 90% RH of less than 1% (Figure 5). Lactose and trehalose, in contrast, showed maximum vapor absorption of approximately 14 wt. % at 55% RH and collapsed at greater RH. The collapse occurs due to a decreased glass transition temperature (Tg) and increased molecular mobility of the amorphous solid [19]. In the case of lactose, a decrease in moisture content to about 3% followed. The loss of the sorbed moisture is due to the transformation of the amorphous lactose to the crystalline state [8]. A mixture of α-lactose monohydrate (theoretical water content of 5%) and anhydrous lactose must have been formed as reported previously by Elamin et al. [8]. Subsequent to the maximum vapor sorption, crystallization occurred also for trehalose forming the dihydrate. This is indicated by the plateau at a water content of 10% [20]. Lysozyme in contrast demonstrated steady moisture sorption up to 26 wt. % without collapse or recrystallization. For cromolyn sodium lyophilisates, Figure 5 demonstrates a maximum vapor absorption of 52 wt. %. The drug is known to be very hygroscopic. Even in its crystalline form, it possesses the unique ability to absorb up to nine molecules of water per molecule of cromolyn sodium into the crystal lattice without collapse [21]. An adsorption up to 24 wt. % water of cromolyn sodium crystals was shown [21]. Such a high water uptake is especially critical when considering powders for pulmonary administration. It is reported that the hygroscopic particle growth can have a negative impact on the respirable dose [22].

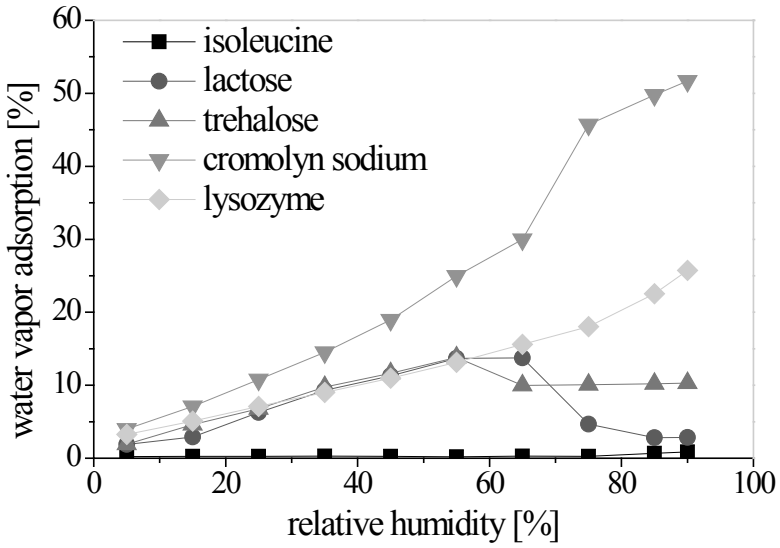

Figure 5: Moisture sorption isotherm at 25°C for lyophilized isoleucine, lactose, trehalose cromolyn sodium and lysozyme.

Small amounts of absorbed water can plasticize amorphous solids, hence exposure to humidity is considered to be an important factor influencing the solid-state properties of amorphous systems [18]. The mechanical properties of the different samples were investigated using the texture analyzer. Figure 6 compares the force necessary to fracture the lyophilisate of the unstressed and moisture stressed samples. As expected, the mechanical behavior of the crystalline lyophilisates of isoleucine and valine did not change after moisture exposure. An interesting aspect is the similar mechanical behavior of the unstressed and moisture stressed lysozyme lyophilisates, in spite of substantial moisture absorption. Lactose and trehalose, in contrast, showed a significant decrease in the force necessary to fracture the lyophilisate for a moisture content of 6%. This decrease is comparable to the force reduction for stored lactose lyophilisates containing at least 1.5% water detected earlier and confirms a maximal softening level that is independent of further moisture absorption. Cromolyn sodium, demonstrating the strongest moisture absorption, showed an immersion-force-curve shift to significantly smaller values only for samples stressed at 50% RH, which corresponds to a moisture content of 16.6%. Thus, the cromolyn sodium lyophilisates which were stored for three months and contained a maximum of 3.2% water showed no significant change in their mechanical behavior. This demonstrates that the plasticizing effect of water for amorphous products does not necessarily result in a softer mechanical property. Additionally, the degree of reduction of the force necessary to fracture the lyophilisate varies between different substances, requiring a different amount of absorbed water for the same effect. The sugars, for

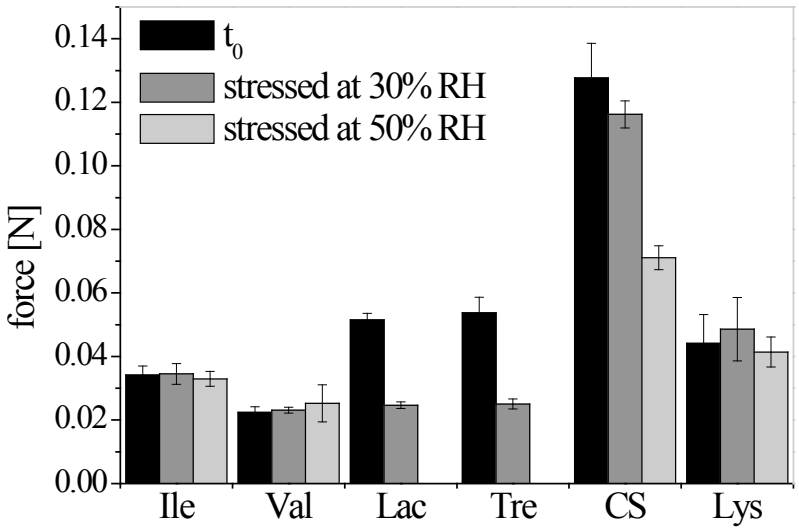

Figure 6: Plateau force values of the immersion-force curves of various lyophilisates immediately after freeze-drying and after moisture stress at 30% and 50% RH in open vials.

example, showed a reduction to about half the force for 1.5% moisture content, whereas cromolyn sodium demonstrated a similar decrease at a moisture content of 16.6%.

In order to explore potential disintegration and lung delivery problems of moisture stressed lyophilisates, ACI measurements were performed. As can be seen from Figure 7, no significant changes in the ED and FPF of various moisture stressed samples compared to the unstressed ones were detectable. The only exception was cromolyn sodium, which demonstrated the strongest moisture absorption. A marginal but not relevant decrease in the FPF related to ED was noticeable, whereas the output from the vial remained the same. Possible explanations for this potential trend include a poorer comminution into fine particles or, more likely, inferior flight qualities of the fractioned particles due to moisture sorption, which results in heavier particles with increased aerodynamic size. The density of cromolyn sodium crystals, for example, varies with increasing humidity as a consequence of the relative rates of moisture uptake and expansion of the lattice. A reduced density is reported to occur between 0 and 10% RH, whereas the density rises rapidly between 60 and 90% RH [21]. Keller et al. [22], for example, reported an increase in mass median aerodynamic diameter for cromolyn sodium DPI from 3.9 to 5.8 µm when aerosolized in a climate box at 95% RH. Overall, however, the stable aerosolization performance of lactose and trehalose lyophilisates revealed no influence of structure softening due to moisture absorption. Thus, the absence of significant changes in ED and FPF for the moisture stressed samples indicates a rather good stability for the formulations even if exposed to higher humidity for short time.

a

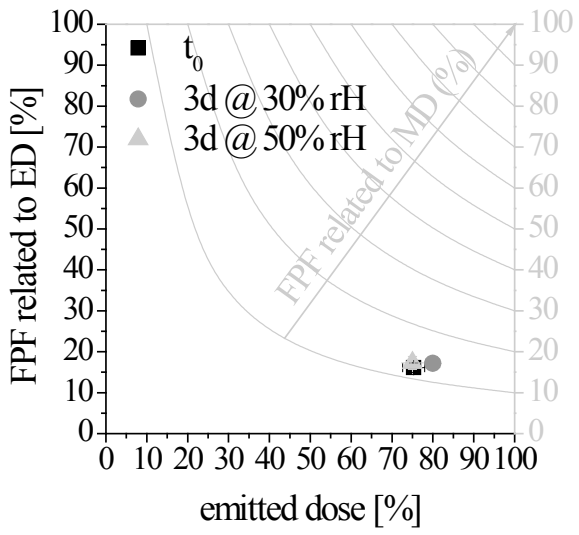

b

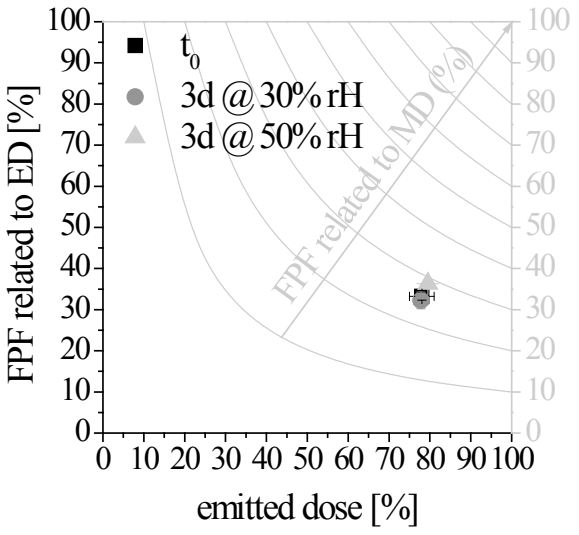

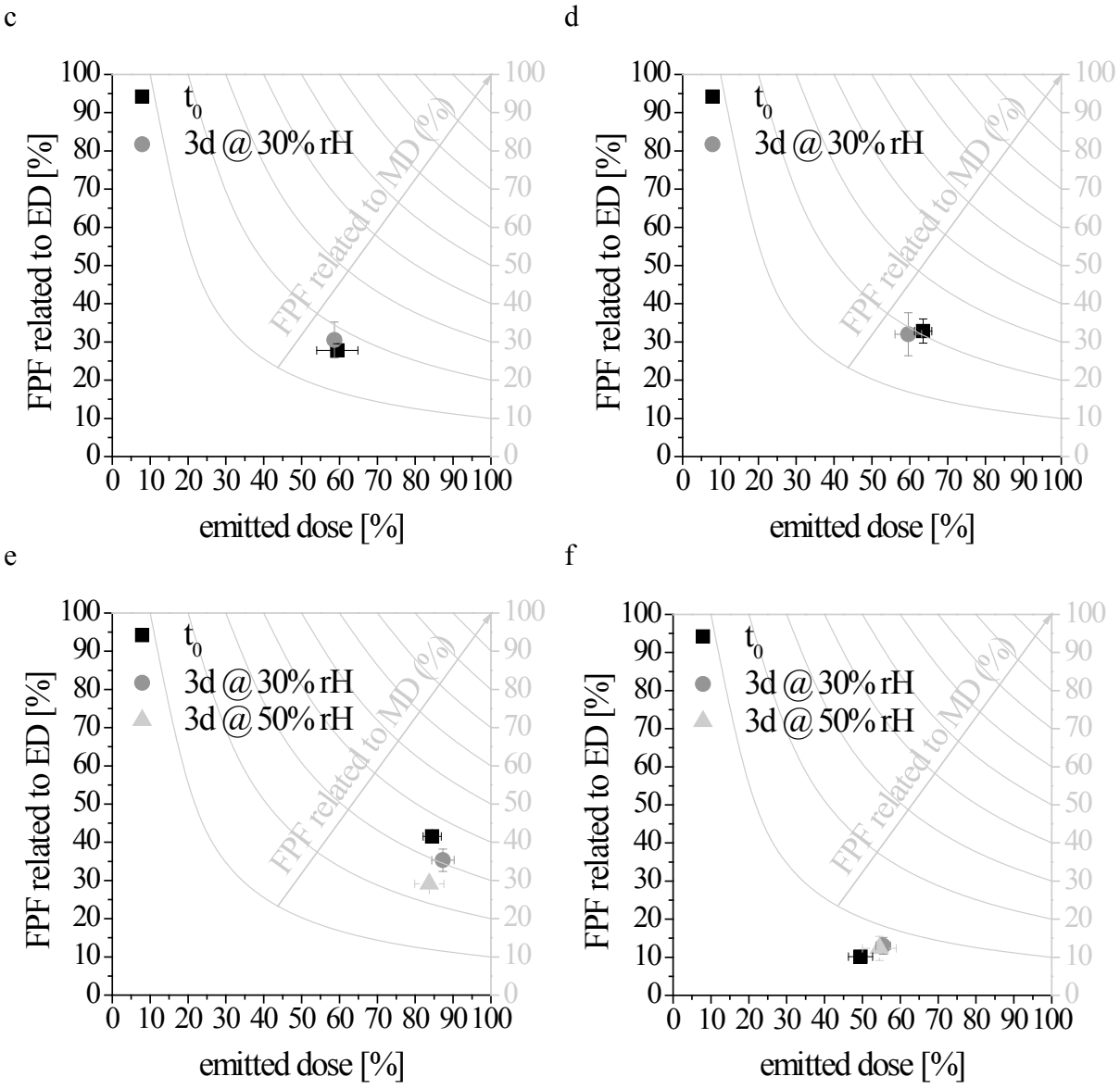

Figure 7: The ED versus its related FPF as well as the FPF related to MD of the different lyophilisates before and after moisture stress: isoleucine (a), valine (b), lactose (c), trehalose (d), cromolyn sodium (e) and lysozyme (f).

4 SUMMARY AND CONCLUSION

Freeze-dried formulations for inhalation were evaluated according to their storage stability. Potential disintegration and lung delivery problems were of special interest. Therefore, three different formulations were studied in a three-month stability study at 25°C/60% RH and 40°C/75% RH. A slight moisture absorption of less than 3% in maximum resulted in a softening of the lyophilisate structure only for lactose, which nevertheless did not hinder

aerosolization performance. The tested lyophilisates for inhalation did not show a decrease in FPF or ED during three months of storage at 25°C/60% RH and 40°C/75% RH. In order to simulate potential higher moisture sorption during short term open storage, various lyophilized substances were evaluated after un-stoppered equilibration at 30% and 50% RH. In contrast to the crystalline lyophilisates, the amorphous samples exhibited substantial moisture uptake up to 16.6% for the hygroscopic drug cromolyn sodium at 50% RH. Due to the plasticizing effect of water, the mechanical strength of the tested lyophilisates decreased to a softer structure for lactose, trehalose and, at higher moisture content, also for cromolyn sodium lyophilisates. Nevertheless, the aerosolization performance remained stable except for the two collapsed sugar lyophilisates. Therefore, it is concluded that freeze-dried formulations for inhalation which are dispersed into aerosols at the time of inhalation show good storage stability.

5 REFERENCES

[1] M.J. Telko, A.J. Hickey, Dry Powder Inhaler Formulation, Respir. Care., 50 (2005) 1209-1227.

[2] G. Pilcer, N. Wauthoz, K. Amighi, Lactose characteristics and the generation of the aerosol, Adv. Drug Delivery Rev., 64 (2012) 233-256.

[3] S. Das, I. Larson, P. Young, P. Stewart, Surface energy changes and their relationship with the dispersibility of salmeterol xinafoate powders for inhalation after storage at high RH, Eur. J. Pharm. Sci., 38 (2009) 347-354.

[4] S. Das, I. Larson, P. Young, P. Stewart, Influence of storage relative humidity on the dispersion of salmeterol xinafoate powders for inhalation, J. Pharm. Sci., 98 (2009) 1015-1027.

[5] I.J. Smith, M. Parry-Billings, The inhalers of the future? A review of dry powder devices on the market today, Pulm. Pharmacol. Ther., 16 (2003) 79-95.

[6] Stability Testing of New Drug Substances and Products Q1A(R2), in, International Confernece on Harmonisation of technical requirements for registration of pharmaceuticals for human use 2003.

[7] X. Tang, M. Pikal, Design of Freeze-Drying Processes for Pharmaceuticals: Practical Advice, Pharm. Res., 21 (2004) 191-200.

[8] A.A. Elamin, T. Sebhatu, C. Ahlneck, The use of amorphous model substances to study mechanically activated materials in the solid state, Int. J. Pharm., 119 (1995) 25-36.

[9] P.W. Winston, D.H. Bates, Saturated Solutions For the Control of Humidity in Biological Research, Ecology, 41 (1960) 232-237.

[10] M.J. Pikal, S. Shah, Moisture transfer from stopper to product and resulting stability implications, Dev. Biol. Stand., 74 (1992) 165-177; discussion 177-169.

[11] M. Le Meste, D. Simatos, J.M. Préaud, P.M. Precausta, Factors influencing changes in moisture content during storage of freeze-dried vaccines in vials, J. Biol. Stand., 12 (1985) 117-184.

[12] E.Y. Shalaev, G. Zografi, How does residual water affect the solid-state degradation of drugs in the amorphous state?, J. Pharm. Sci., 85 (1996) 1137-1141.

[13] Y. Roos, M. Karel, Plasticizing Effect of Water on Thermal Behavior and Crystallization of Amorphous Food Models, J. Food Sci., 56 (1991) 38-43.

[14] J. Liu, Physical Characterization of Pharmaceutical Formulations in Frozen and Freeze-Dried Solid States: Techniques and Applications in Freeze-Drying Development, Pharm. Dev. Technol., 11 (2006) 3-28.

[15] J. Lu, J. Wang, Z. Li, S. Rohani, Characterization and pseudopolymorphism of L-phenylalanine anhydrous and monohydrate forms, Afr. J. Pharm. Pharmacol., 6 (2012) 269-277.

[16] M. Mattern, G. Winter, U. Kohnert, G. Lee, Formulation of Proteins in Vacuum-Dried Glasses. II. Process and Storage Stability in Sugar-Free Amino Acid Systems, Pharm. Dev. Technol., 4 (1999) 199-208.

[17] L.S. Taylor, G. Zografi, Sugar–polymer hydrogen bond interactions in lyophilized amorphous mixtures, J. Pharm. Sci., 87 (1998) 1615-1621.

[18] B.C. Hancock, G. Zografi, Characteristics and significance of the amorphous state in pharmaceutical systems, J. Pharm. Sci., 86 (1997) 1-12.

[19] C. Ahlneck, G. Zografi, The molecular basis of moisture effects on the physical and chemical stability of drugs in the solid state, Int. J. Pharm., 62 (1990) 87-95.

[20] H.A. Iglesias, J. Chirife, M.P. Buera, Adsorption isotherm of amorphous trehalose, J. Sci. Food Agr., 75 (1997) 183-186.

[21] J.S.G. Cox, G.D. Woodard, W.C. McCrone, Solid-state chemistry of cromolyn sodium (disodium cromoglycate), J. Pharm. Sci., 60 (1971) 1458-1465.

[22] M. Keller, J. Schierholz, Have inadequate delivery systems hampered the clinical success of inhaled disodium cromoglycate? Time for reconsideration, Expert Opin. Drug Deliv., 8 (2011) 1-17.

Chapter 8

Summary of the Thesis

Pulmonary drug delivery has developed to an appealing option for the treatment of several lung diseases, which entail, for example, the delivery of high lung doses or the formulation of biopharmaceuticals. New inhaler inventions and formulation strategies for dry powder inhalation emerged. Among them was an interesting concept proposed by Yamashita et al. (US Patent 7735485, 2010) to prepare the formulation by freeze-drying and disintegrate the lyophilisate into inhalable particles by an air impact at the time of inhalation. The evaluation and possible further development of this new concept was the subject of this thesis. The main focus was thereby on the improvement of the formulation towards the delivery of high lung doses.

At first, an output test system with reproducible and optimized performance was developed and characterized. The influence of several variable parameters of the test system on the fine particle output was investigated with a screening design of experiments in order to fix the system to a standard parameter setting with the best possible performance. Additionally, the influence of vial and stopper geometry as well as a mouthpiece with sheath air was investigated. For all following experiments, the test system was used in a default setup consisting of a compressed air volume of 20 ml with a pressure of 3 bar, a diameter of the air inlet and air outlet capillary of 0.75 mm, the basic mouthpiece, and 2R vials equipped with lyophilization stoppers. The characterization of the test system by simulation of the air flow demonstrated great pressure drops across the narrow inlet and outlet capillaries and high air flow velocities of about 90 m/s at impaction on the lyophilisate. Nevertheless, high speed camera recordings revealed that the cake was not compressed by the incoming air jet but was lifted up and broken apart into fragments, which swirled around the endings of the capillaries. The particle aerosol finally left the mouthpiece at a velocity of approx. 3 m/s, which is comparable to pressurized metered dose inhalers. With regard to the size distribution of emitted particles, the test system demonstrated an enhanced particle emission in particular for

larger particles (around 100 µm) due to larger target surfaces offered to the discharging air flow and less wall adhesion. Very fine particles (around 3 µm) also showed an increased emission as a result of superior flight properties.

In order to understand the aerosolization behavior of the lyophilisates by impacting air, various placebo formulations (isoleucine, phenylalanine, valine, lactose, trehalose, and mannitol) at a solution concentration of 4 mg/ml were investigated according to lyophilisate characteristics and particle size distributions. The porous lyophilisates disintegrated into particles of large geometric size up to above 100 µm. The particles consisted of agglomerates of smaller fragments, resulting in a highly porous structure with a low particle density. Due to these characteristics, a substantial fraction (20-50%) of these particles had an aerodynamic size between 1 and 5 µm (fine particle fraction, FPF), and can thus be deposited in the smaller airways of the lung. The amino acid lyophilisates of phenylalanine and valine performed best among the tested samples, which must be caused by material properties other than the physical state of being crystalline or amorphous. Small standard deviations between 1 and 4% of triplicate measurements by cascade impaction demonstrated reproducible lyophilisate aerosolization and fine particle output of the test system and robustness against freeze-drying batch heterogeneity.

To test the suitability of this technology for the delivery of high powder doses, the first approach was to investigate ways and limitations for an elevation of the metered dose (MD). Valine and cromolyn sodium lyophilisates at increasing solution concentration and fill volume were examined. An increase in dose could only be achieved by increasing the solution concentration at a low fill volume because of a distinct reduction in the FPF at increased fill volume. Due to an increased hardness with higher solution concentration, the elevation of MD was however limited. The decrease in FPF at higher fill volume was caused by an impaired disintegration of the lyophilisate. For soft, instantaneous disintegrating cakes (e.g., valine), this was primarily caused by reduced milling efficiency. For harder lyophilisates (e.g., cromolyn sodium), the hindered disintegration was attributed to incomplete fragmentation of the harder cakes into particles due to a lack of space to perform rotational movements. An increased pressure for dispersion of 4 bar resulted in an increased emitted dose (ED) only for the highest fill volume of 2 ml and was not able to further enhance the fine particle dose (FPD) of cromolyn sodium. In 2R vials at default setting, a maximum FPD of 1.2 mg was achieved for valine and of 2.6 mg for cromolyn sodium lyophilisates. By the employment of bigger 6R vials, the now available space for rotational movements improved cromolyn

sodium cake disintegration of larger fill volume (2 ml). In combination with an adapted amount of compressed air to the doubled vial volume (30 ml at 4 bar), which enhanced the ED, the FPD could be further elevated to 3.7 mg.

In a second approach, the possibility to improve the FPF of lysozyme, a substance which showed poor aerosolization properties, was evaluated. The crystalline amino acids phenylalanine and valine, which performed best as single excipient formulations, were added in varying concentration (14-40%) to the high molecular weight model drug lysozyme. The dose independent increase of the FPF from 5% to 17% with phenylalanine and to 14% with valine was possibly a result of enhanced fracture properties of the lyophilisates. Another contributing factor is the reduced particle agglomeration and cohesion due to a rougher surface, which was caused by embedded amino acid crystals in the amorphous lysozyme matrix.

In a third approach for a possible improvement of the FPF, the impact of different cake morphologies on lyophilisate characteristics and their aerosolization performance were investigated. Variations of the solid matrix structure were achieved by changing the freezing process and by addition of tertiary butyl alcohol (TBA) as co-solvent. The applied freezing methods (shelf-ramped freezing, shelf-ramped freezing including two holding steps, shelf-ramped freezing with annealing, freezing on precooled shelf, freezing in liquid nitrogen, and vacuum-induced freezing) partly resulted in different pore structures of the lyophilisates, which again caused a variation of the mechanical properties. Significant changes in the aerosolization performance only became apparent for strong variations of the solid matrix structure. A lamellar-oriented morphology resulted in an increase in ED, whereas a loss of the ordered structure by consolidation caused a decreased ED and FPF compared to the conventional spherulitic morphology. This robust outcome demonstrated that the aerosolization performance is less sensitive to minor changes in the lyophilisate morphology, which can occur due to freeze-drying batch heterogeneity. Samples featuring a fine directional lamellar pore morphology, achieved by freezing in liquid nitrogen, could positively affect the ED and mostly also the FPF. Despite the demonstration of elastic lyophilisate properties, this special structure disaggregated quickly and completely into large but highly porous particles with good aerodynamic properties. The addition of TBA in the range of 5% to 20% as co-solvent rendered needle-shaped ice crystals, resulting in a lamellar-like morphology with the characteristic elastic structure and mostly also high ED of larger particles. The investigation of various freeze-dried substances (phenylalanine, valine, lactose, trehalose, cromolyn

sodium, and lysozyme + phenylalanine/valine) prepared with different freezing procedures emphasized the great influence of the material property on lyophilisate characteristics and the aerosolization performance. Mechanical material properties measured by compaction analysis were not able to fully explain commonalities and differences of the aerosolization performance of different substances. This demonstrated that properties affecting the aerosolization of lyophilisates are very complex and make it difficult to draw general conclusions or predict performance.

Finally, storage stability for three months at 25°C/60% RH and 40°C/75% RH was investigated for selected formulations (8 mg/ml phenylalanine, 12 mg/ml lactose, 20 mg/ml cromolyn sodium, and 12 mg/ml lysozyme + 4 mg/ml phenylalanine). Despite a slight increase in the moisture content which resulted in a softening of lactose lyophilisates, all formulations demonstrated unchanged aerosolization performance. In order to simulate potential higher moisture sorption due to an unintended open storage at high humidity or an alternative moisture-permeable container, an un-stoppered storage at 30% and 50% RH for three days was performed as stress test for several model substances (isoleucine, valine, lactose, trehalose, cromolyn sodium, and lysozyme). In contrast to the amino acid lyophilisates, which demonstrated crystallinity, the amorphous samples exhibited substantial moisture uptake of up to 16.6% for the hygroscopic drug cromolyn sodium at 50% RH. Except of the lyophilized sugars lactose and trehalose, which collapsed at 50% RH, storage at 30% and 50% RH showed hardly any effect on the aerosolization performance of all. It can therefore be concluded that the lyophilisates show good storage stability with regard to their aerosolization performance.

In conclusion, the disintegration of lyophilisates by an air impact represents a promising new concept for dry powder pulmonary delivery. It combines a formulation process which is friendly for thermolabile drugs like biopharmaceuticals with the idea of creating fine particles at the time of inhalation which avoids formulation problems of most respiratory powders like poor flowability and redispersibility. Depending on the lyophilized substance, it demonstrated rather large FPF compared to dry powder inhalation products on the market and it can keep up with products of higher metered dose regarding the FPD. The aerosolization performance was shown to be less sensitive to minor changes in the lyophilisate morphology, which refers to robustness against freeze-drying batch heterogeneities like variation within and between batches. Nevertheless, it is important to note that the aerosolization performance is strongly affected by material properties.

LIST OF ABBREVIATIONS

A	Heckel-intercept
ACI	Andersen cascade impactor
API	active pharmaceutical ingredient
CF	cystic fibrosis
COPD	chronic obstructive pulmonary disease
CS	cromolyn sodium
d_A	aerodynamic diameter
DD	delivered dose
DoE	design of experiment
DPI	dry powder inhaler
D_{rel}	relative porosity
DSC	differential scanning calorimetry
DSPC	distearoylphosphatidylcholine
d_V	volume-equivalent diameter
ED	emitted dose
EMA	european medicines agency
FPD	fine particle dose
FPF	fine particle fraction
ICD	inlet capillary diameter
ICP	inlet capillary position
Ile	L-isoleucine
k	Heckel constant/Heckel-slope
Lac	lactose-monohydrate
LD	laser diffraction
Lys	lysozyme
Man	D-mannitol
MD	metered dose
MLI	multistage liquid impinger
MMAD	mass median aerodynamic diameter
MRSA	methicillin-resistant *Staphylococcus aureus*
OCD	outlet capillary diameter

OCP	outlet capillary position
P	pressure
P0	baffle plate after stage 0 of ACI
P1	baffle plate after stage 1 of ACI
Phe	L-phenylalanine
PLGA	poly(lactide-co-glycolide)
pMDI	pressurized metered dose inhaler
PSD	particle size distribution
RH	relative humidity
SEM	scanning electron microscopy
SIP	suction induction port
TBA	tertiary butyl alcohol
Tg'	glass transition temperature of the max. freeze concentrated solution
Tg	glass transition temperature
TOF	time of flight
Tre	trehalose
Val	L-valine
Vol	volume
XRD	x-ray diffractometry
ρ	density
χ	shape factor

PRESENTATIONS AND PUBLICATIONS ASSOCIATED WITH THIS WORK

Publications

S. Claus, T. Schoenbrodt, C. Weiler, W. Friess, Novel dry powder inhalation system based on dispersion of lyophilisates, Eur. J. Pharm. Sci. 43 (2011) 32-40

S. Claus, C. Weiler, J. Schiewe, W. Friess, Optimization of the fine particle fraction of a lyophilized lysozyme formulation for dry powder inhalation, Pharm. Res. 30 (2013) 1698-1713

S. Claus, C. Weiler, J. Schiewe, W. Friess, How can we bring high drug doses to the lung? (submitted to Eur. J. Pharm. Biopharm.)

Posters

S. Claus, C. Weiler, J. Schiewe, W. Friess; Effect of Freezing Methods on Aerosolization of Lyophilized Lactose for Dry Powder Inhalation, 8th World Meeting on Pharmaceutics, Biopharmaceutics and Pharmaceutical Technology, Istanbul, Turkey, March 19-22, 2012

S. Claus, C. Weiler, J. Schiewe, W. Friess; Optimization of the fine particle fraction of a lyophilized lysozyme formulation for dry powder inhalation, 2011 AAPS Annual Meeting & Exposition, Washington DC, USA, October 23-27, 2011

S. Claus, C. Weiler, W. Friess; How to Optimize the Fine Particle Dose of a Lyophilization-Based Novel Dry Powder Inhalation System, RDD Europe, Berlin, Germany, May 3-6, 2011, pp. 341-344

S. Claus, T. Schoenbrodt, W. Friess; Evaluation of lyophilized powders for inhalation, 7th World Meeting on Pharmaceutics, Biopharmaceutics and Pharmaceutical Technology, Valetta, Malta, March 8-11, 2010